Transformació i metabolisme de fàrmacs al medi aquàtic mitjançant l'espectrometria de masses d'alta resolució

Jaume Aceña i Sánchez

Transformació i metabolisme de fàrmacs al medi aquàtic mitjançant l'espectrometria de masses d'alta resolució

Jaume Aceña i Sánchez

Tesi doctoral - 2017

Programa de Doctorat

"Química Analítica del Medi Ambient i la Pol·lució"

Transformació i metabolisme de fàrmacs al medi aquàtic mitjançant l'espectrometria de masses d'alta resolució

Memòria presentada per optar al grau de

Doctor per la Universitat de Barcelona per

Jaume Aceña i Sánchez

Codirectora

Dra. Sandra Pérez
Cientifica contractada
IDAEA – CSIC

Codirector

Pr. Damià Barceló
Professor investigació
IDAEA – CSIC

Tutora

Dra. Encarnación Moyano
Professora titular
Universitat de Barcelona

Barcelona, Juny 2017

Als meus pares, per fer-ho possible

A la Pilar, per fer-ho realitat

“I’m a greater believer in luck, and I find
the harder I work the more I have of it”

Thomas Jefferson

Aquesta tesi doctoral ha estat finançada principalment per la Generalitat de Catalunya (2014 SGR 418 – Institut de diagnosi Ambiental i Estudis de l'Aigua), el Ministeri d'Economia i Competitivitat mitjançant el projecte SCARCE (Consolider-Ingenio 2010 CSD2009-00065), i el 7è Programa Marc de Finançament de la Unió Europea amb el conveni de subvenció nº 603629-ENV-2013-6.2.1-Globaqua.

AGRAIMENTS

En primer lloc agrair al professor Damià Barceló l'oportunitat i la confiança de poder realitzar aquesta tesis doctoral al seu grup d'investigació, on he disposat de tots els recursos necessaris, l'instrumental més punter i un equip humà de màxima qualitat científica i per sobre de tot humana. Agrair també de forma molt especial a la doctora Sandra Pérez tota la seva dedicació, direcció, correccions i coneixements. Han estat anys de molt treball, on sempre he trobat el seu recolzament. Si avui aquesta tesis és una realitat és sens dubte gracies a la seva confiança i a la seva gran implicació per tirar endavant aquesta tesis, des del primer a l'últim dia; gràcies Sandra! Agrair també a la doctora Encarnación Moyano haver acceptar la tutoria d'aquesta tesis, el seu consell i totes les facilitats donades, tant per ella com per la Universitat de Barcelona.

Aquesta memòria és un resum del treball realitzat durant aproximadament cinc anys en els que he pogut compartir molts moments amb moltes persones d'arreu del món, gràcies per poder ser un més de vosaltres! Tots els agraïments requeririen un altre capítol i segur que em deixaria algunes persones. No obstant, no puc estar-me d'almenys mencionar aquelles que m'heu acompanyat d'una manera especial durant aquest camí.

Tinc clar per on començar, amb el KIKE, contigo empezo todo! Espero que tornem a coincidir!! I també amb el mestre Josep i els meus germans grans de tesis, la Vicky i el Bozo! he après tant de vosaltres!! I com no al Pablo, efjaristó! I clar, mencionar a la Bianca, el Cayo, el Niko, la Paqui, l'Asun, l'Aleksandra, el Dani, la Postigo, la Marina, la Marta1.0, la Marianne, la MeriLu, la Chus, la Paula, l'Alicia, la Laia, la Rebeca, la Giovanna, la Giselle, l'Alex, el D. Molins, la Mar, la Núria, la Maja, les Noelias, la Meri, l'Angels, l'Elena, la Roser, la Dori, la Maria!! Buf, i veig tants amics... Sou collonuts!

Infinites gracies per l'ajuda a la Maia, la Charlotte, la Marine, la Marta2.0, l'Abraham, la Serena, el Michael, el Manuel i el Juan!! Va ser un plaer poder guiar-vos en les vostres primeres passes davant els masses! Però de ben segur vaig aprendre més jo de vosaltres que no al revés!! Juan, gracias amigo!

I tot ha de seguir amb la nova generació; la Dra. Bosch, el Dani, l'Oscar, la Gabriella, la Maria Pau, l'Esther, el Simón, el Carlos, la Gemma...i suma i sigue... Un plaer haver compartit moments amb tots vosaltres!!

No vull oblidar-me de la Marinel·la, la Silvia, l'Ethel, la Miren i l'Antoni, pels que tingut la sort de treballar o col·laborar! Tampoc de l'ajuda inestimable del Peter, el Piero, la M. Vila, el M. Zacchini, la M. Solé, la Cinta Porte, l'Oscar Gonzalez, el Benjamí Piña, l'Esteban Abad i el Jose Luís Abad. Un autèntic plaer col·laborar amb persones de tan nivell! Recordar també a aquells qui estan de pas van deixar un record i grans moments per la memòria; l'Alinne, el Walid, l'Ignacio, l'Abel, l'Ahmed, l'Elisabeth, la Sara, el Rodrigo, el Thiago, l'Alex, la Mónica...I evidentment, tot el grup del Thomaidis, on em vaig sentir com a casa! la Violeta, la Christina, el Reza, el Nikiforos, la Katerina, l'Anna,la Maristina, la Vasiliki, la Sophia, el Dimitris... i com he dit, molts més, gràcies a tots!!

Però he de dir, que tot això no hagués estat possible sense el suport incondicional de la meva família; gracies papes! Escrivint aquestes línies és inevitable pensar en quan redactava les del màster.. així que aprofito per fer extensiva la dedicació d'aquesta tesis a tot el personal sanitari de l'Hospital de Mataró, que ha fet possible dedicar als dos aquesta tesis. I com no, GRÀCIES PILAR! per tota la teva ajuda i suport, per sacrificar el temps que em requeria, per aguantar els moments de més engoixa i en definitiva, per seguir fent possible l'impossible! Gràcies avis, Xavier, Raquel, Ivanna, Juan, Elisa, Juan Antonio, Juan Antonio ("el niño"), Jan, Ona i també a la Laia, la il·lusió que ja ve de camí! I que en vinguin més! SABER QUE PUC COMPTAR AMB TOTS VOSALTRES HO FA TOT MÉS FÀCIL! Us estimo!!

També agrair la comprensió dels amics, de TOTS!! I de tota la família de l'Illuro HC! Als nous companys de Menadiona agrair l'interès i les facilitats donades en el tram final de tesis. He repartit el temps entre tot tant bé com he pogut, però sempre sento que en fa falta més per poder estar més amb vosaltres. En definitiva, GRACIES A TOTHOM, em sento molt afortunat i us puc assegurar que cada dia d'aquesta etapa ha valgut la pena!

INDEX

RESUM 5

RESUMEN 9

SUMMARY ..... **¡Error! Marcador no definido.**

CAPITOL 1. INTRODUCCIÓ 22

1.1 Vies d'entrada i presència dels fàrmacs al medi aquàtic 22

1.2 Transformacions dels fàrmacs als rius 24

1.3 Exposició i metabolisme de fàrmacs en biota 29

1.4 Anàlisi de fàrmacs, els seus productes de transformació i els seus metabòlits amb espectrometria de masses al medi aquàtic i a la biota 38

1.4.1 Anàlisi quantitatiu 42

1.4.2 Anàlisi qualitatiu 46

Article nº 1: Advances in liquid chromatography–high-resolution mass spectrometry for quantitative and qualitative environmental analysis 58

CAPITOL 2. OBJECTIUS I ESTRUCTURA 74

2.1 OBJECTIUS 74

2.2 ESTRUCTURA 75

CAPITOL 3. TRANSFORMACIÓ DE FÀRMACS AL MEDI AQUÀTIC 78

3.1 Processos de transformació: Fotodegradació 79

Article nº 2: Identification of phototransformation products of Sildenafil (Viagra) and its N-demethylated human metabolite under simulated sunlight. 82

Article nº 3: Structure elucidation of phototransformation products of unapproved analogs of the erectile dysfunction drug sildenafil in artificial freshwater with UPLC-Q Exactive-MS. 100

3.2 Processos de transformació: Biodegradació 124

Article nº 4: Degradation of sulphonamides as a microbial resistance mechanism. 126

3.3 Discussió de resultats 160

3.3.1 Aproximacions analítiques 160

3.3.2 Identificació de TPs 163

3.3.3 Detecció de TPs en mostres ambientals 165
CAPITOL 4. ACUMULACIÓ I METABOLISME DE FÀRMACS A LA BIOTA .. 170
4.1 Estudi del metabolisme de fàrmacs en biota a escala laboratori..... 171
Article nº 5: Metabolic profiling of ibuprofen and carbamazepine in juvenile Senegal soles (Solea senegalensis) using high-resolution mass spectrometry. 174
Article nº 6: Ibuprofen exposure in Lemna gibba L.: evaluation of growth and phytotoxic indicators, detection of ibuprofen and identification of its metabolites in plant and in the medium 198
4.2 Avaluació del metabolisme a peixos de riu 206
4.3 Discussió de resultats 210
4.3.1 Identificació de les reaccions metabòliques a escala laboratori . 210
4.3.2 Detecció de metabòlits de fàrmacs en peixos de riu..... 216
CAPITOL 5. CONCLUSIONS 224
BIBLIOGRAFIA 229
INDEX DE TAULES 243
INDEX DE FIGURES 243
LLISTAT D'ACRÒNIMS 245

RESUM

RESUM / RESUMEN / SUMMARY

RESUM

En la societat actual, els fàrmacs són imprescindibles per a millorar la qualitat de vida de les persones. Aquests són àmpliament consumits per tal de pal·liar dolències i prevenir, combatre o curar malalties tant per les pròpies persones com en veterinària. Per tant, la pròpia finalitat dels compostos en provoca una activitat biològica inherent a la seva naturalesa i, en conseqüència, el seu destí ambiental genera una creixent preocupació pels efectes colaterals als ecosistemes. Els fàrmacs estan dissenyats per ser consumits, realitzar la seva funció i finalment ser excretats. El seu rati d'excreció i el dels seus productes de transformació, anomenats metabòlits, és diferent per a cada principi actiu. Aquest conjunt de compostos, considerats contaminants orgànics, arriba a través de les aigües residuals a les estacions depuradores (EDARs). Actualment, les EDARs no estan dissenyades per eliminar aquests compostos i per tant en molts casos poden persistir durant el procés de tractament. Com a resultat d'aquesta persistència i pertinent entrada al medi aquàtic, es produeix una exposició crònica d'organismes als contaminants, els quals poden resultar afectats de diferents formes. Per agreujar encara més la creixent contaminació, les aigües pluvials i d'escorrentia poden constituir una aportació addicional, ja que poden provocar que aquestes aigües no rebin cap mena de tractament abans d'entrar als diferents cursos d'aigua.

Un cop a les aigües superficials, el destí dels fàrmacs i els seus metabòlits encara no esta completament estudiat. En la darrera dècada molts estudis han determinat els diversos principis actius en els diferents ecosistemes i han tractat d'avaluar-ne els seus efectes. Malgrat aquests esforços, molts estudis conclouen que per una avaluació més completa és necessari tenir en compte les possibles transformacions que pateixen aquests compostos al medi ambient. Els productes resultants són anomenats productes de transformació (TPs) i poden retenir l'activitat biològica del pare i fins i tot en ocasions tenir efectes toxicològics superiors als del compost original.

En el desenvolupament d'aquests tesi s'han estudiat les principals transformacions dels fàrmacs al medi aquàtic, incloent processos biòtics i abiòtics. Aquests estudis s'han realitzat mitjançant metodologies basades en la

cromatografia de líquids acoblada a l'espectrometria de masses d'alta resolució (LC-HRMS).

Al capítol 1 s'ha revisat l'estat actual de la LC-HRMS per a diferents aproximacions en mostres ambientals. A la literatura s'han publicat diverses comparacions amb instrumentació de baixa resolució (LRMS) i es pot constatar que actualment, els espectròmetres de nova generació, han superat les limitacions tradicionals d'aquesta tècnica per a l'anàlisi quantitatiu, oferint linealitats i sensibilitats similars als instruments de triple quadrupol. A més, als mètodes multi-residu a través de LC-HRMS, l'augment del nombre de compostos objectiu no en perjudica la sensibilitat. Evidentment, les grans prestacions que ens ofereix aquesta tècnica per a l'elucidació estructural de compostos també la fa idònia per a aquestes finalitats i s'ha pogut demostrar en els diferents estudis realitzats mitjançant la identificació dels TPs. A més, en els darrers anys s'han desenvolupat noves estratègies mitjançant instrumentació HRMS híbrida, aprofitant la elevada resolució que ofereixen aquests instruments, la corresponent exactitud de massa i l'adquisició selectiva o no selectiva d'ions fragments en una única injecció. Aquests mètodes permeten l'anàlisi dirigit de compostos coneguts, l'escombratge de compostos sospitosos a partir de bases de dades i fins i tot l'anàlisi no dirigit de compostos desconeguts. Moltes d'aquestes capacitats han estat utilitzades per a detectar i identificar els TPs dels diferents processos estudiats en aquesta tesi.

Al capítol 3 s'ha avaluat l'efecte de la llum del sol sobre els fàrmacs, conegut com a fotòlisi, i que és considerat el principal mecanisme de transformació abiòtic. De fet, aquest pot ser el mecanisme de degradació més important en ecosistemes amb un gran impacte de la llum. En el capítol 3 s'ha avaluat les reaccions de foto-transformació dels inhibidors de la fosfodiesterasa V mitjançant simulacions a escala laboratori. Per aquest motiu s'ha avaluat la fotòlisi del principi actiu més utilitzat, el sildenafil (SDF). Els darrers anys, aquest principi actiu també ha estat molt falsificat, a través d'anàlegs per adulterar productes naturals de venda per internet. La avaluació conjunta de les rutes de degradació ens ofereix més informació sobre l'efecte de la llum i les transformacions produïdes en la seva estructura. Mitjançant aquests estudis s'ha pogut determinar un patró de fragmentació comú i identificar els TPs

principals pels diferents compostos. Finalment, per tal de contrastar aquestes transformacions en mostres reals, s'han analitzat mostres ambientals per a detectar els TPs identificats. Aquest estudi a significat la primera detecció de dos TPs del SDF i/o dels seus anàlegs al medi ambient.

En ecosistemes on l'efecte de la llum és menor, el principal destí i transformació dels fàrmacs ve marcat pels processos de biodegradació causats per microorganismes. Per tal d'estudiar aquests processos, al capítol 3 també es mostra un estudi que es va realitzar a escala laboratori on es determinen els principals TPs per biodegradació de sulfonamides. En aquesta ocasió la identificació dels TPs es va utilitzar per a poder realitzar un estudi quantitatiu dels mecanismes de resistència bacteriana a les sulfonamides. Els resultats constaten que a altes concentracions el paper de la degradació de les sulfonamides és més important, mentre que a baixes concentracions la adaptació dels bacteris mitjançant la propagació de gens resistents als antibiòtics cobra protagonisme. Els TPs identificats mostren rutes diferents a les observades pels processos abiòtics, demostrant que a les aigües trobem un còctel de compostos els efectes dels quals són difícil de predir.

A la literatura s'ha pogut constatar que els fàrmacs han estat detectats també a la biota que hi esta constantment exposada. Al capítol 4 s'ha volgut avaluar aquesta exposició en diferents organismes aquàtics i com aquests es transformen a través de reaccions bioquímiques en diferents TPs, generalment coneguts com a metabòlits. Per aquest motiu s'han realitzat de nou estudis a escala laboratori per a determinar els metabòlits principals. En primer lloc s'han identificat els metabòlits de l'Ibuprofè i la carbamazepina, dos fàrmacs habitualment detectats a les aigües superficials, mitjançant la injecció intraperitoneal a llenguados. La comparació de mostres control i mostres tractades ha permès detectar els nous pics corresponents a metabòlits. Mitjançant l'estudi dels patrons de fragmentació d'aquests compostos s'han proposat les identitats dels metabòlits. Aquesta aproximació a permès detectar i identificar temptativament 13 metabòlits de l'ibuprofè i 11 metabòlits de la carbamazepina a la bilis dels peixos injectats.

A continuació mitjançant una nova simulació al laboratori, s'han identificat els metabòlits de l'ibuprofè en plantes aquàtiques, concretament en llenties d'aigua (Lemna Gibba). En total s'han identificat 11 metabòlits de l'ibuprofè. Aquests estudis han permès demostrar la variabilitat en el metabolisme d'un mateix fàrmac en diferents organismes aquàtics i com això en fa encara més complexa la seva avaluació, ja que un compost pot resultar gairebé inofensiu per a una espècie i molt tòxic per a una altre.

Finalment, aprofitant tots els coneixements assolits en el desenvolupament d'aquesta tesi i les capacitats màximes de la LC-HRMS, s'ha estudiat el metabolisme dels fàrmacs en mostres de peixos salvatges. Per això s'ha realitzat un mostreig de peixos al riu Llobregat i s'han analitzat mitjançant un sistema Q-TOF. Inicialment s'ha realitzat un escombratge dirigit a les dades obtingudes de més de 2000 contaminants orgànics. Aquesta base de dades havia estat prèviament generada mitjançant la injecció directe de patrons amb el mateix mètode d'anàlisi. Això ens ha permès detectar multitud de contaminants, entre ells més de 12 productes farmacèutics dels 150 que contenia la llista.

Dels fàrmacs detectats s'han seleccionat 6 fàrmacs que ens han despertat més interès, ja sigui per la seva alta detecció o per que només han estat detectats en un punt concret del mostreig. Aquests compostos han estat l'Ibuprofè, el gemfibrozil, la pregabalina, la sertralina i la mepivacaina. A continuació, a través d'un software de predicció de metabòlits i els coneixements adquirits a les simulacions a escala laboratori, s'ha generat una base de dades de més de 150 metabòlits corresponents a les transformacions d'aquests sis fàrmacs. Amb aquesta base de dades s'ha realitzat un escombratge de sospitosos permeten la detecció d'un gran nombre de candidats. Mitjançant l'estudi dels patrons de fragmentació, softwares de predicció de fragments i biblioteques d'espectres s'han proposat les estructures d'alguns d'ells amb un grau de confiança força elevat (grau 2 de l'escala proposada per Shymanski i els seus col·laboradors).

RESUMEN

En la sociedad actual, los productos farmacéuticos son imprescindibles para mejorar la calidad de vida de las personas. Estos son ampliamente consumidos para paliar dolencias y prevenir, combatir o curar enfermedades tanto para las personas como en veterinaria. Por lo tanto, la finalidad de los compuestos les propicia una actividad biológica inherente a su naturaleza y, en consecuencia, su destino ambiental genera una creciente preocupación por los efectos colaterales en los ecosistemas. Los fármacos están diseñados para ser consumidos, realizar su función y finalmente ser excretados. Su ratio de excreción y el de sus productos de transformación, llamados metabolitos, es diferente para cada principio activo. Este conjunto de compuestos, considerados contaminantes orgánicos, llega a través de las aguas residuales a las estaciones depuradoras (EDARs). Actualmente, las EDARs no están diseñadas para eliminar estos compuestos y por tanto en muchos casos pueden persistir durante el proceso de tratamiento. Como resultado de esta persistencia y pertinente entrada al medio acuático, se produce una exposición crónica de organismos a los contaminantes, los cuales pueden resultar afectados de distintas formas. Para agravar aún más la creciente contaminación, las aguas pluviales y de escorrentía pueden constituir un aporte adicional, ya que pueden provocar que estas aguas no reciban ningún tipo de tratamiento antes de entrar a los diferentes cursos de agua.

Una vez en las aguas superficiales, el destino de los fármacos y sus metabolitos aún no está completamente estudiado. En la última década muchos estudios han determinado los diversos principios activos en los diferentes ecosistemas y han tratado de evaluar sus efectos. A pesar de estos esfuerzos, muchos estudios concluyen que para una evaluación más completa es necesario tener en cuenta las posibles transformaciones que sufren estos compuestos en el medio ambiente. Los productos resultantes son llamados productos de transformación (TPs) y pueden retener la actividad biológica del padre e incluso en ocasiones tener efectos toxicológicos superiores a los del compuesto original.

En el desarrollo de ésta tesis se han estudiado las principales transformaciones de los fármacos en el medio acuático, incluyendo procesos bióticos y abióticos.

Estos estudios se han realizado mediante metodologías basadas en la cromatografía de líquidos acoplada a la espectrometría de masas de alta resolución (LC-HRMS).

En el capítulo 1 se ha revisado el estado actual de la LC-HRMS para diferentes aproximaciones en muestras ambientales. En la literatura se han reportado varias comparaciones con instrumentación de baja resolución (LRMS) y se puede constatar que actualmente, los espectrómetros de nueva generación, han superado las limitaciones tradicionales de esta técnica para el análisis cuantitativo, ofreciendo linealidades y sensibilidades similares a los instrumentos de triple cuadrupolo. Además, en los métodos multi-residuo a través de LC-HRMS, el aumento del número de compuestos objetivo no perjudica la sensibilidad. Evidentemente, las grandes prestaciones que nos ofrece esta técnica para la elucidación estructural de compuestos también la hace idónea para estos fines y se ha podido demostrar en los diferentes estudios realizados mediante la identificación de los TPs. Además, en los últimos años se han desarrollado nuevas estrategias mediante instrumentación HRMS híbrida, aprovechando la elevada resolución que ofrecen estos instrumentos, la correspondiente exactitud de masa y la adquisición selectiva o no selectiva de iones fragmento en una única inyección. Estos métodos permiten el análisis dirigido de compuestos conocidos, el barrido de compuestos sospechosos a partir de bases de datos e incluso el análisis no dirigido de compuestos desconocidos. Muchas de estas capacidades han sido utilizadas para detectar e identificar los TPS de los diferentes procesos estudiados en esta tesis.

En el capítulo 3 se ha evaluado el efecto de la luz del sol sobre los fármacos, conocido como fotólisis, y que es considerado el principal mecanismo de transformación abiótico. De hecho, este puede ser el mecanismo de degradación más importante en ecosistemas con un gran impacto de la luz. En el capítulo 3 se ha evaluado las reacciones de foto-transformación de los inhibidores de la fosfodiesterasa V mediante simulaciones a escala laboratorio. Por este motivo se ha evaluado la fotólisis del principio activo más utilizado, el sildenafil (SDF). En los últimos años, este principio activo también ha sido muy falsificado, a través de análogos para adulterar productos naturales de venta

por internet. La evaluación conjunta de las rutas de degradación nos ofrece más información sobre el efecto de la luz y las transformaciones producidas en su estructura. Mediante estos estudios se ha podido determinar un patrón de fragmentación común e identificar los TPS principales por los diferentes compuestos. Finalmente, para contrastar estas transformaciones en muestras reales, se han analizado muestras ambientales para detectar los TPS identificados. Este estudio ha significado la primera detección de dos TPS del SDF y / o de sus análogos al medio ambiente.

En ecosistemas donde el efecto de la luz es menor, el principal destino y transformación de los fármacos viene marcado por los procesos de biodegradación causados por microorganismos. Para estudiar estos procesos, en el capítulo 3 también se muestra un estudio que se realizó a escala laboratorio donde se determinan los principales TPs por biodegradación de sulfonamidas. En esta ocasión la identificación de los TPs se utilizó para poder realizar un estudio cuantitativo de los mecanismos de resistencia bacteriana a las sulfonamidas. Los resultados constatan que a altas concentraciones el papel de la degradación de las sulfonamidas es más importante, mientras que a bajas concentraciones la adaptación de las bacterias mediante la propagación de genes resistentes a los antibióticos cobra protagonismo. Los TPs identificados muestran rutas diferentes a las observadas por los procesos abióticos, demostrando que en las aguas encontramos un cóctel de compuestos cuyos efectos son difícil de predecir.

En la literatura se ha podido constatar que los fármacos han sido detectados también en la biota que está constantemente expuesta. En el capítulo 4 se ha querido evaluar esta exposición en diferentes organismos acuáticos y como estos se transforman a través de reacciones bioquímicas en diferentes TPs, generalmente conocidos como metabolitos. Por este motivo se han realizado de nuevo estudios a escala laboratorio para determinar los metabolitos principales. En primer lugar se han identificado los metabolitos del Ibuprofeno y la carbamazepina, dos fármacos habitualmente detectados en las aguas superficiales, mediante la inyección intraperitoneal a lenguados. La comparación de muestras control y muestras tratadas ha permitido detectar los nuevos picos correspondientes metabolitos. Mediante el estudio de los

patrones de fragmentación de estos compuestos se han propuesto las identidades de los metabolitos. Esta aproximación ha permitido detectar e identificar tentativamente 13 metabolitos del ibuprofeno y 11 metabolitos de la carbamazepina en la bilis de los peces inyectados.

A continuación mediante una nueva simulación en el laboratorio, se han identificado los metabolitos del ibuprofeno en plantas acuáticas, concretamente en lentejas de agua (Lemna gibba). En total se han identificado 11 metabolitos del ibuprofeno. Estos estudios han permitido demostrar la variabilidad en el metabolismo de un mismo fármaco en diferentes organismos acuáticos y como esto hace aún más compleja su evaluación, ya que un compuesto puede resultar casi inofensivo para una especie y muy tóxico por otro.

Finalmente, aprovechando todos los conocimientos adquiridos en el desarrollo de esta tesis y las capacidades máximas de la LC-HRMS se ha estudiado el metabolismo de los fármacos en muestras salvajes. Para ello se ha realizado un muestreo de peces en el río Llobregat y se han analizado mediante un sistema Q-TOF. Inicialmente se ha realizado un barrido dirigido de más de 2000 contaminantes orgánicos. Esta base de datos había sido previamente generada mediante la inyección directa de patrones con el mismo método de análisis. Esto nos ha permitido detectar multitud de contaminantes, entre ellos más de 12 productos farmacéuticos de los 150 que contenía la lista.

De los fármacos detectados se han seleccionado 6 fármacos que nos han despertado más interés, ya sea por su alta detección o para que sólo han sido detectados en un punto concreto del muestreo. Estos compuestos han sido el Ibuprofeno, el gemfibrozilo, pregabalina, la sertralina y la mepivacaina. A continuación, a través de un software de predicción de metabolitos y los conocimientos adquiridos en las simulaciones a escala laboratorio, se ha generado una base de datos de más de 150 metabolitos correspondientes a las transformaciones de estos seis fármacos. Con esta base de datos se ha realizado un barrido de sospechosos que ha permitido la detección de un gran número de candidatos. Mediante el estudio de los patrones de fragmentación, softwares de predicción de fragmentos y bibliotecas de espectros se han

propuesto las estructuras de algunos de ellos con un buen grado de confianza (grado 2 de la escala propuesta por Shymanski y sus colaboradores).

SUMMARY

Nowadays, pharmaceuticals are essential to improve people's quality of life. Pharmaceuticals are widely consumed to alleviate ailments and prevent or cure diseases in humans and animals. Therefore, the purpose of the compounds gives them a biological activity and, consequently, their environmental fate causes a growing concern for the plausible effects in the ecosystems. Following administration and transport/diffusion to the site of action, they exert the desired pharmacological effect. As the organism recognizes drugs as exogenous substances, toxification is achieved either by direct excretion of the intact molecule or after one or more metabolic reactions ultimately generating biotransformation products suitable for urinary or biliary excretion. The major elimination pathway varies largely between drugs. Eventually, Excreted drug and metabolites become organic pollutants as they arrive with the wastewater stream at the wastewater treatment plant (WWTPs). Currently, WWTPs are not designed to remove these synthetic compounds and therefore many pharmaceuticals persist during the treatment process or are only marginally eliminated. As a result of this persistence and their relevant entry into the aquatic environment, wildlife is at risk to be chronically exposed to these pollutants.

Once in surface waters, the fate of drugs and their metabolites is not yet fully understood despite the fact that in the last decade many studies have measured pharmaceuticals in different ecosystems and have evaluated their effects. Many studies have concluded that for a complete evaluation, environmental transformations of drugs must be taken into account. The resulting products are so called transformation products (TPs) and can retain biological activity from the parent compound. Sometimes, TPs can be more toxic than the parent compound.

In the development of this thesis, the main transformations of drugs in the aquatic environment have been studied, including biotic and abiotic processes. These studies have been performed using liquid chromatography coupled to high resolution mass spectrometry (LC-HRMS).

In the Chapter 1 different approaches by LC-HRMS in environmental samples have been reviewed. In the literature, comparisons between low and high resolution instrumentation have been reported. The new generation of high resolution mass spectrometers have overcome the traditional limitations of this technique for quantitative analysis, offering similar linearities and sensitivities of the low resolution instruments. Furthermore, multi-residue methods through LC-HRMS, increasing the number of target compounds, does not impair sensitivity. Obviously, the great benefits offered by this technique for the structural elucidation of compounds also makes it suitable for these purposes and has been demonstrated in the different studies performed by the identification of TPs. In addition, new strategies have been developed using hybrid HRMS instrumentation, taking advantage of the high resolution offered by these instruments, the corresponding mass accuracy and the selective or non-selective acquisition of fragment ions in a single injection. These methods allowed the targeted analysis of known compounds, the scanning of suspect compounds from databases and even the untarget analysis of unknown compounds. Many of these capabilities have been used to detect and identify the TPs of the different processes studied in this thesis.

In chapter 3, the photodegradiation or photolysis of drugs, considered the main mechanism of abiotic environmental transformation, have been evaluated. In fact, this may be the most important degradation mechanism in ecosystems with a large impact of sunlight. In chapter 3 the phototransformation reactions of phosphodiesterase V inhibitors have been studied through laboratory-scale simulations. For this reason we have evaluated the photolysis of the most commonly used active pharmaceutical ingredient, sildenafil (SDF). Nowadays, this drug is frequently falsified through the adulteration of natural products by SDF analogues. The comparison of degradation pathways provided more information about the transformations produced in its structures by light effects. Through these studies, common fragmentation pattern and the major TPs were identified. Finally, to contrast these transformations in real samples, environmental samples have been analyzed to detect the identified TPs. This study reported the first detection of two TPs of SDF and/or its analogues in the environment.

In the ecosystems where the effect of light is less important, biodegradation by microorganisms is more relevant than photodegradation. To study these processes, Chapter 3 also shows a study of biodegradation of sulfonamides and the identification of main TPs at laboratory scale. This time the identification of TPs was used to make a quantitative study of the mechanisms of bacterial resistance to sulphonamides. The results show that at high concentrations the role of sulphonamide degradation is more important, while at low concentrations the adaptation of bacteria through the propagation of antibiotic resistant genes is more relevant. The identified TPs show different routes to those observed by the abiotic processes, demonstrating that in the waters we find a cocktail of compounds whose effects are difficult to predict.

In the literature pharmaceutical residues have also been detected in the exposed biota. In chapter 4, the exposure of different aquatic organisms and their different metabolism was evaluated. Metabolism transformed drugs, through biochemical reactions, in different TPs, generally known as metabolites. For this reason, laboratory-scale studies have been performed to determine the major metabolites of IBU in plant and fish. First, the metabolites of Ibuprofen and carbamazepine, two drugs commonly detected in surface waters, have been identified by intraperitoneal injection of sole. Comparison of control samples and treated samples allowed us to detect the new peaks corresponding to generated metabolites. Fragmentation patterns allowed the tentative identification of phase I and phase II metabolites. With this approach, 13 metabolites of ibuprofen and 11 metabolites of carbamazepine have been tentatively identified in bile of treated fish.

Subsequently, the metabolites of ibuprofen in aquatic plants (Lemna gibba) have been identified by means of new simulation at laboratory scale. In this study, 11 metabolites of ibuprofen have been identified. These studies have demonstrated the variability of different aquatic organisms for the biotransformation of IBU and this makes its evaluation even more complex, since one compound can be almost harmless for several species and very toxic for anothers.

Finally, taking advantage of all the knowledge acquired in the development of this thesis and the maximum capacities of LC-HRMS, the metabolism of drugs in wild samples has been studied. For this purpose, sampling campaing was design along the Llobregat river to collect fish samples. Muscle and bile samples were analyzed by Q-TOF system. Initially, target screeninf of more than 2000 organic pollutants was carried out. This database has been previously generated by Athens University by direct injection of patterns using the same adquisition method. This approach allowed us to detect lot of contaminants, including more than 12 pharmaceutical products out of the 150 contained in this list.

Six of these drugs have been selected for their environmental relevant, either because of their high detection or that they have only been detected at a specific point of sampling. These compounds have been Ibuprofen, gemfibrozil, pregabalin, sertraline and mepivacaine. Then, a database of more than 150 metabolites corresponding to the transformations of these six drugs, through a metabolite prediction software and the knowledge acquired in the simulations at laboratory scale, has been generated. With this database suspect screening approach has been carried out for the detection of a large number of metabolite candidates. Through the study of fragmentation patterns, fragment prediction software and spectral libraries, the structures of some of them have been proposed with a good confidence level (level 2 of the scale proposed by Shymanski et al.).

CAPÍTOL 1.

INTRODUCCIÓ

CAPITOL 1. INTRODUCCIÓ

1.1 Vies d'entrada i presència dels fàrmacs al medi aquàtic

Els fàrmacs són un grup de substàncies químiques que tenen propietats medicinals i són utilitzades per prevenir, diagnosticar, mitigar o curar malalties tant en els éssers humans com en els animals. Així que en primer lloc, és important remarcar que els productes farmacèutics són indispensables pel manteniment de la salut pública i la qualitat de vida de la societat actual i és per aquest motiu que anualment es consumeixen una gran quantitat de fàrmacs arreu del món. El 2015, la indústria farmacèutiva va generar aproximadament un bilió d'ingressos $ US- a tot el món. Els majors mercats es localitzen a Amèrica del Nord, on només als EEUU es consumeixen el 55% dels fàrmacs produïts al món, i a Europa, que en consumeix el 24% del global. A Europa s'estima un consum per habitant variable d'entre 50-150g/persona/any. Malgrat la seva gran utilitat, la seva inherent activitat biològica ha provocat una creixent preocupació pel seu destí ambiental i els seus efectes sobre la fauna i la flora exposada contínuament a diferents concentracions d'un gran nombre d'aquests compostos [1]. Tot i això, fins al 2005 el procés d'autorització per la comercialització de fàrmacs no incloïa cap avaluació de l'impacte ambiental. Actualment estan subjectes a alguns marcs normatius per la producció i comercialització de productes químics a Europa que comencen a incloure una avaluació de la possible persistència, bioacumulació i toxicitat. Malgrat tot, no existeixen regulacions o controls estrictes sobre els efectes farmacèutics al medi ambient, i per tant han comportat multitud d'investigacions científiques i projectes d'investigació centrats en determinar la seva presencia i les possibles conseqüències sobre els diferents ecosistemes .

L'aparició de compostos farmacèutics al medi aquàtic és ubiqua [2-5]. Es considera que la ruta principal d'introducció d'aquests compostos al medi aquàtic és a través de les aigües residuals municipals. Molts productes farmacèutics que s'utilitzen tant per humans com per animals no són metabolitzats completament i per tant s'excreten, tant les seves formes natives com els conjugats, a traves de l'orina i la femta als diferents sistemes d'aigües residuals [6, 7]. Com a resultat, diverses classes de fàrmacs i els seus

possibles metabòlits arriben a les plantes de tractament d'aigües residuals municipals (EDARs). A les EDARs aquests fàrmacs i metabòlits són sotmesos a diferents tractaments primaris, secundaris i fins i tot terciaris. Durant aquests tractaments alguns d'aquests compostos poden ser eliminats però alguns d'ells es mantenen inalterats o produeixen productes de transformació (TPs) que en alguns casos poden ser més perillosos que el propi compost. També és conegut que alguns metabòlits, durant aquests tractaments, poden retornar al fàrmac precursor. Finalment doncs, els fàrmacs, els seus metabòlits i alguns TPS poden ser alliberats a través dels efluents a les aigües superficials, aigües subterrànies, aigües costaneres, i fins i tot en ocasions, poden arribar fins a l'aigua potable [8, 9].

És per aquest motiu que els efluents de les EDARs es consideren el punt més important com a font d'exposició aquàtica i d'entrada en ambients tant d'aigua dolça com marina pels contaminants orgànics polars si no són eficientment eliminats durant el procés de tractament de les aigües residuals [10, 11].

Per agreujar encara més la creixent contaminació, les aigües pluvials i d'escorrentia agrícola constitueixen una aportació addicional de contaminants orgànics, ja que aquestes aigües reben un tractament inadequat o cap mena de tractament abans d'entrar als diferents cursos d'aigua .Tanmateix, hi ha algunes altres vies directes d'entrada que inclourien les aigües residuals de petites comunitats sense sistema de depuració, el vessament d'aigua residual de corrals d'engreix d'animals, les aigües residuals rurals, els hospitals [12] i les aigües residuals industrials, l'aqüicultura incontrolada i/o il·legal, que també poden ser una font significativa d'aquests contaminants al medi aquàtic [13, 14].

Les diferents classes de fàrmacs que es detecten en l'entorn aquàtic inclouen evidentment les diferents famílies del mercat i es relacionen directament amb el seu consum. Així, habitualment es detecten antiinflamatoris, analgèsics, reguladors de lípids en sang, antidepressius, antiepilèptics i antimicrobians [13, 15-17]. La figura 1 mostra els nivells detectats per les diferents tipologies de fàrmacs en aigua superficial del riu Llobregat durant un estudi realitzat al nostre grup l'any 2011 [18].

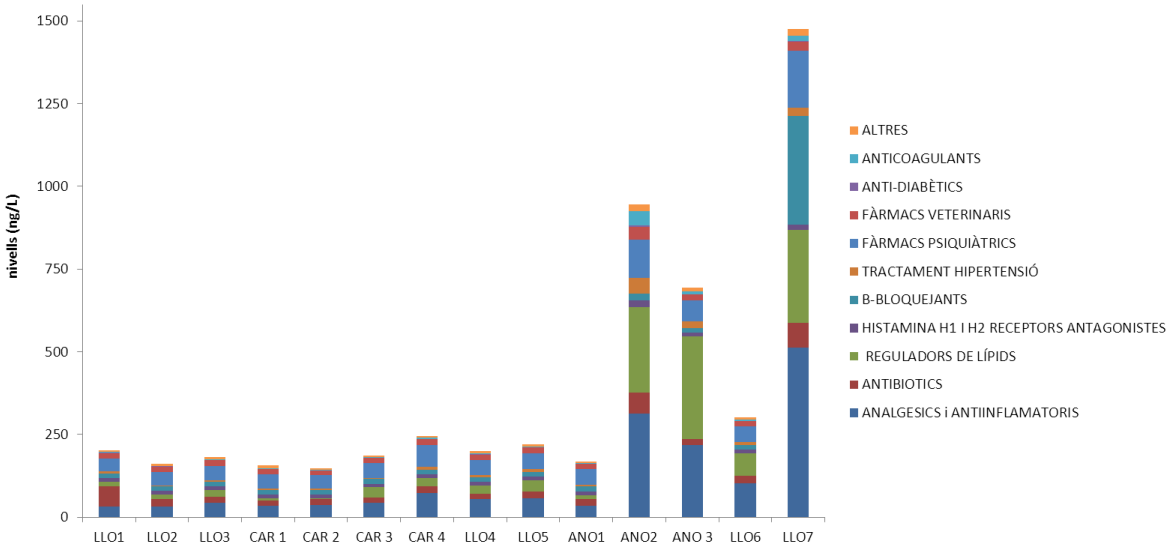

Figura 1. *Concentracions de fàrmacs al riu Llobregat l'any 2011 [18].*

1.2 Transformacions dels fàrmacs als rius

Un cop els fàrmacs han arribat als rius, la seva concentració també pot disminuir de forma natural o artificial, sent aquesta segona la forma planificada per l'home per a la reutilització de l'aigua superficial com aigua potable. Les concentracions de fàrmacs al riu es poden atenuar de manera natural per diferents processos com els biològics, els físics i els químics. Hi ha processos físics de dispersió i dilució els quals no alteren químicament els fàrmacs però si les seves concentracions que poden ser d'un ordre de magnitud inferiors a les concentracions dels efluents de les depuradores. Aquests processos de dilució es produeixen principalment en zones amb grans rius, els quals en rebre aigües residuals contaminades amb fàrmacs poden diluir la seva concentració. Un clar exemple n'és un estudi realitzat al riu Ebre, que és el que més aigua porta de l'estat espanyol, així com als seus efluents pertinents. En aquest estudi es van detectar concentracions totals de fàrmacs màximes de 333 ng/Ll al pròpi riu i de 890 ng/L als efluents [19] demostrant que l'efecte de la dilució sòl ser menor als efluents que als rius cabalosos. Un altre procés d'atenuació natural és la volatilització, però encara que pot ser un procés important en l'eliminació de compostos orgànics d'un riu, per als fàrmacs és un procés molt poc important ja que aquests compostos presenten baixa pressió de vapor, habitualment una polaritat alta i pesos moleculars més alts que les molècules volàtils. Malgrat que en el particulat de l'aire es podrien detectar fàrmacs,

aquestes concentracions són molt baixes i degudes a processos de resuspensió de partícules que es troben als sòls i al riu. No obstant això, en un altre estudi realitzat al particulat de l'aire, han detectat drogues d'abús a concentracions altes ja que pot haver-hi resuspensió d'aquestes substàncies també en el seu ús [20]. En aquest estudi, s'han determinat concentracions diàries de cocaïna de 204 a 480 pg/m3, de tetrahidrocannabinol de 27 a 44 pg/m3, de amfetamina d'1.4 a 2.3 pg/m3 i d'heroïna de 9 a 143 pg/m3 [20].

A més d'existir partícules sòlides a l'aire, al riu també hi ha dos tipus de material sòlid, el material particulat en suspensió i els sediments, on podrien tenir lloc processos d'adsorció dels fàrmacs. Els sòlids en suspensió transporten els fàrmacs pel riu, mentre els sediments són fonts de contaminació més estàtiques. Recentment, en un treball científic, s'han detectat 31 fàrmacs al particulat del riu Ebre sent les classes de compostos més detectats els antiinflamatoris i els analgèsics seguits dels B-antagonistes i els antibiòtics [19].Com a exemple, en aquest estudi es van detectar concentracions màximes d'acetaminofén en particulat de 657 ng/L, 442 ng/L d'ibuprofè i 95 ng/L de l'antibiòtic claritromicina. En canvi, en els sediments les concentracions van ser més baixes pels fàrmacs, com al cas de l'acetaminofén que va presentar concentracions màximes de 222 ng / L, o l'ibuprofè (concentracions màximes de 20.9 ng / L) o la claritromicina de 3.75 ng / L [19]. En aquest estudi també es va calcular la distribució dels fàrmacs entre la fase aquosa i el particulat de l'aigua, observant-se que el 30% dels 43 fàrmacs mesurats eren a la fase particulada. En aquest cas els compostos amb característiques bàsiques (Pka> 7) com la famotidina, timolol i nadolol van presentar major tendència a unir-se a la fase particulada [19].

Pel que fa a l'eliminació mitjançant la transformació dels fàrmacs als rius, tal i com s'ha comentat anteriorment, cal considerar dos processos importants: la fotòlisi i la biodegradació. La fotòlisi és la descomposició d'una substància per l'efecte de la llum. Per avaluar aquests processos en un riu, generalment es fan primer simulacions a nivell laboratori i després es realitzen estudis en el medi ambient. Un clar exemple és l'estudi de l'avaluació de la fotòlisi de l'antiviral oseltamivir i el seu metabòlit humà principal realitzat en mostres d'aigua del riu Ebre [21]. Per a això primer es va avaluar la fotodegradació dels dos

compostos en diferents matrius aquoses i a més es va avaluar com es transformaven en l'aigua superficial real per l'efecte de la llum solar. En aquest experiment es van identificar diversos productes de transformació, i finalment dos d'aquests van ser detectats en mostres d'aigües superficials del riu Ebre, confirmant així que la fotòlisi és un dels processos més importants d'atenuació natural per a aquest tipus de fàrmacs als rius [21]. L'altre procés important per a l'atenuació natural dels fàrmacs als rius és la biodegradació, i aquesta inclou també processos catabòlics de microorganismes, algues, llevats i fongs els quals poden descompondre parcialment o completament els compostos orgànics. Fins a l'actualitat, no existeixen estudis de biodegradació al riu Ebre, però si s'han realitzat estudis d'avaluació de la biodegradació de fàrmacs en altres països com els Estats Units [22]. En aquest estudi, es va poder observar la disminució dels nivells del fàrmac quiral metroprolol al llarg del riu i es va poder atribuir a la biodegradació (considerant la fotodegradació com a procés menys important) ja que es va observar canvi en la fracció enantiomèrica. La taula 1 resumeix les principals publicacions amb estudis de biodegradació al medi ambient.

Com s'ha pogut constatar, els últims anys s'han realitzat moltes comunicacions científiques que han informat de la presència de fàrmacs i els seus TPs en els diferents medis aquàtics, principalment en efluents d'aigües residuals i en rius però també podrien acumular-se en la biota.

TAULA 1. Resum dels principals estudis de biodegradació ambiental, TPs identificats i principals reaccions de transformació.

Compost pare	Proces de biodegradació (número de TPs identificats)	Reaccions	Instrumentació/ Esquema d'identificació	Detecció al medi ambient	Referències
3 ICM (Iohexol, Imeprol, Iopamidol)	Biodegradation (soil/water system) (27)	Transformations at the side chains containing either, carboxylic moieties and/or primary and secondary amide moieties, the triiodoisophthalic acid structure remained unaltered	Qq-LIT-MS (4000 Q Trap, AbSciex) Fragmentation pattern, MS^n NMR	Yes, several TP were detected	[23]
4 ICM (Iohexol, Imeprol, Iopamidol, Diatrizoate)	Biodegradation (soil/water system) (27+7)	New TPs: oxidation, cleavage of the N-C bond and decarboxylation	Qq-LIT-MS (4000 Q Trap, AbSciex) Fragmentation pattern, MS^n NMR	Yes, several TP were detected	[24]
Metformin	Biodegradation (Closed Bottle OECD301D and Zahn-Wellens OECD302B, Manometric Respiratory test (OEDC 301 F) (1)	Amidine hydrolysis to guanylurea	LC-LIT-MS (Bruker Daltonic Esquire3000) Fragmentation pattern, MS^n	Yes	[25]

Compost pare	Proces de biodegradació (número de TPs identificats)	Reaccions	Instrumentació/ Esquema d'identificació	Detecció al medi ambient	Referències
Sulfametoxazol	Anoxic water/sediment test under denitrification (2)	Nitration, deamination and reversible reactions	LC-MS/MS (Varian) Fragmentation pattern of the standards	N/A	[26]
Verapamil	Biodegradation (Closed Bottle OECD301D and Zahn-Wellens OECD302B (3)	O- and N-demethylation	LC-LIT-MS (Bruker Daltonic Esquire3000) Fragmentation pattern, MS^n	N/A	[27]

1.3 Exposició i metabolisme de fàrmacs en biota

Els fàrmacs poden ser dispersats a través del medi ambient, des de la seva font de producció i primers consumidors, fins als diferents cossos d'aigua. La seva persistència a les EDARs i la pertinent entrada continua al medi pot produir una exposició crònica d'organismes als contaminants, els quals podrien resultar afectats de diferents formes [28-33]. A més, els fàrmacs també poden ser bioacumulats en diferents nivells tròfics que afecten a molts tipus de biota. Així, els residus de productes farmacèutics als ecosistemes aquàtics preocupen tant pels possibles efectes en els organismes exposats com en la salut general de l'ecosistema.

Els fàrmacs estan dissenyats específicament per a les interaccions metabòliques principalment en els éssers humans. Els seus possibles efectes adversos en la vida salvatge exposada de forma indirecta són en molts casos desconeguts. Les activitats biològiques inherents d'aquests contaminants suggereixen que poden ser biològicament actius també en aquesta vida silvestre. En particular, se sap que els antibiòtics poden produir resistència antimicrobiana i causar problemes en els ecosistemes aquàtics que hi són exposats contínuament. Fora de l'entorn aquàtic, el 2004, Oaks i col. , va correlacionar els residus del fàrmac antiinflamatori diclofenac amb fallades renals que van causar una disminució de la població de voltors al Pakistan [34].

Naturalment, la biota aquàtica està exposada a productes farmacèutics de dues maneres, directament i a través de la cadena alimentària, i diversos autors han estudiat els possibles efectes del diclofenac als peixos. Aquests estudis van mostrar canvis histològics en el fetge, ronyó, i brànquies i efectes en diferents processos biològics a concentracions similars a les aigües superficials [35]. El 2010, Corcoran i col. [36] va examinar els efectes sobre els peixos dels productes farmacèutics més comunament detectats en el medi aquàtic. Aquesta revisió va mostrar diversos exemples de diferents efectes dels productes farmacèutics, com ara alteracions endocrines i el seu afecte en la reproducció i creixement. D'altra banda, alguns efectes poden ser subestimats a causa de la complexitat de reproduir els efectes crònics i mixtos de diferents fàrmacs en els experiments a escala de laboratori. A més, la manca d'estudis

ambientals relevants requereix més investigació sobre els seus efectes potencials sobre peixos però també en altres organismes. A part de productes farmacèutics, de fet, les noves tendències inclouen també els seus possibles TPs.

Ja el 1997, Nagtegaal i col. [37] va determinar per primera vegada en peixos salvatges la presencia d'una família de contaminants orgànics relacionats amb la cura personal, els filtres UV. El 2012, Gago i col. van estudiar la determinació dels filtres UV orgànics en la biota aquàtica [38]. En general, van observar que a la literatura, els compostos més lipofílics es detecten habitualment en concentracions que van fins als 7112 ng/$g_{lípids}$ en els musclos i fins a 3100 ng/$g_{lípids}$ en el peix. Les majors concentracions determinades en peixos corresponen als compostos 4-methylbenzilidenecamphor i octocrilè. Pel que fa als productes farmacèutics, Brooks i col. [39] va informar de la primera determinació de fàrmacs en peixos salvatges el 2005. En aquest estudi, es van analitzar peixos d'un riu amb aportació d'efluents d'EDARs i es van detectar antidepressius com la fluoxetina i la sertralina en els teixits del fetge, el cervell i filet lateral a nivells que van de 0,1 a 15 ng/g. Ja al 2007, Ramírez i col., va desenvolupar un mètode pel cribratge de 23 productes farmacèutics i dos metabòlits en diferents teixits permetent la detecció de difenhidramina, diltiazem, carbamazepina i norfluoxetina en 11 de les 11 mostres de peixos [40]. Dos anys després, els resultats d'un estudi pilot a nivell nacional als Estats Units van mostrar la presència dels mateixos compostos i també de gemfibrozil en peixos de rius amb l'aportació d'efluents d'EDARs [41]. En aquesta ocasió es van detectar altes concentracions de setralina, 19 ng/g al filet lateral del peix i 545 ng/g al fetge. En el mateix estudi, es van analitzar diversos compostos utilitzats per la cura personal i van revelar l'aparició de galaxolide i tonalide en concentracions màximes de 2100 i 290 ng/g respectivament.

Tornant a Europa, concretament a alemanya, Bikram Subedi i col. [42] va ser el primer en reportar l'aparició de fàrmacs en teixits de peixos, als quals van detectar difenhidramina i desmetilsertralina. A més, els autors van comparar els resultats obtinguts en l'estudi amb els anteriorment esmentats dels Estats Units. En aquest cas, les concentracions de galaxolida i tonalida del 2008 van disminuir respecte les de 1995 i aquestes van ser 19 i 28 vegades,

respectivament, més baixes que als Estats Units. Ja al nostre estat, el 2012, Huerta i col. [43] va reportar la presència de productes farmacèutics a la biota aquàtica i les seves possibles implicacions mediambientals. Recentment, més publicacions han reportat la presència d'altres productes farmacèutics com ara diclofenac, naproxè o ibuprofè en diferents teixits de peix de riu de diferents països a nivells de concentració que van d'1 a 10 ng/g [25-29].

Com es pot constatar, en els estudis publicats s'analitzen òrgans diferents del peix. Cal tenir en compte que, a més de la variabilitat entre especies, les diferents característiques dels teixits poden comportar també una diferent acumulació dels fàrmacs. El 2015, Tanoue i col. [44] va estudiar l'absorció i distribució dels fàrmacs en els diferents teixits de peixos salvatges que viuen en rierols amb impacte d'aigües residuals tractades. En aquest estudi es pretenia posar en relleu la importància de la distribució en els diferents teixits i per això els autors van comparar els seus factors de bioacumulació en els diferents òrgans. A més, també van comparar els factors de bioacumulació mesurats en plasma amb els valors pronosticats i com a conseqüència van observar que les concentracions màximes mesurades de fàrmacs antiinflamatoris eren fins a 17 vegades més altes que els valors teòrics. Mentrestant, Liu i col. [45] també va investigar l'exposició dels peixos a l'antibiòtic roxitromicina i la seva acumulació als diferents teixits. Els resultats d'aquest estudi van mostrar majors concentracions de roxitromicina al fetge, seguit per la bilis, les bränquies i els teixits musculars. En aquest cas, la concentració a la bilis pot ser probablement subestimada pel fet que el fàrmac es metabolitzés.

Aquests resultats emfatitzen doncs la importància de la distribució en els teixits per a l'avaluació dels riscos. Però malgrat que en alguns estudis com aquests s'ha reportat l'acumulació dels productes farmacèutics en els diferents òrgans dels peixos, actualment encara se sap molt poc sobre la seva disposició en el peix. De fet, el mateix procés inicial d'absorció de fàrmacs als peixos no es coneix amb exactitud. Es considera que els fàrmacs poden entrar al organisme principalment a través de les bränquies, però també ho poden fer a través de la pell o el sistema digestiu. A les bränquies els compostos poden ser absorbits a través de cèl·lules epitelials i després distribuïts als diferents òrgans a través del corrent sanguini. A més, és important considerar que els peixos són

coneguts per tenir sistemes de detoxificació hepàtica, cosa que els fa probablement capaços de metabolitzar els contaminants orgànics que contenen les aigües contaminades. El fetge és considerat l'òrgan principal pel metabolisme dels compostos xenobiòtics i els seus metabòlits són excretats a la femta o a l'orina a través de la bilis. Aquests metabòlits es divideixen en dos grups; metabòlits de fase I i de fase II. En les reaccions de fase I generalment s'introdueixen grups reactius (com per exemple –OH o NH2) i en les reaccions de fase II aquests grups reaccionen amb diversos conjugats, com poden ser glucurònics, taurina o glutations. Malgrat la metabolització es considera un procés de detoxificació, en alguns casos el metabòlit pot ser el causant dels efectes adversos. Segons Mehinto i col., aquest podria ser el cas del acil glucurònic del diclofenac, el qual causa alteracions fisiològiques a la truita de riu després d'una exposició prolongada [46]. El metabolisme en cada cas dependrà del tipus d'organisme i probablement de les condicions ambientals.

És per aquest motiu que diversos estudis proposen l'anàlisi de la bilis de peix per a una ràpida avaluació de l'exposició a residus farmacèutics. De fet s'ha observat que les concentracions de fàrmacs o els seus metabòlits en els peixos podrien ser aproximadament 1000 vegades més gran que la concentració que es troba en les aigües circumdants on viuen i per tant la detecció dels productes farmacèutics a la bilis pot resultar menys complexa [47].

En aquest sentit, Brozinski i col. va estudiar la captació i el metabolisme dels diferents productes farmacèutics mitjançant l'exposició de la truita arc de Sant Martí a diferents concentracions de fàrmacs en aigua o mitjançant la dosificació intraperitoneal [47-49]. En aquests estudis, els autors van informar de la identificació dels diferents metabòlits PPCPs en la bilis i els seus factors de bioconcentració a la bilis (BCF_{bilis}). Pel diclofenac, naproxè i ibuprofè, els BCF_{bilis} en peixos eren d'entre 320 a 950 exposats a 1,8 mg/L, de 900 a 1800 també exposats a 1,8 mg/L i de 14.000 a 49.000 exposats a diferents nivells de concentració. A més, els autors van determinar la presència de diclofenac, naproxè i ibuprofè a la bilis dels peixos silvestres per tal d'avaluar i verificar el fet que les concentracions de productes farmacèutics o els seus metabòlits en la bilis del peix podrien ser molt més altes que les concentracions trobades a

les aigües superficials en les quals viuen. En aquests estudis a més s'han pogut identificar els principals metabòlits del naproxè, ibuprofè i diclofenac.

La taula 2 resumeix les principals publicacions d'estudis d'identificació de metabòlits en peixos.

TAULA 2. Metabòlits dels fàrmacs identificats als peixos

Compost pare	Proces de biodegradació (número de TPs identificats)	Reaccions	Instrumentació/ Esquema d'identificació	Referències
cisaprida, chlorpromazina, verapamil,i dextrometorfan	Larves de peix zebra (23 Met identificats)	Oxidació, N-dealquilació, O-de-etilació, sulfatació i glucuronització	LC(1100 agilent)-MS/MS (PE Sciex)	[50]
Diclofenac	Bilis (truita arc de sant martí) (11 Met)	Glucuronització, hidroxilació, sulfatació and glucuronització dels metabòlits hidroxilats	Qq-ToF-MS (micrOTOF-Q, Bruker Daltonics) IT (Agilent 1100 Series LC/MSD Trap) Patró de fragmentació, MSn, masa exacte	[51]
Diclofenac, Ibuprofè, naproxè	Bilis, plasma (truita arc de sant martí) (16 Met)	Glucuronització, hidroxilació, sulfatació and glucuronització dels metabòlits hidroxilats, desmetil.lació	Triple quadrupol MS (Quattro MicroTM Waters)	[52]
Ibuprofé	Plasma (2 Met)	Hidroxilació	LC-LTQ (Thermo)	[53]
Ibuprofè	Larves de peix zebra (1Met identificat i un altre sense identificar)	Hidroxilació	Finnigan ,LTQ-orbitrap (Thermo Electron Corporation, Hertfordshire, UK) Patró de fragmentació	[54]

Compost pare	Proces de biodegradació (número de TPs identificats)	Reaccions	Instrumentació/ Esquema d'identificació	Referències
Ibuprofè	Bilis (truita arc de sant martí) (13 Met)	Glucuronització, hidroxilació, sulfatació and glucuronització dels metabòlits hidroxilats, conjugats amb taurina i glucuronització del metabòlits amb taurina	Qq-ToF-MS (micrOTOF-Q, Bruker Daltonics) IT (Agilent 1100 Series LC/MSD Trap) Patró de fragmentació, MSn, masa exacte	[49]
Difenidramina	Cervell, fetge, bränquies, muscul (2 met)	Desmetil.lació, 2 cops desmetil.lació	(UPLC; Agilent, Waldbronn, Germany) i QqQ-MS (Agilent 6460 triple cuadrupol-MS) Detecció per ions fragment	[55]
Carbamezapina	Cervell, fetge, bränquies, muscul,intestí (2 Met)	Hidroxilació, epoxidació	UPLC-QTRAP-MS (5500 QTRAP Sciex) patrons purs	[56]
Àcid clofibric	Embrions (17 Met)	Conjugació amb sulfat, àcid glucurònic, carnitina, taurina o àcid aminometasulfònic, ciclacions	Synapt G2S LC-QToF-MS (waters)	[57]

La majoria d'aquests treballs suggereixen que els peixos que viuen aigües avall de les EDARs poden acumular els residus dels fàrmacs, els seus metabòlits, o tots dos, sobretot després d'una exposició prolongada o crònica. Però a més, no només els peixos d'aigua dolça poden estar exposats als productes farmacèutics. A causa de la disminució de les poblacions de peixos salvatges i l'increment del consum de peix i marisc, l'aqüicultura és a l'alça. La cria de peixos marins en estuaris és cada vegada més comú i aquestes aigües podrien veures afectades també pels efluents d'EDARs.

A la literatura, actualment es disposa de poques dades sobre la detecció de productes farmacèutics en aigües marines. Només uns pocs estudis han informat de la presència de productes farmacèutics com ara diclofenac, ibuprofè o carbamazepina en diferents estuaris [58-61]. La detecció de productes farmacèutics als estuaris ha fet créixer la preocupació pels possibles efectes adversos sobre les espècies que hi viuen i l'entrada a la nostra cadena tròfica. Malgrat això, avui en dia encara hi ha molts pocs estudis que reportin la presència dels productes farmacèutics per consum humà en especies marines. Kwon i col. [62] va ser el primer en informar de la detecció de fàrmacs en espècies marines salvatges, concretament va reportar la detecció de diazepam en peixos marins recollits a prop d'abocaments d'aigües residuals municipals al mar [62]. Més recentment, Álvarez-Muñoz i col. va informar de la presència de productes farmacèutics i compostos disruptors endocrins en macro-algues, bivalves i peixos de les zones costaneres i va proposar una llista de compostos candidats per a l'establiment de prioritats en altres estudis [63].

A més a més, tant els peixos criats en piscifactories marines com al riu podrien estar exposats deliberadament a antibiòtics mitjançant ingredients del pinso. Per exemple, medicaments d'ús veterinari, com ara les sulfonamides i tetraciclines, són àmpliament utilitzats en l'aqüicultura per tractar infeccions en peixos, i també poden ser acumulats en l'organisme de peix. Fa alguns anys, els antibiòtics es van utilitzar també de forma massiva en la cria de peixos, ja que en milloren el creixement quan s'afegeix a l'alimentació. En l'actualitat, aquesta pràctica ha estat prohibida per la Unió Europea (UE) des de 2006 [64].

La detecció de residus d'antibiòtics en animals comestibles va causar una gran preocupació tant als organismes reguladors com als consumidors. No obstant això, l'aparició d'aquests fàrmacs en teixits de peixos s'associa a efectes no desitjats en els consumidors com ara possibles al·lèrgies, però la ingestió incontrolada d'antibiòtics pot causar el desenvolupament de resistències bacterianes. Aquest últim efecte ha causat més preocupació en el camp dels animals productors d'aliments. En conseqüència, s'han establert diverses legislacions que controlen els usos d'antibiòtics en peix i han establert els límits màxims dels seus residus en diferents productes d'origen animal [65]. Per tal de garantir la seguretat del peix, aquest aliment es pot consumir després d'un temps d'espera que correspon al temps post-tractament en el qual el peix es considera lliure de drogues. Aquests períodes pot oscil·lar entre 3 i 42 dies, depenent de l'antibiòtic, l'espècie i la temperatura de l'aigua [66].

Com s'ha pogut constatar la majoria dels estudis s'han centrat en l'acumulació dels productes farmacèutics en el peix però en altres organismes com plantes, algues o invertebrats aquàtics ha estat molt menys investigat. Tot i això, a la literatura hi ha alguns estudis que reporten la presència de fàrmacs a les gambes i musclos [67-69] però el seu metabolisme en els diferents organismes encara és més desconegut. La detecció de fàrmacs en els diferents organismes ha comportat una conseqüent preocupació pel seus efectes en la cadena tròfica. Vernouillet et al. van determinar els factors de biomagnificació de fàrmacs i productes de cura personal en els diferents nivells tròfics de la cadena alimentària exposats a aigua fortificada amb productes farmacèutics [70]. En aquest estudi, la carbamazepina es va transferir al llarg de la cadena tròfica aquàtica composta per alga verda, crustacis, i els pòlips d'aigua dolça. Resumint, es van obtenir factors de bioacumulació de 2.2 i 12.6 a les algues i en els crustacis, però no es va observar cap bioacumulació significativa en els pòlips d'aigua dolça.

A la majoria d'estudis centrats en la determinació de fàrmacs en diferents matrius ambientals, els anàlisi s'han realitzat principalment per cromatografia líquida acoblada a l'espectrometria de masses (LC-MS). Recentment i a causa de les recents millores en l'anàlisi instrumental, l'espectrometria de masses d'alta resolució (HRMS) acoblada a LC s'ha convertit en l'eina imprescindible

vàlida tant per a l'anàlisi qualitatiu com quantitatiu de les diferents mostres ambientals.

1.4 Anàlisi de fàrmacs, els seus productes de transformació i els seus metabòlits amb espectrometria de masses al medi aquàtic i a la biota

L'impacte de les activitats humanes sobre el medi ambient i l'entrada associada de productes farmacèutics que s'han tractat anteriorment han pogut ser documentats al llarg dels anys gràcies a les capacitats de la instrumentació ofertes principalment per l'espectrometria de masses.

L'espectrometria de masses és un mètode instrumental per a la identificació de la constitució química d'una substància per mitjà de la separació dels ions gasosos d'acord amb la seva diferent relació entre massa i càrrega (m/z). La resolució de massa es defineix com la diferència de massa mínima (m2 - m1) entre dos pics de l'espectre de masses i mesura la capacitat de distingir dos pics de diferent ràtio massa/càrrega [71]. La història de l'espectrometria de masses va lligada a la evolució i l'increment de la seva resolució. El primer exemple de l'aplicació de l'espectrometria de masses el va dur a terme Joseph John Thomson l'any 1913, quan va ser capaç de separar els isòtops de neó per la seva massa (Figura 2). Al segle XX es van assolir molts desenvolupaments nous (Figura 2), com per exemple l'augment de la resolució de l'espectròmetre de masses de 130 a 80.000. Una altre fita important assolida al segle XX va ser la capacitat per acoblar un sistema de separació, com la cromatografia de gasos (GC), amb un espectròmetre de masses (GC-MS) en la dècada de 1950. Els instruments comercials GC-MS però no varen estar disponibles fins a la dècada de 1970. No obstant això, l'anàlisi mitjançant GC-MS va resultar útil sobretot pels compostos volàtils però mancava una nova tècnica adequada per a l'anàlisi de traces de compostos polars. Per aquell temps, la incompatibilitat relativa de les fonts de ionització existents amb un flux continu de cromatografia líquida, va retardar l'acoblament d'aquestes tècniques. Ja a la meitat del segle XX s'havien desenvolupat diverses interfícies per l'acoblament de la cromatografia líquida amb un espectròmetre de masses (LC-MS) però no eren gaire fiables, i per tant, el seu èxit en el mercat era molt limitat. No obstant això,

la situació va canviar amb el desenvolupament de tècniques d'ionització a pressió atmosfèrica (API) que van permetre finalment l'acoblament LC-MS. La font d'ionització per electrospray (ESI), que actualment és la interfície més àmpliament utilitzada, va ser desenvolupada per Fenn a la dècada de 1980 [72, 73]. Les diferents companyies van desenvolupar ràpidament instruments equipats amb fonts ESI ja que proporcionava una interfície simple i robusta, permetent que LC/ESI-MS esdevingués una tècnica de rutina en la determinació d'analits polars. Malgrat aquest avenç, cal destacar que com a principal inconvenient, l'ESI és la interfície més sensibles a possibles efectes de la matriu. Avui en dia, els instruments de LC-MS es basen gairebé exclusivament en interfícies API com és l'ESI, la ionització química a pressió atmosfèrica (APCI), i la ionització per fotoionització a pressió atmosfèrica (APPI), desenvolupada més recentment per a la detecció de compostos orgànics en pràcticament qualsevol tipus de mostra (extracte) que es pugui analitzar mitjançant una columna de LC. Les dues últimes interfícies són capaces fins i tot d'ionitzar els compostos de baixa o mitjana polaritat i per tant són considerades complementàries a l'ESI.

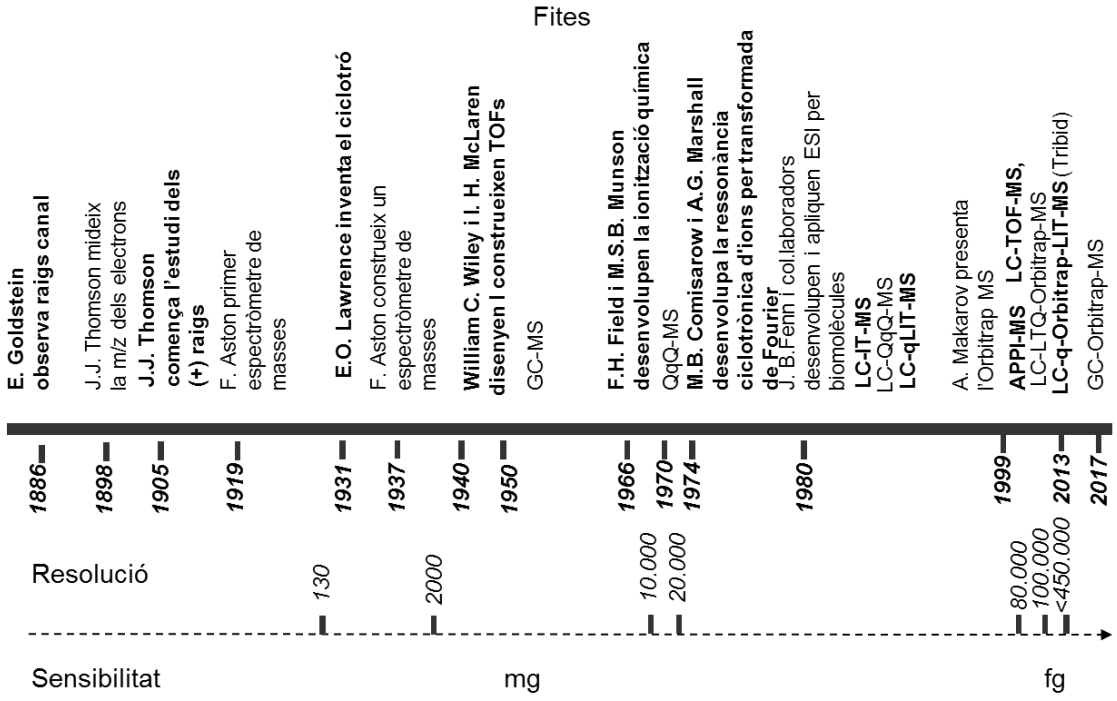

Figura 2. *Història de la espectrometria de masses*

En les dues últimes dècades, diferents analitzadors de baixa resolució (LR) s'han acoblat a LC, però, només alguns d'ells ofereixen la sensibilitat i la selectivitat requerida per a la quantificació fiable de petits compostos polars en diferents tipus de mostres. La LC acoblada amb un espectròmetre de quadrupol individual (Q) ofereix una bona sensibilitat, però quan s'investiguen matrius molt complexes, com les aigües residuals, la selectivitat és insuficient i sovint perjudica la identificació inequívoca dels diferents analits. La MS en tàndem (MS/MS), desenvolupada el 1970 [74], ofereix un rendiment superior en termes de sensibilitat i selectivitat en comparació amb els instruments d'un simple quadrupol i la capacitat d'aïllar, en una primera etapa, l'ió molecular del compost d'interès.

La LC-MS/MS s'aconsegueix mitjançant els instruments de triple quadrupol (QqQ) o als espectròmetre de quadrupol amb trampa lineal d'ions (QqLIT). A causa de la seva elevada sensibilitat i selectivitat, els analitzadors de QqQ esdevenen l'eina principal per a l'anàlisi de traces en tot tipus de matrius. I de fet, passen a ser els espectròmetres de masses més utilitzats als laboratoris per a la quantificació d'un gran nombre de compostos orgànics. Aquests instruments ofereixen aquesta gran sensibilitat i selectivitat mitjançant adquisicions en mode de monitorització selectiva d'ions (SRM), que consisteix en monitoritzar transicions del compost precursor al ió fragment. A la literatura s'han reportat centenars de determinacions de nombroses classes de contaminants emergents utilitzant instruments de QqQ [75-79]. No obstant això, una de les limitacions principals del mode de SRM és la incapacitat per detectar o avaluar els compostos no inclosos inicialment a la llista de transicions, encara que la seva abundància a la mostra sigui molt alta. A més, el requisit d'almenys dues transicions SRM per compost restringeix el nombre d'analits en una sola injecció, degut a que l'increment de temps que se'n deriva en compromet la sensibilitat. Un problema afegit és el fet que alguns compostos de baix pes molecular només proporcionen una transició amb suficient intensitat de senyal per a la detecció sensible i altres components de la matriu poden tenir les mateixes transicions que l'analit d'interès.

Molts d'aquest inconvenients es poden evitar mitjançant l'ús de espectròmetres de masses d'alta resolució (HR). Durant l'última dècada, aquesta tècnica ha sofert una gran transformació ja que l'accés als instruments HR és cada vegada més assequible. Les tres plataformes principals que ara s'utilitzen en els estudis basats en HRMS són el quadrupol amb temps de vol (QTOF)-MS, l'Orbitrap-MS, i de ressonància ciclotrònica d'ions per transformada de Fourier (FT-ICR)-MS. Si bé la tecnologia QTOF s'ha implementat en múltiples aplicacions, sobretot en els seus inicis patia de baixa transmissió d'ions (cosa que afectava a la sensibilitat) i tenia un rang dinàmic limitat [80, 81]. D'altra banda, la majoria de QToFs ofereixen una resolució de 30,000- 40,000 en amplada total a mitja alçada (FWHM), que és molt més baix que les altres dues tecnologies d'alta resolució, i per tant pot no resultar ideal per a la detecció i caracterització d'analits en experiments en què una resolució més gran és essencial. D'altra banda, FT-ICR-MS ens ofereix la resolució més alta de totes les tecnologies actuals (poder de resolució de 1.000.000), i fàcilment s'ha implementat en la caracterització de la matèria orgànica i l'anàlisi de petroli [82-85] No obstant això, aquest analitzador no és tan àmpliament utilitzat a causa del seu elevat cost i complicat funcionament [86]. Finalment, la tecnologia Orbitrap es va introduir fa poc més d'una dècada i ha guanyat ràpidament impuls en els camps del medi ambient i dels anàlisis clínics i forenses, amb múltiples estudis reportats fins a la data [87-94]. Per un cost molt més baix que un instrument FT-ICR-MS, el Orbitrap ofereix una gran sensibilitat (fg per pg), un bon rang dinàmic (> 5.000), exactitud de massa (<2 ppm), i alta resolució [80]. Des de la seva introducció al mercat, els avenços en el disseny instrumental de l'Orbitrap han permès augmentar significativament aquesta resolució. Del LTQ Orbitrap inicial que oferia una resolució de 100.000 FWHM fins al últim membre de la família Orbitrap, l'espectròmetre de masses Orbitrap Fusion Tribrid, que pot arribar fins a una resolució de 500.000 [95].

Gràcies a l'aplicació de HR-MS s'han pogut resoldre multitud de falsos positius i falsos negatius. El problema de la detecció esbiaixada o parcial a través de l'ús de mètodes amb adquisició completa d'ions que permet la detecció de qualsevol espècie ionitzable que surti de la columna de la LC. Alhora, aquests mètodes poden complementar-se amb diferents modes d'adquisició MS/MS.

Els instruments HRMS són capaços d'analitzar simultàniament un nombre virtualment il·limitat de compostos de baixa i alta abundància tant per a la caracterització i identificació dels desconeguts, com per a la detecció i quantificació dels coneguts. Tot això amb una necessitat mínima d'optimització dels mètodes en comparació amb els instruments de baixa resolució [80, 96-99]. Aquestes capacitats dels instruments HR estan relacionades amb poder discriminar en un espectre de masses ions de massa/càrrega molt similars i per tant amb la mesura de la massa exacta dels ions [100, 101]. Tot això, ha provocat que la HRMS hagi cobrat força en el camp de l'anàlisi ambiental. En aquest camp s'han desenvolupat noves estratègies per l'anàlisi dirigit, l'anàlisi de sospitosos, la identificació de TPs i/o metabòlits i l'anàlisi no dirigit. A la literatura s'han reportat aplicacions d'aquestes estratègies demostrant el potencial que a fet tant atractiva aquesta tècnica [99, 102-105]. Per a classificar aquestes diferents aplicacions s'han classificat en dos grups en funció del seu objectiu; l'anàlisi quantitatiu i l'anàlisi qualitatiu.

1.4.1 Anàlisi quantitatiu

L'anàlisi quantitatiu es refereix a la determinació de la concentració de compostos coneguts i en general es realitza utilitzant un conjunt de patrons de referència més els seus anàlegs marcats amb el fi de quantificar els primers. A la literatura hi ha reportats un gran nombre de mètodes que utilitzen aquest enfocament per a una àmplia varietat de compostos [81, 106-109]. Tradicionalment pels mètodes quantitatius s'ha utilitzat la LRMS i els espectròmetres més utilitzats han estat els de QqQ o els de QqLIT. Se sap que els mètodes basats en LRMS requereixen l'optimització dels paràmetres en tàndem MS/MS per a cada analit i per tant s'han de tenir en compte qüestions com la formació d'adductes i les transicions SRM inespecífiques. Com a conseqüència d'això, l'optimització dels mètodes en mode de SRM és essencial pel desenvolupament del mètode però és una part complexa i que requereix de temps i capacitats de l'analista. D'altra banda, la baixa resolució dels QqQ no permet identificar els ions matricials que elueixen amb una finestra molt similar de m/z que l'analit diana. Per tant, una possible solució per superar aquest inconvenient ha estat treballar amb HRMS [108]. Així doncs, durant l'últim parell d'anys, després de resoldre les seves principals carències, l'HRMS s'ha

convertit en una tècnica prometedora per als mètodes quantitatius desafiant els protocols establerts basats en la LRMS. Per exemple Henry i col. [108] van desenvolupar un mètode utilitzant HRMS en mode d'escombratge complet d'ions i l'activació de la funció d'adquisició de dades independents (FIA). En aquest mode l'instrument s'alterna a una freqüència d'aproximadament 2 Hz entre una exploració convencional completa, en el qual els ions moleculars (majoritàriament intactes) generats a la font d'ionització s'envien com paquets al Orbitrap, i una fragmentació induïda per col·lisió d'alta energia (HCD), on els ions que es recullen en l'espectròmetre de masses es dirigeixen primer cap a la cel·la de col·lisió per a la fragmentació no selectiva (sense selecció de l'ió precursor) seguit d'anàlisi al detector Orbitrap. El primer escaneig produeix cromatogrames d'ions totals relativament simples (TICs) a partir dels quals les masses d'ions específics es poden extreure amb alta selectivitat mitjançant l'establiment de finestres molt estretes de masses. El segon és molt més complex ja que requereix desconvolució per identificar tots aquells ions que pertanyen al mateix ió precursor. L'aplicació d'aquest enfocament és particularment valuós per a l'anàlisi qualitatiu que de forma retrospectiva perquè en un sola injecció es recull una gran quantitat d'informació estructural dels diferents compostos. Altres configuracions dels Orbitrap-MS, com ara el LTQ-Orbitrap, han demostrat ser una eina adequada per a la quantificació de molècules petites i la identificació simultània dels seus metabòlits [109].

A la literatura hi ha un nombre creixent d'estudis que es centren en la comparació de la LRMS amb la HRMS però només uns quants d'ells ofereixen un examen més detallat de la seva selectivitat. Henry i col. [108] van comparar les capacitats de HRMS i LRMS utilitzant QqQ en tàndem per l'anàlisi quantitatiu de fàrmacs en mostres de plasma [108]. Es varen utilitzar tres instruments diferents, un Orbitrap-MS (Exactive) de HRMS i dos instruments QqQ, un TSQ Quantum Discovery i un TSQ Quantum Ultra en mode H-SRM. Els instruments es van comparar mitjançant l'avaluació de l'anàlisi de 17 fàrmacs i es van obtenir resultats similars pel que fa selectivitat, precisió, repetibilitat, linealitat i sensibilitat per als tres instruments. El 2010, Kaufmann i col. va avaluar de nou la selectivitat proporcionada per l'Orbitrap-MS (model Exactive) i un instrument LR de QqQ convencional [110]. El resultat va ser

també similar. L'Orbitrap-MS va mostrar una alta selectivitat amb una sensibilitat similar a la del QqQ, fet que suggeria la probabilitat que la HRMS es convertís en una tècnica dominant en el camp de la quantificació de contaminants orgànic polars en un futur pròxim. Kaufmann i col. també va comparar tres plataformes diferents, incloent dos instruments de HRMS com el TOF-MS i l'Orbitrap-MS i un de LRMS de QqQ [111]. Aquest estudi va concloure que els anàlisis mitjançant TOF van proporcionar rendiments analítics més pobres que els anàlisis realitzats per QqQ i Orbitrap-MS, però cal esmentar que l'instrument TOF utilitzat no era d'última generació; ja que estava equipat amb detector de temps a digital (TDC) i no amb el detector més nou d'analògic a digital (ADC). En les generacions més recents de ToF-MS s'han millorat les seves capacitats, especialment en termes de rang dinàmic (mitjançant l'esmentat detector ADC o funcions de millora del rang dinàmic [112] i de la resolució (de 15.000-40.000 FWHM), solventant d'aquesta manera les seves deficiències en sensibilitat i precisió. Avui en dia s'han desenvolupat amb èxit diversos mètodes quantitatius d'acord amb els diferents paràmetres de qualitat [113, 114]. Per exemple diversos autors han comparat els QqQ enfront dels sistemes TOF-MS i/o QTOF HRMS per a la determinació de plaguicides en fruites i verdures [115, 116]. Aquests estudis han confirmat que la LR mitjançant MS/MS encara és més sensible i robust, però que mitjançant QTOF-MS s'obté un bon rendiment, una confirmació més fiable i informació addicional de les mostres. No obstant això, els models més recents de sistemes QqQ són encara més sensibles que els instruments HRMS, particularment quan s'analitza un nombre petit de compostos, i per tant un baix nombre de transicions SRM. A mesura que el nombre d'analits diana dins d'una sola injecció augmenta, s'aconsegueix un punt d'inflexió en el qual el l'adquisició de dades no selectiva en mode d'escombrat complet dels HRMS excedeix la sensibilitat de la detecció mitjançant LRMS.

Així doncs, com s'ha comentat anteriorment, l'anàlisi per HRMS resol en gran mesura el problema d'interferències de compostos provinents de la matriu i per tant resulta de gran ajuda per desemmascarar falsos positius obtinguts per MS/MS. A continuació s'esmenten alguns exemples dels beneficis de l'anàlisi per HRMS, que implica matrius complexes i la capacitat de separació de les

interferències isobàriques dels senyals dels contaminants d'interès. Un és el cas de benzofenona, en el qual Gallart-Ayala et al. va demostrar que una resolució de 50.000 FWHM permetia distingir benzofenona d'un compost d'interferència [117]. Ferrer et al. també va utilitzar aquestes capacitats en un QTOF-MS, que treballava a 30.000 FWHM, per desenvolupar un mètode quantitatiu per a 100 medicaments i els seus productes de degradació entre els quals hi havia un nombre de compostos isobàrics [118]. Per si encara és necessari més selectivitat, actualment també s'han implementat instruments com el tripleTOF, capaços de treballar en SRM en alta resolució.

Un benefici addicional que també es descriu en moltes publicacions és la possibilitat de realitzar anàlisi quantitativa i qualitativa de forma simultània. Aquest avantatge permet el desenvolupament de mètodes per a la quantificació dels analits d'interès i la detecció simultània de compostos sospitosos o desconeguts. Així doncs, aquesta poderosa eina s'utilitza actualment per l'anàlisi ambiental [80, 104, 119] i de suplements alimentaris [120], proporcionant tant informació sobre la concentració de compostos coneguts usant corbes de calibratge de patrons autèntics, com també la presència d'altres compostos.

En resum, la HRMS ofereix diversos avantatges: la possibilitat d'emmagatzemar grans volums de dades i d'informació mitjançant l'exploració d'escombratge complet i l'obtenció dependent o independent de dades de MS/MS amb masses d'alta precisió que permeten un anàlisi retrospectiu, sense oblidar la facilitat de configuració dels mètodes. La robustesa de qualsevol enfocament d'anàlisi complet HR depèn en gran mesura de l'estabilitat de l'exactitud de massa, la precisió i el poder de resolució com un mitjà per distingir entre masses d'ions molt similars. Això fa que avui dia, molts laboratoris estan ja considerant la possibilitat de substituir els mètodes basats en QqQ per l'ús de l'última generació de HRMS.

1.4.2 Anàlisi qualitatiu

Com hem vist, l'anàlisi quantitatiu es pot realitzar tant als instruments HRMS com als LRMS, però això només cobreix la determinació d'una petita fracció de contaminants orgànics coneguts. Per contra, l'ús d'instruments HRMS cobreix un ampli rang de compostos amb anàlisi qualitatiu, i és de gran utilitat per a la caracterització de compostos desconeguts, la identificació i la confirmació de contaminants de baixa i alta abundància i els seus possibles productes de transformació [104, 121, 122]. Així doncs, sense cap mena de dubte, l'HRMS és la instrumentació analítica més utilitzada per a l'anàlisi mediambiental qualitatiu i avui en dia noves s'estan desenvolupant aproximacions aprofitant tot el seu potencial.

Tornant a la visió tradicional de la LC-HRMS, aquesta tècnica, s'ha utilitzat, la majoria de les vegades, com una eina poderosa per a la identificació de TPs o metabòlits de diferents contaminants generats en estudis a escala de laboratori sota condicions controlades. Aquest enfocament consisteix en una comparació entre les mostres control i les mostres tractades. L'alineació i comparació dels cromatogrames totals d'ions de les mostres tractades i de control permeten detectar la formació de nous pics procedents de la transformació dels compostos d'assaig. Generalment, s'accepten errors de precisió en la massa de fins a 5 ppm sense importar l'analitzador de masses utilitzat (ToF o Orbitrap). Aquestes mesures precises de massa i les dades complementàries, com el perfil isotòpic dels ions moleculars, la comparació dels patrons de fragmentació dels productes originals i els temps de retenció relatiu són finalment les que permeten dilucidar de forma temptativa l'estructura del compost. Finalment, els compostos identificats poden ser confirmats mitjançant patrons de referència i s'inclouen en els protocols per a la vigilància del medi ambient.

En general, els TP formats en experiments de laboratori s'identifiquen temptativament seguint l'esquema de treball que es mostra a la Figura 3. Un cop es detecta el TP candidat, la combinació de mesures de massa exactes del compost pare i els dels espectres MS/MS són el més important pel procés d'identificació dels TPs, tant en els sistemes QTOF com als Orbitrap-MS. Malgrat això, sempre és bo posar atenció sobre la forma de generar els TPs

per a facilitar-ne la seva detecció i la seva conseqüent identificació. A més, per certes estructures és possible predir les possibles reaccions de transformació que tenen lloc, gràcies a la literatura o mitjançant la comparació amb altres compostos/processos similars. Com exemple, Jelic et al. va detectar quatre TPs de carbamazepina en mostres de degradades per Trametes versicolor dels quals tres d'ells havien estat predits a un altre procés [123]. Un altre enfocament seria també la detecció d'ions específics com en l'exemple de Calça et al. on espectres de MS^2 i MS^3 van mostrar diversos ions que van permetre la caracterització dels diferents productes de transformació (TP) i distingir fins i tot les espècies isobàriques. La millora de les tècniques de separació també són molt importants. En els últims anys, els nous desenvolupaments permeten millors resultats cromatogràfics o com s'ha vist, millor resolució de massa. En el cas de Zonja et al. , la HRMS i les millores en la retenció cromatogràfica van jugar un paper molt important en la detecció de TPs de zanamivir.

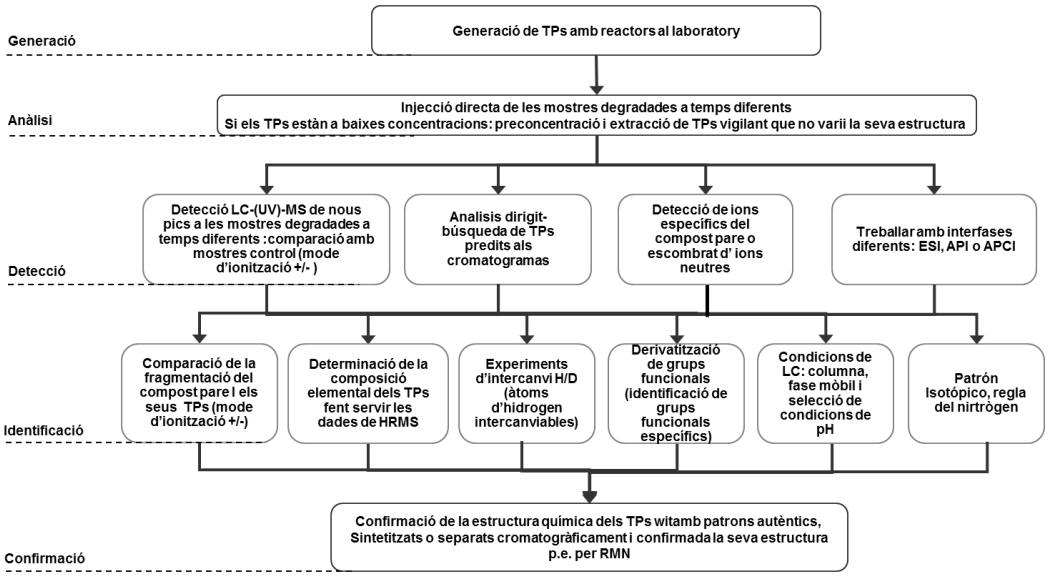

Figura 3. *Esquema de la generació e identificació dels TPs a mostres ambientals*

Al marge de l'elucidació estructural de compostos, pel que fa a l'anàlisi qualitatiu de mostres ambientals, en l'actualitat s'han proposat dos estratègies conceptualment diferents [80]: la detecció de sospitosos i l'anàlisi no dirigit de compostos desconeguts (Figura 3). Tots dos mètodes s'utilitzen generalment de forma complementària permetent la detecció de contaminants sospitosos i la identificació dels desconeguts. Hernández i col. [101] a més també va proposar

el terme anàlisi post-dirigit, quan la recerca d'un contaminant sospitós es realitza després de l'adquisició i sense informació prèvia. Així doncs, les tècniques no dirigides inclouen l'anàlisi de compostos sospitosos i desconeguts utilitzant una combinació d'escombratge complet i experiments MS/MS. Recentment, també hem pogut trobar a la literatura, la utilització de patrons de referència per a crear bases de dades, però sense objectius quantitatius. Aquests anàlisi s'anomena escombratge dirigit i pretén només detectar compostos coneguts inclosos en una llarga llista, normalment amb un objectiu de priorització i/o vigilància.

De les diferents estratègies, la que està guanyant molta popularitat és l'anomenada detecció de sospitosos. Aquesta no requereix utilitzar patrons de referència, com a l'escombratge dirigit, ni és tant complexa com l'anàlisi no dirigit de compostos desconeguts. Per realitzar aquesta tècnica són necessàries bases de dades que es fan servir per detectar també la presència d'analits coneguts mitjançant l'exactitud de massa, la predicció del temps de retenció, la determinació del perfil isotòpic i finalment la confirmació de l'estructura utilitzant informació MS/MS [80, 103, 104, 124]. El fet de no treballar amb patrons de referència implica, evidentment, que no es pugui determinar la concentració a la mostra. Per a l'anàlisi de sospitosos en la seva forma més simple, les composicions elementals dels contaminants amb estructures químiques conegudes s'utilitzen per a calcular les seves masses exactes. Aquests valors es converteixen després en les proporcions m/z exactes dels seus ions moleculars (protonat o desprotonat depenent del mode d'ionització) i de ions relacionats procedents de la formació d'adductes. Un clar exemple són els adductes de sodi en el mode d'ionització positiva o adductes de formiat en la negativa. La base de dades dels valors de m/z generats per aquest procés es poden utilitzar per produir cromatogrames d'ions extrets (XIC) dels cromatogrames d'ions totals corresponents a les dades de rastreig complet. Depenent de l'exactitud de massa i la precisió de l'instrument utilitzat, s'apliquen finestres estretes d'extracció de massa amb un interval típic que va de 5 a 20 ppm. L'observació de pics cromatogràfics als XICs és llavors un indicador de la possible presència del compost sospitós a la mostra. Sovint, aquestes bases de dades cobreixen un gran nombre de contaminants i es

poden ampliar mitjançant la inclusió de metabòlits coneguts (per exemple, de medicaments humans), productes de transformació coneguts (per exemple, els productes de degradació fotoquímica de pesticides), i productes de transformació encara no descrits a la literatura científica, però potencialment formats durant el cicle de vida dels compostos d'origen (per exemple, la formació de derivats de clor en la desinfecció d'aigües residuals). Un cop s'ha detectat una coincidència potencial d'un pic en el seu corresponent XIC amb una entrada de la base de dades, es recull més informació específica del compost per donar suport a la identitat proposada. Això inclou l'anàlisi de l'abundància relativa, la separació dels isòtops més pesats i, en particular, l'examen dels espectres MS/MS amb la detecció d'ions de fragments característics que poden ser o bé obtinguts per estàndards autèntics, en biblioteques d'espectres o predits utilitzant mètodes computacionals. Com evidència addicional per a la detecció d'un analit sospitós, el temps de retenció relatiu es pot utilitzar com a criteri.

A més, les tècniques de detecció de sospitosos s'han aplicat també per a la identificació dels possibles productes de transformació d'analits d'interès en mostres ambientals. Per això, s'utilitzen eines d'identificació de metabòlits en combinació amb models d'elucidació estructural i la confirmació mitjançant la massa exacte dels espectres MS/MS [125, 126]. La possibilitat de trobar falsos positius disminueix quan es disposa de més paràmetres específics de cada compostos. Schymanski et al. proposa un criteri de cinc nivells de confiança en la identificació dels compostos [127]. En aquesta classificació per a la identificació total de la identitat d'un compost s'ha d'utilitzar patrons de referència. En l'estudi de productes de transformació, en molts casos l'obtenció de patrons de referència per a la seva confirmació no és possible i per tant és essencial una identificació precisa. Ja que en l'actualitat l'elucidació estructural dels TPs encara és complexa, Zonja i els seus col·laboradors proposen enfocar els esforços només en l'elucidació dels TPs més rellevants, Amb això, la llista completa dels TPs formats, per exemple en un experiment a escala de laboratori, es pot reduir a uns TPs clau de rellevància mediambiental [128]. Recentment, Bletsou i col. [125] ha revisat l'estat de la LC-HRMS per a la identificació dels TPs al medi ambient aquàtic i de nou, torna a incidir en la

necessitat de implementar aquest pas de prioritització abans d'iniciar el procés d'identificació de compostos que ens consumeixi molt de temps.

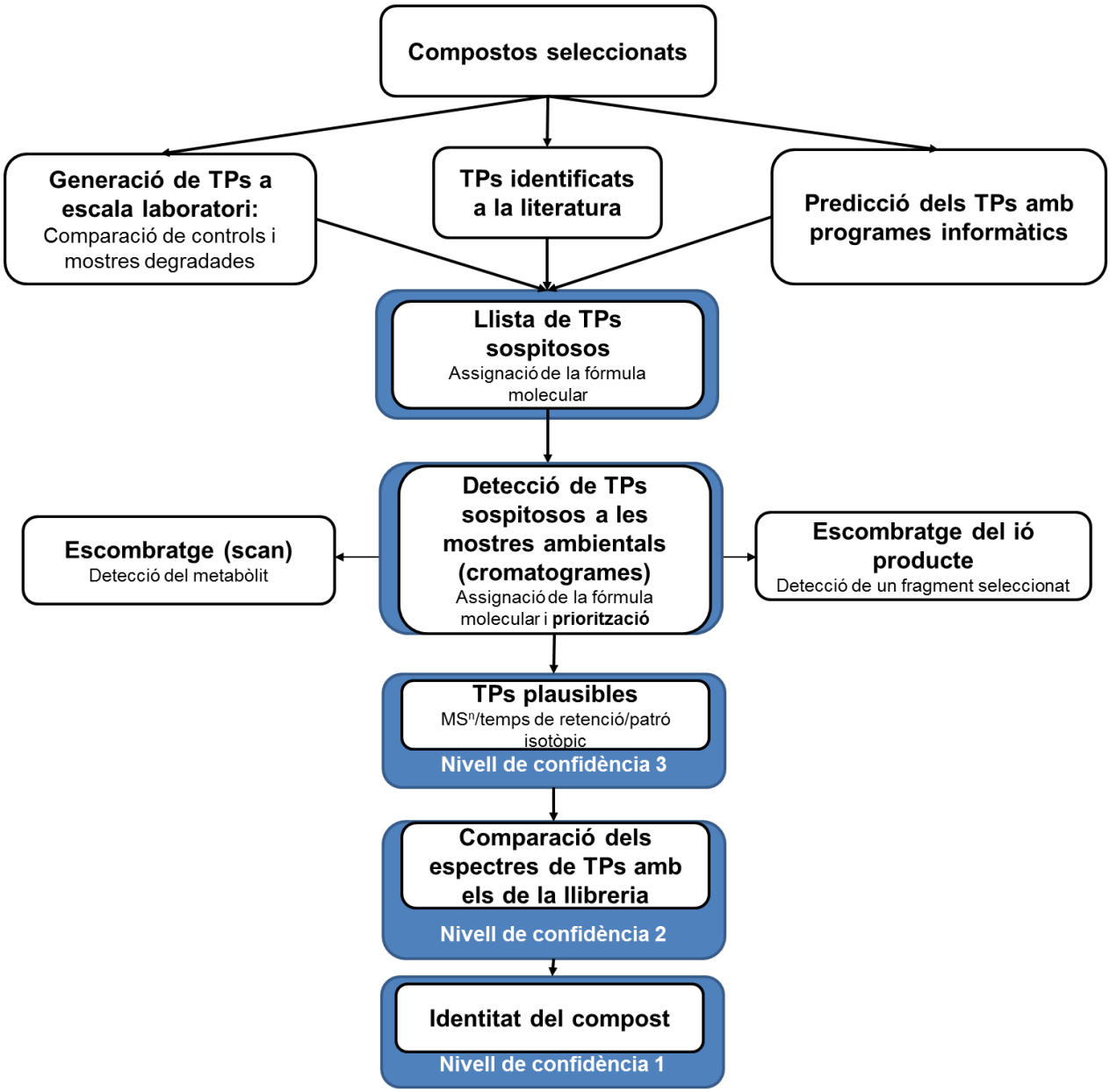

Figura 4. *Detecció de TPs a mostres reals aplicant anàlisi de sospitosos*

La Figura 4 resumeix els plantejaments proposats que s'han utilitzat recentment per a la detecció i identificació dels TPs amb HR-MS en mostres ambientals, incloent aquesta etapa de prioritització. A més, les innovacions en programari per a la predicció de vies de transformació és clau per a la detecció de compostos candidats al escombrat de conjunt de dades, i per a la seva elucidació estructural. A tall d'exemple, per a la predicció de productes de biotransformació de contaminants emergents, Jeon i col. [129] va utilitzar una

combinació d'eines disponibles a Internet, com el sistema de predicció de la Universitat de Minnesota (UM-PPS) i el Meteor Environmental Pathway Prediction System (Lhasa Limited, Regne Unit), o programaris comercials com MetWorks o Sieve per a la detecció dels candidats, Xcalibur per a l'anàlisi de dades, el Mass Frontier (HighChem, Ltd, Bratislava, Eslovàquia) i el MetFrag per a la predicció de les rutes de fragmentació MS/MS i fins i tot el MOLGEN per a la generació de l'estructura molecular. En aquest estudi, els autors prediuen 360 possibles metabòlits però només 23 van ser detectats i identificats. D'aquests, 19 eren metabòlits oxidatius dels quals set metabòlits van ser predits per UM-PPS i 12 van ser identificats com a nous metabòlits. En conseqüència, la combinació de diferents programaris i eines és necessària per l'èxit en la detecció i identificació d'un nombre relatiu dels metabòlits. Malgrat aquests avenços, encara hi ha molt marge de millora en el desenvolupament de programaris més sofisticats que facilitin aquesta tasca.

Un enfocament encara més difícil és l'ús de tècniques de cribratge de sospitosos per a la caracterització dels metabòlits o productes de transformació en les mostres dels estudis de degradació mitjançant HR-MS i programari específic per revelar canvis en la composició elemental de les substàncies d'assaig provocat per la degradació bioquímica o els processos físics [83, 121, 122].

Per exemple, Zonja i col. [128] va utilitzar un enfocament basat en LC-QExactive-Orbitrap-MS per a la detecció i identificació dels productes de transformació de sis agents de contrast iodats, de rellevància ambiental (ICM), que s'utilitzen en medicina per millorar la visibilitat de les estructures vasculars i òrgans durant els procediments de radiografia. Els autors combinen la generació de productes de transformació en un simulador de llum solar (experiments a escala de laboratori) amb la detecció de sospitosos en mostres d'aigua superficial real [128]. L'enfocament va consistir en comparar el control i les mostres tractades seguit de la creació d'una llista de possibles productes de transformació detectats en aquestes mostres (Figura 4). El programari SIEVE es va utilitzar per a l'alineació cromatogràfica dels pics i va permetre la detecció de 108 fotoproductes en les mostres irradiades. La novetat d'aquest estudi és que enlloc de procedir amb l'elucidació estructural de tots els fotoproductes, es

va afegir un nou pas al flux de treball utilitzant la priorització per la detecció d'aquests sospitosos en les mostres reals [128]. Així doncs, es va crear una base de dades amb les masses precises determinades experimentalment, els temps de retenció i les dades de MS / MS per als 108 productes de transformació i aquests van ser cercats als extractes de l'aigua superficial real. Evidentment, es van haver de fixar criteris com els errors de precisió en massa de fins a 5 ppm per a la confirmació [128]. Aquest enfocament va permetre donar prioritat a 11 productes de transformació detectats ja que aquests van ser considerats de rellevància ambiental per la seva alta freqüència de detecció en les mostres reals. La seva elucidació estructural es va realitzar per comparació dels patrons de fragmentació característics amb les dels compostos parentals respectius. Finalment, per tal de quantificar els productes de transformació en les mostres d'aigua superficial, es van obtenir estàndards de referència dels productes de transformació per LC semipreparativa de les mostres irradiades al laboratori. La mitjana de la concentració dels compostos originals va variar de 29 ng/L a 6 g/L (Iomeprol), mentre que els productes de transformació van ser trobats en una mitjana de concentració de 30 ng/L, amb concentracions màximes de fins a 0,4 g/L d'un producte de transformació del Iomeprol [57].

Per tal de predir les estructures dels possibles productes de transformació amb eines computacionals, Kern i col. [130] aplica un enfocament diferent per a detectar productes de transformació de plaguicides i productes farmacèutics directament a les aigües naturals mitjançant LC-HRMS (LTQ Orbitrap). En primer lloc, els autors van crear una llista de contaminants coneguts en aigua superficial i van preveure els seus possibles productes de transformació amb el UM-PPS i utilitzant informació de la literatura. A continuació es va aplicar a les mostres un mètode de cribratge de sospitosos utilitzant una base de dades que contenia la massa exacta de 1794 compostos. Per filtrar els resultats positius d'aquesta llista tant llarga va ser imprescindible aplicar la comparació amb blancs de mostra, la estimació dels temps de retenció i l'anàlisi dels perfils isotòpics. Usant aquest enfocament es van identificar 19 productes de transformació, i després aquests van ser confirmats per patrons de referència.

Com és sabut, l'aigua superficial és en molts casos la principal font d'aigua utilitzada per a la producció d'aigua potable. A l'entrar als sistemes de potabilització, es realitza el tractament físic (per exemple per floculació, sedimentació o filtració), seguit de desinfecció química (per exemple la cloració, l'ozó, i / o radiació ultraviolada) per eliminar la matèria en suspensió i agents patògens [28, 131]. No obstant això, aquests tipus de tractaments poden no ser suficients per eliminar els compostos més persistents. Per exemple, el 2011 Segura i col. [132] van publicar nivells baixos (ng/L) de l'atrazina i la carbamazepina en mostres d'aigua potable de ciutats al Canadà. De la mateixa manera, la presència de la sucralosa ha estat prèviament reportada pel nostre grup, en el qual les concentracions de l'edulcorant artificial van ser tan altes com 465 ng/L en l'aigua potable [133]. Recentment s'ha publicat una revisió de les vies de transformació dels productes farmacèutics durant els processos de desinfecció en la que es detalla clarament la formació de subproductes de desinfecció (DBPs) després del tractaments amb clor, cloramines, ozó, diòxid de clor, UV o UV/H_2O_2 [131].

Com es pot observar, la detecció de sospitosos en l'àmbit del medi ambient s'aplica habitualment a mostres d'aigua però avui dia molt poques publicacions descriuen mètodes de cribratge de sospitosos per a la determinació dels productes farmacèutics a la biota. Sense cap dubte, l'alta selectivitat i sensibilitat de HRMS fan que aquesta tècnica també sigui de gran utilitat per a l'anàlisi de matrius biològiques complexes. Tradicionalment, s'han utilitzat els enfocaments de HRMS per a l'elucidació estructural dels metabòlits d'un fàrmac original i s'utilitzen amb freqüència en l'àmbit dels perfils metabòlics. En experiments de laboratori en condicions controlades, l'eliminació del fons facilita la detecció de compostos emergents i la comparació de la informació de MS/MS dels productes originals proporcionant identificacions temptatives dels productes relacionats. Per aquestes raons, les capacitats de la HRMS suggereixen que pot ser utilitzada com una poderosa eina per a la detecció i identificació d'una àmplia llista de productes farmacèutics als diferents teixits, i, en conseqüència, s'espera que la seva aplicabilitat a d'augmentar encara més ràpidament.

Com s'ha esmentat, aquesta estratègia s'aplica molt menys a la biota però a la literatura ja en podem trobar alguns exemples. Nácher-Mestre i col. [134] van utilitzar la HRMS per dur a terme un examen dirigit a certs productes farmacèutics i altres contaminants orgànics en mostres de peixos i també a la seva alimentació. Després de la detecció de diversos compostos mitjançant l'anàlisi dirigit, es va realitzar un anàlisis de sospitosos amb una llista que contenia al voltant de 1000 compostos més. Amb aquest nou enfocament es van detectar diversos compostos que no s'havien inclòs a l'anàlisi dirigit. En la mesura del possible, es van utilitzar patrons autèntics per confirmar les identitats d'aquests darrers compostos. I quan els patrons no estaven disponibles, les seves identitats van ser proposades provisionalment sobre la base de les seves dades de MS i MS/MS.

En general, els estudis basats en la detecció de sospitosos inclouen més d'una família de contaminants. En molts casos, es realitza una gran llista de contaminants orgànics conjuntament amb els productes farmacèutics. És el cas recent de Plassmann i col. [135], que va examinar mostres d'orina humana amb una llarga llista de contaminants ambientals. En aquest estudi es van poder identificar temptativament 9 compostos sospitosos i finalment quatre d'ells van ser confirmats per estàndards. D'altra banda, la detecció de sospitosos s'aplica normalment de forma conjunta amb els anàlisis no dirigits. Aquest és el cas de Solliec i col. [136], que va realitzar un cribratge mitjançant una llista de residus d'antibiòtics veterinaris sospitosos en una matriu biològica i després va ampliar aquest anàlisi amb la identificació d'altres compostos.

A més dels compostos principals, en mostres biològiques s'ha de tenir en compte la possible aparició de metabòlits dels fàrmacs. Per tal de confirmar les identitats d'aquests metabòlits, resultaria de gran valor la informació de la seva fragmentació però rarament està disponible a les biblioteques d'espectres de masses. Per aquesta raó, els programaris de predicció de fragmentació es podrien utilitzar per ajudar en l'elucidació de l'estructura i per distingir entre metabòlits isobàrics amb fórmules moleculars idèntiques, sense patrons de referència. A més, l'aplicació de la predicció dels temps de retenció facilitaria també la identificació de metabòlits ja que reduiria el nombre de falses

identificacions que d'una altra manera poden aparèixer quan s'utilitza només la massa exacta.

A més a més, els metabòlits es poden classificar en metabòlits comuns i no comuns. Els metabòlits comuns es formen mitjançant una reacció de biotransformació coneguda i es poden predir fàcilment per diferent programari. Per tant, les masses moleculars d'aquests metabòlits podrien ser inclosos en la llista de compostos sospitosos i aquests compostos poden ser detectats juntament amb els compostos parentals en la detecció de sospitosos. Per això, les diferents plataformes ofereixen diferents programaris de predicció i detecció de metabòlits de fàrmacs, tant de fase I com de fase II, en les dades de HRMS. Com exemple, Jeon i col. [129], va proposar les vies de biotransformació d'alguns productes farmacèutics i productes biocides en els crustacis d'aigua dolça a través de la predicció dels seus metabòlits i el seu anàlisi per HRMS. A més, després va determinar diferents nivell de confiança per a la identificació d'aquests metabòlits.

Els metabòlits no comuns es formen per mitjà de reaccions de biotransformació no convencional o de múltiples passos. En conseqüència, els metabòlits no comuns són difícils de predir i incloure en les llistes de sospitosos i per tant es requereixen altres enfocaments. Tradicionalment, en els estudis de perfils metabòlics, la comparació entre les mostres tractades i de control permet la determinació de nous pics i aquests metabòlits poden ser dilucidats en un enfocament no dirigit.

Una nova aproximació és per exemple utilitzar els fragments característics o un grup conjugat específic dels metabòlits per detectar metabòlits comuns i no comuns. Per buscar aquests ions fragment específics en els espectres de ions producte s'utilitza el precursor de ions o el filtrat de pèrdua neutra. L'adquisició de dades dependents també són útils per a la detecció de llistes de compostos coneguts però, és clar, les dades de MS / MS no s'adquireixin pels compostos que no són presents a la llista de sospitosos. Recentment, diversos autors han proposat l'adquisició de dades independent per detectar fragments específics. Aquest enfocament permet la detecció de compostos sospitosos i dels fragments de sospitosos a través d'una anàlisi completa i la generació dels ions

de fragmentació de tots els compostos. A més, també es poden definir finestres de massa específica per a les exploracions dels ions de fragmentació. Kinyua i col. [137] ha utilitzat recentment aquest mètode per a la detecció qualitativa d'una llista de substàncies psicoactives i els seus possibles metabòlits en mostres biològiques. Es van buscar els compostos i els seus possibles metabòlits a les dades de MS d'escombrat complet i els ions producte específics identificats per confirmar les seves estructures. A més, es van buscar alguns fragments específics a les dades d'ions producte per a detectar altres possibles metabòlits d'aquests fàrmacs. Un dels desafiaments més importància d'aquesta estratègia és la dificultat per assignar els ions producte al ió precursor. La forma dels pics pot ser de gran ajuda per a realitzar aquesta assignació i ajudar a confirmar les identitats de metabòlits no predits a partir de fragments específics. En aquest estudi, es van detectar els compostos originals, com la ketamina, 25B-25C-NBOMe i NBOMe i diversos metabòlits de fase I i fase II.

D'altra banda, la HRMS permet l'aplicació d'una altre aproximació, la tècnica del filtrat per defecte de massa (MDF). Aquesta pot permetre la detecció de metabòlits comuns i no comuns a les dades de HRMS. Aquest enfocament es basa en defectes de massa similar entre els metabòlits i el seu compost original. Avui en dia, MDF s'utilitza habitualment en estudis farmacocinètics [109], però es podria estendre a altres camps per completar la detecció i identificació de compostos relacionats. Per aquesta raó, els algoritmes de MDF s'han incorporat recentment als programaris de processament de dades de MS de les diferents companyies.

En resum, els mètodes de detecció de sospitosos avui dia s'utilitzen amb freqüència per determinar una gran quantitat de contaminants, però no s'utilitzen per a estudis de metabolisme en mostres biològiques. Aquest fet es deu probablement a causa de la falta d'estàndards analítics i biblioteques completes d'espectres MS/MS, cosa que dificulta la confirmació de la identitat del metabòlit. És probable que els avenços d'aquesta tècnica proporcionin noves aplicacions per a la detecció sospitosa en mostres biològiques, així com en altres estudis ambientals.

La comunicació científica que es troba a continuació descriu acuradament l'estat actual en quan a la utilització de la cromatografia de líquids acoblada a l'espectrometria de masses d'alta resolució per a l'anàlisi ambiental. En ella s'aprofundeix en el diferent enfoc (quantitatiu/qualitatiu) que s'ha desenvolupat en el transcurs d'aquesta tesis.

Article nº 1: Advances in liquid chromatography–high-resolution mass spectrometry for quantitative and qualitative environmental analysis

J. Aceña, S. Stampachiacchiere, S. Pérez i D. Barceló

Analytical and Bioanalytical Chemistry - 2015

Anal Bioanal Chem
DOI 10.1007/s00216-015-8852-6

REVIEW

Advances in liquid chromatography–high-resolution mass spectrometry for quantitative and qualitative environmental analysis

Jaume Aceña[1] · Serena Stampachiacchiere[2] · Sandra Pérez[1] · Damià Barceló[1,3]

Received: 9 March 2015 / Revised: 30 May 2015 / Accepted: 12 June 2015

Abstract This review summarizes the advances in environmental analysis by liquid chromatography–high-resolution mass spectrometry (LC–HRMS) during the last decade and discusses different aspects of their application. LC–HRMS has become a powerful tool for simultaneous quantitative and qualitative analysis of organic pollutants, enabling their quantitation and the search for metabolites and transformation products or the detection of unknown compounds. LC–HRMS provides more information than low-resolution (LR) MS for each sample because it can accurately determine the mass of the molecular ion and its fragment ions if it can be used for MS–MS. Another advantage is that the data can be processed using either target analysis, suspect screening, retrospective analysis, or non-target screening. With the growing popularity and acceptance of HRMS analysis, current guidelines for compound confirmation need to be revised for quantitative and qualitative purposes. Furthermore, new commercial software and user-built libraries are required to mine data in an efficient and comprehensive way. The scope of this critical review is not to provide a comprehensive overview of the many studies performed with LC–HRMS in the field of environmental analysis, but to reveal its advantages and limitations using different workflows.

Keywords High-resolution mass spectrometry · Liquid chromatography · Transformation products

Published in the topical collection *High-Resolution Mass Spectrometry in Food and Environmental Analysis* with guest editor Aldo Laganà.

✉ Sandra Pérez
spsqam@idaea.csic.es

[1] Water and Soil Quality Research Group, IDAEA-CSIC, c/Jordi Girona 18-26, 08034 Barcelona, Spain

[2] Department of Chemistry, Sapienza Università di Roma, Piazzale Aldo Moro 5, 00185 Rome, Italy

[3] Catalan Institute of Water Research - ICRA, C/Emili Grahit, 101, Edifici H2O, Parc Científic i Tecnològic de la Universitat de Girona, 17003 Girona, Spain

Introduction

The challenges that can be encountered when analyzing polar organic pollutants in environmental samples are diverse. One of the challenges is that there are a plethora of organic contaminants of environmental concern with different physicochemical properties. The number of organic pollutants reported in the literature is increasing annually, with new pollutants, the so-called "contaminants of emerging concern", which are frequently present at low concentrations in the environment, making the analysis of environmental samples evermore challenging. This is mainly caused by the necessity of including large numbers of contaminants in a single analysis because this reduces analysis times. Liquid chromatography coupled to mass spectrometry (LC–MS) is a sophisticated hyphenation of analytical techniques which enables the determination of organic pollutants in complex environmental matrices because of its selectivity and sensitivity. Since the 1990s, when LC coupled to triple-quadrupole mass spectrometry (QqQ-MS) started to be marketed, operating in multiple-reaction-monitoring (MRM) mode, this technique has been the first choice for quantitative analysis because of its high sensitivity and selectivity against a complex matrix background. However, high-resolution mass spectrometry (HRMS) has in recent years become more accessible to research laboratories with the development of Orbitrap-MS-based instruments and the improvements to time-of-flight (TOF) MS systems. Several publications describing the new generation of HRMS systems

Published online: 03 July 2015

[1] and revealing differences between low-resolution (LR) MS and high-resolution capabilities [2,3] testify to the growing importance of HRMS. It should be kept in mind that HRMS analyzers can also be coupled with gas chromatography, but it has been revealed that LC enables analysis of a broader range of contaminants with very different polarities and chemical properties. The use of HRMS enables rapid, selective, and robust analysis in both qualitative and quantitative applications. The ease of setup and the possibility of storing a high volume of full-scan and MS–MS data of high mass accuracy enables retrospective analysis without the need to re-run samples. In addition, the data can be processed using target analysis, suspect screening, and non-target screening (Fig. 1). The reliability of these approaches relies on the main features of the mass analyzer, including mass accuracy, precision, and resolving power; the combination of these characteristics is crucial for correctly measuring ion masses in the presence of interfering matrix components occurring in complex environmental samples. In addition, the creation of compound spectra libraries in conjunction with software packages makes the data analysis and interpretation easier. This opens up the possibility of different specialized types of analysis including screening of suspects, target and non-target analysis, and structural elucidation of novel metabolites and transformation products (TPs).

Several studies have been performed in recent years using LC–HRMS for environmental analysis of different classes of pollutants, and some reviews have been published which discuss these works [4–7]. For these reasons, in this paper we focus on the most recent published articles on environmental analysis using LC–HRMS for qualitative and quantitative purposes. Particular attention has been dedicated to recent aspects related to the use of HRMS for quantitative analysis in comparison to low-resolution analyzers, and to the latest trends in detection and structural identification of contaminants and their related metabolites and TPs, a field where HRMS is surely the standard technique.

Quantitative analysis by LC–HRMS

The sensitive detection and reliable quantitation of a large number of contaminants at low concentrations in environmental studies has been always one of the most important challenges. The use of LC–LRMS in MRM mode requires as a first step the definition of the target analytes to be monitored, and then standards have to be acquired to optimize compound-specific MS conditions including fragment-ion masses, ion-source voltages, and collision energies. In addition the LC gradient has to be adjusted such that all compounds can be accommodated in a large number of retention-time windows. Breaking up the chromatographic time into several experiments is essential to minimize the number of MRM transitions, because this has a direct effect on the sensitivity. Although with modern QqQ-MS analyzers the inter-channel dead time is reduced to a few milliseconds, the increasing number of compounds and therefore of MRM transitions always comes with a loss of sensitivity. When optimizing MRM conditions, several data points per peak always have to be critically considered. Instead of detecting compounds by one or more compound-specific transitions, no pre-selection of precursor ions is necessary when working in scan mode with HRMS because a high selectivity can be achieved in full-scan mode, and thus an unlimited number of analytes can be detected. This means that a theoretically unlimited numbers of analytes can be searched for without compromising sensitivity, because the acquisitions have been made as "all ions all the time". This is useful for both target and so-called post-target analysis where the presence of additional contaminants can be also evaluated by retrospective analysis of the data. Then, if there are positive findings, further quantification can be performed, reducing the cost and time of analysis.

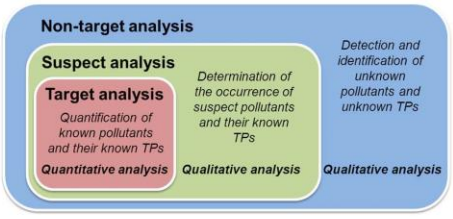

Fig. 1 From target to non-target analysis

Unlike QqQ-LRMS, where selectivity is achieved by selecting one or more suitable MRM transitions, HRMS including (Q)TOFMS and Orbitrap MS usually relies only on the detection of the ions (isotope cluster and isotope spacing can be used as additional criteria for confirmation). Therefore, it is essential that the instrument is operated at a high resolving power such that potentially interfering peaks are resolved. If this is not achieved, mass accuracy is compromised, and when using a mass extraction window of a few ppm (or mDa) the interfering compound is included in this window, resulting in increased signal of the targeted ion and eventually an overestimation of its concentration. This has been emphasized in recent publications that compare selectivity provided by HRMS instruments and QqQ-LRMS [3,8]. In these works the objective of the authors was to identify the HRMS resolution necessary to achieve the same selectivity as the LRMS detector. Using the HRMS Orbitrap Exactive, they concluded that resolution above 50,000 (full width at half maximum, FWHM, at m/z200) afforded selectivity higher than that provided by current unit-resolving QqQ-MS instruments in MRM mode. A relatively novel MS technique is the ABSciex instrument Triple TOFMS, which is designed to offer MRM^{HR} mode for quantitative analysis which measures the

accurate mass of the product ions of a selected precursor ion. Furthermore, the Triple TOFMS in MRM^{HR} aids compound identification with highest confidence via comparison of theoretical and measured mass accuracy and isotopic pattern. Equal or even slightly better quantitative and confirmative performance can be observed for the HRMS instruments [3]. In conclusion, if the resolution of the instrument is not sufficient, false-positive findings can occur even if the experimentally measured exact mass seems to match the ion mass of the compound of interest. The risk of inaccurate quantification is particularly high when two chromatographically coeluting compounds have almost identical *m/z* values, because at insufficient resolving power their intensities combine to form a single peak which eventually leads to overestimation of the analyte concentration. By contrast, underestimation of the concentration may occur when a very narrow mass window is used to extract the analyte mass from such a mixed mass peak. Although the presence of an analyte and unresolved interference might still be detected in a mass spectrum recorded in profile mode (visual inspection reveals a shoulder peak), centroided data can completely shift out of the expected mass-accuracy window. Ferrer and Thurman [9] revealed the possibility of distinguishing analytes from interferences and analytes with very close *m/z* value (i.e. analytes with the same nominal mass) with HRMS. They analyzed lamotrigine and the metabolite of bupropion, hydroxybupropion, with the same nominal mass in wastewater extracts. Both compounds eluted at very similar retention times and the exact masses of the protonated molecules differed by 0.0948 mass units. The authors calculated that the resolving power needed to separate the two compounds was 6000, and performed a reliable quantification with a QTOFMS instrument. Assuming the resolving power is sufficiently high to achieve the necessary selectivity, the variables to be evaluated for method validation are very similar to those for LRMS. These include linearity, repeatability, reproducibility, recovery, matrix effects, and limits of detection (LOD) and quantification.

One of the most commonly used methods to estimate the LOD in LRMS is based on the signal-to-noise (S/N) ratios [10]. By contrast, in HRMS instruments the background noise in the chromatogram is often very low, or even zero for Orbitrap MS instruments in which by default a baseline noise cut-off is applied by the instrument control software to reduce data-file size, making the S/N approach sometimes impracticable. For this reason, alternative methods to calculate LODs have been proposed. One of them defines the LOD as the concentration that gives a peak intensity of at least 1.0×10^4 counts [11]. In another approach [12], instead of LOD, the authors propose to use the limit of identification, which is calculated as the minimum concentration that provides a fragment ion with a mass error <5 ppm [13]. The S/N ratio criterion, however, is still applied in HRMS [14].

As regards the comparison of the linear range, in which (Q)TOFMS and Orbitrap MS provide accurate quantitative measurement over a wide range of analyte concentrations, the Orbitrap has been proved to offer a linear range of at least four orders of magnitude. Modern TOF instruments achieve comparable performance to Orbitrap with respect to linear range, but this is not currently achievable on common hybrid QTOFMS systems. A notable exception is the "Triple TOF" series, which competes directly with triple-quadrupole MS in the field of quantitative analysis. This QTOF-based MS operates at an acquisition frequency of as high as 100 Hz, and promises a linear range of greater than five orders of magnitude and low limits of quantitation equivalent to high-performance triple quadrupoles.

To guarantee reliable confirmation, rules or guidelines are necessary not only for LRMS but also for approaches based on HRMS. In the latter case, the most commonly applied rules for confirming the presence of a target compound in the sample are:

1. detection with a mass error of less than 5 ppm;
2. a matching retention time with respect to the authentic standard retention time within 2.5 % and
3. an isotopic pattern in line with the elemental composition.

Wille et al. [12] quantified pesticides and pharmaceuticals in environmental samples using only the exact mass of the molecular ions deriving from the full-scan acquisition that fulfilled the aforementioned restrictions. Unlike LRMS, for which well-defined criteria have been established for confirming analyte presence, the corresponding criteria for HRMS are still under discussion. According to the EU guideline [15], the presence of a banned drug is confirmed when a specific number of identification points has been achieved. Working with QqQ-MS, one molecular ion gives 1.0 identification point and each of the two transitions 1.5 identification points. In addition, the measured retention time of the suspected peak has to match that of the standard. Finally, the area ratio between the two monitored MRM traces must be identical for the sample and for the standard. As for HRMS, the fact that resolving power may vary largely between instruments and/or techniques makes the definition of general criteria difficult. The EU guidelines state that a monitored ion measured at a resolution of 10,000 yields two identification points. However, this resolution refers to sector MS instruments, for which resolution is defined at 10 % of the peak height. Modern HRMS instruments, including TOF and Orbitrap, use as reference value the peak width at 50 % height. Hence, 10,000 at 10 % corresponds approximately to 20, 000 at 50 % (FWHM). Another point to be taken into account is the *m/z*-value-dependent resolution; i.e., in TOF analyzers the resolution is fairly constant over a broad *m/z* range, whereas in the Orbitrap analyzer resolution drops exponentially with

increasing *m/z* [16–19]. These aspects are discussed in detail in Ref. [20].

The reliable confirmation of an analyte measured by HRMS has been much improved with the availability of hybrid instruments including QTOFMS, Orbitrap MS, and Triple TOFMS. As well as all the characteristics of full-scan acquisition, the selection of precursor ions and subsequent generation of product-ion spectra are highly valuable because they provide compound-specific fragmentation patterns [21]. In fact, there are different ways of generating fragment ions in an unbiased manner. One way is the MS^E mode available on some QTOFMS instruments, consisting of alternating full-spectrum acquisitions at low and high collision energies. The analogous experiment on Orbitrap MS is the so-called all-ion fragmentation (AIF), in which a full MS scan is combined with a nonselective precursor-ion fragmentation performed in the high-energy-collisional-dissociation (HCD) cell. AIF using HCD in Orbitrap MS and collision-induced dissociation (CID) on QqQ-MS often share common main fragments; however, CID and HCD fragmentations in the hybrid Velos Pro-hybrid Ion Trap-Orbitrap MS may be complementary [21,22]. As with QqQ-MS, the extent of fragmentation is compound-specific, and therefore a compromise in the collision-energy setting has to be made to provide as much confirmatory information as possible [23]. Although the generation of fragment ions without precursor-ion selection requires a more careful interpretation when assigning fragment ions to precursor ions, it has proved to be very helpful in confirming compound identity.

As far as the standard approach to precursor-ion selection is concerned, this is undoubtedly the most reliable method and the confirmation of analyte identity is straightforward. Depending on the MS technique the product-ion spectra can contain accurate mass data, as generated by default by QTOFMS and some instruments from the Orbitrap family, or can be low-resolution spectra, e.g. when fragment ions are generated in the ion trap but, instead of being sent to the Orbitrap analyzer, are detected at the ion-trap detector. In contrast with the aforementioned unbiased ion fragmentation (MS^E and AIF), the acquisition of true product-ion spectra always requires a criterion to define the selection of the ion to be isolated for subsequent fragmentation. This can be based on a predefined precursor-ion list or simply based on ion abundance. During this so-called information-dependent acquisition (IDA) or data-dependent acquisition (DDA), the instrument automatically switches after a full-scan-mode acquisition to a product-ion scan mode as the second scan event in the scan cycles.

Literature on this aspect is increasing, and works on the analysis of pharmaceuticals or pesticides in the environment using hybrid instruments have recently been published [11,24]. The high-mass-resolution capabilities of the LTQ Orbitrap MS including an HCD cell were exploited for the determination of trace contaminants, enabling straightforward discrimination between analytes and matrix, and the dependent-scan functions of the Orbitrap MS using LIT MS and an HCD cell were evaluated and compared for the confirmation of analytes at trace concentrations. The authors concluded that data-dependent scanning using LIT MS is more suitable for trace environmental analysis than a data-dependent scan using HCD because of the slower scan times of the latter [24]. The LODs of the HRMS approach were in the low ng L^{-1} range (0.0007–0.0088 μg L^{-1}), revealing a sensitivity comparable to that of the data produced using the QqQ-MS instruments which have been the standard methods for quantitative analysis [24].

It can therefore be concluded that the most important advantage of using hybrid mass spectrometers, rather than QqQ-MS instruments or single-stage HRMS techniques, is to combine different kinds of study in a single method. This is particularly useful in environmental applications where the tasks of target analysis and of structural elucidation of transformation products and determination of their occurrence are equally important. In the recent work by Negreria et al. [25] the applicability of this combined approach was revealed for the elucidation of biotransformation products and subsequent quantitative target analysis.

It should be kept in mind, however, that quantitative studies always require reference standards of the targeted analytes, contaminants to be determined, and their metabolites or transformation products. In many cases their availability is a severe problem: they are either not commercially available, or prohibitively high prices make the purchase unrealistic. A possible work-around of this challenge is in-silico studies which attempt to predict the ionization efficiency in the electrospray-ionization source [26,27]. This interesting approach, however, requires more research to better understand the relevant factors defining ESI efficiency [28].

Qualitative analysis by LC–HRMS

HRMS systems have been primarily used for qualitative environmental analysis. LC–HRMS has mostly been used as a powerful tool for the identification of TPs or metabolites of different contaminants generated in laboratory-scale studies under controlled conditions [29,30]. This approach consists of a manual comparison of control samples and treated samples or detection of the TPs by creating a list of possible TPs from the literature or with in-silico methods (Fig. 2). Alignment and comparison of the total ion chromatograms of treated and control samples from lab-scale experiments enable detection of new peaks originating from the transformation of the test compounds [31,32]. Mass-accuracy errors of up to 5 ppm are usually accepted regardless of the mass analyzers used. These accurate mass measurements and complementary

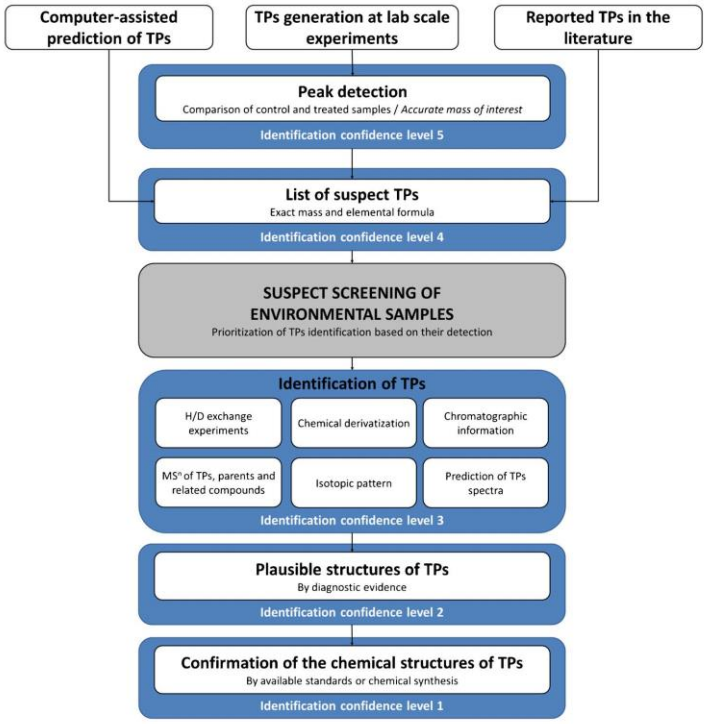

Fig. 2 General workflow for detection of relevant TPs in environmental samples with identification confidence levels in accordance with Schymanski et al. 2014 [38]

data, including the isotope cluster of the molecular ion, the comparison of the fragmentation patterns of the related parent compounds, and retention times, enable elucidation of the compound structure (Fig. 2). Eventually the identified compounds are included in the procedures for environmental monitoring [33,34]. A study using four MS techniques (LIT MS, QqQ-MS, LTQ Orbitrap, and TOFMS) for the identification of human metabolites of amitriptyline and verapamil was performed by Rousu et al. [35]. They compared their suitability for metabolite screening, considering the abilities to detect metabolites and to provide structural information for their identification, and addressed additional aspects of the workload of each instrument including time consumption and data processing. For the detection of metabolites different approaches were used: scan mode for HRMS instruments, a combination of neutral-loss and product-ion spectra for QqQ-MS, and information-dependent acquisition (IDA) with MRM for LIT MS. Data from each instrument was processed separately. Using the TOFMS approach, 28 and 69 metabolites were confirmed for amitriptyline and verapamil, respectively. However, with the other three instruments less than 50 % of these metabolites were detected. Although LTQ Orbitrap had better mass accuracy, TOFMS had more sensitivity and faster data acquisition than LTQ Orbitrap MS because of the inherently low data-acquisition rates in full-scan-type analysis for the latter. The QTRAP and triple-quadrupole MS had poor sensitivity and time-consuming sample analysis [35]. Therefore, the high sensitivity in full-scan mode has made LC–HRMS the most suitable tool for the development of screening methods, enabling the detection of a large number of emerging contaminants without prior selection of compounds [36]. Thus, LC–HRMS-based screening methods are unquestionably an important advance in the determination of environmental pollutants, with hundreds to thousands of organic pollutants and their TPs or metabolites under scrutiny. In general, what is now expected from HRMS instruments is to provide as much as information as possible from a single run of each sample without the need for reanalysis. In 2010 Krauss et al. [5] classified qualitative analysis of environmental samples into two categories: suspect screening and non-target screening (Fig. 3). Both methods are usually used in a complementary way, enabling the detection of

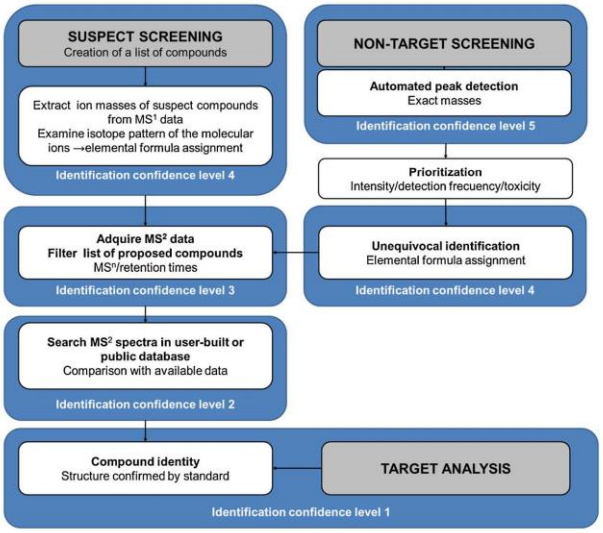

Fig. 3 General workflow for qualitative HRMS approaches

suspect pollutants and the identification of unknowns [37]. Hernandez et al. proposed the additional term post-target for when the search for pollutants is performed after HRMS acquisition without prior information.

For suspect analysis, elemental composition and structure are used to create databases of exact ion masses for the expected protonated or deprotonated molecules or their common adducts (Fig. 3). These libraries are created with suspect emerging pollutants and, sometimes, completed with their metabolites or TPs, either manually or by use of transformation-prediction software. After accurate mass extraction of expected ions, specific information on each compound is used to confirm plausible identities. Isotopic pattern, MS–MS spectra, fragmentation pathways, retention times, or mass defects can be found in the literature or predicted by appropriate software. The probability of false-positive findings decreases when more compound-specific properties are available. Schymanski et al. [38] proposed a system of five levels of confidence in the identification. In the end, reference standards must be used to achieve the top level of confirmation of the compound identity.

For example, Wode et al. [39] recently developed a method for the screening of 2188 compounds with Orbitrap MS. The TraceFinder software provided isotopic-pattern matching of the accurate mass measurement. Suspects with an isotopic-pattern score below 80 % were regarded as false-positive. Finally, 55 compounds were identified by analytical standards. The authors could not take advantage of spectral libraries for the verification of other suspects because there is no possibility of obtaining an MS2 spectrum with a single-stage Orbitrap. In fact, the use of single-stage mass spectrometers in AIF mode, where all precursor ions are fragmented without the possibility of isolating precursor ions, limits the study to all fragment ions derived from the fragmentation in the HCD cell.

With respect to the aforementioned limitation, hybrid HRMS systems are gaining popularity because of their ability to accurately measure product-ion masses. High-quality MS–MS spectra are produced by the two different approaches mentioned previously for quantitative confirmation: non-selective fragmentation and data-dependent MS–MS acquisitions. The major disadvantage of the first approach is the difficulty of assigning fragment ions to the molecular ion, because there is no connection between them; sometimes this task can be delegated to deconvolution software. In contrast, MS–MS acquisitions can provide information for a small set of compounds which then can be searched for in spectra libraries. Inclusion lists are often applied to the screening methods to perform pre-target suspect analysis. Coupling an Orbitrap with an LIT (hybrid LIT series) enables the combination of two complementary product-ion scans in HRMS, HCD, and CID, obtaining more structural data for the identification of TPs and metabolites. Thus, with this approach there is a gain in product-ion information that cannot be obtained on typical ion-trap instruments. The two product-ion scans complement each other by generating different spectra. For instance, in a recent paper the application of dual collision cells in LTQ Orbitrap MS, HCD, and CID in a data-dependent scan enhanced the structural elucidation of human metabolites of

selected pharmaceuticals [40]. Such an acquisition procedure can be an advantage over the approaches that can be performed with QqQ-MS and (Q)TOFMS instruments.

Regardless of whether AIF or data-dependent MS–MS switching modes are run, the use of specific software to streamline the data-mining process, and ultimately the confirmation, is regarded as essential.

As an example of new approaches with Q Exactive Orbitrap HRMS for TP detection and identification, Zonja et al. [41] used the standard approach based on lab-scale experiments combined with suspect screening of real surface-water samples. In this study, a sunlight simulator was used to degrade relevant pollutants of emerging concern, six iodinated contrast media (ICM), in surface-water samples. SIEVE software was used for the chromatographic-peak alignment and enabled the detection of 108 photoproducts in the photodegraded samples. Instead of performing the structural elucidation of and search for all TPs in environmental samples, a database was created with experimentally determined accurate masses, retention times, and MS–MS data of the 108 TPs for further suspect screening of real surface-water extracts. This approach enabled the prioritization of eleven environmentally relevant TPs, on the basis of their detection frequency in real samples, for subsequent structure elucidation. Finally, standards of the TPs were obtained by semipreparative LC, and quantitative analysis of the parent compounds and their prioritized TPs was performed in real surface-water extracts.

In contrast with the lab-scale methods, Kern et al. [42] used a different approach to determine the occurrence of TPs directly in natural waters by HRMS using LTQ Orbitrap. To this end, the authors created a list containing known aquatic contaminants, and predicted their TPs by means of the University of Minnesota Pathway Prediction System (UM-PPS) and literature information. Suspect screening was performed using an accurate database of 1794 compounds. When the target list contains a large number of compounds, comparison with blanks and estimated retention times and isotope patterns is essential to filter for positive results. This approach enabled the identification of 19 TPs, later confirmed by reference standards. In a subsequent study, Kern et al. [43] combined detection of the predicted TPs, degradation in batch reactors, and the calculated mass balances of wastewater treatment plants (WWTPs) to quantify transformation rates.

Wang et al. [44] developed a suspect-screening method to identify phase II metabolites of pharmaceuticals in reclaimed water with Q Exactive Orbitrap MS. In this study, the MetWorks software was used to find expected phase II metabolites of the most commonly detected pharmaceuticals. The identification of metabolites was only performed when the parent drug was detectable. As a criterion for positive findings, they expected an earlier retention time of a metabolite except in the case of acetylation. HRMS analysis was performed in DDA mode, meaning peaks from full-scan chromatograms with intensities lower than 1×10^5 counts were not considered. This study reported the detection and identification of sulfamethoxazole glucuronide and acetylsulfamethoxazole, two phase II metabolites of sulfamethoxazole.

Figure 2 summarizes the approaches used for detection and identification of TPs in environmental samples. Recently, Bletsou et al. [45] reviewed the state-of-the-art of LC–HRMS for the identification of TPs in the aquatic environment. A prioritization step is essential to optimize our efforts in the elucidation of more relevant TPs, and clearly software development is crucial for the prediction of transformations and for detection of candidates and their elucidation. As an example, Jeon et al. [46] used UM-PPS and Meteor Environmental Pathway Prediction System (Lhasa Limited, UK) for biotransformation prediction, MetWorks and SIEVE for candidate detection, Xcalibur for data analysis, Mass Frontier (HighChem, Ltd., Bratislava, Slovakia) and MetFrag for the prediction of MS–MS fragmentation, and even MOLGEN for molecular-structure generation. In this study 23 of the 360 predicted metabolites were detected and identified. Out of the 19 oxidation products identified, 12 metabolites were predicted by Meteor and seven by UM-PPS. Consequently, the combination of different software programs and the development of new ones are required.

In particular, software designed for the management of mass-spectral data provides another possibility for the detection of phase II metabolites or other compounds that provide common fragment ions through fragment-ion search. From these ions, related compounds are detected and tentatively identified [47]. Several authors refer to this approach as a semi-non-target approach because one searches for known fragment ions of unknown pollutants. In this way, Hernandez et al. [6] differentiated between unbiased non-target analysis and biased non-target analysis. In general, the objective of non-target screening is to analyze environmental samples without any information on the compounds present in the sample, and to detect and identify relevant compounds. Thus, the prioritization of compounds that will be selected for identification becomes an important step of non-target analysis [48]. In unbiased non-target analysis, peaks for the identification could be selected on the basis of intensity, detection frequency, and toxicity (for bioassay-directed analysis) and/or in a comparison of samples and blanks. In biased non-target analysis, the method screens for compounds with concrete properties including specific mass defects and distinctive isotope pattern or fragment ions.

The general workflow for non-target studies consists of automatic peak detection, prioritization, determination of elemental composition, structural elucidation, and library spectrum matching and ranking of the candidates (Fig. 3). Automated peak detection and spectra deconvolution algorithms are required, and the success is limited to the prioritized

compounds. The lack of comprehensive (LC–)MS libraries hampers the identification process [48]. In short, non-target screening can be summarized in two steps: the reduction of peaks included in the identification procedure and the reduction and ranking of candidates [37]. Whereas in suspect screening compound identities are known, in non-target analysis calculated molecular formulas must be evaluated. Consequently, the application of non-target screening requires a large investment in data analysis. Some software packages, including MOLGEN and the Seven Golden Rules (7GR) afford an automated analysis [49]. Currently, the identification of unknown pollutants remains a tedious and time-consuming task. Researchers usually have to rely on a combination of complementary software packages, user-built libraries, and literature information to propose plausible compound identities.

In addition, as mentioned above, the use of publicly available LC–HRMS databases, including MassBank, ChemSpider, NIST, HMDB, METLIN, and MetFrag, for the identification of "known unknown" compounds is helpful but still limited.

Usually, qualitative studies have performed non-target, suspect, and target analysis together [50,51] in so-called "all in one" analysis. For instance, the studies by Schymansky et al. [52] revealed the capability of LC–HRMS to perform analysis of wastewaters by taking advantage of these different approaches. First, an accurate mass list was compiled with enviMass and processed by the R package "non-target" (Eawag, Switzerland). This software selects the most intense peak of each unknown compound and creates groups with all related peaks into one component to associate isotope and adduct peaks with the compound. After blank and noise subtraction, an intensity-based prioritization was performed. In (−)ESI MS, four of the 30 most intense peaks were determined by their target screening method; also, 15 of these peaks contained S, enabling the identification of seven compounds by searching a list of 394 compounds which contain sulfur. Finally, non-target workflows were used for the elucidation of the remaining unknown compounds. As a result, of the 26 most intense non-target peaks, seven were tentatively identified and one identified and confirmed by use of a reference standard.

As a promising approach for the screening of unknown toxicant pollutants, LC–HRMS identification could be prioritized through effect-directed analysis (EDA). Weiss et al. [53] used SIEVE to discriminate the peaks between active and non-active fractions and followed a non-target workflow to identify the most toxic unknowns. This approach enabled the identification of eight androgen-disrupting compounds.

As well as false-positive findings, which are reduced by different strategies, false-negative findings are also plausible in qualitative analysis without reference standards. Several compounds might not be ionized or are not extracted by the sample-preparation method. To this end, sample procedures including direct-injection or large-volume-injection LC–HRMS of water samples can be an alternative to avoid selective pre-concentration [54,55]. To increase the range of polarity and volatility, recent studies combined HRMS with both LC and gas chromatography [56].

Conclusions and future advances

In summary, LC–HRMS is a powerful tool for quantitative and qualitative analysis, enabling the quantitation of target compounds and the search for and identification of suspected or unknown pollutants. A recent trend in LC–HRMS-based environmental studies is to perform "all-in-one" analysis, i.e. simultaneous target analysis (quantitative), suspect screening, and non-target determination (qualitative). Comparing the performance for quantitative analysis, LC–HRMS has sensitivity comparable to that of LC–QqQ-MS, whereas the selectivity—achieved on QqQ-MS by choosing suitable MRM transitions—is largely dependent on the resolving power of the instrument. Only sufficiently high resolving power can guarantee that co-eluting matrix components can be distinguished from compounds of interest. The high sensitivity in conjunction with the wealth of unbiased information gathered means that LC–HRMS is increasingly competing with LC–QqQ-MS in environmental research laboratories. With the growing popularity and acceptance, one of the aspects that needs to be addressed is the criteria used in compound confirmation.

There are some differences between different HRMS instruments for quantitative analysis. (Q)TOFMS instruments were initially used for qualitative analysis. However, the latest instruments on the market have improved quantitative capabilities, providing a good approach for quantification combined with the power of exact mass. However, the Orbitrap instruments try to achieve higher sensitivity with higher mass accuracy. A disadvantage of the Orbitrap mass analyzer is that the mass resolution of Orbitrap is inversely related to scan speed, meaning high-resolving-power settings imply low acquisition frequencies. By contrast, TOFMS instruments are known to produce essentially the same resolution across different scan rates. Therefore, to achieve UPLC separations, the acquisition rate of Orbitrap MS needs to be decreased at the expense of resolving power. This disadvantage is particularly important when the minimum number of points per peak cannot be achieved. However, the scan rate for Orbitrap technology is faster and attempts are being made to provide a sufficient number of scans (≥10) across the chromatographic peak in full-scan mode. As regards mass accuracy, whereas most TOFMS instruments require internal calibration for continuous correction of the mass axis, the Orbitrap analyzer is capable of maintaining mass accuracy over several days after

initial calibration. With internal calibration in (Q)TOFMS, the ionization of the calibrant(s) may interfere with the ionization of the analytes. Moreover, the calibrant signal may collapse in the presence of high matrix loads because of ion suppression, and its intensity may vary with changing mobile-phase composition during gradient elution. For obvious reasons, the choice of an appropriate internal calibrant has to be such that spectral interferences with the analytes of interest can be ruled out.

Regarding qualitative analysis, LC–HRMS provides more information about each sample than LRMS instruments, enabling suspect and non-target screening without retrospective analysis. Different workflows based on their accurate mass measurements have been used to reduce the number of false-positive findings. New commercial software and the availability of public HRMS libraries of environmental contaminants and their TPs could help mine the data from controlled laboratory experiments (conducted at high concentrations) in an efficient and comprehensive fashion. Regarding non-target analysis, more studies on the prediction of retention times, ionization behavior, and MS–MS fragmentation are still needed and are expected to eventually deliver the computational tools essential for easier identification of unknowns.

Acknowledgments S. Pérez acknowledges the contract from the Ramon y Cajal Program of the Spanish Ministry of Economy and Competitiveness. This work has been financially supported by the Generalitat de Catalunya (Consolidated Research Groups "2014 SGR 418 - Water and Soil Quality Unit", 2014 SGR 291.

References

1. Eichhorn P, Pérez S, Barceló D (2012) Time-of-flight mass spectrometry versus orbitrap-based mass spectrometry for the screening and identification of drugs and metabolites: is there a winner? Compr Anal Chem 58:217–272
2. J. Aceña, D. Rivas, B. Zonja, S. Péreza, D. Barcelóa, Liquid Chromatography–Mass Spectrometry: Quantification and Confirmation Aspects
3. Kaufmann A, Butcher P, Maden K, Walker S, Widmer M (2011) Quantitative and confirmative performance of liquid chromatography coupled to high-resolution mass spectrometry compared to tandem mass spectrometry. Rapid Commun Mass Spectrom 25: 979–992
4. Hernández F, Sancho J, Ibáñez M, Abad E, Portolés T, Mattioli L (2012) Current use of high-resolution mass spectrometry in the environmental sciences. Anal Bioanal Chem 403:1251–1264
5. Krauss M, Singer H, Hollender J (2010) LC–high resolution MS in environmental analysis: from target screening to the identification of unknowns. Anal Bioanal Chem 397:943–951
6. Hernández F, Ibáñez M, Bade R, Bijlsma L, Sancho J (2014) Investigation of pharmaceuticals and illicit drugs in waters by liquid chromatography-high-resolution mass spectrometry. TrAC Trends Anal Chem 63:140–157
7. Agüera A, Martínez Bueno M, Fernández-Alba A (2013) New trends in the analytical determination of emerging contaminants and their transformation products in environmental waters. Environ Sci Pollut Res 20:3496–3515
8. Kaufmann A, Butcher P, Maden K, Walker S, Widmer M (2010) Comprehensive comparison of liquid chromatography selectivity as provided by two types of liquid chromatography detectors (high resolution mass spectrometry and tandem mass spectrometry): "Where is the crossover point?". Anal Chim Acta 673:60–72
9. Ferrer I, Thurman EM (2012) Analysis of 100 pharmaceuticals and their degradates in water samples by liquid chromatography/quadrupole time-of-flight mass spectrometry. J Chromatogr A 1259:148–157
10. Shrivastava A, Gupta VB (2011) Methods for the determination of limit of detection and limit of quantitation of the analytical methods. Chronicles of Young Sci 2:21
11. Farré M, Picó Y, Barceló D (2014) Application of ultra-high pressure liquid chromatography linear ion-trap orbitrap to qualitative and quantitative assessment of pesticide residues. J Chromatogr A 1328:66–79
12. Wille K, Claessens M, Rappé K, Monteyne E, Janssen CR, De Brabander HF, Vanhaecke L (2011) Rapid quantification of pharmaceuticals and pesticides in passive samplers using ultra high performance liquid chromatography coupled to high resolution mass spectrometry. J Chromatogr A 1218:9162–9173
13. Padilla-Sánchez JA, Plaza-Bolaños P, Romero-González R, Grande-Martínez Á, Thurman EM, Garrido-Frenich A (2012) Innovative determination of polar organophosphonate pesticides based on high-resolution Orbitrap mass spectrometry. J Mass Spectrom 47:1458–1465
14. Vergeynst L, Haeck A, De Wispelaere P, Van Langenhove H, Demeestere K (2015) Multi-residue analysis of pharmaceuticals in wastewater by liquid chromatography–magnetic sector mass spectrometry: Method quality assessment and application in a Belgian case study. Chemosphere 119:S2–S8
15. Commission E (2002) Commission Decision 2002/657/EC of 12 August 2002 implementing Council Directive 96/23/EC concerning the performance of analytical methods and the interpretation of results. Off J Eur Comm L 221:8–36
16. Nurmi J, Pellinen J (2011) Multiresidue method for the analysis of emerging contaminants in wastewater by ultra performance liquid chromatography–time-of-flight mass spectrometry. J Chromatogr A 1218:6712–6719
17. Wille K, Bussche JV, Noppe H, De Wulf E, Van Caeter P, Janssen C, De Brabander H, Vanhaecke L (2010) A validated analytical method for the determination of perfluorinated compounds in surface-, sea- and sewagewater using liquid chromatography coupled to time-of-flight mass spectrometry. J Chromatogr A 1217:6616–6622
18. Lara-Martín PA, González-Mazo E, Brownawell BJ (2011) Multi-residue method for the analysis of synthetic surfactants and their degradation metabolites in aquatic systems by liquid chromatography–time-of-flight-mass spectrometry. J Chromatogr A 1218:4799–4807
19. Farré M, Gros M, Hernandez B, Petrovic M, Hancock P, Barceló D (2008) Analysis of biologically active compounds in water by ultra-performance liquid chromatography quadrupole time-of-flight mass spectrometry. Rapid Commun Mass Spectrom 22:41–51
20. Nielen M, Van Engelen M, Zuiderent R, Ramaker R (2007) Screening and confirmation criteria for hormone residue analysis using liquid chromatography accurate mass time-of-flight, Fourier transform ion cyclotron resonance and orbitrap mass spectrometry techniques. Anal Chim Acta 586:122–129
21. Makarov A, Scigelova M (2010) Coupling liquid chromatography to Orbitrap mass spectrometry. J Chromatogr A 1217:3938–3945
22. K. Comstock, Y (2011) Huang, Multiple fragmentation methods for small molecule characterization on a dual pressure linear ion trap Orbitrap hybrid mass spectrometer, Application Note, 540
23. Coscollà C, León N, Pastor A, Yusà V (2014) Combined target and post-run target strategy for a comprehensive analysis of pesticides in ambient air using liquid chromatography-Orbitrap high resolution mass spectrometry. J Chromatogr A 1368:132–142

24. Cahill MG, Dineen BA, Stack MA, James KJ (2012) A critical evaluation of liquid chromatography with hybrid linear ion trap—Orbitrap mass spectrometry for the determination of acidic contaminants in wastewater effluents. J Chromatogr A 1270:88–95
25. Negreira N, López de Alda M, Barceló D (2015) Degradation of the cytostatic etoposide in chlorinated water by liquid chromatography coupled to quadrupole-Orbitrap mass spectrometry: Identification and quantification of by-products in real water samples. Sci Total Environ 506–507:36–45
26. Chalcraft KR, Lee R, Mills C, Britz-McKibbin P (2009) Virtual Quantification of Metabolites by Capillary Electrophoresis-Electrospray Ionization-Mass Spectrometry: Predicting Ionization Efficiency Without Chemical Standards. Anal Chem 81:2506–2515
27. Kruve A, Kaupmees K, Liigand J, Leito I (2014) Negative electrospray ionization via deprotonation: predicting the ionization efficiency. Anal Chem 86:4822–4830
28. Oss M, Kruve A, Herodes K, Leito I (2010) Electrospray ionization efficiency scale of organic compounds. Anal Chem 82:2865–2872
29. B. Zonja, J. Aceña, S. Pérez, D. Barceló (2013) Chapter 16 - Methods for Elucidation of Transformation Pathways: Identification of Intermediate Products, Chiral, and Isotope-Ratio Mass Spectrometry Analysis, in: D.B. Mira Petrovic, P. Sandra (Eds.) Comprehensive Analytical Chemistry, Elsevier, pp. 593–610
30. Eichhorn P, Ferguson PL, Pérez S, Aga DS (2005) Application of Ion Trap-MS with H/D Exchange and QqTOF-MS in the Identification of Microbial Degradates of Trimethoprim in Nitrifying Activated Sludge. Anal Chem 77:4176–4184
31. Pérez S, Eichhorn P, Celiz MD, Aga DS (2006) Structural Characterization of Metabolites of the X-ray Contrast Agent Iopromide in Activated Sludge Using Ion Trap Mass Spectrometry. Anal Chem 78:1866–1874
32. Pérez S, Barceló D (2008) First Evidence for Occurrence of Hydroxylated Human Metabolites of Diclofenac and Aceclofenac in Wastewater Using QqLIT-MS and QqTOF-MS. Anal Chem 80: 8135–8145
33. Aceña J, Pérez S, Gardinali P, Abad JL, Eichhorn P, Heuett N, Barceló D (2014) Structure elucidation of phototransformation products of unapproved analogs of the erectile dysfunction drug sildenafil in artificial freshwater with UPLC-Q Exactive-MS. J Mass Spectrom 49:1279–1289
34. Zonja B, Gonçalves C, Pérez S, Delgado A, Petrovic M, Alpendurada MF, Barceló D (2014) Evaluation of the phototransformation of the antiviral zanamivir in surface waters through identification of transformation products. J Hazard Mater 265:296–304
35. Rousu T, Herttuainen J, Tolonen A (2010) Comparison of triple quadrupole, hybrid linear ion trap triple quadrupole, time-of-flight and LTQ-Orbitrap mass spectrometers in drug discovery phase metabolite screening and identification in vitro – amitriptyline and verapamil as model compounds. Rapid Commun Mass Spectrom 24:939–957
36. Moschet C, Piazzoli A, Singer H, Hollender J (2013) Alleviating the reference standard dilemma using a systematic exact mass suspect screening approach with liquid chromatography-high resolution mass spectrometry. Anal Chem 85:10312–10320
37. Hug C, Ulrich N, Schulze T, Brack W, Krauss M (2014) Identification of novel micropollutants in wastewater by a combination of suspect and nontarget screening. Environ Pollut 184:25–32
38. Schymanski EL, Jeon J, Gulde R, Fenner K, Ruff M, Singer HP, Hollender J (2014) Identifying small molecules via high resolution mass spectrometry: communicating confidence. Environ Sci Technol 48:2097–2098
39. Wode F, van Baar P, Dünnbier U, Hecht F, Taute T, Jekel M, Reemtsma T (2015) Search for over 2000 current and legacy micropollutants on a wastewater infiltration site with a UPLC-high resolution MS target screening method. Water Res 69:274–283
40. Bushee JL, Argikar UA (2011) An experimental approach to enhance precursor ion fragmentation for metabolite identification studies: application of dual collision cells in an orbital trap. Rapid Commun Mass Spectrom 25:1356–1362
41. Zonja B, Delgado A, Pérez S, Barceló D (2015) LC-HRMS Suspect Screening for Detection-Based Prioritization of Iodinated Contrast Media Photodegradates in Surface Waters. Environ Sci Technol 49: 3464–3472
42. Kern S, Fenner K, Singer HP, Schwarzenbach RP, Hollender J (2009) Identification of transformation products of organic contaminants in natural waters by computer-aided prediction and high-resolution mass spectrometry. Environ Sci Technol 43:7039–7046
43. Kern S, Baumgartner R, Helbling DE, Hollender J, Singer H, Loos MJ, Schwarzenbach RP, Fenner K (2010) A tiered procedure for assessing the formation of biotransformation products of pharmaceuticals and biocides during activated sludge treatment. J Environ Monit 12:2100–2111
44. Wang J, Gardinali PR (2014) Identification of phase II pharmaceutical metabolites in reclaimed water using high resolution benchtop Orbitrap mass spectrometry. Chemosphere 107:65–73
45. A.A. Bletsou, J. Jeon, J. Hollender, E. Archontaki, N.S. Thomaidis (2015) Targeted and non-targeted liquid chromatography-mass spectrometric workflows for identification of transformation products of emerging pollutants in the aquatic environment, TrAC Trends Anal Chem
46. Jeon J, Kurth D, Hollender J (2013) Biotransformation Pathways of Biocides and Pharmaceuticals in Freshwater Crustaceans Based on Structure Elucidation of Metabolites Using High Resolution Mass Spectrometry. Chem Res Toxicol 26:313–324
47. Gómez-Ramos MM, Pérez-Parada A, García-Reyes JF, Fernández-Alba AR, Agüera A (2011) Use of an accurate-mass database for the systematic identification of transformation products of organic contaminants in wastewater effluents. J Chromatogr A 1218:8002–8012
48. Zedda M, Zwiener C (2012) Is nontarget screening of emerging contaminants by LC-HRMS successful? A plea for compound libraries and computer tools. Anal Bioanal Chem 403:2493–2502
49. Kind T, Fiehn O (2007) Seven Golden Rules for heuristic filtering of molecular formulas obtained by accurate mass spectrometry. BMC Bioinforma 8:105
50. Chiaia-Hernandez AC, Schymanski EL, Kumar P, Singer HP, Hollender J (2014) Suspect and nontarget screening approaches to identify organic contaminant records in lake sediments. Anal Bioanal Chem 406:7323–7335
51. Hogenboom A, Van Leerdam J, de Voogt P (2009) Accurate mass screening and identification of emerging contaminants in environmental samples by liquid chromatography–hybrid linear ion trap Orbitrap mass spectrometry. J Chromatogr A 1216:510–519
52. Schymanski EL, Singer HP, Longrée P, Loos M, Ruff M, Stravs MA, Ripollés Vidal C, Hollender J (2014) Strategies to characterize polar organic contamination in wastewater: exploring the capability of high resolution mass spectrometry. Environ Sci Technol 48: 1811–1818
53. Weiss J, Simon E, Stroomberg G, de Boer R, de Boer J, van der Linden S, Leonards PG, Lamoree M (2011) Identification strategy for unknown pollutants using high-resolution mass spectrometry: Androgen-disrupting compounds identified through effect-directed analysis. Anal Bioanal Chem 400:3141–3149
54. Vergeynst L, Van Langenhove H, Joos P, Demeestere K (2014) Suspect screening and target quantification of multi-class pharmaceuticals in surface water based on large-volume injection liquid chromatography and time-of-flight mass spectrometry. Anal Bioanal Chem 406:2533–2547

55. Martínez Bueno MJ, Ulaszewska MM, Gomez MJ, Hernando MD, Fernández-Alba AR (2012) Simultaneous measurement in mass and mass/mass mode for accurate qualitative and quantitative screening analysis of pharmaceuticals in river water. J Chromatogr A 1256:80–88

56. Hernández F, Ibáñez M, Portolés T, Cervera MI, Sancho JV, López FJ (2015) Advancing towards universal screening for organic pollutants in waters. J Hazard Mater 282:86–95

CAPÍTOL 2.

OBJECTIUS I ESTRUCTURA DE TESI

CAPITOL 2. OBJECTIUS I ESTRUCTURA

2.1 OBJECTIUS

Els objectius generals d'aquesta tesi van ser millorar el coneixement dels processos de transformació dels fàrmacs humans en el medi aquàtic.

En particular es pretenia:

- Avaluar les rutes de fotodegradació de la droga "livestyle" sildenafil i el seu metabòlit humà principal en aigües superficials en un simulador de llum solar. A més a mes, comparar la fotòlisis d'estructures químiques rel·lacionades diferenciant-se principalment en l'anell de piperazina. Aquests compostos que han sorgit recentment per evadir la seva detecció en protocols d'anàlisi de drogues il·legals són el norneosildenafil, el tiosildenafil, l'homosildenafil i l'hidroxihomosildenafil. Utilitzar la espectrometria de masses de mitja/alta resolució per a la elucidació estructual dels seus productes de transformació.

- Detectar i quantificar la presència dels metabòlits que provenen de la biodegradació d'uns compostos ampliament detectats a les aigües superficials, la sulfametazina i el sulfametoxazol, en mesocosmos. Utilitzar la espectrometria de masses d'alta resolució per a l'anàlisi qualitatiu i un espectrometre de masses de baixa resolució pel quantitatiu.

- Detectar les principals reaccions metabòliques de la carbamazepina i l'ibuprofè en peixos (Solea Senegalensis) tractas amb aquests dos compostos a escala laboratori. Identificar els productes de biotransformació a les bilis amb espectrometria de masses d'alta resolució i les principals reaccions metabòliques. Comparar les diferents rutes metabòliques en altres organismes aquàtics com per exemple les plantes. Amb aquesta informació, crear una base de dades de productes de biotransformació que es podrien formar potencialment en peixos exposats a residus farmacèutics. Determinar la exposició de peixo salvatges a fàrmacs mitjançant aquesta llsta.

2.2 ESTRUCTURA

La tesi s'ha estructurat en 5 capítols diferents:

- En el capítol 1 s'ha focalitzat en les principals transformacions que pateixen els fàrmacs al medi natural. A més s'ha revisat l'evolució de la HRMS per a l'estudi d'aquests procesos.
- Al capítol 2 es marquen els principals objectius per al desenvolupament d'aquesta tesi.
- Al capítol 3 s'han avaluat els procesos de transformació biòtics i abiòtics que afecten als fàrmacs al medi natural.
- Al capítol 4 s'avalua l'exposició de la biota als residus farmacèutics i el seu metabolisme tant a escala laboratori com al riu.
- En el capítol 5 es resumeixen les conclusions que es deriven de la realització d'aquesta tesi.

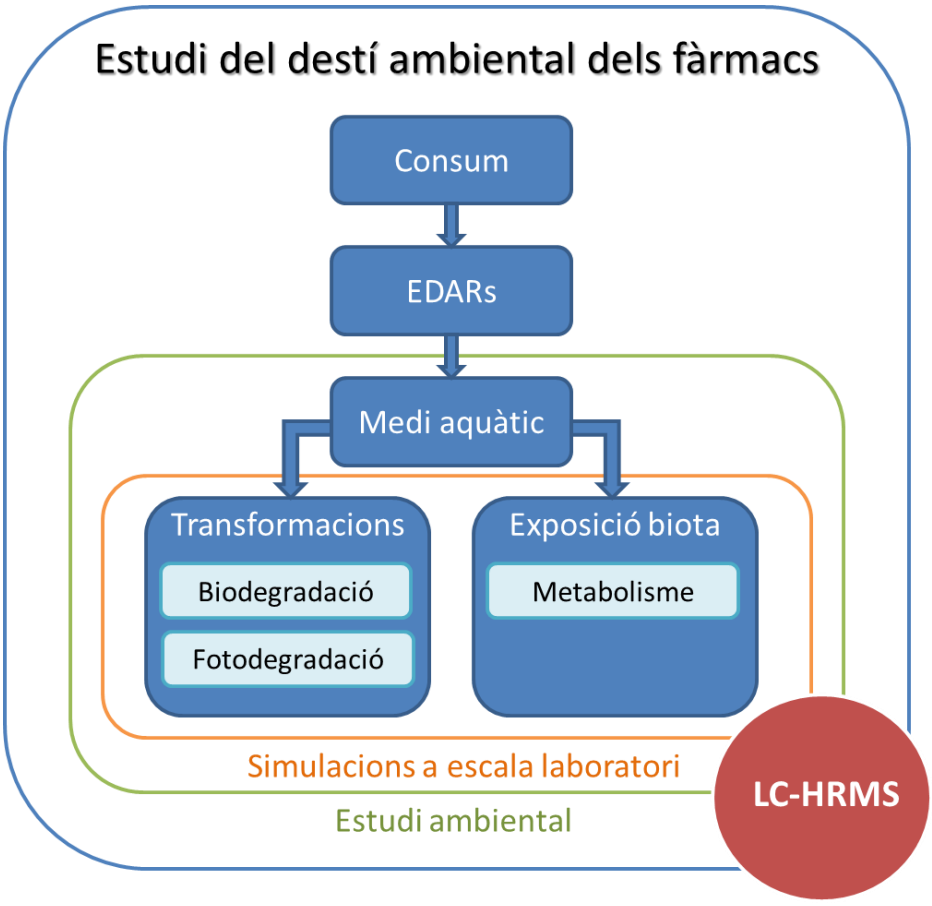

Figura 5. Esquema del estudi ambiental dels fàrmacs

CAPÍTOL 3.

TRANSFORMACIÓ DE FÀRMACS AL MEDI AQUÀTIC

CAPITOL 3. TRANSFORMACIÓ DE FÀRMACS AL MEDI AQUÀTIC

Com s'ha comentat anteriorment, la presència de residus farmacèutics al medi ambient pot representar una amenaça potencial pels ecosistemes i fins i tot pels humans. Un cop al medi aquàtic, els fàrmacs poden ser transportats i distribuïts en les diferents aigües superficials i subterrànies. A més del transport, aquests compostos estan subjectes a la degradació per dues vies, els processos biòtics i els abiòtics. Sovint, el resultat d'aquests processos són la formació de productes de transformació (TPs) que poden ser més mòbils i polars que el compost original i per tant també poden exercir efectes adversos en els organismes aquàtics. A més, en el cas dels compostos bioactius el seu efecte farmacològic pot ser retingut quan la part activa de la molècula roman intacte després de la seva transformació com per exemple l'activitat antibiòtica, com s'ha demostrat per alguns productes deshidratats de tetraciclines [138] i productes de fotodegradació de l'antibiòtic fluoroquinolona ofloxacina [139]. Per tant, l'elucidació de les diferents vies de degradació dels fàrmacs i la identificació dels TPs és de crucial importància per avaluar el destí global i per avaluar el risc d'aquests contaminants emergents al medi aquàtic

Al capítol 1 s'han descrit els principals estudis de les diferents transformacions que poden patir els fàrmacs un cop arriben al medi aquàtic, i principalment a les aigües superficials, fixant com a principals procesos la fotodegradació i la biodegradació. Malgrat això, a la literatura científica es disposa encara de poca informació relacionada amb els possibles efectes tòxics dels TPs formats. A més, en la majoria d'estudis que hi ha, s'avalua la toxicitat de mescles que contenen els fàrmacs d'origen junt amb els seus TPs i per a una avaluació concloent de la toxicitat seria essencial poder identificar, separar i aïllar cada TP de la mostra.

Avui en dia, tot i que la identificació estructural de TPs és actualment un dels procediments més utilitzats pels investigadors per avaluar el destí dels fàrmacs al medi ambient, aquesta tasca és encara complexa i requereix l'aplicació de tècniques instrumentals sofisticades com ara ressonància magnètica nuclear (RMN), GC-MS o LC-MS. En aquest capítol es pretén aprofitar els avenços en el camp de la LC-HRMS

per estudiar aquestes possibles transformacions mitjançant simulacions a escala laboratori.

3.1 Processos de transformació: Fotodegradació

La fotodegradació és la descomposició d'una substància per l'efecte de la llum i és el procés de transformació abiòtic més important, sobretot a les aigües superficials. En els sistemes aquàtics als quals hi arriba força irradiació UV, aquest procés pot ser més rellevant que els processos biòtics, sobretot pels contaminants que han persistit als tractaments biològics de les EDARs.

Al medi aquàtic, la fotòlisi no sempre degrada completament els fàrmacs i en moltes ocasions l'efecte de la llum produeix reaccions complexes. Aquestes reaccions causen transformacions en l'estructura del compost, formant compostos estables de propietats i toxicitat desconegudes, els anomenats TPs.

Habitualment aquests processos s'estudien primer a escala laboratori i després al medi natural degut a la complexitat del medi i als diferents factors que poden afectar al destí dels fàrmacs,. Així doncs, solucions aquoses fortificades amb els fàrmacs són irradiadiades, generalment mitjançant un simulador de llum solar, per tal de formar, detectar i identificar els seus TPs més importants.

En l'actualitat al mercat hi coexisteixin més de 3000 productes farmacèutics [140]. Un dels grups que s'ha detectat més recentment a les aigües superficials són les drogues "life-style". Dins d'aquestes hi ha un grup que són els inhibidors de la fosfodiesterasa V (PDE-V) utilitzats pel tractament de la disfunció erèctil. Actualment, es planteja que la disfunció erèctil pot tenir una afectació de fins al 52 % dels homes entre els 40 i 70 anys [141]. A més, aquesta incidència està augmentant i s'esperen més de 600.000 nous casos per any [142]. Només als Estats Units existeixen més de 30 milions d'homes que presenten algun grau de disfunció que els impedeix tenir relacions sexuals satisfactòries [143]. El nombre d'homes que la pateixen arreu del món s'estima que arribarà fins a uns 320 milions en els següents 15 anys [144]. El sildenafil (SDF) o citrat de SDF, va ser comercialitzat el 1998 pels laboratoris Pfizer com a principi actiu de la Viagra®. Un dels seus principals metabòlits humans és el desmetilsildenafil (DM-

SDF). Diferents publicacions indiquen que la concentració d'aquest metabòlit al plasma, després d'una única ingesta de SDF, pot ser d'entre el 30 i el 40% respecte la concentració del producte inicial [145].

Degut a que fins fa poc temps, aquest medicament requeria prescripció mèdica, ha aparegut un mercat negre emergent que ha comportat que el SDF es consideri un dels fàrmacs més falsificats. A més alguns anàlegs sintètics són utilitzats per adulterar herbes i altres productes medicinals, ofertats com a naturals, que es venen a través d'internet. En aquest sentit, els consumidors poden estar exposats inconscientment a les contraindicacions que presenten aquest conjunt de medicaments. A la literatura es poden trobar multitud d'anàlegs utilitzats en l'adulteració d'herbes i pastilles, principalment a l'est i sud-est asiàtic [146]. La majoria presenten una estructura molt similar amb una petita variació estructural. Tots aquests compostos, no indicats en l'etiquetat i/o no testats clínicament, suposen un risc per a la salut humana.

A més, sumat a la gran producció mundial d'aquests compostos, s'estima que aquests poden ser persistents i/o bioacumulables i per tant també representen un risc ambiental [140]. Dins d'aquest context, en primer lloc es va estudiar la fototransformació del SDF i el seu metabòlit (DM-SDF) a demés de quatre dels anàlegs il·legals més utilitzats, concretament del norneosildenafil (NR-SDF), el tiosildenafil (TS-SDF), l'homosildenafil (H-SDF) i l'hidroxihomosildenafil (HH-SDF).

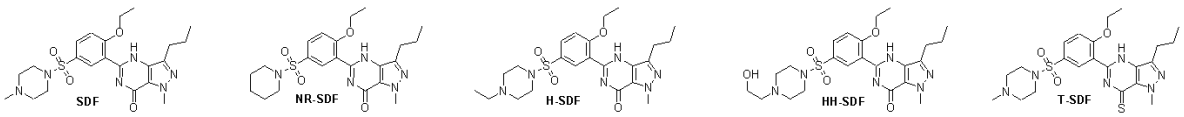

Figura 6. *Estructures del SDF i els seus anàlegs*

Els resultats d'aquests estudis es resumeixen a les dues publicacions que es troben a continuació.

Article nº 2: Identification of phototransformation products of Sildenafil (Viagra) and its N-demethylated human metabolite under simulated sunlight.

P. Eichhorn, S. Pérez, **J. Aceña**, P. Gardinali i D. Barceló.

Journal of Mass Spectrometry - 2012

Research Article

Journal of MASS SPECTROMETRY

Received: 20 November 2011 Revised: 22 March 2012 Accepted: 23 March 2012 Published online in Wiley Online Library

(wileyonlinelibrary.com) DOI 10.1002/jms.2998

Identification of phototransformation products of sildenafil (Viagra) and its N-demethylated human metabolite under simulated sunlight

Peter Eichhorn,[a] Sandra Pérez,[a]* Jaume Aceña,[a] Piero Gardinali,[b] José Luis Abad[c] and Damià Barceló[a,d,e]

Recent publications on pharmaceutical monitoring are increasingly covering the field of illicit drugs and lately the forensic evaluation of designing illegal analogs of lifestyle drugs like the phosphodiesterase type 5 (PDE-5) inhibitors Viagra (sildenafil), Levitra (vardenafil) and Cialis (tadalafil). Recently, the presence of all three erectile dysfunction treatment drugs has been reported in wastewaters at very low concentrations. In the environment, contaminants undergo various physical or chemical processes classified into abiotic (photolysis, hydrolysis) and biotic (biodegradation) reactions. Thus, changes in the chemical structure lead to the formation of new transformation products, which may persist in the environment or be further degraded. This study describes the photolysis of sildenafil (SDF) and its human metabolite N-demethylsildenafil (DM-SDF) under simulated solar radiation (Xenon lamp). Following chromatographic separation of the irradiated samples, eight photoproducts in the SDF samples and six photoproducts for DM-SDF were detected and characterized. The combination of ultra performance liquid chromatography-electrospray ionization-quadrupole time-of-flight-mass spectrometry (UPLC-ESI-QToF-MS), liquid chromatography-atmospheric pressure chemical ionization-triple quadrupole mass spectrometry (LC-APCI-QqQ-MS) and hydrogen/deuterium-exchange experiments allowed to propose plausible chemical structures for the photoproducts, taking into account the characteristic fragmentation patterns and the accurate mass measurements. These mass spectral data provided sound evidence for the susceptibility of the piperazine ring toward photodegradation. A gradual breakdown of this heterocyclic structure gave rise to a series of products, which in part were identical for SDF and DM-SDF. The sulfonic acid, as the formal product of sulfonamide hydrolysis, was identified as key intermediate in the photolysis pathway. In both drug/metabolite molecules, phototransformation processes taking place beyond the sulfonamide group were deemed to be of minor relevance. Copyright © 2012 John Wiley & Sons, Ltd.

Supporting information may be found in the online version of this article.

Keywords: photolysis; emerging contaminants; sildenafil; structure elucidation; UPLC-ESI-QToF-MS

INTRODUCTION

The assessment of the presence of emerging contaminants in wastewater influents or even receiving waters is no longer restricted to potentially toxic substances,[1] endocrine disruptive chemicals, personal care products and prescription drugs.[2] Since the report of the presence of caffeine in river waters back in 1978,[3] the wealth of publications devoted to the assessment of the chemical ecology of surface water has become a burden of proof indicating that traditional water treatment needs to improve substantially if the quality of potable water is to be preserved from further degradation. Moreover, a combination of consumption, limited human metabolism and resistance to treatment for some of these drugs has resulted in the development of noninvasive communal monitoring of drug abuse from both prescribed and illegal markets.[4] One of the last markets to be addressed by chemical ecology is the lifestyle enhancement drugs. Lucrative voluntary use drugs like the phosphodiesterase type 5 (PDE-5) inhibitors Viagra, Levitra and Cialis are usually prescribed to treat erectile dysfunction syndrome (EDS). However, a growing recreational and illegal market has fast developed and now includes not only generic versions of the three common EDS drugs but also a number of nonapproved analogs.[5] Because of this increased utilization and the potential threats posed by uncontrolled consumption of counterfeit or illegal analogs, the first studies relying on LC-ESI-MS/MS protocols have recently looked at the environmental occurrence of EDS drugs in wastewater streams.[4,6] The presence of all three erectile dysfunction treatment drugs was reported in domestic wastewater effluents at low ng/l concentrations.[4] Invariably, SDF was the most commonly detected EDS compound among the three aforementioned drugs likely

* Correspondence to: Sandra Pérez Solsona, IDAEA-CSIC, Department of Environmental Chemistry, Jordi Girona 18-26, Barcelona 08034, Spain. E-mail: spsqam@idaea.csic.es

a IDAEA-CSIC, Department of Environmental Chemistry, Jordi Girona 18-26, Barcelona 08034, Spain

b Florida International University, 11200 SW 8th Street, Miami, Florida 33199-0001, USA

c IQAC-CSIC, Department of Biomedicinal Chemistry, Jordi Girona 18-26, Barcelona 08034, Spain

d Catalan Institute of Water Research, c/Emili Grahit, 101, Edifici H_2O, Parc Científic i Tecnològic de la Universitat de Girona, Girona 17003, Spain

e King Saud University, BOX 2455, Riyadh 11451, Saudi Arabia

Journal of MASS SPECTROMETRY

reflecting prescription trends or the availability of generic formulations. Interestingly, concentrations of sildenafil (SDF) in discharges from fitness centers in Germany[6] were remarkably higher (up to 2082 ng/l), and positive detection of the most relevant human metabolites (i.e. N-demethyl-, N,N-deethyl- and hydroxypropyl SDF) was also accomplished. Because these changes are often small and in substructures easily targeted by biotic and abiotic degradation, metabolites with common structures are likely. Tracking the approved or nonapproved analogs becomes then a function of how well characterized the degradation pathway is when the parent compound is no longer present in the sample, be it due to extensive metabolic clearance in humans or environmental degradation.

With this in mind, the specific goals of this study were to evaluate the susceptibility of SDF and its human key metabolite N-demethylsildenafil (DM-SDF)[7] (Table 1) to undergo phototransformations under the influence of simulated sunlight and to identify their potential photoproducts using the high-resolution MS capabilities of a UPLC-ESI-QToF-MS system in conjunction with MS/MS experiments. In addition, the use of an APCI source to interface an LC system with a QqQ-MS instrument afforded complementary structural information for an unusual heat-sensitive photoproduct. Inclusion of the metabolite, which lacks the N-methyl group in the piperazine, in photodegradation studies conducted in parallel was believed to facilitate the interpretation of the product ion spectra of the photoproducts of the parent drug and to aid in rationalizing the degradation pathways because for several fluoroquinoline antibiotics the piperazine moiety contained therein had been shown to be the preferred target for photolytic processes.[8–11] Thus, SDF and DM-SDF were expected to yield a number of photoproducts of identical chemical structure arising from the light-induced destruction of the aliphatic heterocycle.

EXPERIMENTAL

Chemical Reagents

SDF (CAS No. 171599-83-0) and DM-SDF (CAS No. 139755-82-1) were purchased from Toronto Research Chemicals (Toronto, Canada). All organic solvents used for UPLC were Chromasol LC grade or equivalent. Ultrapure water and LC/MS-grade formic acid were purchased from Sigma Aldrich (Munich, Germany). LC-grade acetonitrile was purchased from Riedel de Häen (Steinheim, Germany). Analytical-grade inorganic salts were obtained from Merck (Darmstadt, Germany).

Phototransformation experiments

Phototransformation experiments were conducted in a Suntest CPS solar simulator (Heraeus, Hanau, Germany) equipped with a Xenon lamp. By using the appropriate window glass filters, the device emitted radiation across a wavelength spectrum similar to that of natural solar radiation. Test solutions of SDF and DM-SDF were prepared at 10 mg/l in ultrapure water; artificial freshwater (AFW), which resembled a moderately hard water (96 mg/l $NaHCO_3$, 60 mg/l $CaSO_4 \cdot 2H_2O$, 60 mg/l $MgSO_4$ and 4 mg/l KCl; pH 6.9); and natural river water (RW, pH 7.6) (see Table S1 for physicochemical characterization). Test solutions were irradiated in capped quartz tubes (not airtight) for up to 48 h. Positive dark control solutions containing the target analyte in the appropriate matrix (HPLC, AFW or RW) and negative irradiated control solutions containing only the matrix were kept inside the exposure chamber to mimic the temperature conditions. Subsamples of dark controls and blanks were taken at the same time points as those from the irradiation experiments. SDF and DM-SDF concentrations remained constant in the dark controls over the test period, and no biotic or thermal degradation products were observed in the vials (data not shown). Identification of the degradates was accomplished by high-resolution MS/MS using a QToF-MS instrument in conjunction with additional experiments on an APCI-QqQ-MS system. To obtain sufficiently intense fragment ions for accurate mass measurements, selected samples were preconcentrated by freeze-drying prior to QToF-MS/MS analysis.

UPLC-ESI-QToF-MS Analysis

Chromatographic separation was performed on a Waters Acquity BEH C_{18} column (50 × 2.1 mm, 1.7 μm particle size) equipped with a guard column (5 × 2.1 mm) of the same packing material. The mobile phases were (A) 0.1% HCOOH and (B) acetonitrile. After 1 min isocratic conditions at 90% A, the proportion of A was linearly decreased to 70% within 3 min. The percentage of A was then maintained at 70% and held for 0.3 min. The initial mobile phase composition was reestablished within 0.7 min followed by a 1.0 min equilibration step at 90% A. The flow rate was 300 μl/min, and the injection volume was 10 μl. Exact mass measurements of SDF, DM-SDF and their phototransformation products formed in the irradiation device were carried out on a Micromass ESI-QToF-system interfaced with a Waters Acquity UPLC system (Micromass, Manchester, UK). All accurate mass measurements were conducted in the positive ion mode. The source parameters were as follows: capillary voltage: +3500 V; nebulizer gas flow: 50 l/h; drying gas flow: 600 l/h; dry gas temperature: 350 °C; ion source block temperature: 120 °C. The ToF analyzer was operated at a resolution of 5000 (full width at half maximum), calculated for the internal lock mass Tyr-Val-Tyr ($[M+H]^+ = m/z$ 380.2185). ESI^+ mass spectra were recorded in 1-s intervals, with automatic switching of the dual sprayer every 11 s for infusion of the lock mass for a duration of 1 s. External mass calibration for positive ESI mode was conducted daily prior to analysis for the mass range of m/z 80–900, infusing a mixture of acetonitrile/0.1 M NaOH/10% HCOOH (98 : 1 : 1) at a flow rate of 10 μl/min. All data acquisition and processing was done using the software package MassLynx V4.0.

LC-QqQ-MS analysis

Quantification of the two test compounds for kinetic analysis (Table S2) was accomplished using a Transcend LC system coupled to a TSQ Quantum Vantage triple–quadrupole MS (both from Thermo Fisher Scientific, San José, CA, USA) equipped with an ESI source. For (+)-APCI experiments, the vaporizer temperature of the source was set to 400 °C. The photoproducts were separated on a HALO C_{18} fused-core technology column (50 × 2.1 mm, 2.7 μm particle size) (Advanced Material Technology, Wilmington, USA). The mobile phases were (A) 0.1% HCOOH and (B) acetonitrile. After 0.5 min isocratic conditions at 90% A, the portion of A was linearly decreased to 50% within 7.0 min. Then, the column was washed at 90% of B for 0.67 min. The initial mobile phase composition was reestablished within 0.25 min followed by 3 min equilibration at 90%. The flow rate was 300 μl/min, and the injection volume was 10 μl. The Xcalibur software version 2.07 (Thermo Fisher Scientific, San José, CA, USA) was used to control the LC/MS system and to process the data.

Table 1. Proposed chemical structures of photoproducts of sildenafil (SDF) and N-demethylsildenafil (DM-SDF)

Structure	Retention time (min)	SDF (R = CH_3) $[M+H]^+$ ($[M_D+D]^+$)	DM-SDF (R = H) $[M+H]^+$ ($[M_D+D]^+$)
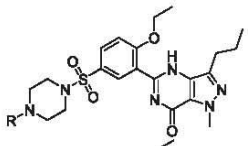	3.07 (SDF) 3.05 (DM-SDF)	SDF *m/z* 475 (*m/z* 477 [1])	DM-SDF *m/z* 461 (m/z 464 [2])
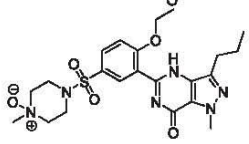	3.11	TP490 *m/z* 491 (*m/z* 493 [±0])	Not possible
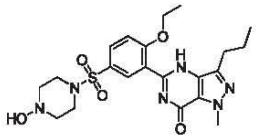	3.38	Not detected	TP476 *m/z* 477 (*m/z* 480 [±0])
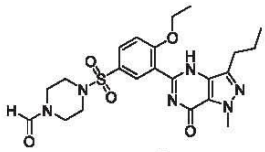	3.62	TP488-C *m/z* 489 (*m/z* 491 [±0])	Not possible
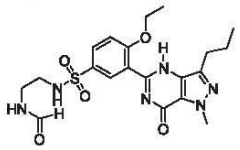	3.27	TP462 *m/z* 463 (*m/z* 467 [+2])	TP462 *m/z* 463 (*m/z* 467 [+1])
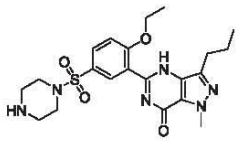	3.06	TP460 *m/z* 461 (DM-SDF) (*m/z* 464 [+1])	(Parent compound)
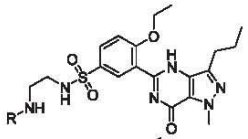	2.88	TP448-A *m/z* 449 (*m/z* 453 [+2])	(see TP434)
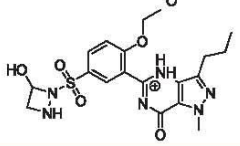	3.39	Not detected	TP448-B *m/z* 449 (*m/z* 453 [+1])

(Continues)

Journal of MASS SPECTROMETRY

Table 1. *(Continued)*

Structure	Retention time (min)	SDF (R = CH_3)	DM-SDF (R = H)
		$[M + H]^+$	$[M + H]^+$
		($[M_D + D]^+$)	($[M_D + D]^+$)
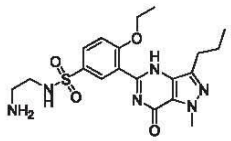	2.89	TP434 *m/z* 435 (*m/z* 440 [+3])	TP434 *m/z* 435 (*m/z* 440 [+2])
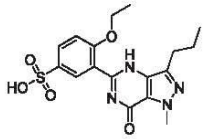	2.76	TP392 *m/z* 393 (*m/z* 396 [+1])	TP392 *m/z* 393 (*m/z* 396 [±0])
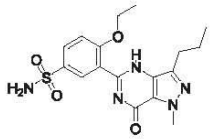	3.40	TP391 *m/z* 392 (*m/z* 396 [+2])	TP391 *m/z* 392 (*m/z* 396 [+1])

Number in square brackets after *m/z* value of $[M_D + D]^+$ ion denotes number of exchangeable hydrogen atoms (parent compounds) or change of number of exchangeable hydrogen atoms relative to parent compounds (photoproducts).

Hydrogen/deuterium-exchange experiments

Besides the acquisition of high mass accuracy MS/MS data, hydrogen/deuterium (H/D)-exchange studies were carried out to determine the number of exchangeable hydrogen atoms in each of the photoproducts. To determine the shifts of the *m/z* values of the molecular ions $[M_D + D]^+$, aliquots of the irradiated 2- and 8-h samples of SDF and DM-SDF in ultrapure water were solvent exchanged to D_2O/CD_3COOD (0.3%) and chromatographically separated using the aforementioned UPLC system (Water Acquity). The mobile phases consisted of (A) D_2O with 0.3% CD_3COOD and (B) acetonitrile.

RESULTS AND DISCUSSION

Fragmentation pattern of SDF and DM-SDF

Following (+)ESI, the acquisition of the product ion spectrum of the protonated SDF molecule gives rise to a number of characteristic fragment ions (Fig. 1A and B), in accordance with previous reports.[4,12,13] The base peak with *m/z* 100 corresponds to the piperazine radical cation deriving from the homolytic cleavage of the sulfonamide bond, whereas heterolytic cleavage and simultaneous proton abstraction of a hydrogen atom from the α-carbon atom by the sulfone–oxygen produce the ion *m/z* 99. If the latter mechanism takes place while the positive charge is located in the other part of the molecule, the ion at *m/z* 377 is generated. Ring-cross fragmentation within the piperazine, commonly observed for this heterocyclic basic amine, leads to the fragment ion at *m/z* 58. As will be illustrated later, this characteristic fragmentation of the photolytically modified piperazine ring provides valuable information facilitating the structural elucidation of the main SDF photoproducts. Besides these low-mass ions, a set of three fragment ions at *m/z* 283, 299 and 311 is also observed upon collision-induced dissociation of the protonated SDF. These are attributed to the cleavage of the sulfonamide from the aromatic ring (*m/z* 311), whereas concurrent loss of the hydrocarbon chain from the ethoxy group generates *m/z* 283 (Table 2). Rationalizing the formation of the fragment ion at *m/z* 299 ($C_{15}H_{15}N_4O_3$) is less straightforward but can be attributed to the C–O cleavage in the ethoxy group (as in *m/z* 313) and rearrangement of the sulfonamide group involving shift of an oxygen atom to the aromatic ring and hydrogen transfer to the leaving group. The resulting hydroquinone can be stabilized through hydrogen shift, forming a structure with an extended π-electron system (Fig. 1B). The three SDF fragment ions (*m/z* 311, 299 and 283) are a common feature in the mass spectra of most of the photoproducts detected in this study and thus served as a fingerprint to differentiate light-induced structural changes in the phenyl pyrazolopyrimidinone area from those occurring in the piperazine ring. The (+)ESI mass spectrum of DM-SDF exhibits a pattern very similar to that of SDF (Fig. 1B): Fragment ions lacking the piperazine ring are common for both compounds, namely, *m/z* 377, 311, 299 and 283. On the other hand, those ions that originate from cleavage of the sulfonamide linkage upon charge retention in the piperazine differ by 14 Da, i.e. the nominal mass of the CH_2 group (Table 3).

Identification of the photoproducts of SDF and DM-SDF

In view of the reported occurrence of both SDF and DM-SDF in wastewaters,[4,6] the photodegradability of the two test

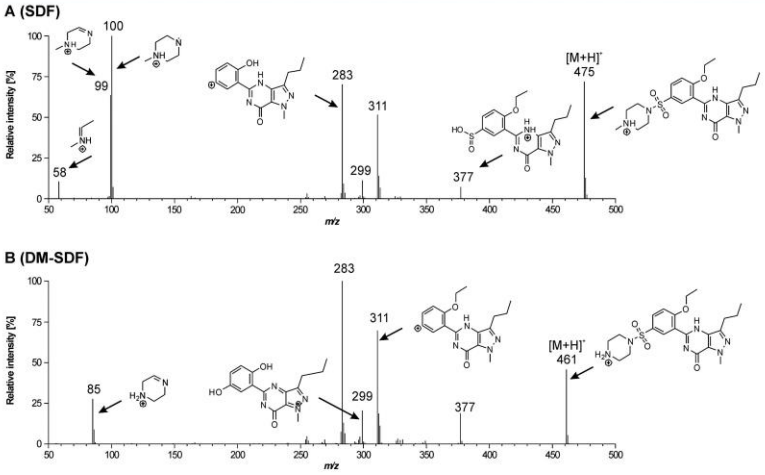

Figure 1. (+)ESI-MS/MS spectra of (A) sildenafil and (B) N-demethylsildenafil.

compounds was evaluated not only in ultrapure water but also in AFW and natural river water. The degradation profiles indicate substantially slower kinetics in matrix-free water as compared with the other two test media (Fig. S1). That these quantitative differences are due to the presence of catalytically acting matrix components in the two media of more complex composition rather than a reflection of distinct photolytical pathways is supported by the observation that the same set of photoproducts was detected regardless of the type of water.

Irradiation of the aqueous solutions of SDF and DM-SDF with artificial sunlight yielded several transformation products (Fig. S2 illustrates chromatographic separation). By combining the accurate mass data and the MS^2 fragmentation patterns with the knowledge on the photodegradation pathways of structurally related compounds (ciprofloxacin and enrofloxacin[8,10,11]), plausible chemical structures for most of the photoproducts were proposed. In the following section, the mass spectral data of the analytes are discussed in the order of decreasing structural similarity to the parent compound. This approach reveals that the piperazine ring is gradually broken down, giving rise to a sulfonated pyrazolopyrimidinone as one of the key intermediates.

The photoproduct TP460 (*m/z* 461) at 3.05 min (Tables 1 and 2), which is hidden under the chromatographic peak of the coeluting SDF, differs in elemental composition by the loss of CH_2 and the gain of one additional exchangeable hydrogen atom ($[M_D + D]^+$ at *m/z* 464). In its (+)ESI-MS^2 spectrum (Fig. 2B), the characteristic SDF ion at *m/z* 99 is shifted to *m/z* 85, indicating that the piperazine ring underwent N-demethylation (TP460) to form DM-SDF. In contrast, the mass spectra of TP488-A (2.61 min) and TP488-B (2.94 min) in turn displayed the fragment ions *m/z* 99 and 100, suggesting structural modification in the right part of the parent molecule (spectra not shown). Unspecific fragmentation did not allow to further assign the site of modification for TP488-A and TP488-B. A third isobaric photoproduct for SDF, TP488-C (3.62 min, not detected in DM-SDF samples), was postulated to originate directly from the parent compound by oxidation of the N-methyl group ($C_{22}H_{31}N_6O_5S$; Tables 1 and 2). The observation of the diagnostic ion series with *m/z* 311, 299 and 283 and the key fragment ion at *m/z* 461 in the product ion profile (Fig. 2C) led to propose the well-known mechanism of hydrogen abstraction by hydroxyl radical and formation of an amide.[11] The fragment ion at *m/z* 461 is formed by neutral loss of CO from the amide, whereas *m/z* 85 is attributed to the piperazine ring, once the molecular ion has lost CO.

As for the TP490 (*m/z* 491), the accurate mass measurement indicates oxygenation of SDF (Table 1), possibly yielding a hydroxylated photoproduct. A first visual examination of the (+) ESI mass spectrum (Fig. 2D), however, indicates that the substructures on either side of the sulfone group are apparently intact: On the one hand, the characteristic SDF fragments ions at *m/z* 283, 297, 311 and 377 are present, whereas on the other hand, the detection of an intense fragment ion at *m/z* 99 is indicative of cleavage of the N-methylpiperazine ring from the sulfone (see Fig. 1A for assignment of respective ion structures). The only distinct fragment ion with respect to the SDF mass spectrum is detected at *m/z* 404, with a likely empirical formula resulting from the elimination of C_4H_9NO out of the $[M+H]^+$ (Table 2). A first hint that TP490 does not correspond to hydroxylation of an aliphatic or aromatic carbon atom is the fact that TP490 eluted slightly after the parent compound (3.11 min *vs* 3.07 min for SDF). The formation of a C-hydroxylated product would have rendered the molecule more polar and thus less chromatographically retained on the reversed-phase column. At this point, H/D-exchange experiments proved very valuable as they revealed TP490 to bear an identical number of exchangeable hydrogen atoms as SDF (Table 1), therefore allowing to definitively preclude C-hydroxylation. Considering the elution order, a hypothetical epoxidation of a double bond in the phenyl ring is also unlikely. The formation of an N-oxide, i.e. oxygenation of a tertiary amine, in turn matches the observed chromatographic pattern: N-oxides behave more like neutral compounds under acidic LC conditions and thus are generally eluted after the parent compound in which protonation of the basic amine (mobile phase pH of 3) leads to a charged, hence more polar, species.[14] To gather additional evidence for

Journal of MASS SPECTROMETRY

Table 2. Accurate ion mass measurements of sildenafil and its phototransformation products obtained by UPLC-(+)ESI-QToF-MS in MS and MS/MS mode

Compound/Photoproduct	Measured ion mass of $[M+H]^+$	Elemental composition	Theoretical ion mass (*m/z*)	Relative error (ppm) (double bond equivalent (DBE))
SDF	475.2128	$C_{22}H_{31}N_6O_4S$	475.2132	+1.9 (10.5)
	377.1285	$C_{17}H_{21}N_4O_4S$	377.1279	+1.6 (9.5)
	311.1514	$C_{17}H_{19}N_4O_2$	311.1503	+3.5 (10.5)
	299.1153	$C_{15}H_{15}N_4O_3$	299.1139	+4.7 (10.5)
	283.1183	$C_{15}H_{15}N_4O_2$	283.1190	−2.5 (10.5)
	100.1033	$C_5H_{12}N_2$	100.0995	+38 (1.0)
	99.0938	$C_5H_{11}N_2$	99.0917	+21.2 (1.5)
TP490	491.2089	$C_{22}H_{31}N_6O_5S$	491.2072	+3.5 (10.5)
	473.1948	$C_{22}H_{29}N_6O_4S$	473.1966	−3.8 (11.5)
	404.1382	$C_{18}H_{22}N_5O_4S$	404.1387	−1.2 (10.5)
	377.1285	$C_{17}H_{21}N_4O_4S$	377.1279	+1.6 (9.5)
	311.1518	$C_{17}H_{19}N_4O_2$	311.1503	+4.8 (10.5)
	299.1152	$C_{15}H_{15}N_4O_3$	299.1139	+4.3 (10.5)
	283.12.5	$C_{15}H_{15}N_4O_2$	283.1190	+4.6 (10.5)
	100.1012	$C_5H_{12}N_2$	100.0995	+17 (1.0)
	99.0940	$C_5H_{11}N_2$	99.0917	+28.3 (1.5)
TP488-C	489.1952	$C_{22}H_{29}N_6O_5S$	489.1910	+4.5 (11.5)
	461.1997	$C_{21}H_{29}N_6O_4S$	461.1966	+6.7 (10.5)
	377.1296	$C_{17}H_{21}N_4O_4S$	377.1279	+4.5 (9.5)
	311.1511	$C_{17}H_{19}N_4O_2$	311.1503	+2.6 (10.5)
	299. 1146	$C_{15}H_{15}N_4O_3$	299.1139	+2.3 (10.5)
	283. 1183	$C_{15}H_{15}N_4O_2$	283.1190	−2.5 (10.5)
	85.0727	$C_4H_9N_2$	85.0760	−38.8 (1.5)
TP462	463.1777	$C_{20}H_{27}N_6O_5S$	463.1758	+4.1 (10.5)
	435.1836	$C_{19}H_{27}N_6O_4S$	435.1809	+4.1 (9.5)
	418.1517	$C_{19}H_{24}N_5O_4S$	418.1544	−6.5 (10.5)
	311.1530	$C_{17}H_{19}N_4O_2$	311.1503	+8.7 (10.5)
	299.1155	$C_{15}H_{15}N_4O_3$	299.1139	+5.3 (10.5)
	283.1178	$C_{15}H_{15}N_4O_2$	283.1190	−4.2 (10.5)
TP460	461.1986	$C_{21}H_{29}N_6O_4S$	461.1966	+4.3 (10.5)
	377.1285	$C_{17}H_{21}N_4O_4S$	377.1279	+1.6 (9.5)
	311.1511	$C_{17}H_{19}N_4O_2$	311.1503	+2.6 (10.5)
	283.1185	$C_{15}H_{18}N_4O_2$	283.1190	−1.8 (10.5)
	85.0769	$C_4H_9N_2$	85.0760	+9.4 (1.5)
TP448-A	449.2163	$C_{20}H_{29}N_6O_4S$	449.1966	+5.1 (9.5)
	418.1529	$C_{19}H_{24}N_5O_4S$	418.1544	−3.6 (10.5)
	392.1363	$C_{19}H_{24}N_5O_4S$	392.1387	−6.1 (9.5)
	377.1290	$C_{17}H_{21}N_4O_4S$	377.1279	+2.9 (9.5)
	311.1489	$C_{17}H_{19}N_4O_2$	311.1503	−4.5 (10.5)
	299. 1151	$C_{15}H_{15}N_4O_3$	299.1139	+4.0 (10.5)
	283. 1203	$C_{15}H_{15}N_4O_2$	283.1190	+4.6 (10.5)
TP434	435.1834	$C_{19}H_{27}N_6O_4S$	435.1814	+5.7 (9.5)
	418.1567	$C_{19}H_{24}N_5O_4S$	418.1544	+5.5 (10.5)
	392.1451	$C_{17}H_{22}N_5O_4S$	392.1387	+5.6 (9.5)
	377.1245	$C_{17}H_{21}N_4O_4S$	377.1279	−9.0 (9.5)[a]
	311.1516	$C_{17}H_{19}N_4O_2$	311.1503	+4.2 (10.5)
	299. 1159	$C_{15}H_{15}N_4O_3$	299.1139	+6.7 (10.5)
	283.1205	$C_{15}H_{15}N_4O_2$	283.1190	+5.3 (10.5)
TP392	393.1234	$C_{17}H_{21}N_4O_5S$	393.1227	+1.5 (9.5)
	365.0903	$C_{15}H_{17}N_4O_5S$	365.0914	−3.0 (9.5)
	336.0637	$C_{14}H_{14}N_3O_5S$	336.0649	−3.6 (9.5)
	284.1279	$C_{15}H_{16}N_4O_2$	284.1268	3.9 (10.0)
	256.1070	$C_{14}H_{14}N_3O_2$	256.1081	−4.3 (9.5)
TP391	392.1365	$C_{17}H_{22}N_5O_4S$	392.1387	−5.6 (9.5)
	364.1056	$C_{15}H_{18}N_5O_4S$	364.1079	−6.3 (9.5)
	299.1157	$C_{15}H_{15}N_4O_3$	299.1139	+6.0 (10.5)
	283.1169	$C_{15}H_{15}N_4O_2$	283.1190	−7.4 (10.5)

Table 3. Accurate ion mass measurements of N-demethylsildenafil and its phototransformation products of obtained by UPLC-(+)ESI-QToF-MS in MS and MS/MS mode

Compound/Photoproduct	Measured ion mass of $[M+H]^+$	Elemental composition	Theoretical ion mass (*m/z*)	Relative error (ppm)
DM-SDF	461.1978	$C_{21}H_{29}N_6O_4S$	461.1966	+2.6 (10.5)
	377.1270	$C_{17}H_{21}N_4O_4S$	377.1279	−2.4 (9.5)
	311.1518	$C_{17}H_{19}N_4O_2$	311.1503	+4.8 (10.5)
	299.1155	$C_{15}H_{15}N_4O_3$	299.1139	+5.3 (10.5)
	283.1203	$C_{15}H_{15}N_4O_2$	283.1190	+4.6 (10.5)
	85.0803	$C_4H_9N_2$	85.0760	−11.8 (1.5)
TP476	477.1959	$C_{21}H_{29}N_6O_5S$	477.1915	+9.2 (10.5)
	404.1404	$C_{18}H_{22}N_5O_4S$	404.1387	+7.9 (10.5)
	377.1295	$C_{17}H_{21}N_4O_4S$	377.1278	+4.5 (9.5)
	331.0836	$C_{15}H_{15}N_4O_3S$	331.0865	−5.7 (10.5)
	312.1597	$C_{17}H_{20}N_4O_2$	312.1581	+5.1 (10.0)
	283.1205	$C_{15}H_{15}N_4O_2$	283.1190	+4.6 (10.5)
	83.0628	$C_4H_7N_2$	83.0604	+28.9 (2.5)
TP462	463.1777	$C_{20}H_{27}N_6O_5S$	463.1758	+4.1 (10.5)
	435.1839	$C_{19}H_{27}N_6O_4S$	435.1809	+6.9 (9.5)
	418.1569	$C_{19}H_{24}N_5O_4S$	418.1544	+6.0 (10.5)
	311.1520	$C_{17}H_{19}N_4O_2$	311.1503	+5.5 (10.5)
	299. 1122	$C_{15}H_{15}N_4O_3$	299.1139	−5.7 (10.5)
	283.1175	$C_{15}H_{15}N_4O_2$	283.1190	−5.3 (10.5)
TP448-B	449.1620	$C_{19}H_{25}N_6O_5S$	449.1602	+4.0 (10.5)
	431.1507	$C_{19}H_{23}N_6O_4S$	431.1496	+2.6 (11.5)
	404.1393	$C_{18}H_{22}N_5O_4S$	404.1387	+0.2 (10.5)
	311.1519	$C_{17}H_{19}N_4O_2$	311.1503	+5.1 (10.5)
	299.1122	$C_{15}H_{15}N_4O_3$	299.1139	−5.7 (10.5)
	283.1206	$C_{15}H_{15}N_4O_2$	283.1190	+5.7 (10.5)
TP434	435.1801	$C_{19}H_{25}N_6O_5S$	435.1810	−2.1 (9.5)
	418.1539	$C_{19}H_{22}N_5O_4S$	418.1544	−1.2 (10.5)
	392.1353	$C_{17}H_{22}N_5O_4S$	392.1387	−8.7 (9.5)
	377. 1281	$C_{17}H_{21}N_4O_4S$	377.1279	+0.5 (9.5)
	311.1514	$C_{17}H_{19}N_4O_2$	311.1503	+3.5 (10.5)
	299.1126	$C_{15}H_{15}N_4O_3$	299.1139	−4.3 (10.5)
	283.1197	$C_{15}H_{15}N_4O_2$	283.1190	+2.5 (10.5)
TP392	393.1248	$C_{17}H_{21}N_4O_5S$	393.1227	+5.3 (9.5)
	365.0922	$C_{15}H_{17}N_4O_5S$	365.0914	+2.2 (9.5)
	336.0627	$C_{14}H_{14}N_3O_5S$	336.0649	−6.5 (9.5)
	284.1290	$C_{15}H_{16}N_4O_2$	284.1268	7.7 (10.0)
	256.1060	$C_{14}H_{14}N_3O_2$	256.1081	−8.2 (9.5)
TP391	392.1405	$C_{17}H_{22}N_5O_4S$	392.1387	+3.1 (9.5)
	364.1105	$C_{15}H_{18}N_5O_4S$	364.1079	−0.5 (9.5)
	299.1158	$C_{15}H_{15}N_4O_3$	299.1139	+6.4 (10.5)
	283.1172	$C_{15}H_{15}N_4O_2$	283.1190	−6.4 (10.5)

N-oxidation, full-scan MS data were acquired on the QqQ-MS under (+)APCI conditions where N-oxides, which are frequently encountered metabolites of small molecule drugs containing tertiary amines or aromatic heterocycles, undergo thermal deoxygenation in the ion source.[15,16] The full-scan mass spectrum recorded at a vaporizer temperature of 400 °C (Fig. 3A) reveals the characteristic loss of the oxygen atom from the molecular ion, whereas thermal dehydration also occurs to some extent. Both heat-induced in-source decomposition processes have been reported for the (+)APCI full-scan spectra of the N-oxides of clozapine[15] and imatinib,[16] which share the N-methylpiperazine moiety with SDF. The acquisition of the pseudo-MS^3 spectrum of the $[M+H\text{-}O]^+$ ion of TP490 yielded a product ion profile (Fig. 3B) that, expectedly, matched the MS^2 spectrum of SDF (Fig. 1A). In conclusion, the experimental findings provide strong evidence for oxygenation of the N-methyl group in the piperazine ring.

The TP448-A (absent in the irradiated DM-SDF samples) with a retention time of 2.88 min is 26 Da lighter than SDF, thus corresponding to formal elimination of C_2H_2 (Tables 1 and 2). The fragmentation pattern (Fig. 2A) shows the characteristic set of *m/z* 311, 299 and 283 but does not produce any ion in the low mass range in which the piperazine-related fragment ions have been observed for the aforementioned analytes. The absence of such a diagnostic ion is indicative of the decomposition of the aliphatic ring, indicating that TP448-A is the product of an N,N-deethylation reaction. Elimination of the ethylene bridge connecting the two nitrogen atoms in the piperazine is in agreement with the increase in the number of exchangeable hydrogens by two counts (Table 1). In its product ion profile, the

Journal of MASS SPECTROMETRY

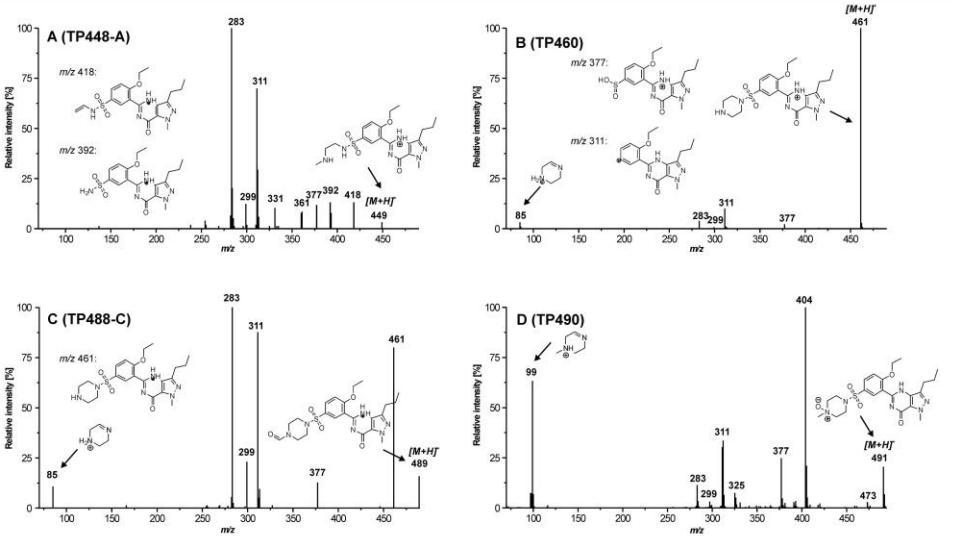

Figure 2. (+)ESI-MS/MS spectra of photoproducts formed by sildenafil (not detected in studies on demethylsildenafil): (A) TP448-A, (B) TP460, (C) TP488-C and (D) TP490. Assignment of site of protonation/charge is tentative.

detection of *m/z* 418 arises then from the elimination of aminomethane (31 Da), and further loss of acetylene produces the ion at *m/z* 392 (Table 2). With respect to the fragment ion at *m/z* 377, this sulfinic acid is the result of S–N bond cleavage as postulated earlier for SDF (Fig. 1A). Interestingly, the TP448-A is identical in structure to the major metabolite identified in pharmacokinetic studies in humans (referred to as UK-150,564 in[17]) and was reported to occur in raw and treated sewage.[6]

As far as the photoproduct TP434 is concerned, its mass spectrum (Fig. 4C) closely resembles the one of TP448-A and can be considered as deriving from N-demethylation of TP448-A ($C_{19}H_{27}N_6O_4S$; Table 2). Similarly to the coelution of SDF and its N-demethylation product TP460, the chromatographic behaviors of TP448-A (2.88 min) and its N-demethyl analog TP434 (2.86 min) are almost identical. The fact that both compound pairs remain virtually unresolved under the applied gradient elution can be attributed to the fact that the decrease in lipophilicity, caused by the loss of the methyl group, is apparently compensated for by a concurrent reduction in basicity of the nitrogen atom, which in turn enhances the retention in the acidic mobile phase. Conversely, the formation of TP462 (3.27 min) can be thought of as to derive either from TP488-C by loss of the ethylene bridge or by oxidation of the methyl group in TP448-A. Apart from these two reaction sequences, a third mechanism involving oxidative C–C bond cleavage of the ethylene bridge is likely to contribute to the formation of TP462 because this photoproduct is also generated during light exposure of DM-SDF (Tables 2 and 3). In this instance, the carbonyl C-atom can only originate from the CH_2 group as the demethylated metabolite of SDF lacks the methyl group. Regarding the MS^2 spectrum of TP462, the fragment ion at *m/z* 435 (Fig. 4D) is assigned to be formed by cleavage of the amide bond, whereas the set of diagnostic signals at *m/z* 311, 299 and 283 confirms the absence of modifications beyond the sulfonamide group.

The (+)ESI-MS^2 spectrum of TP392 (2.76 min; DM-SDF: TP392) in Fig. 4B is consistent with hydrolysis of the sulfonamide bond,

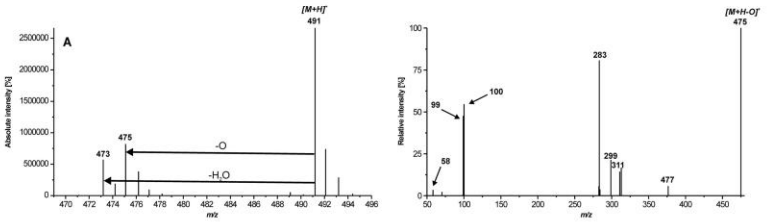

Figure 3. (A) Background-subtracted (+)APCI-MS spectrum of TP490 illustrating the in-source fragmentation of the [M + H] + ion. (B) (+)APCI-pseudo MS3 spectrum on deoxygenated TP490 ([M + H-O] + at *m/z* 475). The vaporizer temperature of the APCI source was set to 400 °C (data acquisition on QqQ-MS instrument).

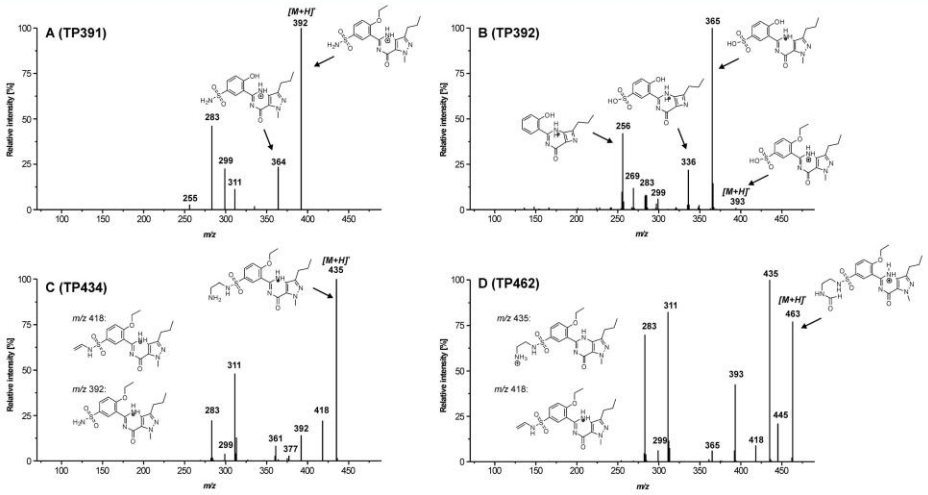

Figure 4. (+)ESI-MS/MS spectra of photoproducts common to sildenafil and demethylsildenafil: (A) TP391, (B) TP392, (C) TP434 and (D) TP462. Assignment of site of protonation/charge is tentative.

which eventually results in a sulfonic acid.[18] Therefore, the collision-induced dissociation (Table 2) can be rationalized as loss of C_2H_4 from the ethoxy side chain (base peak at *m/z* 365) in analogy to the formation of *m/z* 283 out of *m/z* 311, followed by ring contraction of the pyrazole upon expulsion of methanimine (29 Da), thereby generating *m/z* 336. In the next step, SO_3 (80 Da) is released from the aromatic ring to produce the second most intense fragment ion at *m/z* 256 (Table 2). Additional evidence for the structure of TP392 was provided by the product ion spectrum acquired in the (–)ESI mode, showing high ionization efficiency for this strongly acidic species. Upon collision-induced dissociation (spectrum not shown), the deprotonated molecule is proposed to first cleave off methanimine (29 Da) affording *m/z* 362, which is followed by extrusion of SO_2 from the sulfonic acid, thereby generating a phenolic structure with *m/z* 298. Whereas the sulfonic acid TP392 as endproduct of the oxidative breakdown of the piperazine ring is the first to elute among the identified photoproducts, the substantially less polar TP391 (*m/z* 392 in the (+)ESI mode) is detected at 3.40 min in samples from the photolysis experiments of both SDF and DM-SDF (Table 1). The proposed elemental composition of $C_{17}H_{22}N_5O_4S$ (Tables 2 and 3) and the shift in the number of exchangeable hydrogen atoms with respect to the parent compounds (+2 and +1, respectively) suggest formation of the N,N-non-substituted sulfonamide. Besides the diagnostic fragment ions at *m/z* 283, 299 and 311, the product ion mass spectrum shows a neutral loss of C_2H_4 (*m/z* 364) that is most likely cleaved off from the ethoxy group (Fig. 4A).

As the comparison in Table 1 summarizes, DM-SDF formed two photoproducts that were not detectable in any of the irradiated SDF samples. According to the accurate mass measurements, the first one with an $[M+H]^+$ of *m/z* 477 (TP476) corresponds to formal oxygenation of DM-SDF (Table 3). The detection of the ions at *m/z* 283, 299 and 311 points at structural modification in the piperazine ring. This is in agreement with an observed mass shift of the characteristic fragment ion at *m/z* 85 (DM-SDF) to *m/z* 83 in the mass spectrum of TP476 (Fig. 5B). As illustrated earlier in the structural elucidation of the SDF photoproduct TP490, consideration of the elution order and, in particular, interpretation of the findings of the H/D-exchange studies have allowed to propose the chemical structure of the photoproduct with a high level of confidence. An N-hydroxylation of the secondary

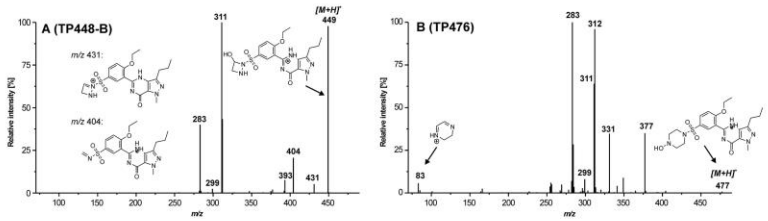

Figure 5. (+)ESI-MS/MS spectra of photoproducts formed by demethylsildenafil (not detected in studies on sildenafil): (A) TP448-B and (B) TP476. Assignment of site of protonation/charge is tentative.

amine in TP476 satisfies both experimental observations: decreased polarity due to loss of the basic character of the amine-nitrogen – and thus stronger retention of TP476 under LC conditions with acidified eluent – and unchanged number of exchangeable hydrogen atoms following insertion of the oxygen atom into the N–H bond (Table 1). The structure of the fragment ion *m/z* 83 can then be rationalized as protonated dihydropyrazine formed by concurrent dehydration of the hydroxylamine and cleavage of the N–S bond in the sulfonamide.

The second phototransformation product being unique to DM-SDF is TP448-B (Table 1). Analysis of its accurate mass data (Table 3) suggests a change in elemental composition consisting of a loss of C_2H_4 and a gain of one oxygen atom. In the (+)ESI-MS^2 spectrum (Fig. 5A), the elimination of water from the protonated molecule (*m/z* 431) indicates the presence of a hydroxyl group. Detection of the diagnostic fragment ions *m/z* 283, 299 and 311 but absence of *m/z* 85 as indicator of an intact piperazine ring point to light-induced modification within the latter. The H/D-exchange data, however, reveal that the number of exchangeable hydrogen atoms remains unchanged with respect to DM-SDF (Table 1). Thus, the apparent loss of the ethylene group (C_2H_4) does not imply the generation of additional N-bound hydrogens. A plausible structure that takes into account these conclusions is based on a contracted four-membered ring with an N–N single bond (Table 1). The formation of the fragment ion detected at *m/z* 404 likely originates from dehydration upon formation of the C–N double bond (see Fig. 5A) followed by cross-ring cleavage.

The stepwise photolytic decomposition of the (N-methyl)piperazine moiety described here for SDF and DM-SDF has been reported for other pharmaceuticals likewise bearing a piperazine ring, namely fluoroquinoline antibiotics.[8–11] Stable intermediates formed during the irradiation of an aqueous solution of enrofloxacin with a Xe lamp (use of identical Suntest CPS apparatus as in the current work) originated from N-deethylation in analogy to the formation of DM-SDF (TP460) and subsequent destruction of the ring upon loss of the bridging ethylene (TP434 for SDF).[8] Further photolytic breakdown of this species by N-dealkylation resulted in the unsubstituted aromatic amines. However, the formation of a lactone in the piperazine ring of enrofloxacin is not observed here for SDF. Recently, Paul and coworkers[9] reported on the effects of photolytic and photocatalytic treatment processes on the antibacterial activity of ciprofloxacin solutions exposed to UVA-VIS or VIS light. Characterization of the transformation products by QToF-MS led to postulate oxidative opening of the piperazine with formation of mono- and dialdehydes. The cleavage of the sulfonamide bond in SDF (TP392), eventually leading to the sulfonic acid, is corroborated by previous findings on the photodegradation of the antibiotic sulfamethoxazole under simulated solar radiation.[18] Based on fragmentation patterns and accurate mass data provided by ToF-MS analysis, two aromatic sulfonic acids were identified with high confidence.

CONCLUSIONS

The findings of the photolysis experiments with SDF and DM-SDF provide sound evidence that the piperazine ring in these molecules can be broken down with relative ease under the influence of artificial sunlight. The various photoproducts identified clearly indicate a stepwise degradation of the aliphatic heterocyclic moiety until reaching the stage of the sulfonic acid as a key intermediate. It is worth noting that the fate of SDF under the photolysis conditions followed a similar route this PDE-5 inhibitor follows in the human body where as many as seven metabolites have been described to arise from oxygenation and N-dealkylation reactions in the piperazine ring,[17] including the photoproducts TP476, TP460 and TP434 (additional human metabolites were reported to correspond to aliphatic hydroxylations in the portion of the molecule beyond the sulfonamide). Taking into consideration this cocktail of human metabolites released into the environment through wastewater discharges, the potential generation of microbial transformation products during the biological sewage treatment – currently being investigated in our group – and the susceptibility of DM-SDF to undergo photoreactions, any attempt to provide a comprehensive evaluation of the environmental fate of SDF will undoubtedly be a very challenging one.

ACKNOWLEDGEMENTS

This work has been funded by the Spanish Ministry of Economy and Competitiveness through the projects SCARCE (Consolider-Ingenio 2010 CSD2009-00065) and CEMAGUA (CGL2007-64551/HID). It reflects only the authors' views, and the European Community is not liable for any use that may be made of the information contained therein. SP acknowledges the contract from the Ramón y Cajal Program of the Spanish Ministry of Economy and Competitiveness. Prof. Barceló acknowledges King Saud University (Riyadh, Saudi Arabia) for his contract position as Visiting Professor.

Supporting Information

Supporting information may be found in the online version of this article.

References

[1] P. H. Howard, D. C. G. Muir. Identifying new persistent and bioaccumulative organics among chemicals in commerce. *Environ. Sci. Technol.* **2010**, *44*, 2277.
[2] P. H. Howard, D. C. G. Muir. Identifying new persistent and bioaccumulative organics among chemicals in commerce II: Pharmaceuticals. *Environ. Sci. Technol.* **2011**, *45*, 6938.
[3] L. S. H. Sheldon, R. A. Hites. Organic compounds in Delaware river. *Environ. Sci. Technol.* **1978**, *12*, 1188.
[4] A. Nieto, M. Peschka, F. Borrull, E. Pocurull, R. M. Marcé, T. P. Knepper. Phosphodiesterase type V inhibitors: Occurrence and fate in wastewater and sewage sludge. *Water Res.* **2010**, *44*, 1607.
[5] S. Singh, B. Prasad, A. A. Savaliya, R. P. Shah, V. M. Gohil, A. Kaur. Strategies for characterizing sildenafil, vardenafil, tadalafil and their analogues in herbal dietary supplements, and detecting counterfeit products containing these drugs. *TrAC Trends Anal. Chem.* **2009**, *28*, 13.
[6] H. Schröder, W. Gebhardt, M. Thevis. Anabolic, doping, and lifestyle drugs, and selected metabolites in wastewater - detection, quantification, and behaviour monitored by high-resolution MS and MS/MS; before and after sewage treatment. *Anal. Bioanal. Chem.* **2010**, *398*, 1207.
[7] D. K. Walker. Pharmacokinetics and metabolism of sildenafil in mouse, rat, rabbit, dog and man. *Xenobiotica* **1999**, *29*, 297.
[8] J. Burhenne, M. Ludwig, M. Spiteller. Polar photodegradation products of quinolones determined by HPLC/MS/MS. *Chemosphere* **1999**, *38*, 1279.
[9] T. Paul, M. C. Dodd, T. J. Strathmann. Photolytic and photocatalytic decomposition of aqueous ciprofloxacin: Transformation products and residual antibacterial activity. *Water Res.* **2010**, *44*, 3121.
[10] K. Tomiainen, C.-P. Askolin, J. Mattinen. Isolation and structure elucidation of an intermediate in the photodegradation of ciprofloxacin. *J. Pharm. Biomed. Anal.* **1997**, *16*, 439.

[11] T. G. Vasconcelos, D. M. Henriques, A. König, A. F. Martins, K. Kümmerer. Photo-degradation of the antimicrobial ciprofloxacin at high pH: Identification and biodegradability assessment of the primary by-products. *Chemosphere* **2009**, *76*, 487.
[12] S. R. Gratz, B. M. Gamble, R. A. Flurer. Accurate mass measurement using Fourier transform ion cyclotron resonance mass spectrometry for structure elucidation of designer drug analogs of tadalafil, vardenafil and sildenafil in herbal and pharmaceutical matrices. *Rapid Commun. Mass Spectrom.* **2006**, *20*, 2317.
[13] W. Weinmann, M. Bohnert, A. Wiedemann, M. Renz, N. Lehmann, S. Pollak. Post-mortem detection and identification of sildenafil (viagra) and its metabolites by LC/MS and LC/MS/MS. *Int. J. Legal Med.* **2001**, *114*, 252.
[14] L. A. Marques, I. Maada, F. J. J. de Kanter, H. Lingeman, H. Irth, W. M. A. Niessen, M. Giera. Stability-indicating study of the anti-alzheimer's drug galantamine hydrobromide. *J. Pharm. Biomed. Anal.* **2011**, *55*, 85.
[15] S. Ma, S. K. Chowdhury, K. B. Alton. Thermally induced N-to-O rearrangement of tert-N-oxides in atmospheric pressure chemical ionization and atmospheric pressure photoionization mass spectrometry: Differentiation of N-oxidation from hydroxylation and potential determination of N-oxidation site. *Anal. Chem.* **2005**, *77*, 3676.
[16] S. Ma, Y. Xu, M. Shou. Characterization of imatinib metabolites in rat and human liver microsomes: Differentiation of hydroxylation from N-oxidation by liquid chromatography/ atmospheric pressure chemical ionization mass spectrometry. *Rapid Commun. Mass Spectrom.* **2009**, *23*, 1446.
[17] G. J. Muirhead, D. J. Rance, D. K. Walker, P. Wastall. Comparative human pharmacokinetics and metabolism of single-dose oral and intravenous sildenafil citrate. *Brit. J. Clin. Pharmacol.* **2002**, *53*, S13.
[18] A. G. Trovó, R. F. P. Nogueira, A. Agüera, C. Sirtori, A. R. Fernández-Alba. Photodegradation of sulfamethoxazole in various aqueous media: Persistence, toxicity and photoproducts assessment. *Chemosphere* **2009**, *77*, 1292.

Supporting Information

Identification of Phototransformation Products of Sildenafil (Viagra) and its N-Demethylated Human Metabolite under Simulated Sunlight

Peter Eichhorn[1], Sandra Pérez[1*], Jaume Aceña[1], Piero Gardinali[2], José Luis Abad[3], Damià Barceló[1,4,5]

[1] IDAEA-CSIC, Department of Environmental Chemistry, Jordi Girona 18-26, Barcelona 08034 (Spain)

[2] Florida International University, 11200 SW 8th Street, Miami, FL 33199-0001 (USA)

[3] IQAC-CSIC, Department of Biomedicinal Chemistry, Jordi Girona 18-26, Barcelona 08034 (Spain)

[4] Catalan Institute of Water Research, c/Emili Grahit, 101, Edifici H_2O, Parc Científic i Tecnològic de la Universitat de Girona, Girona 17003 (Spain)

[5] King Saud University, BOX 2455, Riyadh 11451 (Saudi Arabia)

Table S1: Physico-chemical characterization of the surface water from the Llobregat river (Catalonia, Spain) used in the photodegradation studies. Metals were determined by ICP-MS, nitrate by molecular absorbance spectrophotometry (EAM) in the UV-VIS region, and total organic carbon (TOC) by a Shimadzu TOC-V CPH analyzer.

Parameter	Sant Joan Despi
pH	7.6
Conductivity [μS/cm]	1440
Na^+ [mg/L]	182
K^+ [mg/L]	34
Ca^{2+} [mg/L]	116
Mg^{2+} [mg/L]	32
Sr^{2+} [mg/L]	2.0
Fe^{3+} [μg/L]	<20
NO_3^- [mg/L]	<5
Cl^- [mg/L]	379
TOC [mg/L]	7.5

Figure S-1. Time course of sildenafil degradation in three different aqueous matrices: ultra-pure water (◆), artificial freshwater (○), and natural freshwater (△).

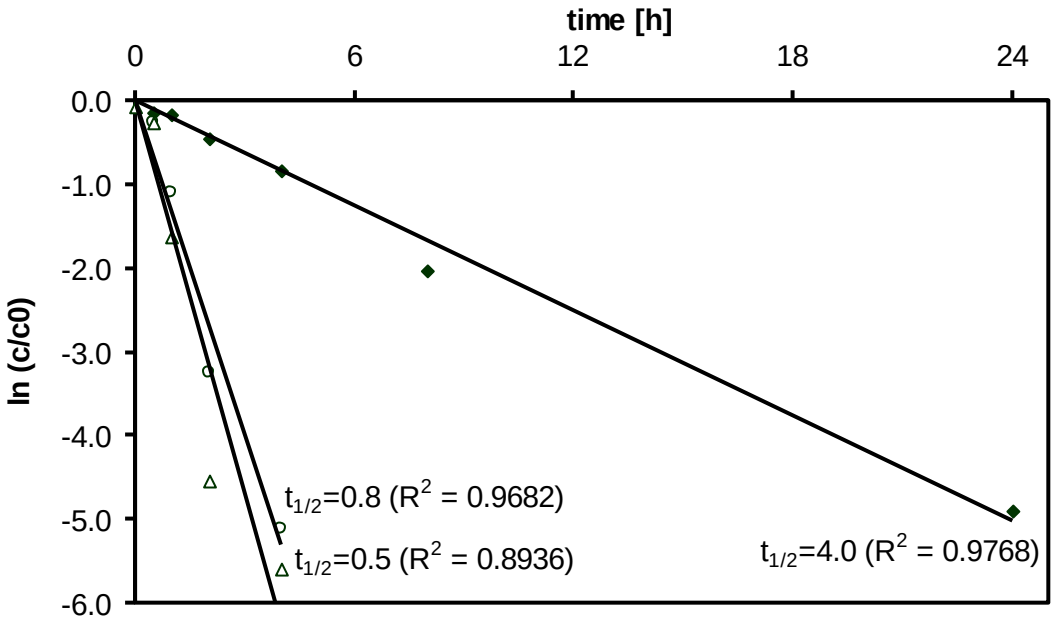

Figure S-2. UPLC-(+)ESI-QToF chromatograms of the samples collected at 0, 60 and 120 min from the irradiated artificial surface water sample spiked with sildenafil at 10 mg/L.

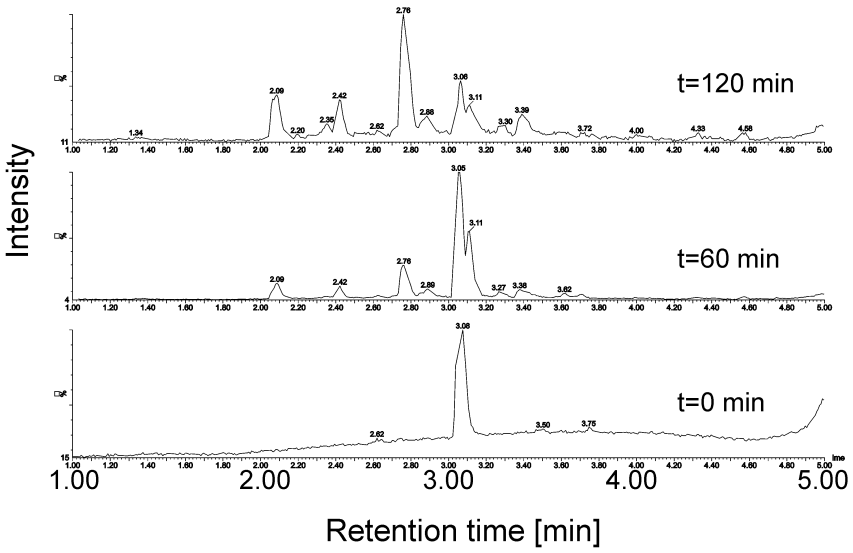

Article nº 3: Structure elucidation of phototransformation products of unapproved analogs of the erectile dysfunction drug sildenafil in artificial freshwater with UPLC-Q Exactive-MS.

J. Aceña, S. Pérez, P. Gardinali, J.L. Abad, P. Eichhorn i D. Barceló

Journal of Mass Spectrometry - 2014

Research article

Journal of MASS SPECTROMETRY

Received: 25 March 2014 Revised: 2 August 2014 Accepted: 5 August 2014 Published online in Wiley Online Library

(wileyonlinelibrary.com) DOI 10.1002/jms.3461

Structure elucidation of phototransformation products of unapproved analogs of the erectile dysfunction drug sildenafil in artificial freshwater with UPLC-Q Exactive-MS

Jaume Aceña,[a] Sandra Pérez,[a]* Piero Gardinali,[b] José Luis Abad,[c] Peter Eichhorn,[a] Nubia Heuett[b] and Damià Barceló[a,d]

In this study, four unapproved analogues of Sildenafil (SDF) were photodegraded under synthetic sunlight in artificial freshwater. Homosildenafil (H-SDF), hydroxyhomo-sildenafil (HH-SDF), norneosildenafil (NR-SDF) and thiosildenafil (T-SDF) were selected because they are frequently detected as adulterants in natural herbal products. Using UPLC-Orbitrap (Q Exactive)-MS, six photoproducts common to H-SDF, HH-SDF and T-SDF and nine unique transformation products of different molecular weights were identified based on their high-resolution (+)ESI product ion spectra. Mass spectral analysis of deuterated H-SDF, labeled on the N-ethyl group, allowed to gain mechanistic insight into the fragmentation pathway of the substituted piperazine ring and to support the postulated photoproduct structures. The mass spectral fragmentation confirmed the stepwise destruction of the piperazine ring eventually producing a sulfonic acid derivative ($C_{17}H_{20}N_4O_5S$: 392.1151 Da). In contrast, the photodegradation of NR-SDF, which lacks a piperazine ring in its structure, formed only two prominent photoproducts originating from *N,N*-dealkylation of the sulfonamide followed by hydrolysis. The current work constitutes the first study on the photodegradation of analogs of erectile dysfunction drugs and the first detection of two transformation products (*m/z* 449 and 489) in environmental samples.

Additional supporting information may be found in the online version of this article at the publisher's web site.

Keywords: analogs of erectile dysfunction drugs; photolysis; transformation products; high-resolution mass spectrometry

Introduction

In the European Union three drugs are approved for the treatment of erectile dysfunction, namely sildenafil citrate, vardenafil hydrochloride (Levitra™, Bayer) and tadalafil (Cialis™, Elli Lilly). These phosphodiesterase type V (PDE-5) inhibitors act on the smooth muscle cells lining blood vessels, especially in the corpus cavernosum of the penis. While these approved lifestyle drugs are in principle only available exclusively by medical prescription, growing evidence points to the undeclared presence of these PDE-5 inhibitors and structurally closely related analogs in herbal medicines and dietary supplements for erectile dysfunction[1] Many cases of adulterated products have been reported from East and Southeast Asian countries.[2,3] Consumers in other parts of the world may also be exposed unknowingly to such adulterated products that they can readily purchase through internet portals. Besides the unintentional exposure to any of the three aforementioned erectile dysfunction drugs, human health risks arise particularly from the presence of unapproved analogs containing minor structural modifications because they have not undergone extensive safety testing. Since the first detection of homosildenafil (H-SDF) in 2003 in herbal formulations,[4] a series of derivatives of SDF, vardenafil and tadalafil have been identified in adulterated products.[1,5,6] As the chemical structures of many of them are claimed in patents, they can be expected to exert pharmacological effects in humans, but toxicological safety profiles, as available for the three approved compounds, which underwent comprehensive preclinical testing and subsequently clinical studies, are not released for any of the derivatives.

Regarding the first-in-class PDE-5 inhibitor SDF, its synthetic analogs that have been identified include the so-called homo-SDF (H-SDF), homohydroxy-SDF (HH-SDF), thio-SDF (T-SDF) and norneo-SDF (NR-SDF) (for structures see Scheme 1).[7] As little as is known about the pharmacodynamics of the adulterants that have been tracked down in a number of dietary supplements,[8–12] their disposition in the human body is expectedly unknown. Ultimately, however, all these exogenous substances are subject to excretory

* Correspondence to: Sandra Pérez, IDAEA-CSIC, Water and Soil Quality Research Group, Jordi Girona 18-26, Barcelona 08034, Spain. E-mail: spsqam@idaea.csic.es

a Water and Soil Quality Research Group, IDAEA-CSIC, c/Jordi Girona 18-26, 08034, Barcelona, Spain

b Florida International University, 11200 SW 8th Street, Miami, Florida, 33199-0001, USA

c IQAC-CSICDepartment of Biomedicinal ChemistryJordi Girona 18-26, 08034, Barcelona, Spain

d Catalan Institute of Water Research, ICRA Catalan Institute for Water Research-ICRA, C/Emili Grahit, 101, Edifici H_2O, Parc Científic i Tecnològic de la Universitat de Girona, E-17003, Girona, Spain

Journal of MASS SPECTROMETRY

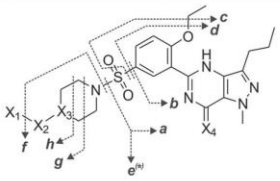

Compound	Substituent				Fragmentation								
	X_1	X_2	X_3	X_4	*a*	*b*	*c*	*d*	*e*	*e**	*f*	g	h
SDF	H	CH_2	N	O	377	311	299	283	99	100	-	70	58
H-SDF	CH_3	CH_2	N	O	377	311	299	283	113	114	99	84	72
T-SDF	H	CH_2	N	S	393	327	315	299	99	100	-	70	58
HH-SDF	CH_2OH	CH_2	N	O	377	311	299	283	129	130	99	100	88
NR-SDF	-	-	CH_2	O	377	311	299	283	84	85	-	-	-
H-SDF-d_5	CD_3	CD_2	N	O	377	311	299	283	118	119	101	89	77

Scheme 1. Fragmentation scheme for sildenafil and analogues.

processes and are discharged as parent compound, and possibly metabolites, eventually into sewage. Recent monitoring studies conducted on raw and treated sewage from municipal wastewater treatment plants (WWTP) have provided evidence for the occurrence of PDE-5 inhibitors, including SDF and several human metabolites.[13,14] As with many other human pharmaceuticals, common sewage treatment does not completely remove these compounds from the wastewater stream and eventually leads to discharge into receiving water bodies.[15] Once the aquatic environment has been reached, their fate is governed by a combination of biotic and abiotic processes. Into the latter category fall photochemical reactions which are considered an important mechanism in the natural attenuation of organic environmental micropollutants.[16] To address the possibility of photolysis of PDE-5 inhibitors in the environment, recent research efforts in our group were devoted to assessing the photodegradability of SDF under simulated sunlight.[17] In these studies we could demonstrate that the aliphatic piperazine ring was the principal target of the photolytical processes. With the aid of high-resolution mass spectrometry (quadrupole-time of flight instrument), coupled to ultra-high performance liquid chromatography (UHPLC), a total of 18 photoproducts could be identified through their unique mass spectral fragmentation patterns.

With this in mind, the current work builds on the outcomes of the previous study and aims to extend the spectrum of investigated compounds by including a number of structural derivatives of SDF, all of which reported to occur as analogs of erectile dysfunction drugs in various natural herbal products.[1,18–21] Specifically, the objective consisted of elucidating the phototransformation reactions of the four SDF analogs H-SDF, HH-SDF, T-SDF and NR-SDF (Scheme 1), in aqueous solution under the influence of simulated solar radiation. Based on the findings of the SDF studies,[17] we expected that the photodegradation pathways for the former three compounds (NR-SDF does not contain a piperazine ring in its structure), and therefore the spectra of their intermediates formed were very similar to those identified for SDF with a first generation quadrupole time-of-flight MS instrument. Largely improved sensitivity, resolution and mass accuracy of the Q Exactive-Orbitrap-MS platform held great promise in achieving more robust identification results.

Experimental

Chemical reagents

SDF, DM-SDF, H-SDF, H-SDF-d_5, HH-SDF, NR-SDF and T-SDF were purchased from Toronto Research Chemicals (Toronto, Canada). All organic solvents used for UPLC and TLC were Chromasol LC grade or equivalent. Ultra pure water and LC/MS grade formic acid were purchased from Sigma Aldrich (Munich, Germany). LC-grade acetonitrile was purchased from Riedel de Häen (Steinheim, Germany).

Photolysis experiments

Phototransformation experiments were conducted in a Suntest CPS solar simulator (Heraeus, Hanau, Germany) equipped with a Xenon lamp. Appropriate window glass filters were installed between the light source and the test solution in order to generate an emission spectrum similar to that of natural solar radiation. Test solutions of H-SDF, HH-SDF, NR-SDF and T-SDF at 10 mg/l and 1 μg/l were prepared in artificial freshwater (AFW) resembling a moderately hard water (96 mg/l $NaHCO_3$, 60 mg/l $CaSO_4{\cdot}2H_2O$, 60 mg/l $MgSO_4$ and 4 mg/l KCl; pH: 6.9). Test solutions were irradiated in capped quartz tubes (not airtight) for up to 58 h. Dark control solutions containing the target analytes and the selected matrix were kept inside the exposure chamber to mimic the temperature conditions. Subsamples of dark controls were taken at the same time points as those from the irradiation experiments. H-SDF, HH-SDF, NR-SDF and T-SDF concentrations remained constant in the dark controls over the test period and no bio or thermal degradation products were observed in the vials (data not shown).

Sampling and sample preparation

Reclaimed water (16 l) from the North District Wastewater Treatment Plant (North Miami, FL) was collected during the month of June of 2014 in pre-cleaned stainless steel containers. The sample produced reclaimed water for irrigation by using primary and secondary treatment followed by final disinfection. Because the nature and functionalities of the metabolites targeted was completely unknown sample extraction was performed in three 4-l aliquots by liquid–liquid extraction against methylene chloride.

Journal of MASS SPECTROMETRY

For two of the aliquots pH was modified prior to extraction as follows: aliquot A was acidified to pH 3.56 using 200 μl of formic acid; aliquot B was basified to pH 9.66 using 3000 μl of ammonium hydroxide. Aliquot C was extracted as untreated (neutral). Liquid–liquid extractions were performed using multiple 2-l separatory funnels, and analytes were extracted using a total of 300 mL of methylene chloride (3 x 100 mL) per sample aliquot. Extracts were dried over anhydrous sodium sulfate and their volumes reduced to 1000 μl of methylene chloride using a combination of a water bath and a stream of purified nitrogen gas. Prior to analysis the extracts with UPLC-HR-MS (see next section) were diluted with a mixture of methanol and water containing a suitable modifier such as formic acid of ammonium formate.

UHPLC/ESI-MS/MS analysis

Photolysis samples

Chromatographic separation was performed on a Waters ACQUITY BEH C_{18} column (50 × 2.1 mm, 1.7-μm particle size) equipped with a guard column (5 × 2.1 mm) of the same packing material. The mobile phases were (A) 0.1% HCOOH or 20 mM of NH_4OAc for acid and neutral conditions respectively, and (B) acetonitrile. After 0.5-min isocratic elution at 90% A, the proportion of A was linearly decreased to 10% within 6.5 min. The percentage of A was then maintained at 10% and held for 1.0 min. The initial mobile phase composition was reestablished within 1.0 min followed by a 2.0-min equilibration step at 90% A. The flow rate was 300 μl/min, and the injection volume was 10 μl. Exact mass measurements of the SDF analogs and their phototransformation products formed in the irradiation device were carried out in full-scan and product ion scan mode on a Q Exactive mass spectrometer (Thermo Fisher Scientific, San Jose, CA, USA). All MS experiments were performed in the positive ion mode using Heated Electro Spray Ionization (HESI). The source parameters were as follows: spray voltage: +3000 V; sheath gas pressure: 40 psi; auxiliary gas flow: 10 (arbitrary units); capillary temperature: 350 °C; heater temperature: 300 °C. The Orbitrap mass analyzer was operated at a resolving power of 70 000 (FWHM) in full-scan mode and of 17 500 (FWHM) in the data-dependent MS^2 mode (normalized collision energy of 40). The accurate mass of diisooctyl phthalate (*m/z* 391.28429) as a ubiquitous contaminant in LC-MS systems was used as a lock mass. External mass calibration for positive ESI mode was conducted every 5 days for the mass range of *m/z* 50–2000 by infusing a Pierce LTQ Velos ESI Positive Ion calibration solution from Thermo Fisher Scientific. All MS data acquisition and processing were done using the software package Xcalibur 2.2.

Environmental samples

Liquid chromatography analysis was carried out using a quaternary Accela 1200 pump equipped with a CTC PAL autosampler. Twenty microliters of the extract was used for analysis. Separation of analytes was achieved using a Hypersil Gold aQ (150 × 2.1 mm × 3 μm) analytical column and a gradient composition of methanol, HPLC grade water and HPLC water with 1% formic acid and 100 mM ammonium formate. Detection of analytes was performed using a Thermo QExactive Orbitrap high resolution mass spectrometer equipped with a HESI ionization source operated in the positive mode. Full scan analysis (R = 140 000) followed by target MS2 analysis (R = 35 000, NCE 35) was carried out for identification and confirmation purposes. Samples were acquired in both ESI positive and negative ion mode and processed for target compound identification using a combination of Xcalibur, Metworks and Mass Frontier software packages (Thermo Scientific, San Jose CA).

Results and discussion

Irradiation of the aqueous solutions degraded efficiently undeclared erectile dysfunction drugs in all studied matrices at high and low concentration. Figure S1, provided in the Supporting Information, shows the degradation profiles at different concentrations. Common phototransformation products were obtained in each sample, regardless of the concentration of the test compound (Figure S4). Plausible chemical structures were proposed by combining chromatographic information, accurate mass and MS^2 fragmentation data based on the knowledge of the photodegradation pathways of SDF.[17]

Comparison of the TICs of the control samples with those of the irradiated samples showed several new peaks indicating the presence of phototransformation products (Fig. S2). Their retention times relative to the test compound provided first hints on the polarity of the photodegradates. *N*-Oxide-SDF was confirmed with a chemically synthetized standard in the irradiated samples from T-SDF. In order to identify the formation of more *N*-oxides of the two other piperazine-analogs of SDF (H-SDF and HH-SDF), the change of pH of the mobile phase was evaluated. Figure S3 compares the effect of mobile phase pH (3.2 *vs* 6.8) on the retention times of H-SDF and TP504. In case of H-SDF increasing the pH from 3.2 to 6.8 led in stronger retention. This behavior was expected because the lower degree of protonation of the tertiary amine (pK_b) in the piperazine ring resulted in a less polar molecule. Results indicated that the new TP corresponds to a neutral molecule probably to an *N*-oxide. If other polar compounds would have been formed, when changing the pH of the mobile phase a shift in the retention time of the new TP on the reversed-phase column would have been observed. The effect of the pH on the retention times of TPs allow us to gain insight on the formation of *N*-oxides of the two analogs containing the piperazine ring in their structures.[22,23]

Fragmentation patterns of H-SDF, HH-SDF, T-SDF and NR-SDF

In order to identify the structures of the TPs formed under simulated sunlight, the first step was to elucidate and compare the fragmentation patterns of the four related parent compounds obtained under (+)ESI conditions. The high-resolving Q Exactive mass spectrometer delivered consistently low mass errors in both full-scan and product ion mode, thereby greatly facilitating the assignment of fragment ion compositions (Tables 1 and 2). Moreover, previous experience gained on a QToF-MS for SDF and its photoproducts allowed for straightforward interpretation of the (+)ESI-MS^2 spectra (for the sake of comparability Fig. 1 includes the mass spectrum of SDF).[17,24] The generic fragmentation pathway depicted in Scheme 1 summarizes the main fragment ions. While the right portion of the molecule containing the phenyl-pyrazolopyrimidin (ethi)one remains largely intact upon collision-induced dissociation, several bond cleavages occur at, and in the proximity of, the sulfonamide bond as well as within the piperazine ring. The fragmentations ***a***, ***b***, ***c*** and ***d*** lead to a characteristic set of ions with *m/z* ratios of 377, 311, 299 and 283 for SDF, H-SDF, HH-SDF and NR-SDF. In T-SDF where the oxygen atom of the pyrimidinone ring is replaced by a sulfur atom, the corresponding cleavages produce fragment ions that are 16 *m/z* units heavier (*m/z* 393 (***a***), 327 (***b***), 315 (***c***) and 299 (***d***)). Given the distinct substitution pattern in the piperazine

Journal of MASS SPECTROMETRY

Table 1. Accurate mass measurements of H-SDF($-d_5$), HH-SDF, T-SDF and NR-SDF obtained by UPLC-(+)ESI-Orbitrap-MS in MS or MS/MS mode

Compound	Measured ion mass [*m/z*]	Elemental composition	Theoretical ion mass [*m/z*]	Rel. error [ppm]
H-SDF	489.2281	$C_{23}H_{33}N_6O_4S$	489.2279	0.5
	461.1969	$C_{21}H_{29}N_6O_4S$	461.1966	0.8
	377.1281	$C_{17}H_{21}N_4O_4S$	377.1278	0.7
	311.1503	$C_{17}H_{19}N_4O_2$	311.1503	0.2
	283.1195	$C_{15}H_{15}N_4O_2$	283.1190	1.8
	113.1078	$C_6H_{13}N_2$	113.1073	3.8
	99.0923	$C_5H_{11}N_2$	99.0917	5.8
	84.0815	$C_5H_{10}N$	84.0808	8.1
	72.0816	$C_4H_{10}N$	72.0808	10.7
	58.0660	C_3H_8N	58.0651	15.4
H-SDF-d_5	494.2589	$C_{23}H_{28}D_5N_6O_4S$	494.2592	0.6
	461.1973	$C_{21}H_{29}N_6O_4S$	461.1966	1.7
	377.1284	$C_{17}H_{21}N_4O_4S$	377.1278	1.6
	311.1500	$C_{17}H_{19}N_4O_2$	311.1503	−0.9
	283.1188	$C_{15}H_{15}N_4O_2$	283.1190	−0.4
	118.1391	$C_6H_8D_5N_2$	118.1387	3.0
	101.1047	$C_5H_9D_2N_2$	101.1042	4.7
	89.1128	$C_5H_5D_5N$	89.1122	7.5
	77.1129	$C_4H_5D_5N$	77.1122	10.0
	62.0911	$C_3H_4D_4N$	62.0902	14.0
HH-SDF	505.2232	$C_{23}H_{33}N_6O_5S$	505.2228	0.9
	487.2129	$C_{23}H_{31}N_6O_4S$	487.2122	1.5
	461.1970	$C_{21}H_{29}N_6O_4S$	461.1966	1.0
	377.1281	$C_{17}H_{21}N_4O_4S$	377.1278	0.8
	311.1505	$C_{17}H_{19}N_4O_2$	311.1503	0.6
	299.1142	$C_{15}H_{15}N_4O_3$	299.1139	1.2
	283.1192	$C_{15}H_{15}N_4O_2$	283.1190	0.9
	129.1026	$C_6H_{13}N_2O$	129.1022	2.9
	112.1000	$C_6H_{10}NO$	112.0757	4.5
	99.0923	$C_5H_{11}N_2$	99.0917	6.3
	88.0765	$C_4H_{10}NO$	88.0757	9.0
	74.0609	C_3H_8NO	74.0600	11.6
	58.0661	C_3H_8N	58.0651	16.3
T-SDF	491.1896	$C_{22}H_{31}N_6O_3S_2$	491.1894	0.6
	393.1046	$C_{17}H_{21}N_4O_3S_2$	393.1050	−0.8
	327.1274	$C_{17}H_{19}N_4OS$	327.1274	−0.1
	299.1138	$C_{15}H_{15}N_4OS$	299.1139	0.4
	100.1002	$C_5H_{12}N_2$	100.0995	6.5
	99.0923	$C_5H_{11}N_2$	99.0917	6.4
	85.0767	$C_4H_9N_2$	85.0760	8.4
	70.0660	C_4H_8N	70.1651	11.8
	58.0660	C_3H_8N	58.0651	15.2
NR-SDF	460.2015	$C_{22}H_{30}N_5O_4S$	460.2013	0.4
	432.1702	$C_{20}H_{26}N_5O_4S$	432.1700	0.5
	377.1274	$C_{17}H_{21}N_4O_4S$	377.1278	−1.0
	329.1611	$C_{17}H_{21}N_4O_3$	329.1608	1.0
	311.1504	$C_{17}H_{19}N_4O_2$	311.1503	0.6
	299.1142	$C_{15}H_{15}N_4O_3$	299.1139	1.0
	283.1193	$C_{15}H_{15}N_4O_2$	283.1190	1.2
	256.0953	$C_{13}H_{12}N_4O_2$	256.0955	−0.8
	84.0815	$C_5H_{10}N$	84.0808	8.6

ring (piperidine in case of NR-SDF) of the SDF analogs, fragment ions arising from cleavage of the sulfonamide bond (**e**) or dissociation of the aliphatic ring (**f**, **g** and **h**) have compound-specific *m/z* values. All

Table 2. Accurate mass measurements of photoproducts obtained by UPLC-(+)ESI-Orbitrap-MS in MS or MS/MS mode. For those TPs formed by more than one parent compound the listed data correspond to the one labeled with an asterisk. The accurate mass data for the other parent compounds are provided in Tables S1, 2 and 3 in the Supporting Information

Photoproduct	Formed by…	Measured ion mass [*m/z*]	Elemental composition	Theoretical ion mass [*m/z*]	Rel. error [ppm]
TP520	HH-SDF	521.2182	$C_{23}H_{33}N_6O_6S$	521.2177	1.0
		473.1975	$C_{22}H_{29}N_6O_4S$	473.1966	2.0
		404.1389	$C_{18}H_{22}N_5O_4S$	404.1387	0.4
		377.1282	$C_{17}H_{21}N_4O_4S$	377.1278	1.1
		344.1482	$C_{17}H_{20}N_4O_4$	344.1479	1.0
		311.1502	$C_{17}H_{19}N_4O_2$	311.1503	0.1
		283.1191	$C_{15}H_{15}N_4O_2$	283.1190	0.6
		129.1025	$C_6H_{13}N_2O$	129.1022	2.3
		98.0846	$C_5H_{10}N_2$	98.0839	7.2
		83.0611	$C_4H_7N_2$	83.0604	9.3
TP506	HH-SDF	507.2026	$C_{22}H_{31}N_6O_6S$	507.2020	1.0
		489.1926	$C_{22}H_{29}N_6O_5S$	489.1915	2.3
		461.1969	$C_{21}H_{29}N_6O_4S$	461.1966	0.6
		418.1552	$C_{19}H_{24}N_5O_4S$	418.1544	2.0
		311.1507	$C_{17}H_{19}N_4O_2$	311.1503	1.4
		299.1143	$C_{15}H_{15}N_4O_3$	299.1139	1.5
		283.1196	$C_{15}H_{15}N_4O_2$	283.1190	2.4
		115.0871	$C_5H_{11}N_2O$	115.0860	4.3
		88.0765	$C_4H_{10}NO$	88.0757	9.5
		70.0661	C_4H_8N	70.0651	13.6
TP504	H-SDF	505.2230	$C_{23}H_{33}N_6O_5S$	505.2228	0.2
		477.1918	$C_{21}H_{29}N_6O_5S$	477.1915	0.8
		404.1388	$C_{18}H_{22}N_5O_4S$	404.1387	0.1
		377.1278	$C_{17}H_{21}N_4O_4S$	377.1278	0.1
		344.1479	$C_{17}H_{20}N_4O_4$	344.1479	−0.1
		311.1501	$C_{17}H_{19}N_4O_2$	311.1503	−0.4
		283.1190	$C_{15}H_{15}N_4O_2$	283.1190	0.1
		113.1078	$C_6H_{13}N_2$	113.1073	3.8
		98.0845	$C_5H_{10}N_2$	98.0839	6.2
		83.0611	$C_4H_7N_2$	83.0604	8.3
TP490-A	H-SDF	491.2075	$C_{22}H_{31}N_6O_5S$	491.2071	0.7
		473.1972	$C_{22}H_{29}N_6O_4S$	473.1966	1.4
		463.2127	$C_{21}H_{31}N_6O_4S$	463.2122	1.1
		99.0924	$C_5H_{11}N_2$	99.0917	6.8
		72.0816	$C_4H_{10}N$	72.0808	11.8
TP490-B	T-SDF	491.2073	$C_{22}H_{31}N_6O_5S$	491.2071	0.4
		463.1756	$C_{20}H_{27}N_6O_5S$	463.1758	−0.4
		404.1389	$C_{18}H_{22}N_5O_4S$	404.1387	0.5
		377.1279	$C_{17}H_{21}N_4O_4S$	377.1278	0.3
		344.1479	$C_{17}H_{20}N_4O_4$	344.1479	−0.1
		311.1501	$C_{17}H_{19}N_4O_2$	311.1503	−0.5
		299.1138	$C_{15}H_{15}N_4O_3$	299.1139	−0.3
		283.1190	$C_{15}H_{15}N_4O_2$	283.1190	0.3
		99.0922	$C_5H_{11}N_2$	99.0917	5.1
		70.0659	C_4H_8N	70.1651	11.5
		58.0660	C_3H_8N	58.0651	14.9
TP488	H-SDF[a]	489.1919	$C_{22}H_{29}N_6O_5S$	489.1915	0.8
	HH-SDF	461.1970	$C_{21}H_{29}N_6O_4S$	461.1966	0.9
	T-SDF	377.1279	$C_{17}H_{21}N_4O_4S$	377.1278	0.2
		311.1507	$C_{17}H_{19}N_4O_2$	311.1503	1.3
		299.1146	$C_{15}H_{15}N_4O_3$	299.1139	2.3

(Continues)

Journal of MASS SPECTROMETRY

Table 2. (Continued)

Photoproduct	Formed by…	Measured ion mass [m/z]	Elemental composition	Theoretical ion mass [m/z]	Rel. error [ppm]
		283.1195	$C_{15}H_{15}N_4O_2$	283.1190	1.9
		85.0768	$C_4H_9N_2$	85.0760	9.6
TP478	HH-SDF	479.2074	$C_{21}H_{31}N_6O_5S$	479.2071	0.6
		461.1964	$C_{21}H_{29}N_6O_4S$	461.1966	−0.3
		418.1550	$C_{19}H_{24}N_5O_4S$	418.1544	1.6
		435.1813	$C_{19}H_{27}N_6O_4S$	435.1809	1.0
		392.1394	$C_{17}H_{22}N_5O_4S$	392.1387	1.7
		344.1488	$C_{17}H_{20}N_4O_4$	344.1479	2.6
		311.1502	$C_{17}H_{19}N_4O_2$	311.1503	−0.2
		299.1140	$C_{15}H_{15}N_4O_3$	299.1139	0.5
		283.1192	$C_{15}H_{15}N_4O_2$	283.1190	0.8
		149.0383	$C_4H_9N_2O_2S$	149.0379	2.5
		88.0764	$C_4H_{10}NO$	88.0757	7.5
		70.06595	C_4H_8N	70.0651	11.8
TP476	T-SDF	477.1917	$C_{21}H_{29}N_6O_5S$	477.1915	0.5
		449.1971	$C_{20}H_{29}N_6O_4S$	449.1966	1.2
		418.1545	$C_{19}H_{24}N_5O_4S$	418.1544	0.3
		392.1393	$C_{17}H_{22}N_5O_4S$	392.1387	1.4
		311.1504	$C_{17}H_{19}N_4O_2$	311.1503	0.4
		283.1193	$C_{15}H_{15}N_4O_2$	283.1190	1.4
		85.0768	$C_4H_9N_2$	85.0760	9.6
		58.0661	C_3H_8N	58.0651	16.1
TP474	T-SDF	475.2125	$C_{22}H_{31}N_6O_4S$	475.2122	0.6
(SDF)		377.1287	$C_{17}H_{21}N_4O_4S$	377.1278	2.4
		311.1505	$C_{17}H_{19}N_4O_2$	311.1503	0.8
		283.1193	$C_{15}H_{15}N_4O_2$	283.1190	1.4
		100.1001	$C_5H_{12}N_2$	100.0995	6.3
		99.0923	$C_5H_{11}N_2$	99.0917	6.2
		70.0660	C_4H_8N	70.1651	11.8
		58.0660	C_3H_8N	58.0651	15.7
TP462-A	H-SDF	463.2124	$C_{21}H_{31}N_6O_4S$	463.2122	0.3
		435.1829	$C_{19}H_{27}N_6O_4S$	435.1809	4.6
		418.1548	$C_{19}H_{24}N_5O_4S$	418.1544	1.0
		392.1382	$C_{17}H_{22}N_5O_4S$	392.1387	−1.3
		344.1486	$C_{17}H_{20}N_4O_4$	344.1479	2.0
		311.1502	$C_{17}H_{19}N_4O_2$	311.1503	−0.1
		299.1142	$C_{15}H_{15}N_4O_3$	299.1139	1.0
		283.1193	$C_{15}H_{15}N_4O_2$	283.1190	1.2
		151.0537	$C_4H_{11}N_2O_2S$	151.0536	0.9
		72.0816	$C_4H_{10}N$	72.0808	11.4
		58.0660	C_3H_8N	58.0651	15.7
TP462-B	H-SDF[a]	463.1760	$C_{20}H_{27}N_6O_5S$	463.1758	0.4
	HH-SDF	435.1811	$C_{19}H_{27}N_6O_4S$	435.1809	0.4
	T-SDF	418.1545	$C_{19}H_{24}N_5O_4S$	418.1544	0.4
		393.1223	$C_{17}H_{21}N_4O_5S$	393.1227	−1.1
		311.1502	$C_{17}H_{19}N_4O_2$	311.1503	−0.1
		299.1142	$C_{15}H_{15}N_4O_3$	299.1139	1.0
		283.1193	$C_{15}H_{15}N_4O_2$	283.1190	1.1
		71.0611	$C_3H_7N_2$	71.0604	10.2
		59.0612	$C_2H_7N_2$	59.0604	13.5
TP460	H-SDF[a]	461.1967	$C_{21}H_{29}N_6O_4S$	461.1966	0.2
	HH-SDF	377.1278	$C_{17}H_{21}N_4O_4S$	377.1278	0.1
	T-SDF	311.1507	$C_{17}H_{19}N_4O_2$	311.1503	1.4
		299.1140	$C_{15}H_{15}N_4O_3$	299.1139	0.6

(Continues)

Table 2. (Continued)

Photoproduct	Formed by…	Measured ion mass [m/z]	Elemental composition	Theoretical ion mass [m/z]	Rel. error [ppm]
		283.1195	$C_{15}H_{15}N_4O_2$	283.1190	1.8
		85.0768	$C_4H_9N_2$	85.0760	9.3
TP448	T-SDF	449.1968	$C_{20}H_{29}N_6O_4S$	449.1966	0.4
		418.1546	$C_{19}H_{24}N_5O_4S$	418.1544	0.6
		392.1389	$C_{17}H_{22}N_5O_4S$	392.1387	0.4
		377.1278	$C_{17}H_{21}N_4O_4S$	377.1278	−0.1
		311.1502	$C_{17}H_{19}N_4O_2$	311.1503	−0.3
		283.1189	$C_{15}H_{15}N_4O_2$	283.1190	−0.1
		137.0375	$C_3H_9N_2O_2S$	137.0379	−2.8
		73.0768	$C_3H_9N_2$	73.0760	10.5
		58.0660	C_3H_8N	58.0651	14.4
TP434	H-SDF[a]	435.1811	$C_{19}H_{27}N_6O_4S$	435.1809	0.4
	HH-SDF	418.1545	$C_{19}H_{24}N_5O_4S$	418.1544	0.5
	T-SDF	392.1386	$C_{17}H_{22}N_5O_4S$	392.1387	−0.4
		377.1285	$C_{17}H_{21}N_4O_4S$	377.1278	1.7
		311.1502	$C_{17}H_{19}N_4O_2$	311.1503	−0.1
		299.1141	$C_{15}H_{15}N_4O_3$	299.1139	0.8
		283.1191	$C_{15}H_{15}N_4O_2$	283.1190	0.5
TP392	H-SDF[a]	393.1224	$C_{17}H_{21}N_4O_5S$	393.1227	−0.8
	HH-SDF	365.0916	$C_{15}H_{17}N_4O_5S$	365.0914	0.5
	T-SDF	336.0521	$C_{13}H_{12}N_4O_5S$	336.0523	−0.7
	NR-SDF	284.1269	$C_{15}H_{16}N_4O_2$	284.1268	0.4
		256.0956	$C_{13}H_{12}N_4O_2$	256.0955	0.4
TP391	H-SDF[a]	392.1386	$C_{17}H_{22}N_5O_4S$	392.1387	−0.3
	HH-SDF	364.1078	$C_{15}H_{18}N_5O_4S$	364.1074	1.2
		335.0683	$C_{13}H_{13}N_5O_4S$	335.0683	0.1
		311.1505	$C_{17}H_{19}N_4O_2$	311.1503	0.7
	T-SDF	299.1140	$C_{15}H_{15}N_4O_3$	299.1139	0.4
	NR-SDF	283.1192	$C_{15}H_{15}N_4O_2$	283.1190	1.0
		256.0955	$C_{13}H_{12}N_4O_2$	256.0955	0.1

[a]Homolytic cleavage of sulfonamide bond.

of the analytes undergo cleavage of the sulfonamide bond according to ***e*** – in contrast to pathway ***a*** the positive charge remains in the left part of the molecule – but the cross-ring cleavages ***g*** and ***h*** are exclusively observed for the piperazine-bearing compounds (SDF, H-SDF, HH-SDF and T-SDF; $X_3 = N$ in generic structure in Scheme 1) in which. That NR-SDF does not produce any charged species apart from *m/z* 84 (see Fig. 1E) is due to the lack of a readily protonatable nitrogen in this moiety. It is worth mentioning that the dissociation of the sulfonamide bond according to the aforementioned pathway ***e*** can also proceed homolytically (indicated as ***e**** in Scheme 1), thereby generating radical cations that differ from the ions in series ***e*** by an additional hydrogen atom.

As there are a few subtle yet distinct features present in the mass spectra of the SDF analogs, closer examination of commonalities and differences is warranted. The mass spectra of both SDF and its thio-analog T-SDF show expectedly the formation of the ions at *m/z* 99 (100) and *m/z* 58 originating from fragmentations $\mathbf{e}^{(*)}$ and ***h***, respectively. Replacement of the *N*-methyl group by an ethyl group in H-SDF (Fig. 1A), in turn, leads to the homologues ions at *m/z* 113 (114) and *m/z* 72 in the (+)ESI-MS^2 spectrum. Unexpected though is the observation of intense ions with *m/z 99* and *m/z* 58 which differ from the two former ions by a CH_2 unit. What at first glance suggests cross-ring cleavage involving rupture of the C—C

Journal of MASS SPECTROMETRY

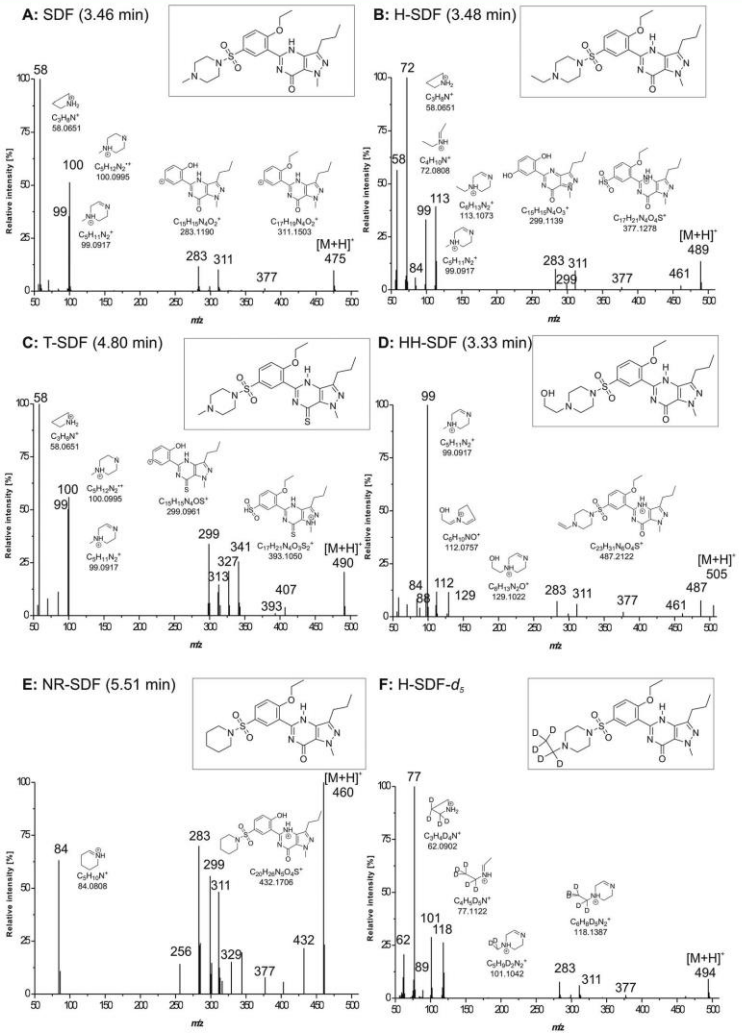

Figure 1. (+)ESI-MS/MS spectra of SDF, H-SDF, T-SDF, HH-SDF, NR-SDF and H-SDF-d_5.

bond in the ethylene bridge of the piperazine ring corresponds in fact to elimination of the terminal methyl group. By recording the (+)ESI product ion mass spectrum of H-SDF-d_5, the mass shifts relative to H-SDF provide valuable information on the site of fragmentation. In H-SDF-d_5 all five deuterium atoms are located in the *N*-ethyl group. Therefore, the fragmentations ***a***, ***b***, ***c*** and ***d*** produce the same set of ions as in H-SDF (see Scheme 1). On the other hand, the ions *m/z* 118 and 77 in the spectrum of H-SDF-d_5 are 5 *m/z* units higher than the corresponding ions in the H-SDF product ion profile, being in line with conservation of all five deuterium atoms in these two ion species. Determination of the elemental composition of the ion at *m/z* 101, however, reveals the presence of only two deuterium atoms in this ion ($C_5H_9D_2N_2$) thus providing evidence for loss of the CD_3 group at some point during the collision-induced dissociation. As for the fragment ion *m/z* 62, the accurate mass data suggest a formula of $C_3H_4D_4N$, i.e. one deuterium has been lost during the fragmentation process. The inset in Fig. 1C shows a plausible structure of this ion in which rearrangement has led to a four-membered ring. As far as *N*-hydroxyethyl analog HH-SDF is concerned (Fig. 1D), the

protonated molecule can undergo dehydration of the aliphatic hydroxyl group to generate *m/z* 487. Cleavage of the precursor ion according to pathway ***e*** gives rise to ion *m/z* 129. The base peak in the mass spectrum (*m/z* 99) corresponds to the formula $C_5H_{11}N_2$ thus being identical in composition to *m/z* 99 in SDF. It is proposed to correspond to the elimination of methanol (30 Da) from *m/z* 129. A fragment ion with a unique structure is detected at *m/z* 112. Here, the accurate mass strongly points at simultaneous cleavage of the C—N bonds between the carbons of the two ethylene groups and the sulfonamide-N. To produce an unsubstituted sulfonamide as neutral fragment, two hydrogen atoms have to be transferred to the sulfonamide-N, thereby generating the unsaturated species shown in the inset in Fig. 1C.

Identification of the photoproducts

Upon irradiation of the spiked AFW solutions with simulated sunlight, all four test compounds (H-SDF, HH-SDF, T-SDF and NR-SFD) underwent extensive photodegradation. The UPLC-based separation revealed the conversion of the SDF analogs into mixtures of different complexity. Compilation of retention time and molecular weight information provided already hints on the presence of several identical photoproducts across compounds. This came as no surprise because previous studies performed on SDF had demonstrated the gradual breakdown of the piperazine ring up to the point where hydrolysis of the sulfonamide yielded a stable sulfonic acid derivative. Since, with the exception of T-SDF, all other analogs bore modifications in this aliphatic heterocycle, its light-induced destruction would eventually lead to the generation of photoproducts with identical structures. In case of T-SDF none of the mass spectra of the photoproducts showed the diagnostic series of ions at *m/z* 299, 315, 327 and 393 produced by fragmentation of the protonated parent compound. Instead, they were all shifted to the SDF-specific series of *m/z* 283, 299, 313 and 377, and, in fact, SDF was unequivocally identified in the samples from the T-SDF photolysis experiments by the perfect match of retention time and product ion profile. The absence of thioketone-containing photoproducts indicated a rapid oxidation of this moiety and therefore allowed to anticipate a degradation pathway comparable to that of SDF.

The (+)ESI mass spectra of six photoproducts common to H-SDF, HH-SDF and T-SDF are depicted in Fig. 2 with the corresponding accurate mass data listed in the Table 2. The heaviest of them (TP488) had an elemental composition of $C_{22}H_{28}N_6O_5S$ and showed an intense fragment ion at *m/z* 461 corresponding to the loss of CO from the molecular ion (Fig. 2A). The same difference in *m/z* values and elemental compositions was observed between the low-intensity fragment ion at *m/z* 113 and the abundant ion with *m/z* 85. The accurate mass data of the latter indicated a composition of $C_4H_9N_2$ which led to propose the cyclic structure shown in the inset of Fig. 2-A. The dissociation of CO from the protonated molecule and from fragment ion *m/z* 113 is consistent with an amide that results from oxidation of the *N*-alkyl group in H-SDF, HH-SDF and T-SDF (converted into SDF after oxidation of the thioketone). Complete loss of the N-substituent is then postulated to generate TP460 exhibiting a very similar fragmentation pattern with the characteristic ion at *m/z* 85 (Fig. 2C). The formation of this secondary-amine bearing compound was ultimately confirmed by comparison with the authentic standard, N-demethylated SDF, which was commercially available and reported to be a major human metabolite of SDF. The TP434 ($C_{19}H_{26}N_6O_4S$) in turn differs in chemical formula from TP460 by the elimination of C2H2 and while it maintains the diagnostic series at *m/z* 283, 299, 311 and 377, it lacks prominent fragment ions in the low mass range (Fig. 2D). A key fragment ion in the mass spectrum of TP434 originates from loss of ammonia in the precursor ion which points at the presence of a terminal amine group as proposed in the *N,N*-deethylated structure shown in Fig. 2D. If dissociation of the sulfur-nitrogen bond in the sulfonamide group precedes the neutral loss of NH_3 from the precursor ion, the result is the low-intensity ion at *m/z* 59 (C_3H_8N). Further photo-induced degradation of TP434 upon loss of the aminoethyl substituent of the sulfonamide is then postulated to generate TP391 ($C_{17}H_{22}N_5O_4S$). With an unsubstituted sulfonamide remaining, no low-mass fragment ions are observed under the applied CID conditions (Fig. 2F). Instead, the first step of dissociation corresponds to the loss of ethylene producing the base peak at *m/z* 364 ($C_{15}H_{18}N_5O_4S$). This cleavage is proposed to occur in the ethoxy group in analogy to the difference in generic fragmentations ***b*** and ***d*** in Scheme 1 (see also inset in Fig. 1A). In contrast, fragmentation according to pathway ***a*** cannot take place in the N-unsubstituted sulfonamide TP391, and hence the class-specific fragment ion at *m/z* 377 is not anymore detected in the mass spectrum. The emergence of fragment ions at *m/z* 335 and 256, however, cannot be rationalized using straightforward heterolytic cleavages. Since the accurate mass data clearly point to chemical formulae of $C_{13}H_{13}N_5O_4S$ and $C_{13}H_{12}N_4O_2$, respectively (these two differ in composition by $HNSO_2$), the fact that computing the double-bond equivalents of these charged species produce integer values can only be attributed to the presence of ions with unpaired electrons. As for *m/z* 335, successive elimination from the molecular ion of first C_2H_4 (ethoxy group: *m/z* 364) and then of C_2H_5 from the propyl side chain give rise to this fragment ion bearing an exo-methylene group. The relative stability of this radical is thought to be due to resonance stabilization involving the adjacent imine group. The same sequence of neutral losses is apparent in the mass spectrum of TP392 (Fig. 2E) where a hydroxyl group replaces the amino group in the sulfonamide to yield the corresponding sulfonic acid ($C_{17}H_{20}N_4O_5S$). Under the applied CID conditions, the radical ion at *m/z* 256 – as in case of TP391 – represents the final stage of fragmentation.

Of the aforementioned photoproducts identified in the irradiated solutions of H-SDF, HH-SDF and T-SDF, only TP391 and TP392 were formed during exposure of NR-SDF in the sunlight simulator. This is fully in line with the structural differences between the four SDF analogs: lacking the tertiary amine, the *N,N*-pentylene bridge in NR-SDF does not give rise to any oxidative intermediates but produces directly the *N,N*-dealkylated compound TP391.

Beside those TPs that were observed for more than one of the test compounds, a number of unique photoproducts was detected suggesting the conservation of the substance-specific N-alkyl substituent on the respective piperazine rings. Comparison of the elemental compositions of the molecular ions as well as examination of the product ion spectra (Fig. 3) for commonalities revealed the presence of three series, of which the first one comprised TPs arising from monooxygenation (TP504 for H-SDF; TP520 for HH-SDF; TP490-B for T-SDF after conversion to SDF). With chromatographic retention times being longer than those of the test compounds (taking SDF as reference in case of T-SDF), C-hydroxylation on an aliphatic or aromatic position appeared unlikely as this would have generated more polar, and thus less retained, entities. At first glance the corresponding (+)ESI mass spectra (Fig. 3A, 3D and 3G) display an apparent inconsistency in that on the one hand they contain the characteristic series of ions comprising *m/z* 404, 311, 299 and 283

Journal of MASS SPECTROMETRY

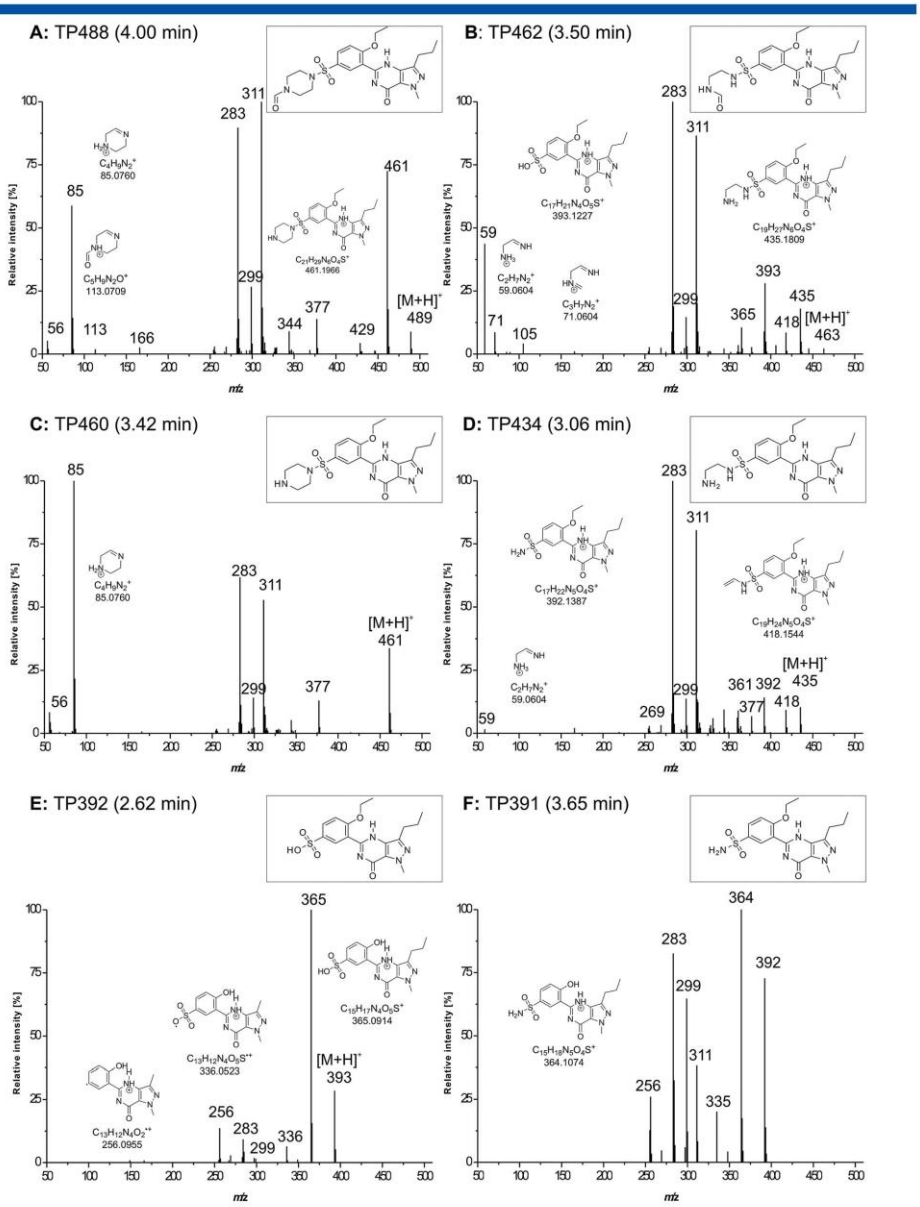

Figure 2. (+)ESI-MS/MS spectra of the common TPs obtained for H-SDF, HH-SDF and T-SDF irradiated samples.

indicating the absence of any modification beyond the sulfonamide, while on the other hand, fragment ions arising from cleavage according to process ***a*** in Scheme 1 are observed in all three spectra (*m/z* 113, 129 and 99, respectively). Based on compelling evidence presented in our previous work on the photodegradation of SDF under identical experimental conditions as in the current study,[17]

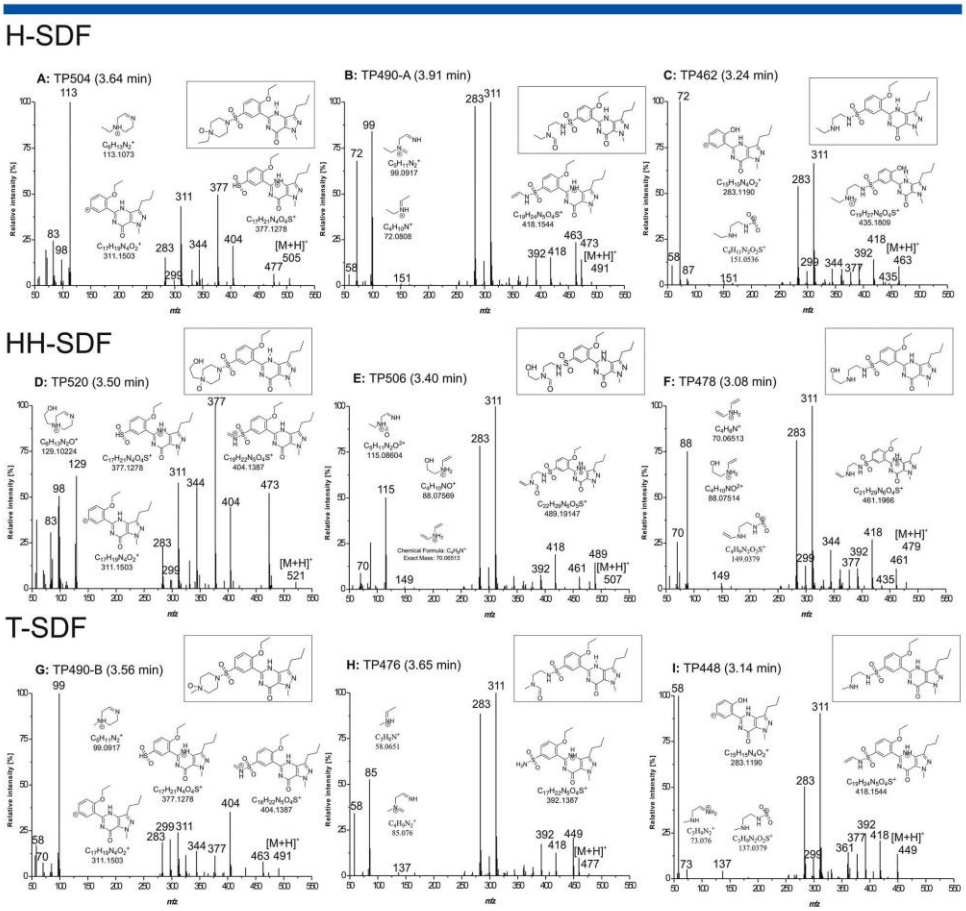

Figure 3. (+)ESI-MS/MS spectra of novel TPs obtained for H-SDF, HH-SDF and T-SDF irradiated samples.

the three TPs are attributed to N-oxygenation of the tertiary amine in the piperazine ring. In fact, the mass spectrum of TP490-B (Fig. 3G) is essentially identical to that of the eponymous photoproduct in Eichhorn *et al.*,[17] i.e. the N-oxide of SDF. As with TP490-B, formed from SDF after rapid initial oxidation of the thiocarbonyl group in T-SDF, the slower elution of TP504 and TP520 as compared to the precursor compound is due to the loss of basicity of the aliphatic amine by conversion into the neutral N-oxide.

Figure 3B, 3E and 3H shows a second series of TPs differing in elemental composition from the parent compounds (SDF in case of the T-SDF) by $-CH_2+O$. As with the three afore discussed TPs or in all three instances the fragment ions at *m/z* 283 and 311 indicate that the modification is in the left part of the molecule. As compared to the parent compounds, the piperazine ring-specific fragment ions at *m/z* 113, 129 and 99 (SDF) are shifted to *m/z* 99, 115 and 85 for H-SDF, HH-SDF and T-SDF (SDF), respectively. At the same time, the molecular ions of the TPs all show a loss of water producing *m/z* 473 (H-SDF), *m/z* 489 (HH-SDF) and *m/z* 459 (T-SDF/SDF) as well as decarbonilation of similar intensity. Plausible structures being consistent with these fragmentation patterns arise from oxidative cleavage of one ethylene bridge upon loss of one carbon atom. Fragmentation of the resulting amide produces the loss of CO or dehydration. Although the latter mechanism is uncommon, the loss of water from has been previously reported.[25]

A third series of homologous TPs comprises TP462 (H-SDF), TP478 (HH-SDF) and TP448 (T-SDF after oxidation to SDF). In terms of elemental formulae, they differ from their precursor compounds by removal of C_2H_2 (26 Da) (see Table 2). The heaviest fragment ion common to all three TPs (Fig. 3C, 3F, and 3I) is the even-electron species with *m/z* 418 ($C_{19}H_{24}N_5O_4S^+$). Taking into account that the three product ion spectra contain the characteristic series of ions at *m/z* 377, 311, 299 and 283, the most plausible photodegradation pathway giving rise to the TPs is *N,N*-deethylation. Hence, the

common ion at *m/z* 418 corresponds to the loss of the substituent on the secondary amine, e.g. of methylamine (C_2H_5N = 31 Da) in case of TP448. Apart from the mass spectral information, the chromatographic behavior is also in agreement with the structural modification insofar as the loss of lipophilicity, i.e. the bridging *N,N*-ethylene moiety, translates into weaker chromatographic retention and therefore earlier elution than the precursor compounds (H-SDF: 3.48 *vs* 3.64 min; HH-SDF: 3.33 *vs* 3.50 min; (T-)SDF: 3.46 *vs* 3.56 min).

Environmental occurrence

The environmental survey of SDF, SDF analogues and their TPs in waters allowed the first detection of TP488 and TP448 in effluent samples. SDF and SDF analogues were not detected in the effluent of WWTP and nor in surface waters. The implementation of UV treatment in the WWTPs could be an important factor in the formation of these TPs. Furthermore, these TPs could be produced from different treatments such as biodegradation in WWTP. Accurate masses and MS2 spectra are given in the Supporting Information (Figure S4) and confirmed TPs identities. Because authentic standards are currently not commercially available, the concentrations of TPs cannot be accurately determined.

Conclusion

In the present study, we examined the photodegradation pathways of several SDF analogues based on the elucidation of high-resolution MS/MS data. Thanks to distinct fragmentation patterns with a number of highly diagnostic fragment ions across the entire *m/z* range, and the possibility to rationalize the formation of the photoproducts by comparing the TP spectrum between the different SDF analogues, the structures of a large number of both unique and common photoproducts could be proposed. It was demonstrated that the piperazine-bearing analogues H-SDF, HH-SDF and T-SDF displayed a similar behavior as SDF in that the aliphatic ring was gradually broken down upon exposure to simulated sunlight. In case of the thioketone-containing T-SDF, all of the identified photoproducts were devoid of the C=S group thereby providing evidence for the instability of this moiety. With the thioketone being subject to rapid oxidation to the corresponding ketone group, i.e. becoming SDF, the set of generated photoproducts was therefore very similar to those reported in our previous work on the photolysis of SDF under identical experimental conditions. Lacking the basic nitrogen atom in the aliphatic ring, NR-SDF, in turn, gave rise to only two prominent photoproducts (TP391 and TP392). These were also found in the solutions of the experiments performed with H-SDF, HH-SDF and T-SDF indicating that the photodegradation pathways of all four SDF analogues eventually converged in the formation of the stable sulfonic acid TP392. Assuming that the findings from the photodegradation studies carried out under controlled laboratory conditions are predictive of the photofate under real conditions in the environment, e.g. in sunlit surface waters having received treated effluents from sewage treatment plants, the detection of one TP or another in the samples would likely not allow to unequivocally determine the identity of the discharged drug. On the other hand, the polar TP392 might serve as a tracer compound for detecting the contamination of surface waters with SDF-related compounds.

Environmental analysis allowed the first detection of TP488 and TP448 in wastewater effluents. It worth noting that their detection does not allow to unequivocally determine the identity of the initially discharged precursor compound, because the two TPs can originate from different SDF analogs.

Acknowledgements

This work has been supported by the Spanish Ministry of Science and Innovation [project Consolider-Ingenio 2010 Scarce CSD2009-00065]. This work reflects only the authors' views, and the European Community is not liable for any use that may be made of the information contained therein. SP acknowledges the contract from the Ramón y Cajal Program of the Spanish Ministry of Economy and Competitiveness. This work was partly financially supported by the Generalitat de Catalunya (Consolidated Research Group: Water and Soil Quality Unit 2014-SGR-418) and 2014 SGR 291-ICRA.

References

[1] B. J. Venhuis, D. de Kaste. Towards a decade of detecting new analogues of sildenafil, tadalafil and vardenafil in food supplements: A history, analytical aspects and health risks. *J. Pharm. Biomed. Anal.* **2012**, *69*, 196–208.
[2] S. Singh, B. Prasad, A. A. Savaliya, R. P. Shah, V. M. Gohil, A. Kaur. Strategies for characterizing sildenafil, vardenafil, tadalafil and their analogues in herbal dietary supplements, and detecting counterfeit products containing these drugs. *TrAC Trends Anal. Chem.* **2009**, *28*, 13–28.
[3] M. Y. Low, Y. Zeng, L. Li, X. W. Ge, R. Lee, B. C. Bloodworth, H. L. Koh. Safety and Quality Assessment of 175 Illegal Sexual Enhancement Products Seized in Red-Light Districts in Singapore. *Drug-Safety* **2009**, *32*, 1141–1146.
[4] M. H. Shin, M. K. Hong, W. S. Kim, Y. J. Lee, Y. C. Jeoung. Identification of a new analogue of sildenafil added illegally to a functional food marketed for penile erectile dysfunction. *Food Addit. Contam.* **2003**, *20*, 793–796.
[5] C. L. Kee, X. Ge, M.-Y. Low, H. L. Koh. Structural elucidation of a new sildenafil analogue using high-resolution Orbitrap mass spectrometry. *Rapid Commun. Mass Spectrom.* **2013**, *27*, 1380–1384.
[6] F. Shi, C. Guo, L. Gong, J. Li, P. Dong, J. Zhang, P. Cui, S. Jiang, Y. Zhao, S. Zeng. Application of a high resolution benchtop quadrupole-Orbitrap mass spectrometry for the rapid screening, confirmation and quantification of illegal adulterated phosphodiesterase-5 inhibitors in herbal medicines and dietary supplements, *J. Chromatogr. A. 1344*, 91–98.
[7] B. J. Venhuis, D. M. Barends, M. E. Zwaagstra, D.d. Kaste. Recent developments in counterfeits and imitations of Viagra, Cialis and Levitra, in: RIVM (Ed.), Bilthoven, 2000-2010.
[8] Y. C. Liao, K. C. Lai, H. C. Lee, Y. C. Liu, Y. L. Lin, D. Y. C. Shih. Isolation and Identification of New Sildenafil Analogues from Dietary Supplements. *J. Food Drug Anal.* **2013**, *21*, 40–49.
[9] L. Kuo-Chih, L. Yi-Chu, L. Yung-Chih, L. Yun-Lian, T. Li-Yao, L. Jer-Huei, L. Chi-Fang. Isolation and Identification of Three Thio-sildenafil Analogues in Dietary Supplements. *J. Food Drug Anal.* **2010**, *18*, 269–278.
[10] X. Ge, L. Li, H. L. Koh, M. Y. Low. Identification of a new sildenafil analogue in a health supplement. *J. Pharm. Biomed. Anal.* **2011**, *56*, 491–496.
[11] H. J. Park, H. K. Jeong, M. I. Chang, M. H. Im, J. Y. Jeong, D. M. Choi, K. Park, M. K. Hong, J. Youm, S. B. Han, D. J. Kim, J. H. Park, S. W. Kwon. Structure determination of new analogues of vardenafil and sildenafil in dietary supplements. *Food Addit. Contam.* **2007**, *24*, 122–129.
[12] J. C. Reepmeyer, J. T. Woodruff. Use of liquid chromatography–mass spectrometry and a chemical cleavage reaction for the structure elucidation of a new sildenafil analogue detected as an adulterant in an herbal dietary supplement. *J. Pharm. Biomed. Anal.* **2007**, *44*, 887–893.
[13] A. Nieto, M. Peschka, F. Borrull, E. Pocurull, R. M. Marcé, T. P. Knepper. Phosphodiesterase type V inhibitors: Occurrence and fate in wastewater and sewage sludge. *Water Res.* **2010**, *44*, 1607–1615.
[14] H. F. Schröder, W. Gebhardt, M. Thevis. Anabolic, doping, and lifestyle drugs, and selected metabolites in wastewater—detection, quantification, and behaviour monitored by high-resolution MS and MSn before and after sewage treatment. *Anal. Bioanal. Chem.* **2010**, *398*, 1207–1229.

[15] R. L. Oulton, T. Kohn, D. M. Cwiertny. Pharmaceuticals and personal care products in effluent matrices: A survey of transformation and removal during wastewater treatment and implications for wastewater management. *J. Environ. Monit.* **2010**, *12*, 1956–1978.
[16] T. E. Doll, F. H. Frimmel. Fate of pharmaceuticals—photodegradation by simulated solar UV-light. *Chemosphere* **2003**, *52*, 1757–1769.
[17] P. Eichhorn, S. Pérez, J. Aceña, P. Gardinali, J. L. Abad, D. Barceló. Identification of phototransformation products of sildenafil (Viagra) and its N-demethylated human metabolite under simulated sunlight. *J. Mass Spectrom.* **2012**, *47*, 701–711.
[18] L. Blok-Tip, B. Zomer, F. Bakker, K. D. Hartog, M. Hamzink, J. ten Hove, M. Vredenbregt, D. de Kaste. Structure elucidation of sildenafil analogues in herbal products. *Food Addit. Contam.* **2004**, *21*, 737–748.
[19] Reepmeyer J. C., D. A. d'Avignon. Structure elucidation of thioketone analogues of sildenafil detected as adulterants in herbal aphrodisiacs. *J. Pharm. Biomed. Anal.* **2009**, *49*, 145–150.
[20] B. J. Venhuis, M. E. Zwaagstra, J. D. J. van den Berg, A. J. H. P. van Riel, H. W. G. Wagenaar, K. van Grootheest, D. M. Barends, D. de Kaste. Illicit erectile dysfunction products in the Netherlands: A decade of trends and a 2007-2010 product update, in: Illegale erectiemiddelen in Nederland: Analyses van producten (2007-2010) en een decennium van trends, Rijksinstituut voor Volksgezondheid en Milieu RIVM, Dutch Customs Laboratory, Royal Dutch Association for the Advancement of Pharmacy.
[21] M. Alp, M. Coşkun, H. Göker. Isolation and identification of a new sildenafil analogue adulterated in energy drink: Propoxyphenyl sildenafil. *J. Pharm. Biomed. Anal.* **2013**, *72*, 155–158.
[22] S. Ma, Y. Xu, M. Shou. Characterization of imatinib metabolites in rat and human liver microsomes: differentiation of hydroxylation from N-oxidation by liquid chromatography/atmospheric pressure chemical ionization mass spectrometry. *Rapid Commun. Mass Spectrom.* **2009**, *23*, 1446–1450.
[23] R. Ramanathan, A. D. Su, N. Alvarez, N. Blumenkrantz, S. K. Chowdhury, K. Alton, J. Patrick. Liquid Chromatography/Mass Spectrometry Methods for Distinguishing N-Oxides from Hydroxylated Compounds. *Anal. Chem.* **2000**, *72*, 1352–1359.
[24] D. Zhong, J. Xing, S. Zhang, L. Sun. Study of the electrospray ionization tandem mass spectrometry of sildenafil derivatives. *Rapid Commun. Mass Spectrom.* **2002**, *16*, 1836–1843.
[25] R. D. Morrison, A. L. Blobaum, F. W. Byers, T. S. Santomango, T. M. Bridges, D. Stec, K. A. Brewer, R. Sanchez-Ponce, M. M. Corlew, R. Rush, A. S. Felts, J. Manka, B. S. Bates, D. F. Venable, A. L. Rodriguez, C. K. Jones, C. M. Niswender, P. J. Conn, C. W. Lindsley, K. A. Emmitte, J. S. Daniels. The Role of Aldehyde Oxidase and Xanthine Oxidase in the Biotransformation of a Novel Negative Allosteric Modulator of Metabotropic Glutamate Receptor Subtype 5. *Drug Metab. Dispos.* **2012**, *40*, 1834–1845.

Supporting information

Additional supporting information may be found in the online version of this article at the publisher's web site.

Structure elucidation of phototransformation products of analogs of the erectile dysfunction drug sildenafil in artificial freshwater UPLC-Q Exactive-MS

Supporting Information

Jaume Aceña[1], Sandra Pérez[1*], Piero Gardinali[2], José Luis Abad[3], Peter Eichhorn[1], Nubia Heuett[2],Damià Barceló[1,4]

[1] Department of Environmental Chemistry, IDAEA-CSIC, c/Jordi Girona 18-26, 08034 Barcelona (Spain)
[2] Florida International University, 11200 SW 8th Street, Miami, FL 33199-0001 (USA)

[3] IQAC-CSIC, Department of Biomedicinal Chemistry, Jordi Girona 18-26, 08034 Barcelona (Spain)

[4] Catalan Institute of Water Research, ICRA Catalan Institute for Water Research- ICRA, C/Emili Grahit, 101, Edifici H_2O, Parc Científic i Tecnològic de la Universitat de Girona, E-17003 Girona (Spain)

Table S1. Accurate mass measurements of phototransformation products of HH-SDF obtained by UPLC–(+)ESI-Orbitrap-MS in MS or MS/MS mode.

Compound/ Photoproduct	Measured ion mass [m/z]	Elemental composition	Theoretical ion mass [*m/z*]	Rel. error [ppm]
TP488	489.1919	$C_{22}H_{29}N_6O_5S$	489.1915	1.0
	461.1967	$C_{21}H_{29}N_6O_4S$	461.1966	0.4
	377.1279	$C_{17}H_{21}N_4O_4S$	377.1278	0.3
	311.1503	$C_{17}H_{19}N_4O_2$	311.1503	0.2
	299.1141	$C_{15}H_{15}N_4O_3$	299.1139	0.7
	283.1191	$C_{15}H_{15}N_4O_2$	283.1190	0.5
	85.0767	$C_4H_9N_2$	85.0760	8.2
TP462-B	463.1760	$C_{20}H_{27}N_6O_5S$	463.1758	0.5
	435.1805	$C_{19}H_{27}N_6O_4S$	435.1809	-0.9
	418.1541	$C_{19}H_{24}N_5O_4S$	418.1544	-0.5
	311.1503	$C_{17}H_{19}N_4O_2$	311.1503	0.1
	299.1140	$C_{15}H_{15}N_4O_3$	299.1139	0.5
	283.1189	$C_{15}H_{15}N_4O_2$	283.1190	-0.1
	71.0612	$C_3H_7N_2$	71.0604	10.9
TP460	461.1967	$C_{21}H_{29}N_6O_4S$	461.1966	0.4
	377.1279	$C_{17}H_{21}N_4O_4S$	377.1278	0.3
	311.1503	$C_{17}H_{19}N_4O_2$	311.1503	0.2
	283.1191	$C_{15}H_{15}N_4O_2$	283.1190	0.5
	85.0767	$C_4H_9N_2$	85.0760	8.4
TP434	435.1812	$C_{19}H_{27}N_6O_4S$	435.1809	0.6
	418.1551	$C_{19}H_{24}N_5O_4S$	418.1544	1.8
	392.1393	$C_{17}H_{22}N_5O_4S$	392.1387	1.6

	377.1285	$C_{17}H_{21}N_4O_4S$	377.1278	2.0
	311.1506	$C_{17}H_{19}N_4O_2$	311.1503	1.1
	299.1141	$C_{15}H_{15}N_4O_3$	299.1139	0.9
	283.1194	$C_{15}H_{15}N_4O_2$	283.1190	1.7
TP392	393.1223	$C_{17}H_{21}N_4O_5S$	393.1227	-1.0
	365.0915	$C_{15}H_{17}N_4O_5S$	365.0914	0.2
	336.0522	$C_{13}H_{12}N_4O_5S$	336.0523	-0.2
	284.1270	$C_{15}H_{16}N_4O_2$	284.1268	0.7
	256.0955	$C_{13}H_{12}N_4O_2$	256.0955	-0.1
TP391	392.1385	$C_{17}H_{22}N_5O_4S$	392.1387	-0.5
	364.1074	$C_{15}H_{18}N_5O_4S$	364.1074	-0.1
	299.1140	$C_{15}H_{15}N_4O_3$	299.1139	0.4
	283.1191	$C_{15}H_{15}N_4O_2$	283.1190	0.6

Table S2. Accurate mass measurements of T-SDF and its phototransformation products obtained by UPLC–(+)ESI-Orbitrap-MS in MS or MS/MS mode.

Compound/ Photoproduct	Measured ion mass [m/z]	Elemental composition	Theoretical ion mass [*m/z*]	Rel. error [ppm]
TP488	489.1918	$C_{22}H_{29}N_6O_5S$	489.1915	0.7
	461.1974	$C_{21}H_{29}N_6O_4S$	461.1966	1.8
	377.1279	$C_{17}H_{21}N_4O_4S$	377.1278	0.3
	311.1505	$C_{17}H_{19}N_4O_2$	311.1503	0.8
	299.1141	$C_{15}H_{15}N_4O_3$	299.1139	0.7
	283.1192	$C_{15}H_{15}N_4O_2$	283.1190	0.8
	85.0768	$C_4H_9N_2$	85.0760	8.9
TP462-B	463.1761	$C_{20}H_{27}N_6O_5S$	463.1758	0.6
	435.1814	$C_{19}H_{27}N_6O_4S$	435.1809	1.1
	418.1551	$C_{19}H_{24}N_5O_4S$	418.1544	1.7
	311.1505	$C_{17}H_{19}N_4O_2$	311.1503	0.7
	299.1144	$C_{15}H_{15}N_4O_3$	299.1139	1.8
	283.1192	$C_{15}H_{15}N_4O_2$	283.1190	0.8
	71.0612	$C_3H_7N_2$	71.0604	11.9
TP460	461.1967	$C_{21}H_{29}N_6O_4S$	461.1966	0.2
	377.1280	$C_{17}H_{21}N_4O_4S$	377.1278	0.5
	311.1505	$C_{17}H_{19}N_4O_2$	311.1503	0.7
	283.1194	$C_{15}H_{15}N_4O_2$	283.1190	1.4
	85.0768	$C_4H_9N_2$	85.0760	9.3
TP434	435.1810	$C_{19}H_{27}N_6O_4S$	435.1809	0.3
	418.1548	$C_{19}H_{24}N_5O_4S$	418.1544	1.0
	392.1391	$C_{17}H_{22}N_5O_4S$	392.1387	1.1

	377.1288	$C_{17}H_{21}N_4O_4S$	377.1278	2.7
	311.1504	$C_{17}H_{19}N_4O_2$	311.1503	0.6
	299.1140	$C_{15}H_{15}N_4O_3$	299.1139	0.4
	283.1192	$C_{15}H_{15}N_4O_2$	283.1190	0.8
TP392	393.1224	$C_{17}H_{21}N_4O_5S$	393.1227	-0.7
	365.0917	$C_{15}H_{17}N_4O_5S$	365.0914	0.7
	336.0528	$C_{13}H_{12}N_4O_5S$	336.0523	1.4
	284.1276	$C_{15}H_{16}N_4O_2$	284.1268	2.9
	256.0954	$C_{13}H_{12}N_4O_2$	256.0955	-0.3
TP391	392.1386	$C_{17}H_{22}N_5O_4S$	392.1387	-0.2
	364.1071	$C_{15}H_{18}N_5O_4S$	364.1074	-0.9
	299.1139	$C_{15}H_{15}N_4O_3$	299.1139	0.2
	283.1194	$C_{15}H_{15}N_4O_2$	283.1190	1.5

Table S3. Accurate mass measurements of phototransformation products of NR-SDF obtained by UPLC–(+)ESI-Orbitrap-MS in MS or MS/MS mode.

Compound/ Photoproduct	Measured ion mass [m/z]	Elemental composition	Theoretical ion mass [*m/z*]	Rel. error [ppm]
TP392	393.1226	$C_{17}H_{21}N_4O_5S$	393.1227	-0.4
	365.0905	$C_{15}H_{17}N_4O_5S$	365.0914	-2.6
	336.0518	$C_{13}H_{12}N_4O_5S$	336.0523	-1.6
	284.1260	$C_{15}H_{16}N_4O_2$	284.1268	-2.7
	256.0950	$C_{13}H_{12}N_4O_2$	256.0955	-2.0
TP391	392.1391	$C_{17}H_{22}N_5O_4S$	392.1387	1.0
	364.1080	$C_{15}H_{18}N_5O_4S$	364.1074	1.7
	299.1144	$C_{15}H_{15}N_4O_3$	299.1139	1.6
	283.1192	$C_{15}H_{15}N_4O_2$	283.1190	0.9

Figure S1: Phototransformation profiles for the experiments at high and low concentration.

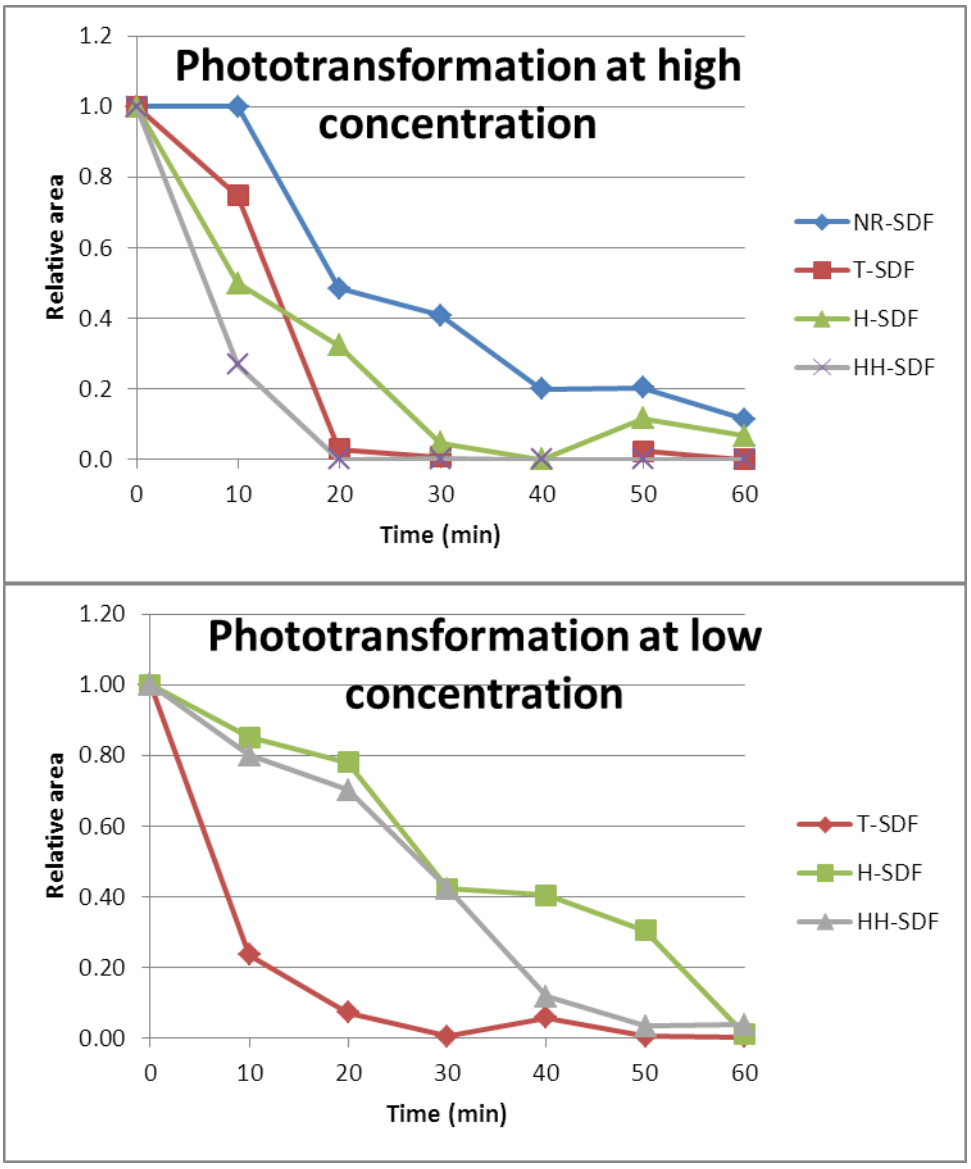

Figure S2: Extracted Ion Chromatograms of TPs of analogues of SDF formed at 1µg/L.

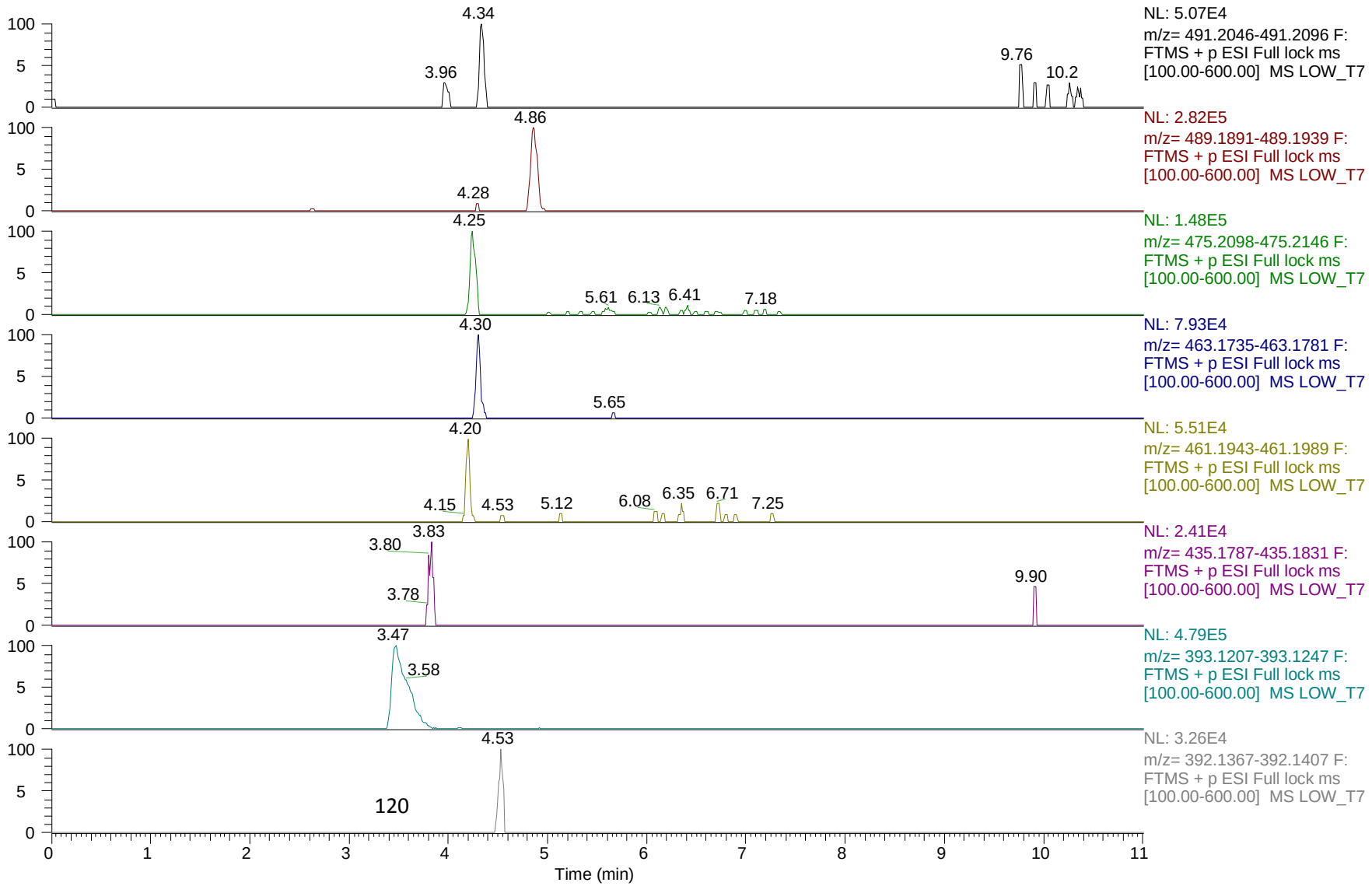

Figure S3: Extracted Ion Chromatograms of H-SDF and TP504 for the comparison of the effect of mobile phase pH (3.2 vs. 6.8) on the retention times.

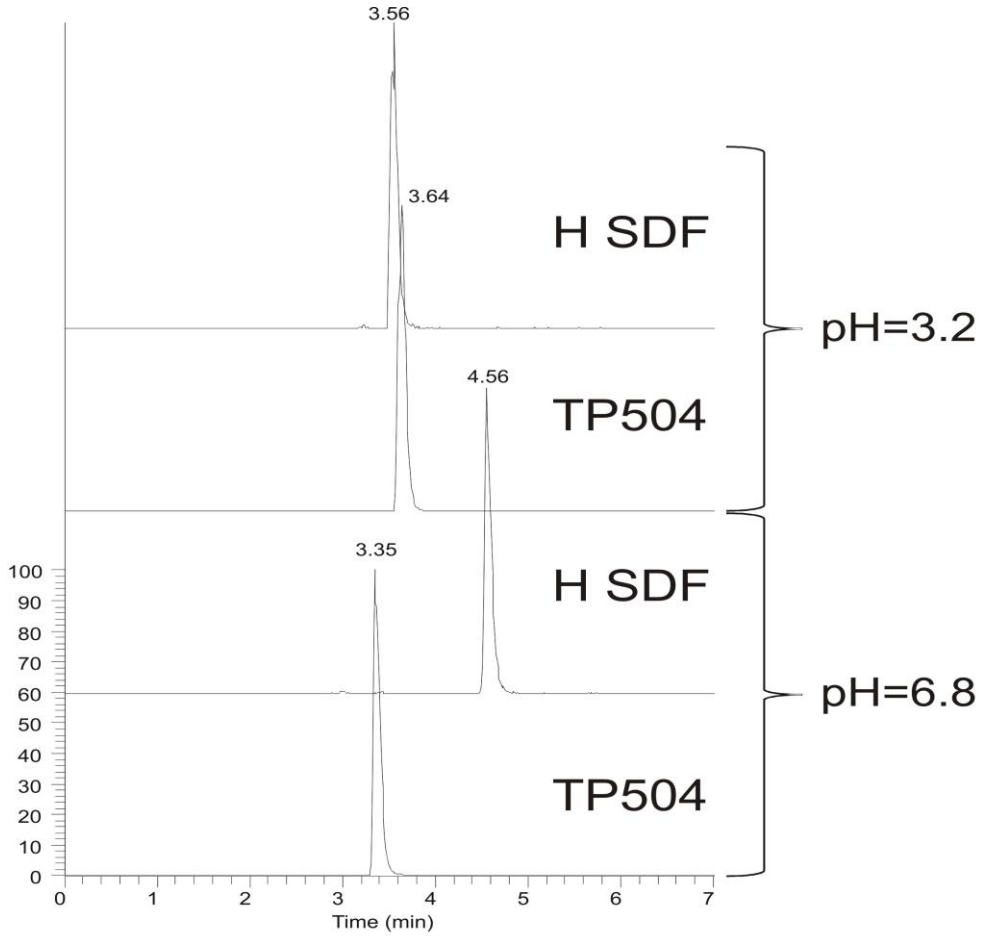

Figure S4: MS2 spectra of A) TP448 and B) TP499 detected in environmental samples.

A)

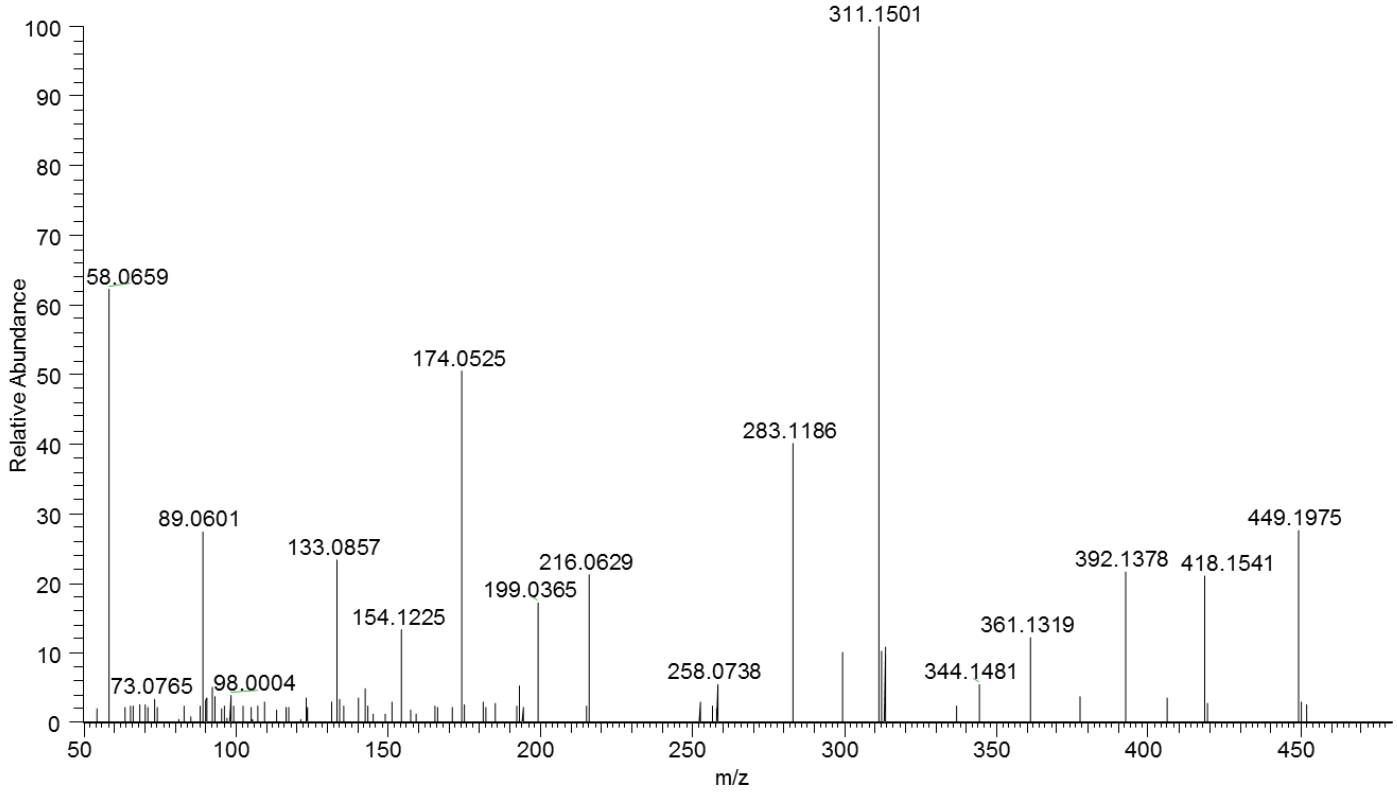

B)

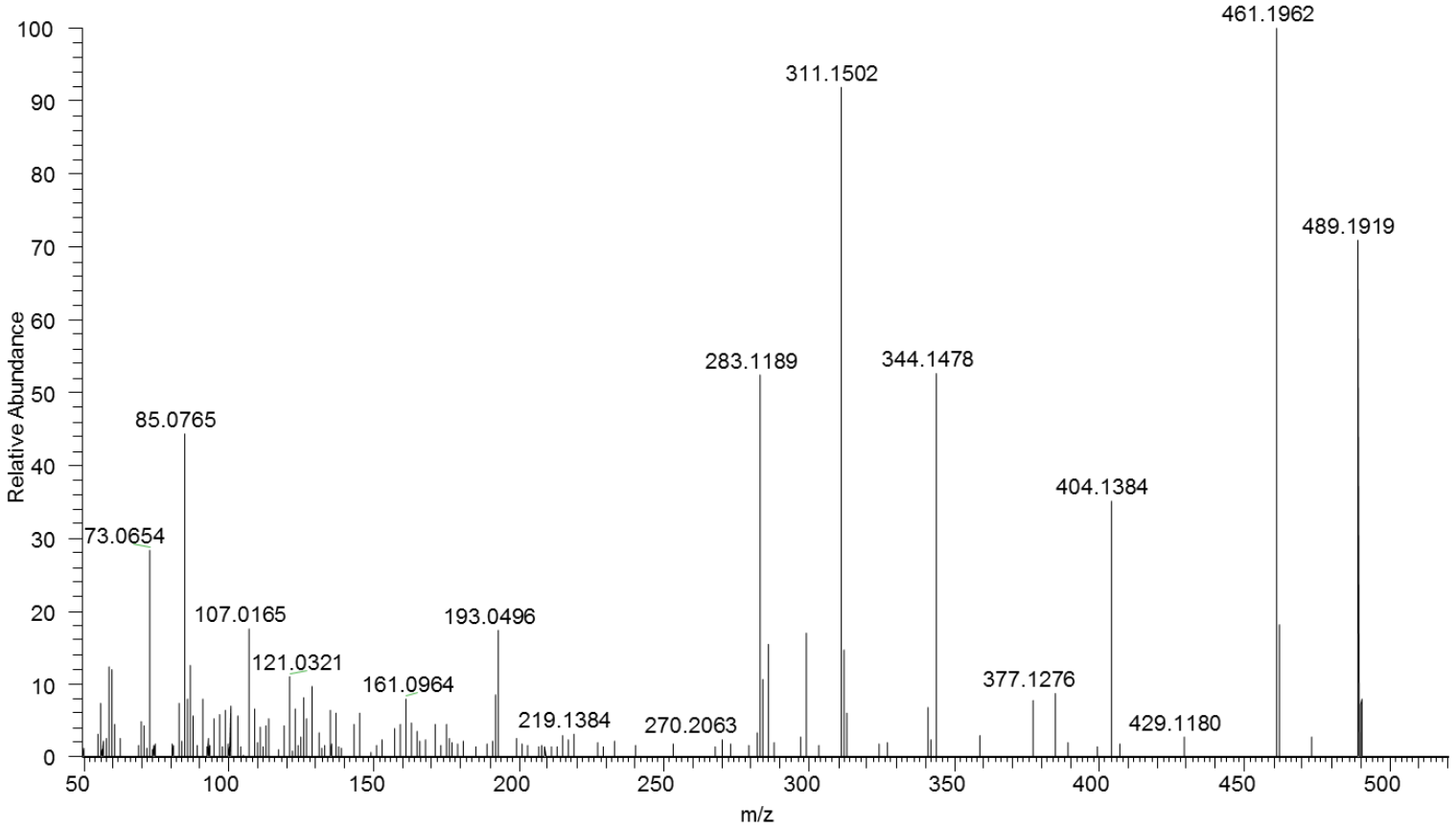
461.1962
311.1502
489.1919
283.1189
344.1478
85.0765
404.1384
73.0654
107.0165
193.0496
121.0321
161.0964
377.1276
219.1384
270.2063
429.1180
Relative Abundance
m/z
100
90
80
70
60
50
40
30
20
10
0
50
100
150
200
250
300
350
400
450
500

3.2 Processos de transformació: Biodegradació

Com s'ha vist, el destí d'un producte farmacèutic al medi aquàtic depèn de nombrosos factors, incloent les seves propietats fisicoquímiques, els factors ambientals, les condicions climàtiques i/o la presència i activitat de microorganismes amb capacitat per biodegradar-lo. Malgrat l'important paper que té la fotodegradació, hi ha diferents causes per les quals compostos que poden evadir les reaccions fotoquímiques, ja sigui per la pròpia naturalesa del compost o simplement perquè no estan exposats a la llum del sol. En aquests casos, el factor predominant en l'eliminació d'aquests compostos és la biodegradació, realitzada principalment mitjançant transformació microbiana. La biodegradació inclou processos catabòlics de microorganismes, algues, llevats i fongs els quals poden descompondre parcial o completament els compostos orgànics. Així doncs, els microorganismes ambientals juguen un paper clau i indispensable pel manteniment de la qualitat del medi aquàtic.

Molts contaminants orgànics es biodegraden per organismes que utilitzen els compostos com a font d'energia. Tanmateix cal tenir en compte un altre procés de biodegradació important, el co-metabolisme. El co-metabolisme consisteix també en la transformació d'un compost orgànic per part de microorganismes però sense ser una font d'energia ni finalitats nutritives [69]. El poder de degradació microbiana per a la eliminació de contaminants és de sobres conegut. Conseqüentment, la presència d'una comunitat microbiana natural és un prerequisit necessari per a una resposta eficaç als diversos contaminants i TPs que s'alliberen als ecosistemes. Malgrat això, l'eliminació d'aquesta contaminació només és possible si la toxicitat no obstaculitza dita activitat microbiana. Recentment, Anna Barra i col. [147] han revisat els diferents estudis de biodegradació de les diferents famílies de fàrmacs que hi ha a la literatura. En aquesta revisió es conclou que en general els fàrmacs no són persistents per si mateixos i que el ràtio de la seva biodegradació depèn de factors com la temperatura i el contingut de matèria orgànica al riu. No obstant això, l'entrada contínua de fàrmacs al medi aquàtic provoca que alguns d'aquests compostos siguin considerats com a contaminants orgànics pseudo-persistents, a causa del seu gran volum de producció i consum, malgrat la seva

curta vida mitjana al medi ambient. L'exposició continua a residus farmacèutics pot comprometre l'estructura de les comunitats microbianes i per tant alterar l'activitat de degradació de contaminants. A més, la presència de residus d'antibiòtics al medi ambient també pot provocar el desenvolupament i expansió d'organismes patògens resistents als agents antimicrobians. Fet que ha comportat una preocupació creixent per a la salut pública amb l'anomenada resistència als antibiòtics.

En aquest camp doncs, són necessaris més estudis per tal de determinar les vies completes de degradació, els diferents processos i els efectes sobre els ecosistemes, però sobretot controlar i disminuir l'entrada i eliminació dels antibiòtics al medi, ja que podent repercutir fins i tot sobre la salut humana. En aquest context, en aquest capítol ens hem proposat estudiar la biodegradació d'antibiòtics al riu tot estudiant els principals mecanismes de resistència bacteriana. P

Dels diferents antibiòtics que podem trobar al medi ambient, ens hem centrat en la família de les sulfonamides ja que la seva presència als efluents de les EDARs i als rius ha estat àmpliament documentada. Les sulfonamides van ser els primers fàrmacs utilitzats de forma eficaç per a tractar infeccions bacterianes a humans. Actualment, el desenvolupament d'algunes alternatives n'esta limitant el seu ús però encara s'utilitzen tan en tractaments humans com en veterinària. El 2010 Gutierrez i col. i col [148] va estudiar la influència de les sulfonamides sobre comunitats bacterianes i va observar que a llarg termini, malgrat siguin en baixes concentracions, poden afectar al funcionament i a la diversitat estructural de les mateixes. Per tal de tenir un una visió més acurada del mecanisme de residència i dels processos de biodegradació, és essensial l'estudi dels seus TPs principals. Per aquest motiu s'han estudiat els mecanismes de resistència a sulfametoxazole, utilitzat principalment pel tractament d'infeccions urinàries en humans, i a sulfametazina, utilitzat freqüentment en veterinària.

La següent publicació mostra els resultats principals d'aquest estudi i les conclusions que s'en deriven.

Article nº 4: Degradation of sulphonamides as a microbial resistance mechanism.

M. Vila-Costa, R. Gioia, **J. Aceña**, S. Perez, E. Casamayor i Jordi Dachs.

Water Research - 2017

Water Research 115 (2017) 309–317

Contents lists available at ScienceDirect

Water Research

journal homepage: www.elsevier.com/locate/watres

Degradation of sulfonamides as a microbial resistance mechanism

Maria Vila-Costa [a, b, *], Rosalinda Gioia [a, **], Jaume Aceña [a], Sandra Pérez [a], Emilio O. Casamayor [b], Jordi Dachs [a]

[a] Department of Environmental Chemistry, IDAEA-CSIC, Jordi Girona 18-24, Barcelona 08034, Catalunya, Spain
[b] Integrative Freshwater Ecology Group, Centre for Advanced Studies of Blanes, CEAB-CSIC, Accés Cala St. Francesc 14, E-17300 Blanes, Spain

ARTICLE INFO

Article history:
Received 28 October 2016
Received in revised form
2 February 2017
Accepted 4 March 2017
Available online 6 March 2017

Keywords:
Microbial sulfonamide degradation
Sulfonamides
Riverine
Biofilms
Antibiotic resistance
Degradation products

ABSTRACT

Two of the main mechanisms of bacterial resistance to sulfonamides in aquatic systems, spread of antibiotic resistance genes (ARG) among the microbial community and in-situ bacterial sulfonamide degradation, were studied in mesocosms experiments using water and cobble biofilms from upstream (pristine waters) and downstream (polluted waters) from the Llobregat river, NE Iberian Peninsula. Mesocosms were prepared at two different concentrations (5000 ng/L and 1000 ng/L) of sulfonamides antibiotics (sulfamethazine and sulfamethoxazole). Concentrations of ARG, nutrients, sulfonamides and their degradation products were measured during the time course of the experiments. Sulfonamides were efficiently degraded by the biofilms during the first four weeks of the experiment. The abundance of ARG in biofilms sharply decreased after addition of high concentrations of sulfonamides, but this was not observed in the mesocosms treated with low concentrations of sulfonamides. Sulfonamide degradation was faster in polluted waters and at high concentrations of sulfonamide (and lower ARG abundances), suggesting that both degradation and ARG are two complementary resistance strategies employed by the microbial community. This study shows that microbial degradation of antibiotics is an efficient resistance mechanism coupled with the presence of ARG, and suggests that *in situ* degradation prevails at high concentrations of antibiotics whereas physiological adaptation by ARG spread would be more important under relatively lower concentrations of antibiotics.

1. Introduction

Antibiotics are widely used, and often abused, in human medicine and stockbreeding operations, for both infectious disease therapy and growth promotion. Antibiotics are ubiquitously found in rivers and there is a raising concern about the wide occurrence of antibiotic resistance bacteria (ARB) in natural waters (Ding and He, 2010; Martinez, 2008; Stoll et al., 2012). Antibiotic resistance in microbial communities can arise through: (1) microbial antibiotic degradation, that is, chemical transformation of the antibiotic by an existing enzyme of the cell, (2) by spontaneous mutation or acquisition of antibiotic resistance genes (ARG) from other cells by lateral gene transfer that yield alterated enzymes in a way that the antibiotic target site is not recognized by the antibiotic, (3) physical removal of intracellular antibiotic by activating membrane efflux pumps (Allen et al., 2010; Dever and Dermody, 2013; Pu et al., 2016). Not all microorganisms have all three mechanisms, and in fact, the relative importance of each mechanism and factors influencing their occurrence in natural systems is not well understood.

Allen et al. (2010) states that some organisms and some environments harbour ARGs irrespective of human activity which leads to the hypothesis that native roles of resistance exist in natural communities. However, little is known about the selection of pressures on ARGs in environments where there is little or no human activity, and how the ARG mechanism is coupled with microbial degradation of the antibiotics.

Sulfonamides such as sulfamethoxazole (SMX) and sulfamethazine (SMZ) were widely used in the past as antibiotics for human treatments. Nowadays, there are limited uses for sulfonamide antibiotics due to increasing bacterial resistance, potential for adverse effects, and the availability of more active antibiotics. Nevertheless, sulfonamides are frequently used in pigs and cattle for the treatment of bacterial diseases (Hruska and Franek, 2012). Sulfonamides

* Corresponding author. Department of Environmental Chemistry, IDAEA-CSIC, Jordi Girona 18-24, Barcelona 08034, Catalunya, Spain.
** Corresponding author. Current address: The REACH Centre, Lancaster University, Lancaster, LA1 4YQ, UK.
E-mail addresses: maria.vila@idaea.csic.es (M. Vila-Costa), r.gioia@thereachcentre.com (R. Gioia).

http://dx.doi.org/10.1016/j.watres.2017.03.007
0043-1354/

Abbreviations

ARG	antibiotic resistance genes
ARB	antibiotic-resistant bacteria
SMX	sulfamethoxazole
SMZ	sulfamethazine
TP	transformation products
Chla	chlorophyll *a*
AFDM	ash free dry mass
MeOH	methanol
qPCR	quantitative polymerase chain reaction
DNA	Deoxyribonucleic acid
TCA	Trichloroacetic acid
N-Hydroxy-SMX	Hydroxy-sulfamethoxazole
desamino-SMX	desamino-sulfamethoxazole
N-acetyl-SMX	acetyl-sulfamethoxazole
4-nitro-SMX	nitro-sulfamethoxazole
N-acetyl-SMZ	acetyl sulfamethazine
NH_4	ammonium

have been detected at relatively high concentrations in sewage treatment plant effluents, surface waters and ground water in diverse world regions (Auerbach et al., 2007; Pei et al., 2006; Pruden et al., 2007; Zhang et al., 2009). Antimicrobial resistance to sulfonamides by propagation of ARG occurred quite rapidly after their first introduction (Davies and Davies, 2010). Resistance to sulfonamides has been thought to be caused by the acquisition of the genes *sul1*, *sul2*, and *sul3* (Randall, 2004; Sköld, 2000). *Sul1* and *sul2* genes are widespread in the environment and they have been detected in lagoons (McKinney et al., 2010; Pei et al., 2007), rivers and surface waters around the globe (Luo et al., 2010; Pruden et al., 2006; Stoll et al., 2012). The microbial degradation of sulfonamides as a microbial resistance mechanism has received little attention, so far.

Stream biofilms play an important role in controlling the aquatic biogeochemical cycle of nutrients and regulate exchange between the water and the hyporheic zone, and is the habitat of important microbial communities. Through mutating or acquiring degradative genes, bacteria can adapt and proliferate in the environment as a result of the selective pressures created by pollutants (van der Meer, 2006). For example, biofilms grown in water from different river sites before and after the exposure to high levels of antibiotics, have shown that the continuous entrance of antibiotics in running waters cause significant structural and functional changes in attached microbial communities (Proia et al., 2013). Degradation of synthetic chemicals is especially efficient in rivers (Gioia and Dachs, 2012), and several studies have shown that stream biofilms play a primary role in attenuating riverine pollutants (Writer et al., 2011a; Battin et al., 2016; Roman and Sabater, 1999; Writer et al., 2011b). Besides abiotic transformation of sulfonamides by photooxidation (Rizzo et al., 2012; Batchu et al., 2014), microbial degradation of sulfonamides and some of the transformation products (TP) has been described in laboratory microcosms (Cetecioglu et al., 2016; Kassotaki et al., 2016; Liao et al., 2016; Su et al., 2016) and sludge (Yang et al., 2016). Microbial degradation of sulfonamides may be a complementary mechanism to ARG alteration, attenuating the effects of antibiotics on bacteria in rivers. However, little is known on the coupling of microbial degradation with the propagation of ARG as antibiotic resistance mechanisms. A priori, the bacterial potential for sulfonamide degradation do not need to be coupled with the presence of ARG, since degradation could be driven by bacterial communities different than those containing ARG.

The purpose of this study was to evaluate the relative importance of sulfonamide degradation versus the spread of sulfonamide-resistance genes in natural benthic biofilm communities as mechanisms of resistance to sulfonamides. Spread of ARG was studied quantifying the presence of *sul1* and *sul2* genes, whereas sulfonamide degradation was tracked quantifying sulfonamides concentrations and transformation products, since genes encodying for sulfonamide-degrading enzymes are not described in natural communities. Both mechanisms were studied under different concentrations of SMX and SMZ in mesocosmos experiments using upstream (pristine waters) and downstream (polluted waters) samples from the Llobregat river.

2. Materials and methods

2.1. Chemicals and materials

All solvents used: MeOH, acetonitrile and water were purchased from Merck (Darmstadt, Germany). Ammonium acetate and formic acid were obtained from VWR (Darmstadt, Germany). SMX and SMZ were purchased from Sigma Aldrich (Steinheim, Germany). The internal standards of SMZ and SMX were obtained from Toronto Research Chemicals (Toronto, Canada). The transformation products of SMX and SMZ such as N-acetyl-SMX, desamino-SMX, N-Hydroxy-SMX, 4-nitro-SMX and N-acetyl-SMZ (see structural formula in Fig. S1) were purchased from Toronto Research Chemicals (Toronto, Canada). Formic acid (98%–100%) was ACS grade and purchased from Sigma Aldrich (Schnelldorf, Germany). Oasis HLB (60 mg), solid-phase extraction cartridges were purchased from Waters (Waters, Milford, MA).

2.2. Field sampling

The Llobregat river (~165 km long) flows from the Pyrenees mountains to the south of Barcelona (NE Iberian Peninsula), and drains a catchment area of 4948 km^2 inhabited by a dense population of more than 3 million people, mostly living in the mid-lower part of the river. This part of the river has the biggest anthropogenic impacts by receiving discharges from urban and industrial wastewater treatment plants, sewer overflows, and diffuse pollution from agricultural fields. Antibiotic concentrations have been reported for the lower section of the Llobregat river, with SMX concentrations ranging between 213 ng/L and 907 ng/L. In contrast, the upper part of the river is pristine with a low population density and almost absent industrial, urban and agricultural inputs (Ginebreda et al., 2010; Masiá et al., 2015).

River water and cobbles were collected at six sites along the Llobregat from upstream (pristine waters) to downstream (polluted waters) in order to map out the concentration gradient of sulfonamide resistance genes along the river. A map of the sites is shown in Fig. 1. Sampling was conducted in July 2012 and water temperature varied between 17 °C at "Les Fonts de Llobregat" (pristine waters) to 24.4 °C at "St Boi" (polluted waters). At these two sites, a large number of cobbles and water were collected to be used in the mesocosm experiements.

2.3. Laboratory experiment

River water and cobbles were used to prepare mesocosms (3.5 L) in polypropylene bakers at two different concentrations (5 μg/L and 1 μg/L) of sulfonamides antibiotics (SMZ and SMX) and for the two sites; fonts del Llobregat (pristine) and St Boi (polluted). Previous to performing these experiments, preliminary experiments performed on glass beakers had shown that glass adsorbs

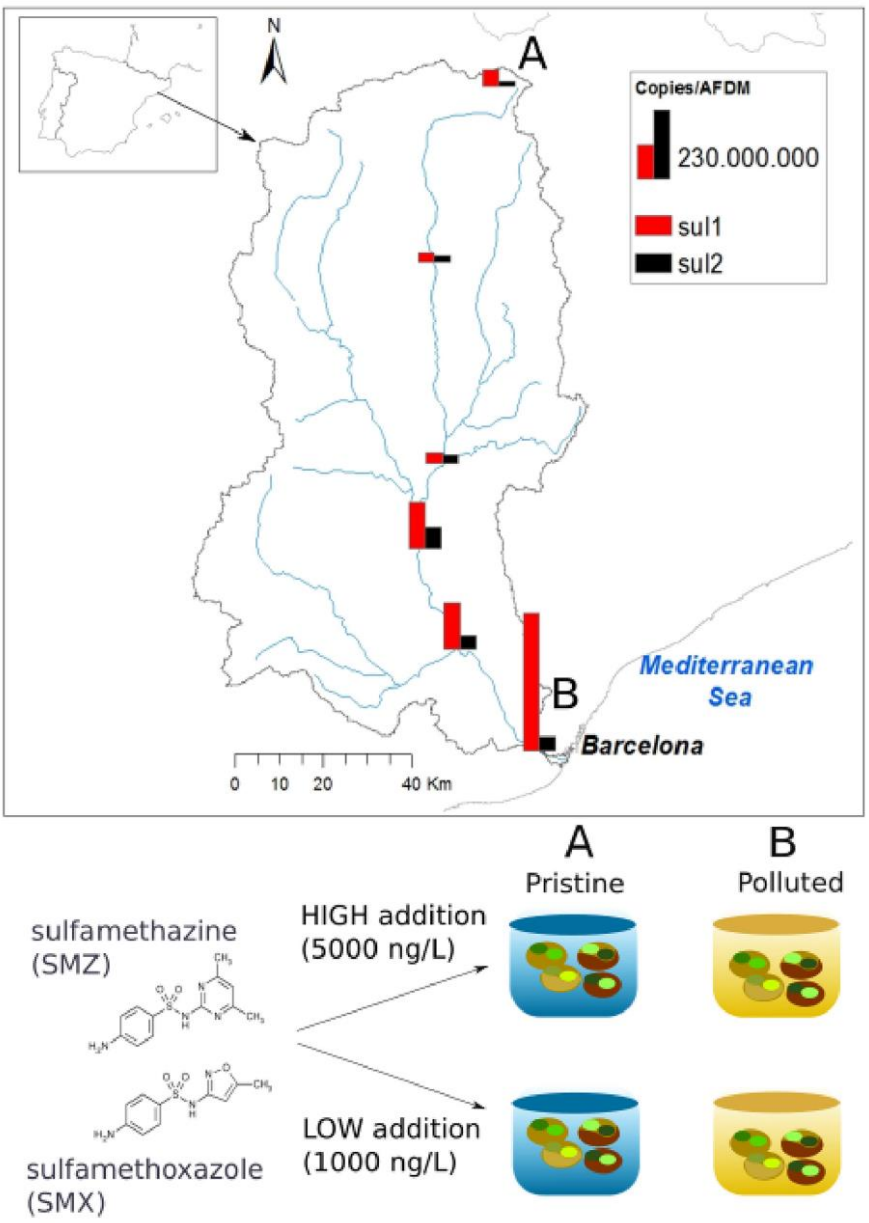

Fig. 1. Map of the sampling locations that shows the abundance of genes *sul1* and *sul2* corrected by biofilm ash free dry mass (AFDM) at each site and conceptual diagram of the experiment set up.

sulfonamides and therefore were deemed to be unsuitable for the experiment. The mesocosms were prepared ensuring that approximately the same area of cobbles was included in each polypropylene baker in order to obtain the same amount of benthic microbial biofilms in each treatment. A conceptual diagram of the experiment is shown in Fig. 1 and S2. Samples from the bakers were

collected at time 0 and every 15 days thereafter for approximately 8 weeks. Eight 'Chemical mesocosms' (2 mesocosms with the high concentration addition and 2 with the low concentrations addition for each one of the two sites) were used to collect duplicate samples for the analysis of sulfonamides and their transformation products (TP) in water. Twenty 'biological mesocosms' were prepared and used to collect cobbles for the analysis of the ARG and other ancillary measurements (5 at high concentration addition and 5 at low concentration addition of sulfonamides for each one of the two sites). Four of the bakers containing the biological mesocosm were sampled every 15 days, corresponding to the two concentration levels for the pristine and polluted sites, respectively. As the cobbles were removed for biofilm sampling, these bakers could not be used for the following sampling times (Fig. S1). Chemical and biological mesocosms were treated in the same manner during the course of the experiment, and thus it is assumed that all the mesocosms with the same initial addition concentration of sulfonamides were similar in respect of water concentration of sulfonamides and biological activity. Chemical controls to monitor abiotic degradation were prepared with MilliQ-water with no cobbles by adding the antibiotics at the high concentration, while microbiological controls were prepared with river water and cobbles without the addition of antibiotics (Fig. S1).

Mesocosms were incubated in replicates for 60 days in 12L:12D photoperiods under white light (120 μE/s m^2). Samples of river water (100 mL) and river cobbles biofilm were collected from the 'chemical mesocosms' and analysed for chemical concentration of sulfonamides. Samples of cobbles were collected from the 'biological mesocosms' at each sampling time and analysed for chemical concentrations of sulfonamide resistance genes and ancillary parameters. Cobbles were scrapped with clean metal brushes and washed with MilliQ-water as described elsewhere (Bartrons et al., 2012). Two stones generated a total pooled volume of 100–150 mL and were used for chlorophyll *a* (Chla) and ash free dry mass (AFDM) analysis by filtering triplicate subsamples of 4 mL through ashed, pre-weighed Whatmann GF/F glass fiber filters. Filters were stored at −20 °C until processing. Replicate samples for DNA analysis were collected from 5 to 10 stones, generating a total volume of approximately 30 mL/stone. Each volume was centrifuged at 5000 rpm, the supernatant was discarded and the biofilm was collected into sterile 2 mL tubes and stored at −20 °C until DNA extraction. Cobble scraped surfaces were estimated using aluminum foil and following a weight-to-area relationship.

2.4. Analytical methods

Water samples were extracted using an OASIS SPE cartridge (Waters). Forty μL of recovery standard d4-SMX at a concentration of 25 ppm was added to the sample prior to the SPE extraction. The water samples were passed through SPE cartridges at a relatively low flow rate (one drop every 2 s). Cartridges were eluted with 4 x 2 mL of methanol (MeOH) (Gros et al., 2009). The MeOH was evaporated under a gentle stream of N_2 to about 0.250 mL. The extract was then transferred to LC white vials and solvent exchanged to 50:50 MeOH: H_2O. An aqueous and MeOH solution of d4-SMZ, used as internal standard for quantification, was spiked at a final concentration of 100 ng/L. The final volume of the extracts was 0.5 mL. Biofilm samples were freeze-dried- for 3–4 days to eliminate or reduce the undesirable effects of water. Samples were then homogenised by mixing and stirring of the biofilm. Forty μL of the recovery standard d4-SMX (25 mg/L) was added to 1 g of sample. Samples were sonicated with 80:20 H2O:MeOH (3 × 10 mL x 15 min). The extract was solvent exchanged to a H_2O solution containing 5% of MeOH. Seventy-five mL of this solution was extracted through a SPE cartridge following the same procedure used for water samples. Samples were analysed by liquid chromatography and mass spectrometry as reported elsewhere (Gros et al., 2009). The MRM transitions of the transformation products were as follows: N-acetyl-SMX: m/z 296/134 and m/z 296/65; desamino-SMX: m/z 237/141 and m/z 237/77; N-hydroxy-SMX: m/z 270/172 and m/z 270/154, and 4-nitro-SMX: m/z 282/138 and m/z 282/186. A reversed-phase Purospher Star RP-18 end-capped column (125 mm × 2.0 mm, particle size 5 μm) was sourced from Merck (Dramstadt, Germany). For MS/MS analyses, Symbiosis™ Pico was connected in series with a 4000QTRAP hybrid triple quadrupole-linear ion trap mass spectrometer equipped with a Turbo Ion Spray source from Applied Biosystems-Sciex (Foster City, California, USA), where mass spectrometry detection was carried out. 4000QTrap was controlled by means of the Analyst 1.4.2 Software from Applied Biosystems-Sciex (Foster City, California, USA) and a companion software appendix for controlling the Symbiosis™ Pico from Spark Holland (Emmen, The Netherlands). Method quantification limits (MQLs) according to a signal-to-noise ratio (S/N) of 10 ranged from 0.9 to 9.5 ng/L and from 78 to 95 ng/L for the targeted compounds which were suitable for water and biofilm sample analysis, respectively. Recoveries for d4-SMX ranged from 60% to 85% for biofilm samples, and from 81 to 110% for water samples. Concentrations were recovery corrected. The concentration of sulfonamides in the chemical control remained constant through the duration of the experiment showing that there was no abiotic degradation or adsorption of the chemical in the mesocosm in the absence of biofilm.

2.5. AFDM and Chla

Biomass of epilithic biofilms (on cobbles) was measured as ash free dry mass (AFDM). AFDM material contains both autotrophic and heterotrophic organisms, live and senescent organisms, and abiotic carbon. To estimate AFDM, biofilm samples collected on glass fiber filters were dried at 60 °C until constant weight (c. 0.1 mg, Mettler Toledo MS204S/01 analytical balance), further combusted at 500 °C for 5 h, dried in a desiccator and weighted. The AFDM was estimated as the mass difference between dry and combusted filters. Chla was determined in acetone extracts by spectrophotometry (UV–Visible spectrophotometer Varian Cary 300 Bio) following Steinman and Lamberti (1996), and corrected for phaeopigments by further acidification.

2.6. DNA extraction and quantification of sul genes by quantitative PCR (qPCR)

DNA was extracted from 0.3 to 1.4 g of wet biofilm using FastDNA® SPIN Kit for Soil (Qbiogene, Carlsbad, CA) following the manufacturer instructions with the only modification of the use of the homogenizer. Cells were broken by vortexing the mixture of lysing matrix and sample using a MoBio vortex in 2 periods of 10 min instead of using the FastPrep instrument. Extracted DNA was quantified fluorometrically using the Quant-iT dsDNA Assay kit (Invitrogen, Paisley, UK) and Qubit fluorometer (Invitrogen). Subsamples of DNA were amplified by 16S PCR to check DNA quality. Quantification of sulfonamide resistance genes was performed by qPCR which quantified the gene copy numbers of the previously described primers *sul1* and *sul2* (Pei et al., 2006). See Table S1 in Supplemental Information for details on the primers and the qPCR conditions used. Standards were obtained after serial dilutions of environmentally cloned *sul1* and *sul2* sequences which were subsequently purified by QIAquick (QIAGEN), quantified by fluorescence (Qubit fluorometer, Invitrogen), and sequenced to check the identity of the target gene. Overall, average efficiencies of all quantification reactions ranged from 90% to 110%. Controls without

templates resulted in undetectable values in all samples. The appropriate size of qPCR products and absence of unspecific PCR products were checked by agarose gel electrophoresis (data not shown). Gene abundances were normalized to cobble area (cm^2) and to AFDM (i.e. organic matter) to allow comparison of results among samples.

2.7. Bacterial production

Bacterial secondary production was determined in the water column at the final time point after incorporation of ^{3}H-leucine into protein using the method of Kirchman et al. (1985) with the modifications of Smith and Azam (1992). Briefly, 1.2 mL of quadruplicate live and duplicate killed (5% TCA) subsamples were incubated with ^{3}H-leucine (40 nmol l^{-1} final concentration) for about 3 h at dark and at the *in situ* temperature. Incubations were stopped by addition of 120 mL of cold 50% TCA and then frozen (−20 °C) until further processing by centrifugation and TCA rinsing.

3. Results and discussion

3.1. Concentration of sulfonamides and their degradation products during the 60 days laboratory experiment

The concentrations of sulfonamides and their degradation products, AFDM, Chla, nutrients, the ARG abundances, and bacterial production are reported in Tables S2 and S3. The averages and standard deviations are reported in Tables S4 and S5. Since the concentrations of sulfonamides in cobbles biofilm were always found below detection limit, only the concentrations of sulfonamides in water are reported.

Fig. 2 shows the concentration of sulfamethazine (SMZ) and sulfamethoxazole (SMX) in both experiments (pristine and polluted sites) for the high (5000 ng/L) and low (1000 ng/L) sulfonamide additions from time zero to the end of the experiment (60 days). The concentrations of both sulfonamides decreased rapidly during the first 30 days reaching steady-state concentrations. The decrease in chemical concentrations during the first 30 days follows the first-order kinetics:

$$\ln\left(\frac{[Sulf]_t}{[Sulf]_0}\right) = -kt \quad (1)$$

where $[Sulf]_{time}$ is the sulfonamide concentrations at initial time and time t. The half-life is given by:

$$t_{1/2} = \frac{\ln 2}{k} \quad (2)$$

Half-lives of SMZ and SMX are reported in Table 1. The half-lives showed that degradation was generally faster in the polluted waters with high concentration addition of SMZ and SMX, in which the half-lives ranged from 2.5 to 3.4 d, averaging 2.9 d. Conversely, the half-lives of SMZ and SMX in the same polluted water mesocosms but with low antibiotic addition ranged from 11d to 22d, averaging 17d, showing a slower degradation rate. The degradation of SMZ in the experiment with pristine waters and high concentration addition also showed a relatively short half-life (half-life averaged 8.7 d with a standard deviation of 3.6d). Half-lives for SMX in the pristine low addition mesocosms could not be calculated because the regression of ln [SMX] versus exposure time were not statistically significant ($p > 0.01$) due to variability between replicates. Therefore, it is concluded that irrespective of the initial status of the river water (polluted vs pristine), the degradation of sulfonamides was faster in the mesocosms with high concentration of sulfonamides.

Fig. 3 shows the transformation products (TPs) of sulfamethoxazole during the experiments (Hydroxy-sulfamethoxazole,

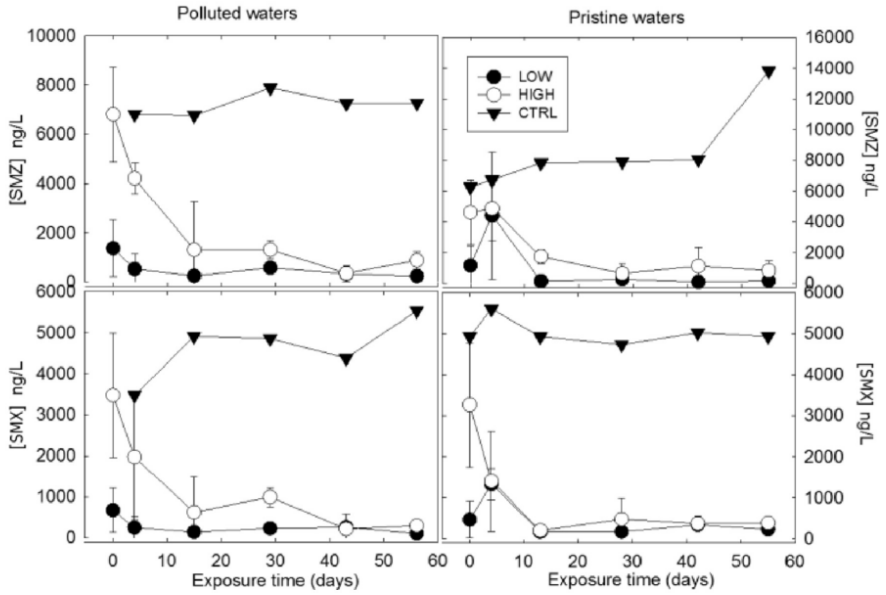

Fig. 2. Concentrations of sulfamethazine and sulfamethoxazole (ng/L) during the curse of the experiment. LOW, HIGH and CTRL refer to the concentrations for the experiments with high and low addition of sulfonamide and the abiotic controls, respectively.

Table 1
Half-lives (ranged, mean and standard deviation) for sulfamethazine (SMZ) and sulfamethoxazole (SMX) for the first 30 days of the experiment.

Half lives (days)				
	Polluted HIGH	Polluted LOW	Pristine HIGH	Pristine LOW
SMZ	2.5–3 2.8 ± 0.3	17–22 20 ± 2.4	6.1–11 8.7 ± 3.6	8.1–14 11 ± 4.6
SMX	2.8–3.4 3.1 ± 0.4	11–16 14 ± 3.8	Not statistically significant (P > 0.01)	Not statistically significant (p > 0.01)

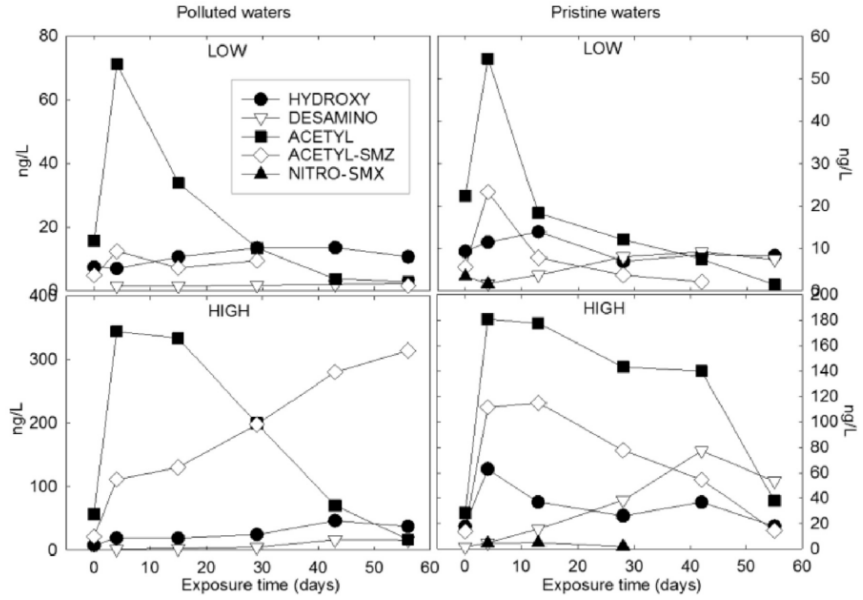

Fig. 3. Concentrations of sulfonamides transformation products (Hydroxysulfamethoxazole (HYDORXY), desamino-sulfamethoxazole (DESAMINO), acetylsulfamethoxazole (ACETYL), acetyl sulfamethazine (ACETYL-SMZ), nitrosulfamethoxazole (NITRO-SMX)) in ng/L during the duration of the experiment. See structural formula in Fig. S1.

desamino-sulfamethoxazole, acetyl-sulfamethoxazole, nitro-sulfamethoxazole) and sulfamethazine TPs (acetyl sulfamethazine). The concentration of hydroxy-sulfametoxazole increased between time 0 and 30 days and then decreased rapidly. The other TPs showed a variable time trend, with desamino-SMX and acetyl-SMZ generally showing increasing concentrations over time. The decrease/increase trend of SMX and SMZ and their TPs supports the evidence that degradation of SMX and SMZ occurred within the first 30 days of the experiments but it also shows that other chemical transformations were occurring. However, as not all the TPs were identified and quantified, it was not possible to close the mass balance.

3.2. ARG abundance in the Llobregat River and during the experiments

Abundance of genes *sul1* and *sul2* along the Llobregat River are shown in Fig. 1. Table S3 shows the mean and the standard deviation for each gene abundance at each sampling location; *sul1* was always the most abundant gene ($4.7*10^8$–$6.9*10^7$copies/AFDM) at all sites, followed by *sul2* ($9.0*10^7$–$7.8*10^6$copies/AFDM). The absolute abundance of *sul1* and *sul2* genes was the highest at St. Boi and, in general, increased from upstream to downstream. Therefore, *in situ sul1* and *sul2* were more abundant at the polluted site (St. Boi) and less abundant at the pristine site (Les Fonts de Llogregat). These two values were also the abundances of *sul1* and *sul2* in the mesocosm experiments at initial time.

Fig. 4 shows the ARG abundances during the course of the experiments. There is a significant difference in ARG abundances between high and low sulfonamide addition treatments; for the high addition, there is a decrease after time zero and then an increase of ARG abundances, whereas in the low concentration addition experiments there is no initial decrease of ARG abundances after time zero. For the mesocosms with low sulfonamide addition in pristine waters, there was a decrease at time 30 days for both *sul1* and *sul2*, but this could be due to an outlier of the AFDM measurement at this time point (see also evolution of Chla concentrations over the experiment in Fig. S3). Abundance of *sul1* and *sul2* increased during the last 30 days of the experiments irrespective of the concentrations and the origin of the river water.

The initial decrease of *sul1* and *sul2* abundance for the mesocosms with high sulfonamide addition of SMX and SMZ, but not under lower concentrations of SMX and SMZ, is consistent with a toxicity effect of sulfonamides to the bacterial groups harboring *sul1* and *sul2* genes. The effect of the concentration of a chemical

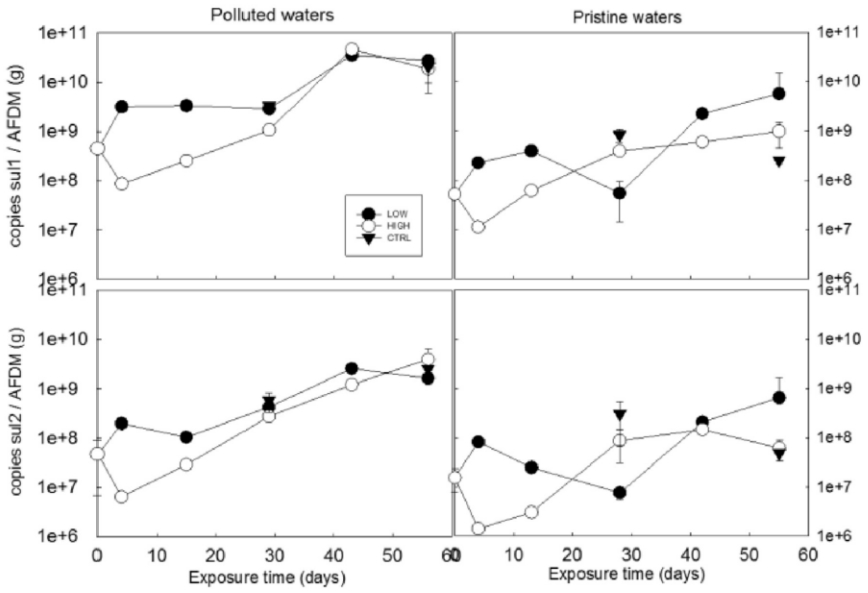

Fig. 4. Abundance of the ARG *sul1* and *sul2* during the curse of the experiment. LOW, HIGH and CTRL refer to the concentrations for the experiments with high and low addition of sulfonamide and the biotic controls without sulfonamide addition, respectively.

(SMX and SMZ in this work) on a biological response (*sul1* or *sul2* abundances) can be represented with dose-response curves following a sigmoidal model with horizontal asymptotes at both extremes of the dose range (Ritz, 2010). Fig. 5 shows that when plotting the abundance of ARG versus the concentration of SMX and SMZ normalized by the abundance of the ARG genes, a typical sigmoid-type curve is obtained. For the experiments with low addition of sulfonamides, there is no decrease in ARG abundance due to the fact that the toxicity thresholds of SMX and SMZ are not achieved. Conversely, if the concentrations of SMZ and SMX are higher than a certain threshold value, then there is a sharp decrease in the abundance of *sul1* and *sul2* genes as observed during the experiments with high concentration addition of sulfonamides (Figs. 4 and 5). This type of sigmoid curve is obtained only if the concentration of SMX + SMZ is normalized by the ARG abundances, indicating that these toxicological thresholds are related to the levels of the ARG genes, and thus suggesting a coupling of the change of *sul1* and *sul2* abundances and degradation of sulfonamide as antibiotic resistance mechanisms. The concentration threshold of SMX + SMZ (normalized by *sul1* and *sul2* genes) at which a reduction of *sul1* and *sul2* genes is observed (Fig. 5) was surprisingly lower for the polluted waters than for the pristine waters. This could either indicate a lack of acclimation to high sulfonamide concentrations of the microbial community containing *sul1* and *sul2* genes from polluted waters, which had been previously exposed to sulfonamides at concentrations 5 fold lower, or that antibiotic resistance is primarily driven by degradation rather than by *sul1* and *sul2* genes at high concentrations of sulfonamides (see below). The microbial community recovered (increase in the genes abundance) after the first 30 days, which coincided with the end of the biodegradation period. Therefore, in the first half of the experiment the bacterial community was degrading the antibiotics; when the concentration of the antibiotic reached steady-state low concentrations, the abundance of ARG started to increase. The residual of sulfonamides and some of the TP might induce potential antimicrobial activity. In the low sulfonamide addition treatments, the sulfonamide concentrations were below the toxicity threshold, with no decrease in ARG abundance although degradation was still observed but with a slower kinetics than when sulfonamide concentrations where higher (Table 1).

3.3. Degradation of antibiotic versus spread of ARG

The structure of the bacterial community may change after exposure to sulfonamides (Liao et al., 2016; Proia et al., 2013). The spread of *sul* genes by horizontal gene transfer occurs rapidly in natural communities thanks to their linkage to class 1 integrons which are often embedded in DNA mobile elements such as plasmids and transposons (Gillings et al., 2015; Sköld, 2000). The two antibiotic resistant mechanisms considered here such as the increase of ARG and sulfonamide degradation pathways probably did not occur in the same bacterial groups. One possibility is that the population of *sul*-harboring bacteria is in part overlapped by the bacterial community with the capacity to degrade SMZ and SMX. Even though this is possible, it may not be the generalized case, since in the mesocosms with polluted water and high addition of sulfonamide (above the toxicity threshold), the degradation was faster (Table 1) with a concurrent decrease of ARG. Therefore, when there was a decrease of ARG, the bacterial degradation was faster suggesting that in polluted waters there was an acclimated population, not found in pristine waters, able to resist sulfonamides by degradation. This resistance mechanism seemed not only complementary to the spread of ARG, but also more effective when the concentration of sulfonamides was highest. It has been suggested that degradation of SMX is enhanced by co-metabolism of ammonia oxidizing bacteria which are not targeted by *sul1* and *sul2*

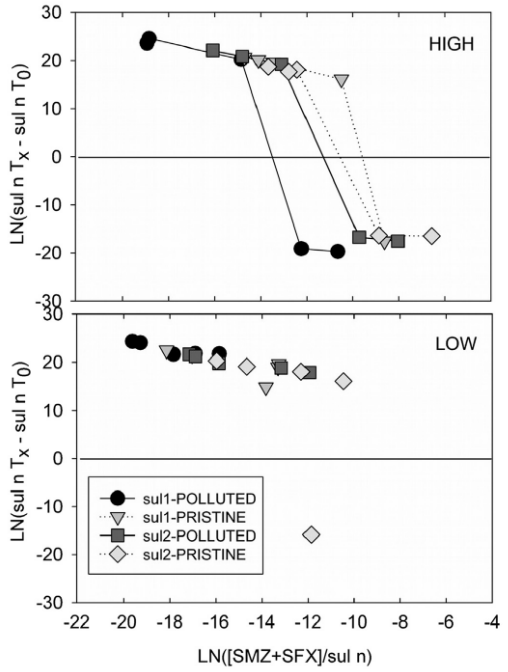

Fig. 5. The logarithm of the *sul1* or *sul2* genes abundances versus the logarithm of the concentration of total sulfonamides normalized by the genes abundance at any given time, and for the experiments with high (upper panel) and low (lower panel) addition of sulfonamides.

primers (Kassotaki et al., 2016; Pei et al., 2006). Fig. S4 shows the nutrient concentrations in the experiments. In polluted waters, there was a quick decrease of ammonia and a steady increase of nitrates and phosphate which would have been consistent with SMZ and SMX degradation due to co-metabolism of nitrification. This was in contrast with the NH_4 time course in pristine waters where there is an initial increase in NH_4 concentrations and then a decrease. For pristine waters, the degradation of sulfonamides was slower than in polluted waters (Table 1).

The results from the bacterial production (Fig. S5) show that there were differences between waters (pristine vs polluted) but not between treatments which suggests that the bacterial communities were recovered from antibiotics from the point of view of this ecological function. For the last sample (60 days), the abundance of ARG in controls were not significantly different from those treated with low or high concentrations of sulfonamides for polluted waters (Fig. 4). However, for pristine waters, the ARG abundance after 60 days in the controls was similar to that observed in mesocosms where sulfonamides were added at high concentrations, but were lower than those observed in the mesocosms at low concentrations. These results suggest that the potential ARG altering resistance mechanism may not have been changed in polluted waters, and the community resistance relies on its capacity to degrade the antibiotics. Conversely, in pristine waters, the degradation rates were always slower than in polluted waters. The differences of ARG abundance after 60 days, could indicate that the ARG altering mechanism may have been promoted when the bacterial community was challenged with relatively low concentrations of antibiotics, but this did not occur at high concentrations. This could be related to sulfonamide concentrations above the toxicity threshold value (Fig. 5), which may have been triggered by changes in the community favoring biodegradation of sulfonamides; however, this could not be demonstrated in this study.

4. Conclusions

The work performed here highlights that two of the main mechanisms of sulfonamide resistance, that is, microbial sulfonamide degradation and spread of sulfonamide-resistant genes are complementary used in natural ephilitic communities. The relative importance of each mechanism seems to be determined by *in situ* concentration of sulfonamides. Whereas sulfonamide degradation might prevail at high concentrations of sulfonamides, ARG spread would be more important under moderate/low concentrations. Further research should focus on the phylogenetic identification of the main players of both mechanisms and the assessment of the relative role of the third mechanisms of resistance not included in this study, the increase of membrane efflux pumps (Pu et al., 2016).

Authors's contributions

MVC, RG, JD, EOC designed the experiment. MVC and RG performed the experiments and analysed data. JA and SP analysed the degradation products. MVC, RG, and JD wrote the paper. All authors contributed to the discussion and final version of the manuscript.

Acknowledgements

This work has been supported by Marie Curie Actions—Intra-European Fellowships (IEF), project number 275863 and by the Spanish Ministry of Economy and Competitiveness project DARKNESS CGL2012-32747 to E.O.C. M.T. Pinnetta, G. Caballero and M.J. Ojeda are acknowledged for sampling assistance, E.Martí for kindly providing river art and M. Kuzmanovic for support with GIS.

Appendix A. Supplementary data

Supplementary data related to this article can be found at http://dx.doi.org/10.1016/j.watres.2017.03.007.

References

Allen, H.K., Donato, J., Wang, H.H., Cloud-Hansen, K.A., Davies, J., Handelsman, J., 2010. Call of the wild: antibiotic resistance genes in natural environments. Nat. Rev. Microbiol. 8, 251–259. http://dx.doi.org/10.1038/nrmicro2312.

Auerbach, E.A., Seyfried, E.E., McMahon, K.D., 2007. Tetracycline resistance genes in activated sludge wastewater treatment plants. Water Res. 41, 1143–1151. http://dx.doi.org/10.1016/j.watres.2006.11.045.

Batchu, S.R., Panditi, V.R., O'Shea, K., Gardinali, P.R., 2014. Photodegradation of antibiotics under stimulated solar radiation: implications for their environmental fate. Sci. Total Environ. 470–471, 299–310.

Battin, T.J., Besemer, K., Bengtsson, M.M., Romani, A.M., Packmann, A.I., 2016. The ecology and biogeochemistry of stream biofilms. Nat. Rev. Microbiol. 14, 251–263. http://dx.doi.org/10.1038/nrmicro.2016.15.

Bartrons, M., Catalan, J., Casamayor, E.O., 2012. High bacterial diversity in ephilitic biofilms of oligotrophic mountain lakes. Microb. Ecol. 64 (4), 860–869.

Cetecioglu, Z., Ince, B., Orhon, D., Ince, O., 2016. Anaerobic sulfamethoxazole degradation is driven by homoacetogenesis coupled with hydrogenotrophic methanogenesis. Water Res. 90, 79–89. http://dx.doi.org/10.1016/j.watres.2015.12.013.

Davies, J., Davies, D., 2010. Origins and evolution of antibiotic resistance. Microbiol. Mol. Biol. Rev. 74, 417–433. http://dx.doi.org/10.1128/MMBR.00016-10.

Dever, L.A., Dermody, T.S., 2013. Mechanisms of Bacterial Resistance to Antibiotics.

Ding, C., He, J., 2010. Effect of antibiotics in the environment on microbial populations. Appl. Microbiol. Biotechnol. 87, 925–941. http://dx.doi.org/10.1007/s00253-010-2649-5.

Gillings, M.R., Gaze, W.H., Pruden, A., Smalla, K., Tiedje, J.M., Zhu, Y.-G., 2015. Using the class 1 integron-integrase gene as a proxy for anthropogenic pollution. ISME J. 9, 1269–1279. http://dx.doi.org/10.1038/ismej.2014.226.

Ginebreda, A., Muñoz, I., de Alda, M.L., Brix, R., López-Doval, J., Barceló, D., 2010. Environmental risk assessment of pharmaceuticals in rivers: relationships between hazard indexes and aquatic macroinvertebrate diversity indexes in the Llobregat River (NE Spain). Environ. Int. 36, 153–162. http://dx.doi.org/10.1016/j.envint.2009.10.003.

Gioia, R., Dachs, J., 2012. The riverine input-output paradox for organic pollutants. Front. Ecol. Environ. 10, 405–406. http://dx.doi.org/10.1890/12.WB.017.

Gros, M., Petrovic, M., Barceló, D., 2009. Tracing pharmaceutical residues of different therapeutic classes in environmental waters by using liquid chromatography/quadrupole-linear ion trap mass spectrometry and automated library searching. Anal. Chem. 81, 898–912.

Hruska, K., Franek, M., 2012. Sulfonamides in the environment: a review and a case report. Vet. Med. (Praha) 57, 1–35.

Kassotaki, E., Buttiglieri, G., Ferrando-Climent, L., Rodriguez-Roda, I., Pijuan, M., 2016. Enhanced sulfamethoxazole degradation through ammonia oxidizing bacteria co-metabolism and fate of transformation products. Water Res. 94, 111–119. http://dx.doi.org/10.1016/j.watres.2016.02.022.

Kirchman, D., Nees, E.K., Hodson, R., 1985. Leucine incorporation and its potential. Environ. Microbiol. 49, 599–607.

Liao, X., Li, B., Zou, R., Xie, S., Yuan, B., 2016. Antibiotic sulfanilamide biodegradation by acclimated microbial populations. Appl. Microbiol. Biotechnol. 100, 2439–2447. http://dx.doi.org/10.1007/s00253-015-7133-9.

Luo, Y., Mao, D., Rysz, M., Zhou, Q., Zhang, H., Xu, L., Alvarez, P.J.J., 2010. Trends in antibiotic resistance genes occurrence in the Haihe River, China. Environ. Sci. Technol. 44, 7220–7225. http://dx.doi.org/10.1021/es100233w.

Martinez, J.L., 2008. Antibiotics and antibiotic resistance genes in natural environments. Science 321 (80), 365–367. http://dx.doi.org/10.1126/science.1159483.

Masiá, A., Campo, J., Barceló, D., Picó, Y., 2015. Pesticide monitoring in the basin of Llobregat River (Catalonia, Spain) and comparison with historical data. Sci. Total Environ. 503, 58–68. http://dx.doi.org/10.1016/j.scitotenv.2014.06.095.

McKinney, C.W., Loftin, K.A., Meyer, M.T., Davis, J.G., Pruden, A., 2010. Tet and sul antibiotic resistance genes in livestock lagoons of various operation type, configuration, and antibiotic occurrence. Environ. Sci. Technol. 44, 6102–6109. http://dx.doi.org/10.1021/es9038165.

Pei, R., Cha, J., Carlson, K.H., Pruden, A., 2007. Response of antibiotic resistance genes (ARG) to biological treatment in dairy lagoon water. Environ. Sci. Technol. 41, 5108–5113. http://dx.doi.org/10.1021/es070051x.

Pei, R., Kim, S.C., Carlson, K.H., Pruden, A., 2006. Effect of River Landscape on the sediment concentrations of antibiotics and corresponding antibiotic resistance genes (ARG). Water Res. 40, 2427–2435. http://dx.doi.org/10.1016/j.watres.2006.04.017.

Proia, L., Lupini, G., Osorio, V., Pérez, S., Barceló, D., Schwartz, T., Amalfitano, S., Fazi, S., Romaní, A.M., Sabater, S., 2013. Response of biofilm bacterial communities to antibiotic pollutants in a Mediterranean river. Chemosphere 92, 1126–1135. http://dx.doi.org/10.1016/j.chemosphere.2013.01.063.

Pruden, A., Messner, N., Pereyra, L., Hanson, R.E., Hiibel, S.R., Reardon, K.F., 2007. The effect of inoculum on the performance of sulfate-reducing columns treating heavy metal contaminated water. Water Res. 41, 904–914. http://dx.doi.org/10.1016/j.watres.2006.11.025.

Pruden, A., Pei, R., Storteboom, H., Carlson, K.H., 2006. Antibiotic resistance genes (ARG) as emerging contaminants: studies in northern Colorado. Environ. Sci. Technol. 40, 7445–7450.

Pu, Y., Zhao, Z., Li, Y., Zou, J., Ma, Q., Zhao, Y., Ke, Y., Zhu, Y., Chen, H., Baker, M.A.B., Ge, H., Sun, Y., Xie, X.S., Bai, F., 2016. Enhanced efflux activity facilitates drug tolerance in dormant bacterial cells. Mol. Cell 62, 284–294. http://dx.doi.org/10.1016/j.molcel.2016.03.035.

Randall, L.P., 2004. Antibiotic resistance genes, integrons and multiple antibiotic resistance in thirty-five serotypes of Salmonella enterica isolated from humans and animals in the UK. J. Antimicrob. Chemother. 53, 208–216. http://dx.doi.org/10.1093/jac/dkh070.

Romaní, A.M., Sabater, S., 1999. Effect of primary producers on the heterotrophic metabolism of a stream biofilm. Freshw. Biol. 41, 729–736. http://dx.doi.org/10.1046/j.1365-2427.1999.00413.x.

Ritz, C., 2010. Toward a unified approach to dose-response modeling in ecotoxicology. Environ. Toxic. Chem. 29, 220–229.

Rizzo, L., Fiorentino, A., Anselmo, A., 2012. Effect of solar radiation on multidrug resistant E.coli strains and antibiotic mixture photodegradation in wastewater polluted stream. Sci. Total Environ. 427–428, 263–268.

Sköld, O., 2000. Sulfonamide resistance: mechanisms and trends. Drug Resist. Updat 3, 155–160. http://dx.doi.org/10.1054/drup.2000.0146.

Smith, D.C., Azam, F., 1992. A simple, economical method for measuring bacterial protein synthesis rates in seawater using tritiated-leucine. Mar. Microb. Food Webs 6, 107–114.

Steinman, A.D., Lamberti, G.A., 1996. Biomass and pigments of benthic algae. P. 297. In: Hauer, F.R., Lamberti, G.A. (Eds.), Methods in Stream Ecology. Academic Press, San Diego, CA.

Stoll, C., Sidhu, J.P.S., Tiehm, A., Toze, S., 2012. Prevalence of clinically relevant antibiotic resistance genes in surface water samples collected from Germany and Australia. Environ. Sci. Technol. 46, 9716–9726. http://dx.doi.org/10.1021/es302020s.

Su, T., Deng, H., Benskin, J.P., Radke, M., 2016. Biodegradation of sulfamethoxazole photo-transformation products in a water/sediment test. Chemosphere 148, 518–525. http://dx.doi.org/10.1016/j.chemosphere.2016.01.049.

van der Meer, J.R., 2006. Environmental pollution promotes selection of microbial degradation pathways. Front. Ecol. Environ. 4, 35–42 doi:10.1890/1540-9295(2006)004[0035:EPPSOM]2.0.CO;2.

Writer, J.H., Barber, L.B., Ryan, J.N., Bradley, P.M., 2011a. Biodegradation and attenuation of steroidal hormones and alkylphenols by stream biofilms and sediments. Environ. Sci. Technol. 45, 4370–4376. http://dx.doi.org/10.1021/es2000134.

Writer, J.H., Ryan, J.N., Barber, L.B., 2011b. Role of biofilms in sorptive removal of steroidal hormones and 4-nonylphenol compounds from streams. Environ. Sci. Technol. 45, 7275–7283. http://dx.doi.org/10.1021/es2008038.

Yang, C.-W., Hsiao, W.-C., Chang, B.-V., 2016. Biodegradation of sulfonamide antibiotics in sludge. Chemosphere 150, 559–565. http://dx.doi.org/10.1016/j.chemosphere.2016.02.064.

Zhang, X., Wu, B., Zhang, Y., Zhang, T., Yang, L., Fang, H.H.P., Ford, T., Cheng, S., 2009. Class 1 integronase gene and tetracycline resistance genes tetA and tetC in different water environments of Jiangsu Province, China. Ecotoxicology 18, 652–660. http://dx.doi.org/10.1007/s10646-009-0332-3.

Table S1. Quantitative PCR conditions for the targeted *sul* genes. Reactions were carried out on 96-well white plates with adhesive seals (Bio-Rad) in a DNA Engine thermal cycler (Bio-Rad, Hercules) equipped with a Chromo 4 Real-Time Detector (Bio-Rad). Reactions were performed in a final volume of 20 µL of reaction mixture containing a 10-µL solution of SsoFast EvaGreen supermix (BioRad), 5 ng of template genomic DNA, 10 µM (each) primer, 1.33 µL of bovine serum albumin (BSA, 6mg/ml) and molecular biology-grade water (Sigma). The temperature program consisted of initial denaturation at 95ºC, followed by 45 cycles of 15s at 95ºC, 30s at the annealing temperature (65.4ºC for *sul1*, 62.2ºC for *sul2*), 30s at 72ºC and a final extension step for 1 min at 95ºC and 1 min at 65ºC to ensure stringent coupled DNA fragments (modified form Pei et al. 2006). Fluorescence signal was read after each elongation step. All reactions were finished with a melting curve starting at 60ºC and increasing by 0.5 ºC until 95 ºC to verify amplicon specificity. Each assay was run in triplicate including no template controls and standard curves spanning from 10^2 to 10^8 copies of DNA genes ($r^2 > 0.99$ for standard curves).

Target gene	**Primer set**	**Sequence (5'-3')**	**Amplicon Length (bp)**	**Annealing tempertaure (ºC)**
sul1	sul1-F	CGCACCGGAAACATCGCTGCAC	163	65.4
	sul1-R	TGAAGTTCCGCCGCAAGGCTCG		
sul2	sul2-F	TCCGGTGGAGGCCGGTATCTGG	191	62.2
	sul2-R	CGGGAATGCCATCTGCCTTGAG		

Table S2. Concentrations of sulfamethazine (SMZ), sulfamethoxazole(SMX) and their degradation products.

				[SMZ]	[SMX]	HYDROXY	DESAMINO	ACETYL	ACETYL-SMZ	NITRO_SMX
EXP	SULF ADDITION	TIME POINT	LABEL	ng/L	ng/L	ng/L	ng/L	ng/L	ng/L	ng/L
Polluted	Before addition	T0	EXP1-T0	NA	NA	NA	NA	NA	NA	NA
Polluted	Before addition	T0	EXP1-T0	NA	NA	NA	NA	NA	NA	NA
Polluted	Before addition	T0	EXP1-T0	NA	NA	NA	NA	NA	NA	NA
Polluted	Before addition	T0	EXP1-T0	NA	NA	NA	NA	NA	NA	NA
Polluted	Before addition	T0	EXP1-T0	NA	NA	NA	NA	NA	NA	NA
Polluted	Before addition	T0	EXP1-T0	NA	NA	NA	NA	NA	NA	NA
Polluted	HIGH	T0	EXP1-T0-HIGH	8777	4550	7	BDL	45	20	BDL
Polluted	HIGH	T0	EXP1-T0-HIGH	6723	4119	8	BDL	70	23	BDL
Polluted	HIGH	T0	EXP1-T0-HIGH	4935	1745	NA	NA	NA	NA	NA
Polluted	LOW	T0	EXP1-T0-LOW	321	152	7	BDL	13	5	BDL
Polluted	LOW	T0	EXP1-T0-LOW	2586	1247	BDL	BDL	19	5	BDL
Polluted	LOW	T0	EXP1-T0-LOW	1197	624	NA	NA	NA	NA	NA
Polluted	HIGH	T1	EXP1-T1-HIGH	3490	223	17	2	312	112	BDL
Polluted	HIGH	T1	EXP1-T1-HIGH	4703	2992	21	2	376	111	BDL
Polluted	HIGH	T1	EXP1-T1-HIGH	4443	2688	NA	NA	NA	NA	NA
Polluted	LOW	T1	EXP1-T1-LOW	1227	556	7	1	59	8	BDL
Polluted	LOW	T1	EXP1-T1-LOW	113	74	7	1	84	17	BDL
Polluted	LOW	T1	EXP1-T1-LOW	229	109	NA	NA	NA	NA	NA
Polluted	control	t1								
Polluted	HIGH	T2	EXP1-T2-HIGH	149	119	21	2	376	111	BDL
Polluted	HIGH	T2	EXP1-T2-HIGH	195	125	17	4	291	150	BDL
Polluted	HIGH	T2	EXP1-T2-HIGH	3573	1620	NA	NA	NA	NA	NA
Polluted	LOW	T2	EXP1-T2-LOW	149	119	8	1	26	4	BDL

Polluted	LOW	T2	EXP1-T2-LOW	NA	NA	13	1	42	10	BDL
Polluted	LOW	T2	EXP1-T2-LOW	342	163	NA	NA	NA	NA	NA
Polluted	control	t2		NA	NA	NA	NA	NA	NA	NA
Polluted	HIGH	T3	EXP1-T3-HIGH	1046	829	17	4	291	150	BDL
Polluted	HIGH	T3	EXP1-T3-HIGH	1575	1158	32	6	108	245	BDL
Polluted	HIGH	T3	EXP1-T3-HIGH	NA	NA	NA	NA	NA	NA	NA
Polluted	HIGH	T3	EXP1-T3-HIGH	NA	NA	NA	NA	NA	NA	NA
Polluted	HIGH	T3	EXP1-T3-HIGH	NA	NA	NA	NA	NA	NA	NA
Polluted	HIGH	T3	EXP1-T3-HIGH	NA	NA	NA	NA	NA	NA	NA
Polluted	LOW	T3	EXP1-T3-LOW	536	220	11	2	7	BDL	BDL
Polluted	LOW	T3	EXP1-T3-LOW	610	236	16	2	20	9	BDL
Polluted	LOW	T3	EXP1-T3-LOW	NA	NA	NA	NA	NA	NA	NA
Polluted	LOW	T3	EXP1-T3-LOW	NA	NA	NA	NA	NA	NA	NA
Polluted	LOW	T3	EXP1-T3-LOW	NA	NA	NA	NA	NA	NA	NA
Polluted	LOW	T3	EXP1-T3-LOW	NA	NA	NA	NA	NA	NA	NA
Polluted	CONTROL	T3	EXP1-T3-CONTROL	NA	NA	NA	NA	NA	NA	NA
Polluted	CONTROL	T3	EXP1-T3-CONTROL	NA	NA	NA	NA	NA	NA	NA
Polluted	CONTROL	T3	EXP1-T3-CONTROL	NA	NA	NA	NA	NA	NA	NA
Polluted	CONTROL	T3	EXP1-T3-CONTROL	NA	NA	NA	NA	NA	NA	NA
Polluted	CONTROL	T3	EXP1-T3-CONTROL	NA	NA	NA	NA	NA	NA	NA
Polluted	CONTROL	T3	EXP1-T3-CONTROL	NA	NA	NA	NA	NA	NA	NA
Polluted	HIGH	T4	EXP1-T4-HIGH	526	391	32	6	108	245	BDL
Polluted	HIGH	T4	EXP1-T4-HIGH	155	93	61	27	32	314	BDL
Polluted	HIGH	T4	EXP1-T4-HIGH	362	160	NA	NA	NA	NA	NA
Polluted	LOW	T4	EXP1-T4-LOW	236	103	14	2	1	BDL	BDL
Polluted	LOW	T4	EXP1-T4-LOW	68	36	13	2	6	BDL	BDL
Polluted	LOW	T4	EXP1-T4-LOW	675	632	NA	NA	NA	NA	NA

Polluted	control	t4		NA	NA	NA	NA	NA	NA	NA
Polluted	HIGH	CHEM-T5	EXP1-CHEM-T5-HIGH1	586	217	61	27	32	314	BDL
Polluted	HIGH	CHEM-T5	EXP1-CHEM-T5-HIGH1	1274	440	14	5	2	BDL	BDL
Polluted	HIGH	CHEM-T5	EXP1-CHEM-T5-HIGH1	757	237	NA	NA	NA	NA	NA
Polluted	HIGH	CHEM-T5	EXP1-CHEM-T5-HIGH2	NA	NA	NA	NA	NA	NA	NA
Polluted	HIGH	CHEM-T5	EXP1-CHEM-T5-HIGH2	NA	NA	NA	NA	NA	NA	NA
Polluted	HIGH	CHEM-T5	EXP1-CHEM-T5-HIGH2	NA	NA	NA	NA	NA	NA	NA
Polluted	LOW	CHEM-T5	EXP1-CHEM-T5-LOW1	286	118	11	2	2	BDL	BDL
Polluted	LOW	CHEM-T5	EXP1-CHEM-T5-LOW1	350	151	10	3	4	2	BDL
Polluted	LOW	CHEM-T5	EXP1-CHEM-T5-LOW1	75	36	NA	NA	NA	NA	NA
Polluted	LOW	CHEM-T5	EXP1-CHEM-T5-LOW2	NA	NA	NA	NA	NA	NA	NA
Polluted	LOW	CHEM-T5	EXP1-CHEM-T5-LOW2	NA	NA	NA	NA	NA	NA	NA
Polluted	LOW	CHEM-T5	EXP1-CHEM-T5-LOW2	NA	NA	NA	NA	NA	NA	NA
Polluted	CONTROL	CHEM-T5	EXP1-CHEM-T5-CONTROL	NA	NA	NA	NA	NA	NA	NA
Polluted	CONTROL	CHEM-T5	EXP1-CHEM-T5-CONTROL	NA	NA	NA	NA	NA	NA	NA
Polluted	CONTROL	CHEM-T5	EXP1-CHEM-T5-CONTROL	NA	NA	NA	NA	NA	NA	NA
Polluted	CONTROL	CHEM-T5	EXP1-CHEM-T5-CONTROL	NA	NA	NA	NA	NA	NA	NA
Polluted	CONTROL	CHEM-T5	EXP1-CHEM-T5-CONTROL	NA	NA	NA	NA	NA	NA	NA
Polluted	CONTROL	CHEM-T5	EXP1-CHEM-T5-CONTROL	NA	NA	NA	NA	NA	NA	NA
Polluted	CONTROL	BIO-T5	EXP1-BIO-T5-CONTROL	NA	NA	NA	NA	NA	NA	NA
Polluted	CONTROL	BIO-T5	EXP1-BIO-T5-CONTROL	NA	NA	NA	NA	NA	NA	NA
Polluted	CONTROL	BIO-T5	EXP1-BIO-T5-CONTROL	NA	NA	NA	NA	NA	NA	NA
Polluted	CONTROL	BIO-T5	EXP1-BIO-T5-CONTROL	NA	NA	NA	NA	NA	NA	NA
Polluted	CONTROL	BIO-T5	EXP1-BIO-T5-CONTROL	NA	NA	NA	NA	NA	NA	NA
Polluted	CONTROL	BIO-T5	EXP1-BIO-T5-CONTROL	NA	NA	NA	NA	NA	NA	NA
Polluted	LOW	BIO-T5	EXP1-BIO-T5-LOW	NA	NA	NA	NA	NA	NA	NA
Polluted	LOW	BIO-T5	EXP1-BIO-T5-LOW	NA	NA	NA	NA	NA	NA	NA

Polluted	LOW	BIO-T5	EXP1-BIO-T5-LOW	NA	NA	NA	NA	NA	NA	NA
Polluted	LOW	BIO-T5	EXP1-BIO-T5-LOW	NA	NA	NA	NA	NA	NA	NA
Polluted	LOW	BIO-T5	EXP1-BIO-T5-LOW	NA	NA	NA	NA	NA	NA	NA
Polluted	LOW	BIO-T5	EXP1-BIO-T5-LOW	NA	NA	NA	NA	NA	NA	NA
Polluted	HIGH	BIO-T5	EXP1-BIO-T5-HIGH	NA	NA	NA	NA	NA	NA	NA
Polluted	HIGH	BIO-T5	EXP1-BIO-T5-HIGH	NA	NA	NA	NA	NA	NA	NA
Polluted	HIGH	BIO-T5	EXP1-BIO-T5-HIGH	NA	NA	NA	NA	NA	NA	NA
Polluted	milliQ-HIGH	T1	Polluted_T1HIGH	6772	4914	NA	NA	NA	NA	NA
Polluted	milliQ-HIGH	T3	Polluted_T3	7884	4856	NA	NA	NA	NA	NA
Polluted	milliQ-HIGH	T4	Polluted_T4	7265	4380	NA	NA	NA	NA	NA
Polluted	milliQ-HIGH	T5	Polluted_T5	7274	5532	NA	NA	NA	NA	NA
TRANSECT	Martorell	S1-T0-Martorell	S1-T0-Martorell	NA	NA	NA	NA	NA	NA	NA
TRANSECT	Martorell	S1-T0-Martorell	S1-T0-Martorell	NA	NA	NA	NA	NA	NA	NA
TRANSECT	Martorell	S1-T0-Martorell	S1-T0-Martorell	NA	NA	NA	NA	NA	NA	NA
TRANSECT	Castellbell	S2-T0-Castellbell	S2-T0-Castellbell	NA	NA	NA	NA	NA	NA	NA
TRANSECT	Castellbell	S2-T0-Castellbell	S2-T0-Castellbell	NA	NA	NA	NA	NA	NA	NA
TRANSECT	Castellbell	S2-T0-Castellbell	S2-T0-Castellbell	NA	NA	NA	NA	NA	NA	NA
TRANSECT	Navarcles	S3-T0-Navarcles	S3-T0-Navarcles	NA	NA	NA	NA	NA	NA	NA
TRANSECT	Navarcles	S3-T0-Navarcles	S3-T0-Navarcles	NA	NA	NA	NA	NA	NA	NA
TRANSECT	Navarcles	S3-T0-Navarcles	S3-T0-Navarcles	NA	NA	NA	NA	NA	NA	NA
TRANSECT	Navarcles	S3-T0-Navarcles	S3-T0-Navarcles	NA	NA	NA	NA	NA	NA	NA
TRANSECT	Navarcles	S3-T0-Navarcles	S3-T0-Navarcles	NA	NA	NA	NA	NA	NA	NA
TRANSECT	Navarcles	S3-T0-Navarcles	S3-T0-Navarcles	NA	NA	NA	NA	NA	NA	NA
TRANSECT	Gironella	S4-T0-Gironella	S4-T0-Gironella	NA	NA	NA	NA	NA	NA	NA
TRANSECT	Gironella	S4-T0-Gironella	S4-T0-Gironella	NA	NA	NA	NA	NA	NA	NA
TRANSECT	Gironella	S4-T0-Gironella	S4-T0-Gironella	NA	NA	NA	NA	NA	NA	NA

Pristine	T0	T0	EXP2-T0	NA	NA	NA	NA	NA	NA	NA
Pristine	T0	T0	EXP2-T0	NA	NA	NA	NA	NA	NA	NA
Pristine	T0	T0	EXP2-T0	NA	NA	NA	NA	NA	NA	NA
Pristine	T0	T0	EXP2-T0	NA	NA	NA	NA	NA	NA	NA
Pristine	T0	T0	EXP2-T0	NA	NA	NA	NA	NA	NA	NA
Pristine	T0	T0	EXP2-T0	NA	NA	NA	NA	NA	NA	NA
Pristine	HIGH	T0	EXP2-T0-HIGH	6245	4084	16	BDL	31	10	BDL
Pristine	HIGH	T0	EXP2-T0-HIGH	5377	4195	20	1	26	18	BDL
Pristine	HIGH	T0	EXP2-T0-HIGH	2243	1516	NA	NA	NA	NA	NA
Pristine	LOW	T0	EXP2-T0-LOW	176	61	10	BDL	22	6	3
Pristine	LOW	T0	EXP2-T0-LOW	2576	949	8	BDL	23	6	BDL
Pristine	LOW	T0	EXP2-T0-LOW	707	389	NA	NA	NA	NA	NA
Pristine	control	t0	NA	NA	NA	NA	NA	NA	NA	NA
Pristine	HIGH	T1	EXP2-T1-HIGH	6861	2607	74	5	193	106	5
Pristine	HIGH	T1	EXP2-T1-HIGH	4985	166	51	4	168	117	BDL
Pristine	HIGH	T1	EXP2-T1-HIGH	2763	1444	NA	NA	NA	NA	NA
Pristine	LOW	T1	EXP2-T1-LOW	4197	1000	12	2	40	21	2
Pristine	LOW	T1	EXP2-T1-LOW	400	1250	11	2	70	26	BDL
Pristine	LOW	T1	EXP2-T1-LOW	8675	1750	NA	NA	NA	NA	NA
Pristine	control	t1	NA	NA	NA	NA	NA	NA	NA	NA
Pristine	HIGH	T2	EXP2-T2-HIGH	1896	178	31	15	171	108	5
Pristine	HIGH	T2	EXP2-T2-HIGH	2085	179	43	16	183	121	4
Pristine	HIGH	T2	EXP2-T2-HIGH	1229	255	NA	NA	NA	NA	NA
Pristine	LOW	T2	EXP2-T2-LOW	172	133	12	3	17	7	BDL
Pristine	LOW	T2	EXP2-T2-LOW	81	159	16	5	19	8	BDL
Pristine	LOW	T2	EXP2-T2-LOW	181	213	NA	NA	NA	NA	NA
Pristine	control	t2	NA	NA	NA	NA	NA	NA	NA	NA

Pristine	HIGH	T3	EXP2-T3-HIGH	1837	1333	26	51	153	93	BDL
Pristine	HIGH	T3	EXP2-T3-HIGH	214	146	26	26	133	62	2
Pristine	HIGH	T3	EXP2-T3-HIGH	948	870	NA	NA	NA	NA	NA
Pristine	HIGH	T3	EXP2-T3-HIGH	NA	NA	NA	NA	NA	NA	NA
Pristine	HIGH	T3	EXP2-T3-HIGH	NA	NA	NA	NA	NA	NA	NA
Pristine	HIGH	T3	EXP2-T3-HIGH	NA	NA	NA	NA	NA	NA	NA
Pristine	LOW	T3	EXP2-T3-LOW	368	209	7	7	14	3	BDL
Pristine	LOW	T3	EXP2-T3-LOW	175	153	7	9	11	5	BDL
Pristine	LOW	T3	EXP2-T3-LOW	299	149	NA	NA	NA	NA	NA
Pristine	Low	T3	EXP2-T3-Low	NA	NA	NA	NA	NA	NA	NA
Pristine	Low	T3	EXP2-T3-Low	NA	NA	NA	NA	NA	NA	NA
Pristine	Low	T3	EXP2-T3-Low	NA	NA	NA	NA	NA	NA	NA
Pristine	CONTROL	T3	EXP2-T3-CONTROL	NA	NA	NA	NA	NA	NA	NA
Pristine	CONTROL	T3	EXP2-T3-CONTROL	NA	NA	NA	NA	NA	NA	NA
Pristine	CONTROL	T3	EXP2-T3-CONTROL	NA	NA	NA	NA	NA	NA	NA
Pristine	CONTROL	T3	EXP2-T3-CONTROL	NA	NA	NA	NA	NA	NA	NA
Pristine	CONTROL	T3	EXP2-T3-CONTROL	NA	NA	NA	NA	NA	NA	NA
Pristine	CONTROL	T3	EXP2-T3-CONTROL	NA	NA	NA	NA	NA	NA	NA
Pristine	HIGH	T4	EXP2-T4-HIGH	711	588	27	67	139	43	BDL
Pristine	HIGH	T4	EXP2-T4-HIGH	173	238	46	87	141	66	BDL
Pristine	HIGH	T4	EXP2-T4-HIGH	2488	300	NA	NA	NA	NA	NA
Pristine	LOW	T4	EXP2-T4-LOW	89	367	9	7	10	BDL	BDL
Pristine	LOW	T4	EXP2-T4-LOW	52	250	8	12	5	2	BDL
Pristine	LOW	T4	EXP2-T4-LOW	183	399	NA	NA	NA	NA	NA
Pristine	control	t4		NA	NA	NA	NA	NA	NA	NA
Pristine	HIGH	CHEM-T5	EXP2-CHEM-T5-HIGH1	972	376	14	34	39	5	BDL
Pristine	HIGH	CHEM-T5	EXP2-CHEM-T5-HIGH1	139	266	22	73	37	24	BDL

Pristine	HIGH	CHEM-T5	EXP2-CHEM-T5-HIGH1	1386	519	NA	NA	NA	NA	NA
Pristine	HIGH	CHEM-T5	EXP2-CHEM-T5-HIGH2	NA	NA	NA	NA	NA	NA	NA
Pristine	HIGH	CHEM-T5	EXP2-CHEM-T5-HIGH2	NA	NA	NA	NA	NA	NA	NA
Pristine	HIGH	CHEM-T5	EXP2-CHEM-T5-HIGH2	NA	NA	NA	NA	NA	NA	NA
Pristine	LOW	CHEM-T5	EXP2-CHEM-T5-LOW1	268	168	8	7	3	BDL	BDL
Pristine	LOW	CHEM-T5	EXP2-CHEM-T5-LOW1	106	294	9	8	0	BDL	BDL
Pristine	LOW	CHEM-T5	EXP2-CHEM-T5-LOW1	160	237	NA	NA	NA	NA	NA
Pristine	LOW	CHEM-T5	EXP2-CHEM-T5-LOW2	NA	NA	NA	NA	NA	NA	NA
Pristine	LOW	CHEM-T5	EXP2-CHEM-T5-LOW2	NA	NA	NA	NA	NA	NA	NA
Pristine	LOW	CHEM-T5	EXP2-CHEM-T5-LOW2	NA	NA	NA	NA	NA	NA	NA
Pristine	CONTROL	CHEM-T5	EXP2-CHEM-T5-CONTROL	NA	NA	NA	NA	NA	NA	NA
Pristine	CONTROL	CHEM-T5	EXP2-CHEM-T5-CONTROL	NA	NA	NA	NA	NA	NA	NA
Pristine	CONTROL	CHEM-T5	EXP2-CHEM-T5-CONTROL	NA	NA	NA	NA	NA	NA	NA
Pristine	CONTROL	BIO-T5	EXP2-BIO-T5-CONTROL	NA	NA	NA	NA	NA	NA	NA
Pristine	CONTROL	BIO-T5	EXP2-BIO-T5-CONTROL	NA	NA	NA	NA	NA	NA	NA
Pristine	CONTROL	BIO-T5	EXP2-BIO-T5-CONTROL	NA	NA	NA	NA	NA	NA	NA
Pristine	CONTROL	BIO-T5	EXP2-BIO-T5-CONTROL	NA	NA	NA	NA	NA	NA	NA
Pristine	CONTROL	BIO-T5	EXP2-BIO-T5-CONTROL	NA	NA	NA	NA	NA	NA	NA
Pristine	CONTROL	BIO-T5	EXP2-BIO-T5-CONTROL	NA	NA	NA	NA	NA	NA	NA
Pristine	LOW	BIO-T5	EXP2-BIO-T5-LOW	NA	NA	NA	NA	NA	NA	NA
Pristine	LOW	BIO-T5	EXP2-BIO-T5-LOW	NA	NA	NA	NA	NA	NA	NA
Pristine	LOW	BIO-T5	EXP2-BIO-T5-LOW	NA	NA	NA	NA	NA	NA	NA
Pristine	LOW	BIO-T5	EXP2-BIO-T5-LOW	NA	NA	NA	NA	NA	NA	NA
Pristine	LOW	BIO-T5	EXP2-BIO-T5-LOW	NA	NA	NA	NA	NA	NA	NA
Pristine	LOW	BIO-T5	EXP2-BIO-T5-LOW	NA	NA	NA	NA	NA	NA	NA
Pristine	HIGH	BIO-T5	EXP2-BIO-T5-HIGH	NA	NA	NA	NA	NA	NA	NA
Pristine	HIGH	BIO-T5	EXP2-BIO-T5-HIGH	NA	NA	NA	NA	NA	NA	NA

Pristine	HIGH	BIO-T5	EXP2-BIO-T5-HIGH	NA	NA	NA	NA	NA	NA	NA
Pristine	HIGH	BIO-T5	EXP2-BIO-T5-HIGH	NA	NA	NA	NA	NA	NA	NA
Pristine	HIGH	BIO-T5	EXP2-BIO-T5-HIGH	NA	NA	NA	NA	NA	NA	NA
Pristine	HIGH	BIO-T5	EXP2-BIO-T5-HIGH	NA	NA	NA	NA	NA	NA	NA
Pristine	milliQ-HIGH	T0	Pristine_T0HIGH	6280	4930	15	0	0	0	0
Pristine	milliQ-HIGH	T1	Pristine_T1HIGH	6738	5599	28	0	3	2	0
Pristine	milliQ-HIGH	T2	Pristine_T2	7842	4930	46	0	5	3	0
Pristine	milliQ-HIGH	T3	Pristine_T3	7917	4731	119	0	11	5	0
Pristine	milliQ-HIGH	T4	Pristine_T4	8065	5025	403	0	20	4	0
Pristine	milliQ-LOW	T5	Pristine_T5	13816	4935	508	0	40	8	0

Table S3. Genes abundance of sul1 and sul2, AFDM, Chla, Nutrients.

EXP	SULF ADDITION	TIME POINT	pPCR *Sul 1* copies/cm2	qPCR *Sulf2* copies/cm2	pPCR *Sul 1* copies/AFDM	qPCR *Sul 2* copies/AFDM	AFDM mg/cm 2	Chla ug/cm2	Margalef's index	430/410	[PO4] µmols/L	[NH4] µmols/L	[NO3]+[NO2] µmols/L
Polluted	Before addition	T0	6.53E+08	1.51E+07	4.51E+08	1.05E+07	1.45	9.44	1.80	1.25	11	239	252
Polluted	Before addition	T0	6.81E+08	1.54E+07	4.71E+08	1.06E+07	NA	NA	NA	NA	NA	NA	NA
Polluted	Before addition	T0	6.75E+08	1.44E+07	4.67E+08	9.97E+06	NA	NA	NA	NA	NA	NA	NA
Polluted	Before addition	T0	6.35E+08	2.26E+07	4.39E+08	8.04E+07	NA	NA	NA	NA	NA	NA	NA
Polluted	Before addition	T0	6.51E+08	2.41E+07	4.50E+08	8.98E+07	NA	NA	NA	NA	NA	NA	NA
Polluted	Before addition	T0	6.32E+08	1.90E+07	4.37E+08	8.08E+07	NA	NA	NA	NA	NA	NA	NA
Polluted	HIGH	T0	NA	NA	NA	NA	NA	NA	NA	NA	8	236	212
Polluted	HIGH	T0	NA	NA	NA	NA	NA	NA	NA	NA	9	255	247
Polluted	HIGH	T0	NA	NA	NA	NA	NA	NA	NA	NA	NA	NA	NA
Polluted	LOW	T0	NA	NA	NA	NA	NA	NA	NA	NA	9	260	244
Polluted	LOW	T0	NA	NA	NA	NA	NA	NA	NA	NA	10	258	237
Polluted	LOW	T0	NA	NA	NA	NA	NA	NA	NA	NA	NA	NA	NA
Polluted	HIGH	T1	9.91E+07	7.62E+06	9.27E+07	7.13E+06	1.05	13.71	1.81	1.22	40	11	541
Polluted	HIGH	T1	1.02E+08	6.75E+06	9.54E+07	6.32E+06	1.09	NA	NA	NA	31	11	624
Polluted	HIGH	T1	7.57E+07	5.95E+06	7.09E+07	5.57E+06	NA	NA	NA	NA	29	9	429
Polluted	LOW	T1	2.83E+09	1.74E+08	2.68E+09	1.64E+08	0.99	10.40	1.92	1.22	28	11	765
Polluted	LOW	T1	3.58E+09	2.31E+08	3.39E+09	2.18E+08	0.98	4.51	1.90	1.21	39	11	584
Polluted	LOW	T1	3.55E+09	2.18E+08	3.36E+09	2.06E+08	1.20	4.88	1.86	1.18	32	11	568
Polluted	control	t1	NA	NA	NA	NA	NA	NA	NA	NA	37	11	669
Polluted	HIGH	T2	3.05E+08	3.35E+07	2.66E+08	2.91E+07	1.53	4.68	1.85	1.21	107	12	1841
Polluted	HIGH	T2	2.95E+08	3.29E+07	2.56E+08	2.87E+07	1.42	1.50	1.82	1.22	80	12	1443

Polluted	HIGH	T2	2.75E+08	3.31E+07	2.40E+08	2.88E+07	0.50	7.80	1.78	1.21	NA	NA	NA
Polluted	LOW	T2	3.66E+09	1.18E+08	3.06E+09	9.83E+07	0.84	5.41	1.87	1.21	81	12	2029
Polluted	LOW	T2	4.17E+09	1.32E+08	3.48E+09	1.10E+08	1.21	2.51	1.89	1.19	107	11	1819
Polluted	LOW	T2	4.16E+09	1.25E+08	3.48E+09	1.04E+08	1.54	7.62	1.85	1.18	NA	NA	NA
Polluted	control	t2	NA	NA	NA	NA	NA	NA	NA	NA	87	12	1668
Polluted	HIGH	T3	8.96E+08	2.35E+08	1.25E+09	3.28E+08	0.67	1.75	1.76	1.17	93	9	2154
Polluted	HIGH	T3	8.95E+08	2.22E+08	1.25E+09	3.10E+08	0.94	0.56	1.75	1.16	106	9	1805
Polluted	HIGH	T3	6.66E+08	1.93E+08	9.29E+08	2.70E+08	0.54	4.43	1.78	1.15	NA	NA	NA
Polluted	HIGH	T3	6.43E+08	2.71E+08	8.98E+08	2.23E+08	NA	NA	NA	NA	NA	NA	NA
Polluted	HIGH	T3	7.53E+08	2.51E+08	1.05E+09	2.54E+08	NA	NA	NA	NA	NA	NA	NA
Polluted	HIGH	T3	7.41E+08	2.46E+08	1.04E+09	2.55E+08	NA	NA	NA	NA	NA	NA	NA
Polluted	LOW	T3	9.05E+08	6.14E+07	2.18E+09	1.48E+08	0.38	0.23	2.08	1.23	76	8	2659
Polluted	LOW	T3	1.10E+09	8.73E+07	2.65E+09	2.10E+08	0.55	1.21	1.92	1.13	98	7	2587
Polluted	LOW	T3	1.08E+09	8.92E+07	2.59E+09	2.15E+08	0.32	2.66	1.89	1.08	NA	NA	NA
Polluted	LOW	T3	1.37E+09	1.63E+07	3.30E+09	6.74E+08	NA	NA	NA	NA	NA	NA	NA
Polluted	LOW	T3	1.38E+09	1.71E+07	3.31E+09	6.55E+08	NA	NA	NA	NA	NA	NA	NA
Polluted	LOW	T3	1.39E+09	1.77E+07	3.34E+09	6.43E+08	NA	NA	NA	NA	NA	NA	NA
Polluted	CONTROL	T3	2.03E+09	3.27E+08	3.28E+09	5.27E+08	0.53	5.45	1.79	1.10	111	8	2684
Polluted	CONTROL	T3	2.17E+09	3.59E+08	3.50E+09	5.80E+08	0.87	4.12	1.79	1.11	NA	NA	NA
Polluted	CONTROL	T3	2.02E+09	3.00E+08	3.25E+09	4.84E+08	0.46	2.59	1.70	1.13	NA	NA	NA
Polluted	CONTROL	T3	2.00E+09	5.51E+08	3.22E+09	6.00E+08	NA	NA	NA	NA	NA	NA	NA
Polluted	CONTROL	T3	2.04E+09	5.81E+08	3.29E+09	6.34E+08	NA	NA	NA	NA	NA	NA	NA
Polluted	CONTROL	T3	2.02E+09	5.68E+08	3.25E+09	6.57E+08	NA	NA	NA	NA	NA	NA	NA
Polluted	HIGH	T4	1.38E+10	3.47E+08	4.73E+10	1.19E+09	0.28	0.34	1.53	1.14	109	7	2489
Polluted	HIGH	T4	1.38E+10	3.51E+08	4.73E+10	1.21E+09	0.36	1.05	1.78	1.15	98	7	2360
Polluted	HIGH	T4	1.30E+10	3.54E+08	4.47E+10	1.22E+09	0.23	1.26	1.72	1.14	92	10	2710
Polluted	LOW	T4	1.81E+10	1.38E+09	3.86E+10	2.94E+09	0.42	1.10	1.79	1.07	77	7	2939

Polluted	LOW	T4	1.77E+10	1.28E+09	3.77E+10	2.72E+09	0.57	0.66	1.88	1.11	114	7	2514
Polluted	LOW	T4	1.42E+10	9.38E+08	3.04E+10	2.00E+09	0.42	1.82	1.90	1.09	102	6	1876
Polluted	control	t4	NA	NA	NA	NA	NA	NA	NA	NA	122	6	3197
Polluted	HIGH	CHEM-T5	2.13E+09	3.44E+08	1.12E+10	1.81E+09	0.18	0.23	1.67	1.15	147	6	3075
Polluted	HIGH	CHEM-T5	2.27E+09	4.20E+08	1.20E+10	2.22E+09	0.27	1.43	1.78	1.13	NA	NA	NA
Polluted	HIGH	CHEM-T5	2.18E+09	3.87E+08	1.15E+10	2.04E+09	0.12	1.32	1.75	1.14	NA	NA	NA
Polluted	HIGH	CHEM-T5	7.25E+09	7.17E+08	3.28E+10	3.24E+09	0.13	1.18	1.83	1.19	NA	NA	NA
Polluted	HIGH	CHEM-T5	7.35E+09	7.67E+08	3.32E+10	3.47E+09	NA	1.14	1.83	1.18	NA	NA	NA
Polluted	HIGH	CHEM-T5	7.15E+09	6.83E+08	3.23E+10	3.09E+09	0.32	1.26	1.79	1.17	NA	NA	NA
Polluted	LOW	CHEM-T5	7.10E+09	2.01E+08	3.80E+10	1.08E+09	0.13	0.90	1.81	1.14	76	6	2542
Polluted	LOW	CHEM-T5	4.54E+09	2.20E+08	2.43E+10	1.18E+09	0.19	0.90	1.86	1.16	NA	NA	NA
Polluted	LOW	CHEM-T5	4.37E+09	2.14E+08	2.34E+10	1.15E+09	0.24	1.22	1.83	1.15	NA	NA	NA
Polluted	LOW	CHEM-T5	1.04E+10	2.42E+08	3.72E+10	8.64E+08	0.31	0.30	1.69	1.11	NA	NA	NA
Polluted	LOW	CHEM-T5	9.23E+09	2.46E+08	3.30E+10	8.79E+08	0.15	1.01	1.86	1.12	NA	NA	NA
Polluted	LOW	CHEM-T5	7.33E+09	2.02E+08	2.62E+10	7.22E+08	0.38	1.75	1.83	1.11	NA	NA	NA
Polluted	CONTROL	CHEM-T5	3.64E+09	1.36E+08	1.33E+10	4.95E+08	0.23	1.34	1.92	1.06	114	6	3610
Polluted	CONTROL	CHEM-T5	3.96E+09	1.95E+08	1.45E+10	7.13E+08	0.33	0.94	1.81	1.06	NA	NA	NA
Polluted	CONTROL	CHEM-T5	3.89E+09	1.89E+08	1.42E+10	6.91E+08	0.26	1.22	1.89	1.07	NA	NA	NA
Polluted	CONTROL	CHEM-T5	3.24E+09	1.41E+08	1.18E+10	2.93E+09	NA	NA	NA	NA	NA	NA	NA
Polluted	CONTROL	CHEM-T5	3.18E+09	1.28E+08	1.16E+10	2.93E+09	NA	NA	NA	NA	NA	NA	NA
Polluted	CONTROL	CHEM-T5	3.28E+09	1.23E+08	1.20E+10	2.95E+09	NA	NA	NA	NA	NA	NA	NA
Polluted	CONTROL	BIO-T5	9.59E+09	1.52E+08	3.17E+10	4.66E+08	0.26	1.81	1.86	1.08	NA	NA	NA

Polluted	CONTROL	BIO-T5	9.57E+09	1.48E+08	3.16E+10	4.22E+08	0.31	1.14	1.79	1.09	NA	NA	NA
Polluted	CONTROL	BIO-T5	9.31E+09	1.42E+08	3.07E+10	4.05E+08	0.34	2.15	1.90	1.08	NA	NA	NA
Polluted	CONTROL	BIO-T5	7.71E+09	8.45E+08	2.54E+10	5.95E+09	NA	NA	NA	NA	NA	NA	NA
Polluted	CONTROL	BIO-T5	7.90E+09	9.10E+08	2.61E+10	6.23E+09	NA	NA	NA	NA	NA	NA	NA
Polluted	CONTROL	BIO-T5	7.63E+09	8.12E+08	2.52E+10	5.80E+09	NA	NA	NA	NA	NA	NA	NA
Polluted	LOW	BIO-T5	1.10E+10	1.57E+07	2.41E+10	1.85E+09	0.48	2.43	1.79	1.16	NA	NA	NA
Polluted	LOW	BIO-T5	7.80E+09	1.56E+07	1.71E+10	1.99E+09	0.44	2.23	1.78	1.18	NA	NA	NA
Polluted	LOW	BIO-T5	7.76E+09	1.49E+07	1.70E+10	1.77E+09	NA	3.14	1.83	1.19	NA	NA	NA
Polluted	LOW	BIO-T5	1.85E+10	1.98E+08	4.05E+10	4.17E+09	NA	NA	NA	NA	NA	NA	NA
Polluted	LOW	BIO-T5	6.81E+09	1.98E+08	1.49E+10	4.20E+09	NA	NA	NA	NA	NA	NA	NA
Polluted	LOW	BIO-T5	6.50E+09	2.03E+08	1.42E+10	3.59E+09	NA	NA	NA	NA	NA	NA	NA
Polluted	HIGH	BIO-T5	1.07E+10	1.96E+07	1.41E+10	7.52E+09	0.91	2.45	1.69	1.12	NA	NA	NA
Polluted	HIGH	BIO-T5	8.77E+09	2.41E+07	1.16E+10	6.32E+09	0.71	4.12	1.77	1.15	NA	NA	NA
Polluted	HIGH	BIO-T5	6.76E+09	2.27E+07	8.91E+09	5.98E+09	0.66	6.05	1.82	1.18	NA	NA	NA
Polluted	milliQ-HIGH	T1	NA	NA	NA	NA	NA	NA	NA	NA	NA	NA	NA
Polluted	milliQ-HIGH	T3	NA	NA	NA	NA	NA	NA	NA	NA	NA	NA	NA
Polluted	milliQ-HIGH	T4	NA	NA	NA	NA	NA	NA	NA	NA	NA	NA	NA
Polluted	milliQ-HIGH	T5	NA	NA	NA	NA	NA	NA	NA	NA	12	12	473
TRANSECT	Martorell	S1-T0-Martorell	1.96E+08	1.51E+07	1.35E+08	2.14E+07	1.45	9.04	1.97	1.27	4	7	111
TRANSECT	Martorell	S1-T0-Martorell	2.36E+08	1.54E+07	1.63E+08	5.61E+07	NA	9.04	1.97	1.27	NA	NA	NA
TRANSECT	Martorell	S1-T0-Martorell	2.32E+08	1.44E+07	1.60E+08	5.97E+07	NA	9.04	1.97	1.27	NA	NA	NA
TRANSECT	Castellbell	S2-T0-Castellbell	5.83E+07	1.16E+08	1.52E+08	7.20E+07	0.36	2.63	1.91	1.17	2	4	63
TRANSECT	Castellbell	S2-T0-Castellbell	5.86E+07	1.30E+08	1.53E+08	7.10E+07	0.40	2.63	1.91	1.17	NA	NA	NA

TRANSECT	Castellbell	S2-T0-Castellbell	5.78E+07	1.17E+08	1.51E+08	6.67E+07	NA	2.63	1.91	1.17	NA	NA	NA
TRANSECT	Navarcles	S3-T0-Navarcles	3.36E+07	7.62E+06	2.58E+07	1.66E+07	1.31	2.63	1.91	1.17	2	4	63
TRANSECT	Navarcles	S3-T0-Navarcles	3.32E+07	6.75E+06	2.54E+07	1.61E+07	NA	2.63	1.91	1.17	NA	NA	NA
TRANSECT	Navarcles	S3-T0-Navarcles	3.28E+07	5.95E+06	2.52E+07	1.75E+07	NA	2.63	1.91	1.17	NA	NA	NA
TRANSECT	Navarcles	S3-T0-Navarcles	6.18E+07	1.74E+08	4.73E+07	5.96E+07	NA	2.63	1.91	1.17	NA	NA	NA
TRANSECT	Navarcles	S3-T0-Navarcles	6.37E+07	2.31E+08	4.88E+07	4.59E+07	NA	2.63	1.91	1.17	NA	NA	NA
TRANSECT	Navarcles	S3-T0-Navarcles	5.44E+07	2.18E+08	4.17E+07	0.00E+00	NA	2.63	1.91	1.17	NA	NA	NA
TRANSECT	Gironella	S4-T0-Gironella	9.67E+06	3.35E+07	2.79E+07	2.06E+07	0.35	2.50	2.06	1.29	1	2	42
TRANSECT	Gironella	S4-T0-Gironella	1.12E+07	3.29E+07	3.24E+07	1.96E+07	0.35	2.50	2.06	1.29	NA	NA	NA
TRANSECT	Gironella	S4-T0-Gironella	1.03E+07	3.31E+07	2.97E+07	1.89E+07	NA	2.50	2.06	1.29	NA	NA	NA
Pristine	T0	T0	1.51E+07	1.18E+08	4.32E+07	1.13E+07	0.35	34.08	1.83	1.21	1	2	44
Pristine	T0	T0	1.54E+07	1.32E+08	4.40E+07	7.85E+06	NA	NA	NA	NA	NA	NA	NA
Pristine	T0	T0	1.44E+07	1.25E+08	4.12E+07	7.78E+06	NA	NA	NA	NA	NA	NA	NA
Pristine	T0	T0	2.26E+07	2.35E+08	6.45E+07	2.12E+07	NA	NA	NA	NA	NA	NA	NA
Pristine	T0	T0	2.41E+07	2.22E+08	6.88E+07	2.52E+07	NA	NA	NA	NA	NA	NA	NA
Pristine	T0	T0	1.90E+07	1.93E+08	5.42E+07	2.00E+07	NA	NA	NA	NA	NA	NA	NA
Pristine	HIGH	T0	NA	NA	NA	NA	NA	NA	NA	NA	2	9	18
Pristine	HIGH	T0	NA	NA	NA	NA	NA	NA	NA	NA	1	10	17

Pristine	HIGH	T0	NA	NA	NA	NA	NA	NA	NA	NA	NA	NA	NA
Pristine	LOW	T0	NA	NA	NA	NA	NA	NA	NA	NA	1	20	14
Pristine	LOW	T0	NA	NA	NA	NA	NA	NA	NA	NA	2	20	16
Pristine	LOW	T0	NA	NA	NA	NA	NA	NA	NA	NA	NA	NA	NA
Pristine	control	t0	NA	NA	NA	NA	NA	NA	NA	NA	1	7	20
Pristine	HIGH	T1	7.62E+06	1.59E+08	1.28E+07	1.46E+06	0.69	2.27	2.23	1.22	1	65	31
Pristine	HIGH	T1	6.75E+06	1.82E+08	1.13E+07	1.50E+06	0.41	1.13	2.34	1.24	1	66	25
Pristine	HIGH	T1	5.95E+06	1.83E+08	9.95E+06	1.30E+06	0.69	1.97	2.10	1.22	1	72	40
Pristine	LOW	T1	1.74E+08	6.14E+07	1.89E+08	7.28E+07	0.77	1.02	2.14	1.15	1	127	27
Pristine	LOW	T1	2.31E+08	8.73E+07	2.50E+08	9.15E+07	0.98	3.20	2.17	1.17	1	126	31
Pristine	LOW	T1	2.18E+08	8.92E+07	2.37E+08	8.33E+07	1.02	2.36	2.11	1.19	1	121	39
Pristine	control	t1	NA	NA	NA	NA	NA	NA	NA	NA	1	75	45
Pristine	HIGH	T2	3.35E+07	2.80E+08	6.30E+07	3.31E+06	0.82	0.32	1.82	1.41	1	60	317
Pristine	HIGH	T2	3.29E+07	2.72E+08	6.20E+07	2.85E+06	0.28	0.38	2.04	1.20	1	83	513
Pristine	HIGH	T2	3.31E+07	2.67E+08	6.22E+07	3.04E+06	0.49	1.28	1.96	1.28	NA	NA	NA
Pristine	LOW	T2	1.18E+08	3.27E+08	3.74E+08	2.30E+07	0.09	1.05	2.16	1.21	1	80	432
Pristine	LOW	T2	1.32E+08	3.59E+08	4.19E+08	2.66E+07	0.46	0.15	1.87	1.27	1	38	404
Pristine	LOW	T2	1.25E+08	3.00E+08	3.97E+08	2.49E+07	0.39	0.60	1.97	1.24	NA	NA	NA
Pristine	control	t2	NA	NA	NA	NA	NA	NA	NA	NA	1	36	553
Pristine	HIGH	T3	2.35E+08	3.72E+08	3.92E+08	3.69E+07	0.45	1.16	1.84	1.19	1	3	813
Pristine	HIGH	T3	2.22E+08	3.93E+08	3.71E+08	3.82E+07	0.93	0.77	1.98	1.21	NA	NA	NA
Pristine	HIGH	T3	1.93E+08	4.07E+08	3.22E+08	3.33E+07	0.41	1.04	1.89	1.24	1	3	1480
Pristine	HIGH	T3	2.71E+08	3.47E+08	4.51E+08	1.41E+08	NA	NA	NA	NA	NA	NA	NA
Pristine	HIGH	T3	2.51E+08	3.51E+08	4.19E+08	1.42E+08	NA	NA	NA	NA	NA	NA	NA
Pristine	HIGH	T3	2.46E+08	3.54E+08	4.10E+08	1.35E+08	NA	NA	NA	NA	NA	NA	NA
Pristine	LOW	T3	6.14E+07	1.38E+09	7.06E+07	8.75E+06	0.75	1.47	1.89	1.13	1	3	1212
Pristine	LOW	T3	8.73E+07	1.28E+09	1.00E+08	9.98E+06	0.95	1.81	2.05	1.14	1	3	2093

Pristine	LOW	T3	8.92E+07	9.38E+08	1.02E+08	1.02E+07	0.91	3.59	1.76	1.16	NA	NA	NA
Pristine	Low	T3	1.63E+07	3.44E+08	1.87E+07	5.40E+06	NA	NA	NA	NA	NA	NA	NA
Pristine	Low	T3	1.71E+07	4.20E+08	1.96E+07	6.00E+06	NA	NA	NA	NA	NA	NA	NA
Pristine	Low	T3	1.77E+07	3.87E+08	2.04E+07	5.86E+06	NA	NA	NA	NA	NA	NA	NA
Pristine	CONTROL	T3	3.27E+08	7.17E+08	6.12E+08	8.68E+07	0.56	1.10	1.61	1.07	1	3	1561
Pristine	CONTROL	T3	3.59E+08	7.67E+08	6.73E+08	9.18E+07	0.60	0.90	2.06	1.23	NA	NA	NA
Pristine	CONTROL	T3	3.00E+08	6.83E+08	5.62E+08	8.80E+07	0.44	0.82	1.82	1.17	NA	NA	NA
Pristine	CONTROL	T3	5.51E+08	2.01E+08	1.03E+09	5.04E+08	NA	NA	NA	NA	NA	NA	NA
Pristine	CONTROL	T3	5.81E+08	2.20E+08	1.09E+09	5.31E+08	NA	NA	NA	NA	NA	NA	NA
Pristine	CONTROL	T3	5.68E+08	2.14E+08	1.06E+09	5.10E+08	NA	NA	NA	NA	NA	NA	NA
Pristine	HIGH	T4	3.47E+08	2.42E+08	6.01E+08	1.48E+08	0.36	0.95	1.90	1.24	1	3	1700
Pristine	HIGH	T4	3.51E+08	2.46E+08	6.07E+08	1.48E+08	0.70	0.45	2.10	1.31	1	3	1784
Pristine	HIGH	T4	3.54E+08	2.02E+08	6.12E+08	1.48E+08	0.67	0.88	2.06	1.26	1	3	1624
Pristine	LOW	T4	1.38E+09	1.36E+08	2.60E+09	2.16E+08	0.40	0.27	1.58	1.18	1	2	1503
Pristine	LOW	T4	1.28E+09	1.95E+08	2.40E+09	2.13E+08	0.64	0.54	2.14	1.23	1	3	2469
Pristine	LOW	T4	9.38E+08	1.89E+08	1.76E+09	1.96E+08	0.55	1.20	2.21	1.19	1	3	1976
Pristine	control	t4	NA	NA	NA	NA	NA	NA	NA	NA	1	2	2137
Pristine	HIGH	CHEM-T5	3.44E+08	8.03E+08	4.69E+08	3.09E+07	0.81	2.44	2.00	1.21	1	3	2674
Pristine	HIGH	CHEM-T5	4.20E+08	8.03E+08	5.73E+08	3.70E+07	0.79	3.02	2.10	1.23	1	3	3014
Pristine	HIGH	CHEM-T5	3.87E+08	8.09E+08	5.27E+08	3.59E+07	0.60	1.47	2.09	1.24	NA	NA	NA
Pristine	HIGH	CHEM-T5	7.17E+08	1.41E+08	1.59E+09	9.40E+07	0.50	0.95	2.02	1.20	NA	NA	NA
Pristine	HIGH	CHEM-T5	7.67E+08	1.28E+08	1.70E+09	8.97E+07	0.42	0.64	2.13	1.24	NA	NA	NA
Pristine	HIGH	CHEM-T5	6.83E+08	1.23E+08	1.51E+09	8.44E+07	0.44	0.88	2.12	1.24	NA	NA	NA
Pristine	LOW	CHEM-T5	2.01E+08	1.80E+09	2.02E+08	1.67E+07	0.96	1.63	2.13	1.20	1	2	2490
Pristine	LOW	CHEM-T5	2.20E+08	1.89E+09	2.20E+08	1.62E+07	1.16	1.25	2.20	1.18	1	3	3679

Pristine	LOW	CHEM-T5	2.14E+08	1.76E+09	2.15E+08	1.88E+07	0.88	0.45	2.10	1.15	NA	NA	NA
Pristine	LOW	CHEM-T5	2.42E+08	8.45E+08	9.29E+08	1.38E+08	0.32	0.27	2.00	1.22	NA	NA	NA
Pristine	LOW	CHEM-T5	2.46E+08	9.10E+08	9.44E+08	1.37E+08	0.35	0.70	2.16	1.14	NA	NA	NA
Pristine	LOW	CHEM-T5	2.02E+08	8.12E+08	7.76E+08	1.26E+08	0.11	NA	NA	NA	NA	NA	NA
Pristine	CONTROL	CHEM-T5	1.36E+08	1.91E+09	1.77E+08	4.45E+07	0.42	0.11	1.23	1.27	1	2	2820
Pristine	CONTROL	CHEM-T5	1.95E+08	1.92E+09	2.55E+08	5.34E+07	1.07	0.25	2.14	1.22	1	3	3241
Pristine	CONTROL	CHEM-T5	1.89E+08	1.64E+09	2.47E+08	5.34E+07	0.81	0.59	2.13	1.16	NA	NA	NA
Pristine	CONTROL	BIO-T5	1.41E+08	5.70E+09	2.91E+08	1.06E+08	0.63	0.63	1.93	1.18	NA	NA	NA
Pristine	CONTROL	BIO-T5	1.28E+08	4.80E+09	2.63E+08	8.01E+07	0.31	1.62	2.14	1.19	NA	NA	NA
Pristine	CONTROL	BIO-T5	1.23E+08	4.54E+09	2.53E+08	1.09E+08	0.51	1.81	2.24	1.21	NA	NA	NA
Pristine	CONTROL	BIO-T5	1.52E+08	3.10E+07	3.12E+08	9.18E+07	NA	NA	NA	NA	NA	NA	NA
Pristine	CONTROL	BIO-T5	1.48E+08	8.15E+07	3.05E+08	9.59E+07	NA	NA	NA	NA	NA	NA	NA
Pristine	CONTROL	BIO-T5	1.42E+08	8.66E+07	2.91E+08	9.15E+07	NA	NA	NA	NA	NA	NA	NA
Pristine	LOW	BIO-T5	8.45E+08	2.76E+07	3.15E+10	2.87E+09	0.03	0.07	1.56	1.30	1	2	2537
Pristine	LOW	BIO-T5	9.10E+08	2.72E+07	3.40E+10	3.24E+09	NA	0.28	2.20	1.28	NA	NA	NA
Pristine	LOW	BIO-T5	8.12E+08	2.55E+07	3.03E+10	3.38E+09	NA	0.27	2.19	1.27	NA	NA	NA
Pristine	LOW	BIO-T5	1.57E+07	2.16E+07	5.86E+08	5.70E+08	NA	NA	NA	NA	NA	NA	NA
Pristine	LOW	BIO-T5	1.56E+07	2.11E+07	5.84E+08	7.66E+08	NA	NA	NA	NA	NA	NA	NA
Pristine	LOW	BIO-T5	1.49E+07	2.28E+07	5.55E+08	0.00E+00	NA	NA	NA	NA	NA	NA	NA
Pristine	HIGH	BIO-T5	1.98E+08	7.78E+07	1.54E+09	8.18E+07	0.14	0.13	1.54	1.16	1	2	2079
Pristine	HIGH	BIO-T5	1.98E+08	5.99E+07	1.53E+09	9.02E+07	0.14	0.24	2.14	1.35	NA	NA	NA
Pristine	HIGH	BIO-T5	2.03E+08	NA	1.57E+09	1.35E+08	0.11	0.31	2.18	1.28	NA	NA	NA
Pristine	HIGH	BIO-T5	1.96E+07	7.14E+06	1.52E+08	1.95E+07	NA	NA	NA	NA	NA	NA	NA
Pristine	HIGH	BIO-T5	2.41E+07	6.80E+06	1.87E+08	2.19E+07	NA	NA	NA	NA	NA	NA	NA
Pristine	HIGH	BIO-T5	2.27E+07	6.53E+06	1.76E+08	2.24E+07	NA	NA	NA	NA	NA	NA	NA

Pristine	milliQ-HIGH	T0	NA	NA	NA	NA	NA	NA	NA	NA	NA	NA	NA
Pristine	milliQ-HIGH	T1	NA	NA	NA	NA	NA	NA	NA	NA	NA	NA	NA
Pristine	milliQ-HIGH	T2	NA	NA	NA	NA	NA	NA	NA	NA	NA	NA	NA
Pristine	milliQ-HIGH	T3	NA	NA	NA	NA	NA	NA	NA	NA	NA	NA	NA
Pristine	milliQ-HIGH	T4	NA	NA	NA	NA	NA	NA	NA	NA	NA	NA	NA
Pristine	milliQ-LOW	T5	NA	NA	NA	NA	NA	NA	NA	NA	1	15	91

Table S4. Average and standard deviation of concentration of SMZ, SMX and their degradation products.

				Average							Standard deviation						
				[SMZ]	[SMX]	HYDROXY	DESAMINO	ACETYL	ACETYL-SMZ	NITRO_SMX	[SMZ]	[SMX]	HYDROXY	DESAMINO	ACETYL	ACETYL-SMZ	NITRO_SMX
EXP	SULF ADDITION	TIME POINT	days	ng/L	ng/L	ng/L	ng/L	ng/L	ng/L	ng/L	ng/L	ng/L	ng/L	ng/L	ng/L	ng/L	ng/L
Polluted	-	T0	0														
Polluted	HIGH	T0	0	6812	3471	8	BDL	57	21	BDL	1923	1510	0.4	BDL	18	2	BDL
Polluted	LOW	T0	0	1368	674	7	BDL	16	5	BDL	1142	549		BDL	4	0	BDL
Polluted	HIGH	T1	4	4212	1968	19	2	344	111	BDL	639	1519	2.5	0.0	45	1	BDL
Polluted	LOW	T1	4	523	246	7	1	71	12	BDL	613	269	0.4	0.0	18	6	BDL
Polluted	CONTROL	T1	NA	NA	NA	NA	NA	NA	NA	NA	NA	NA	NA	NA	NA	NA	NA
Polluted	HIGH	T2	15	1306	621	19	3	333	130	BDL	1964	865	2.6	1.5	60	28	BDL
Polluted	LOW	T2	15	246	141	11	1	34	7	BDL	137	32	3.6	0.1	12	4	BDL
Polluted	CONTROL	T2	15	NA	NA	NA	NA	NA	NA	NA	NA	NA	NA	NA	NA	NA	NA
Polluted	HIGH	T3	29	1311	994	25	5	199	198	BDL	374	233	10.5	1.3	129	68	BDL
Polluted	LOW	T3	29	573	228	13	2	13	9	BDL	53	11	3.8	0.1	9	BDL	BDL
Polluted	CONTROL	T3	29	NA	NA	NA	NA	NA	NA	NA	NA	NA	NA	NA	NA	NA	NA
Polluted	HIGH	T4	43	348	215	47	16	70	280	BDL	186	157	20.6	15.0	54	49	BDL
Polluted	LOW	T4	43	327	257	13	2	4	BDL	BDL	313	326	0.4	0.1	4	BDL	BDL
Polluted	CONTROL	T4	43	NA	NA	NA	NA	NA	NA	NA	NA	NA	NA	NA	NA	NA	NA
Polluted	HIGH	T5	56	872	298	38	16	17	314	BDL	358	124	33.4	15.6	21	BDL	BDL
Polluted	LOW1	T5	56	237	101	11	2	3	2	BDL	144	59	0.4	0.4	2	BDL	BDL
Polluted	CONTROL	T5	56	NA	NA	NA	NA	NA	NA	NA	NA	NA	NA	NA	NA	NA	NA

Pristine	HIGH	T0	0	4869	1406	63	5	181	111	5	2051.3	1221.2	16.4	0.8	18.1	7.6	BDL
Pristine	LOW	T0	0	4424	1333	11	2	55	23	2	4142.2	381.9	0.4	0.0	21.3	3.2	BDL
Pristine	CONTROL	T0	0	NA	NA	NA	NA	NA	NA	NA	NA	NA	NA	NA	NA	NA	NA
Pristine	HIGH	T1	4	4869	1406	63	5	181	111	5	2051.3	1221.2	16.4	0.8	18.1	7.6	BDL
Pristine	LOW	T1	4	145	168	14	4	18	8		55.0	40.7	3.2	1.5	1.5	0.6	BDL
Pristine	CONTROL	T1	4	NA	NA	NA	NA	NA	NA	NA	NA	NA	NA	NA	NA	NA	NA
Pristine	HIGH	T2	13	1000	783	26	38	143	77	2	813.1	598.5	0.3	17.4	14.2	21.7	BDL
Pristine	LOW	T2	13	280	170	7	8	12	4	BDL	97.8	33.7	0.3	1.1	2.2	1.2	BDL
Pristine	CONTROL	T2	13	NA	NA	NA	NA	NA	NA	NA	NA	NA	NA	NA	NA	NA	NA
Pristine	HIGH	T3	28	1124	375	37	77	140	54	BDL	1211.7	186.7	13.7	13.6	1.7	16.6	BDL
Pristine	LOW	T3	28	280	170	7	8	12	4	BDL	97.8	33.7	0.3	1.1	2.2	1.2	BDL
Pristine	CONTROL	T3	28	NA	NA	NA	NA	NA	NA	NA	NA	NA	NA	NA	NA	NA	NA
Pristine	HIGH	T4	42	1124	375	37	77	140	54	BDL	1211.7	186.7	13.7	13.6	1.7	16.6	BDL
Pristine	LOW	T4	42	108	339	9	9	8	2	BDL	67.6	78.5	1.2	3.5	3.1	BDL	BDL
Pristine	CONTROL	T4	42	NA	NA	NA	NA	NA	NA	NA	NA	NA	NA	NA	NA	NA	NA
Pristine	HIGH1	T5	55	832	387	18	53	38	15	BDL	635.0	126.7	6.2	27.4	1.4	13.5	BDL
Pristine	LOW1	T5	55	178	233	8	7	1	BDL	BDL	82.5	63.0	0.8	0.2	1.9	BDL	BDL
Pristine	CONTROL	T5	55	NA	NA	NA	NA	NA	NA	NA	NA	NA	NA	NA	NA	NA	NA

Table S5. Average and standard deviation of genes abundance of sul1 and sul2, AFDM, Chla, Nutrients

				Average											stdev										
				pPCR *Sul1*	qPCR *Sul2*	pPCR *Sul1*	qPCR *Sul2*	AFDM	Chla	Margalef's index	430/410	[PO4]	[NH4]	[NO3]+[NO2]	pPCR *Sul1*	qPCR *Sul2*	pPCR *Sul1*	qPCR *Sul2*	AFDM	Chla	Margalef's index	430/410	[PO4]	[NH4]	[NO3]+[NO2]
EXP	SULF ADDITION	TIME POINT	days	copies/cm2	copies/cm2	copies/AFDM	copies/AFDM	mg/cm2	ug/cm2			µmols/L	µmols/L	µmols/L	copies/cm2	copies/cm2	copies/AFDM	copies/AFDM	mg/cm2	ug/cm2			µmols/L	µmols/L	µmols/L
Polluted	-	T0	0	6.55E+08	1.84E+07	4.52E+08	4.70E+07	1.45E+00	9.44E+00	1.80E+00	1.25E+00	10.6	239.2	252.1	2.02E+07	4.14E+06	1.40E+07	4.03E+07	NA	NA	NA	NA	NA	NA	NA
Polluted	HIGH	T0	0	NA	NA	NA	NA	NA	NA	NA	NA	8.6	245.6	229.7	NA	NA	NA	NA	NA	NA	NA	NA	0.36	12.90	24.58
Polluted	LOW	T0	0	NA	NA	NA	NA	NA	NA	NA	NA	9.5	258.7	240.4	NA	NA	NA	NA	NA	NA	NA	NA	0.61	1.20	5.24
Polluted	HIGH	T1	4	9.22E+07	6.77E+06	8.63E+07	6.34E+06	1.07E+00	1.37E+01	1.81E+00	1.22E+00	33.1	10.5	531.4	1.44E+07	8.38E+05	1.35E+07	7.85E+05	0.02	NA	NA	NA	6.14	1.13	97.77
Polluted	LOW	T1	4	3.32E+09	2.07E+08	3.15E+09	1.96E+08	1.06E+00	6.60E+00	1.89E+00	1.20E+00	33.0	10.9	638.9	4.23E+08	2.99E+07	4.01E+08	2.83E+07	0.12	3.30	0.03	0.02	5.93	0.22	109.15
Polluted	CONTROL	T1	4	NA	NA	NA	NA	NA	NA	NA	NA	37.4	10.7	669.4	NA	NA	NA	NA	NA	NA	NA	NA	NA	NA	NA
Polluted	HIGH	T2	15	2.92E+08	3.32E+07	2.54E+08	2.88E+07	1.15E+00	4.66E+00	1.82E+00	1.21E+00	93.5	12.1	1641.8	1.52E+07	2.82E+05	1.32E+07	2.45E+05	0.56	3.15	0.03	0.01	18.86	0.34	281.85
Polluted	LOW	T2	15	4.00E+09	1.25E+08	3.34E+09	1.04E+08	1.20E+00	5.18E+00	1.87E+00	1.19E+00	93.7	11.3	1924.3	2.94E+08	7.13E+06	2.45E+08	5.95E+06	0.35	2.57	0.02	0.02	18.63	0.60	148.41
Polluted	CONTROL	T2	15	NA	NA	NA	NA	NA	NA	NA	NA	86.6	11.5	1668.4	NA	NA	NA	NA	NA	NA	NA	NA	NA	NA	NA
Polluted	HIGH	T3	29	7.66E+08	2.36E+08	1.07E+09	2.73E+08	7.16E-01	2.25E+00	1.76E+00	1.16E+00	99.9	9.0	1979.6	1.09E+08	2.67E+07	1.52E+08	3.91E+07	0.21	1.98	0.01	0.01	9.16	0.40	246.91
Polluted	LOW	T3	29	1.20E+09	4.82E+07	2.90E+09	4.24E+08	4.15E-01	1.37E+00	1.96E+00	1.15E+00	87.2	7.5	2622.9	2.04E+08	3.55E+07	4.91E+08	2.57E+08	0.12	1.22	0.10	0.08	15.49	0.20	50.39
Polluted	CONTROL	T3	29	2.05E+09	4.48E+08	3.30E+09	5.80E+08	6.20E-01	4.05E+00	1.76E+00	1.12E+00	110.9	8.4	2683.8	6.27E+07	1.32E+08	1.01E+08	6.51E+07	0.22	1.43	0.05	0.02	NA	NA	NA
Polluted	HIGH	T4	43	1.35E+10	3.51E+08	4.64E+10	1.21E+09	2.91E-01	8.83E-01	1.68E+00	1.14E+00	99.5	7.8	2519.6	4.31E+08	3.40E+06	1.48E+09	1.17E+07	0.07	0.48	0.13	0.00	8.70	1.55	176.72
Polluted	LOW	T4	43	1.67E+10	1.20E+09	3.55E+10	2.55E+09	4.69E-01	1.19E+00	1.85E+00	1.09E+00	97.6	6.5	2442.9	2.12E+09	2.31E+08	4.52E+09	4.93E+08	0.09	0.58	0.06	0.02	18.70	0.29	534.87
Polluted	CONTROL	T4	43	NA	NA	NA	NA	NA	NA	NA	NA	121.6	6.4	3197.5	NA	NA	NA	NA	NA	NA	NA	NA	NA	NA	NA
Polluted	HIGH	T5	56	6.06E+09	3.76E+08	1.86E+10	3.97E+09	4.11E-01	2.13E+00	1.77E+00	1.16E+00	147.4	6.0	3075.4	3.13E+09	3.04E+08	1.07E+10	2.10E+09	0.30	1.83	0.06	0.02	NA	NA	NA
Polluted	LOW1	T5	56	8.45E+09	1.64E+08	2.58E+10	1.95E+09	2.89E-01	1.54E+00	1.81E+00	1.15E+00	76.1	5.8	2542.0	3.75E+09	9.11E+07	9.37E+09	1.30E+09	0.13	0.91	0.05	0.03	NA	NA	NA

Polluted	CONTROL	T5	56	6.08E+09	3.27E+08	2.07E+10	2.50E+09	2.89E-01	1.43E+00	1.86E+00	1.07E+00	113.8	6.2	3609.6	2.74E+09	3.20E+08	8.44E+09	2.35E+09	0.04	0.46	0.05	0.01	NA	NA	NA
Polluted	milliQ-HIGH	T1		NA	NA	NA	NA	NA	NA	NA	NA	NA	NA	NA	NA	NA	NA	NA	NA	NA	NA	NA	NA	NA	NA
Polluted	milliQ-HIGH	T3		NA	NA	NA	NA	NA	NA	NA	NA	NA	NA	NA	NA	NA	NA	NA	NA	NA	NA	NA	NA	NA	NA
Polluted	milliQ-HIGH	T4		NA	NA	NA	NA	NA	NA	NA	NA	NA	NA	NA	NA	NA	NA	NA	NA	NA	NA	NA	NA	NA	NA
Polluted	milliQ-HIGH	T5		0.00E+00	0.00E+00	0.00E+00	0.00E+00	0.00E+00	0.00E+00	0.00E+00	0.00E+00	12.0	12.1	472.6	NA	NA	NA	NA	NA	NA	NA	NA	12.04	12.10	472.64
TRANSECT	Martorell	S1-T0-Martorell		2.22E+08	1.50E+07	1.53E+08	4.57E+07	1.45E+00	9.04E+00	1.97E+00	1.27E+00	4.2	6.6	110.9	2.19E+07	5.06E+05	1.51E+07	2.12E+07	NA	NA	0.00	NA	NA	NA	NA
TRANSECT	Castellbell	S2-T0-Castellbell		5.82E+07	1.21E+08	1.52E+08	6.99E+07	3.83E-01	2.63E+00	1.91E+00	1.17E+00	2.2	4.1	62.9	4.31E+05	7.69E+06	1.13E+06	2.84E+06	0.03	NA	0.00	NA	NA	NA	NA
TRANSECT	Navarcles	S3-T0-Navarcles		4.66E+07	1.07E+08	3.57E+07	2.60E+07	1.31E+00	2.63E+00	1.91E+00	1.17E+00	1.7	3.6	63.3	1.50E+07	1.12E+08	1.15E+07	2.22E+07	NA	0.00	0.00	NA	NA	NA	NA
TRANSECT	Gironella	S4-T0-Gironella		1.04E+07	3.32E+07	3.00E+07	1.97E+07	3.46E-01	2.50E+00	2.06E+00	1.29E+00	1.3	2.3	42.5	7.79E+05	2.82E+05	2.25E+06	8.76E+05	NA	NA	NA	NA	NA	NA	NA
Pristine	T0	T0	0	1.84E+07	1.71E+08	5.27E+07	1.55E+07	3.50E-01	3.41E+01	1.83E+00	1.21E+00	1.2	2.2	44.0	4.14E+06	5.24E+07	1.18E+07	7.52E+06	NA	NA	NA	NA	NA	NA	NA
Pristine	HIGH	T0	0	NA	NA	NA	NA	NA	NA	NA	NA	1.6	9.6	17.5	NA	NA	NA	NA	NA	NA	NA	NA	0.21	0.48	1.18
Pristine	LOW	T0	0	NA	NA	NA	NA	NA	NA	NA	NA	1.4	20.0	15.2	NA	NA	NA	NA	NA	NA	NA	NA	0.12	0.59	1.59
Pristine	CONTROL	T0	0	NA	NA	NA	NA	NA	NA	NA	NA	1.3	7.0	20.4	NA	NA	NA	NA	NA	NA	NA	NA	1.28	7.00	20.43
Pristine	HIGH	T1	4	6.77E+06	1.75E+08	1.13E+07	1.42E+06	5.98E-01	1.79E+00	2.23E+00	1.23E+00	1.2	67.5	31.9	8.38E+05	1.33E+07	1.40E+06	1.06E+05	0.16	0.59	0.12	0.01	0.08	3.80	7.17
Pristine	LOW	T1	4	2.07E+08	7.93E+07	2.25E+08	8.25E+07	9.21E-01	2.19E+00	2.14E+00	1.17E+00	1.2	124.7	32.2	2.99E+07	1.55E+07	3.25E+07	9.38E+06	0.14	1.10	0.03	0.02	0.12	2.94	6.48
Pristine	CONTROL	T1	4	NA	NA	NA	NA	NA	NA	NA	NA	1.0	74.7	44.9	NA	NA	NA	NA	NA	NA	NA	NA	1.04	74.72	44.91
Pristine	HIGH	T2	13	3.32E+07	2.73E+08	6.24E+07	3.06E+06	5.31E-01	6.57E-01	1.94E+00	1.30E+00	0.9	71.7	414.9	2.82E+05	6.57E+06	5.31E+05	2.30E+05	0.27	0.54	0.11	0.11	0.12	16.71	138.96
Pristine	LOW	T2	13	1.25E+08	3.29E+08	3.97E+08	2.48E+07	3.15E-01	6.00E-01	2.00E+00	1.24E+00	1.1	59.1	417.9	7.13E+06	2.97E+07	2.26E+07	1.79E+06	0.20	0.45	0.15	0.03	0.07	29.44	19.88
Pristine	CONTROL	T2	13	NA	NA	NA	NA	NA	NA	NA	NA	1.0	35.8	553.1	NA	NA	NA	NA	NA	NA	NA	NA	1.04	35.78	553.12
Pristine	HIGH	T3	28	2.36E+08	3.71E+08	3.94E+08	8.76E+07	5.99E-01	9.90E-01	1.90E+00	1.21E+00	1.1	3.1	1146.6	2.67E+07	2.47E+07	4.45E+07	5.65E+07	0.29	0.20	0.07	0.03	0.05	0.07	471.36
Pristine	LOW	T3	28	4.82E+07	7.91E+08	5.53E+07	7.69E+06	8.70E-01	2.29E+00	1.90E+00	1.14E+00	1.2	3.0	1652.7	3.55E+07	4.70E+08	4.08E+07	2.19E+06	0.10	1.14	0.15	0.02	0.05	0.11	622.99
Pristine	CONTROL	T3	28	4.48E+08	4.67E+08	8.38E+08	3.02E+08	5.34E-01	9.41E-01	1.83E+00	1.16E+00	1.0	2.6	1561.3	1.32E+08	2.81E+08	2.47E+08	2.33E+08	0.09	0.14	0.23	0.08	NA	NA	NA

Pristine	HIGH	T4	42	3.51E+08	2.30E+08	6.07E+08	1.48E+08	5.78E-01	7.61E-01	2.02E+00	1.27E+00	1.1	2.7	1702.8	3.40E+06	2.42E+07	5.88E+06	3.99E+05	0.19	0.27	0.11	0.04	0.06	0.20	79.95
Pristine	LOW	T4	42	1.20E+09	1.73E+08	2.25E+09	2.08E+08	5.32E-01	6.70E-01	1.97E+00	1.20E+00	1.2	2.5	1982.3	2.31E+08	3.29E+07	4.35E+08	1.09E+07	0.12	0.48	0.34	0.03	0.11	0.09	483.28
Pristine	CONTROL	T4	42	NA	NA	NA	NA	NA	NA	NA	NA	1.1	2.5	2136.5	NA	NA	NA	NA	NA	NA	NA	NA	1.11	2.45	2136.52
Pristine	HIGH1	T5	55	3.32E+08	2.70E+08	9.60E+08	6.19E+07	4.38E-01	1.12E+00	2.04E+00	1.24E+00	1.1	2.5	2589.2	2.72E+08	3.47E+08	6.55E+08	3.82E+07	0.27	1.01	0.19	0.05	0.01	0.15	473.25
Pristine	LOW1	T5	55	3.28E+08	6.80E+08	8.40E+09	9.39E+08	5.43E-01	6.16E-01	2.07E+00	1.22E+00	1.2	2.4	2901.9	3.31E+08	7.72E+08	1.42E+10	1.36E+09	0.45	0.55	0.22	0.06	0.11	0.12	673.38
Pristine	CONTROL	T5	55	1.50E+08	2.30E+09	2.66E+08	8.05E+07	6.26E-01	8.35E-01	1.97E+00	1.20E+00	1.2	2.5	3030.1	2.55E+07	2.19E+09	4.10E+07	2.41E+07	0.28	0.71	0.38	0.04	0.01	0.17	297.68
Pristine	milliQ-HIGH	T0		NA	NA	NA	NA	NA	NA	NA	NA	NA	NA	NA	NA	NA	NA	NA	NA	NA	NA	NA	NA	NA	NA
Pristine	milliQ-HIGH	T1		NA	NA	NA	NA	NA	NA	NA	NA	NA	NA	NA	NA	NA	NA	NA	NA	NA	NA	NA	NA	NA	NA
Pristine	milliQ-HIGH	T2		NA	NA	NA	NA	NA	NA	NA	NA	NA	NA	NA	NA	NA	NA	NA	NA	NA	NA	NA	NA	NA	NA
Pristine	milliQ-HIGH	T3		NA	NA	NA	NA	NA	NA	NA	NA	NA	NA	NA	NA	NA	NA	NA	NA	NA	NA	NA	NA	NA	NA
Pristine	milliQ-HIGH	T4		NA	NA	NA	NA	NA	NA	NA	NA	NA	NA	NA	NA	NA	NA	NA	NA	NA	NA	NA	NA	NA	NA
Pristine	milliQ-LOW	T5		NA	NA	NA	NA	NA	NA	NA	NA	1.2	14.5	91.2	NA	NA	NA	NA	NA	NA	NA	NA	1.238	14.521	91.211

3.3 Discussió de resultats

3.3.1 Aproximacions analítiques

En aquest capítol s'han estudiat els processos de transformació mitjançant la seva simulació a escala laboratori. En aquesta estratègia les mostres control cobren gran importància ja que s'han de comparar amb les mostres degradades. Així doncs, aquests controls a poder ser han de ser en les mateixes matrius i tenen que ser sotmesos als mateixos agents externs i condicions ambientals a excepció del paràmetre objectiu de l'estudi. Aquests fet pot incrementar de gran manera la complexitat de la simulació i per tant sempre queden sotmesos a la seva pertinent viabilitat. Un cop s'ha simulat el procés i per tant, s'han generat els diferents TPs, hi ha diferents estratègies analítiques per a detectar i identificar aquests TPs. En aquest capítol s'han utilitzat dues aproximacions diferents, l'alineació cromatogràfica i l'escombratge de sospitosos.

Als estudis de fototransformació en aigües superficials, on l'efecte de la matriu pot simplificarr-se fent una comparació cromatogràfica entre mostres irradiades i mostres control. En aquesta aproximació la detecció del TP queda subjecta a la capacitat de distingir els nous pics generats en les mostres irradiades. Els diferents estudis d'identificació de TPs que hem fet durant aquesta tesi ens han permès també constatar l'evolució de la LC-HRMS a través dels diferents analitzadors que s'han pogut utilitzar. En l'estudi d'identificació dels TPs del SDF es va utilitzar UPLC acoblada a un espectròmetre QToF (micromass) equipat amb ESI. Amb aquest equip, de l'any 1999, es va poder treballar a una resolució de 5000 (FWHM). A la següent publicació, per identificar els TPs dels seus anàlegs, també es va treballar amb UPLC-ESI però en aquest cas es va disposar d'un Orbitrap Q Exactive, fabricat l'any 2011. Amb aquest instrument, considerat de nova generació, es va poder treballar a una resolució de 70000 (FWHM) a l'escombratge total d'ions i de 17500 en l'obtenció dependent dels ions producte. Això va permetre treballar al laboratori a concentracions similars a les que trobem als rius, evitant la necessitat de pre-concentrar les mostres per obtenir una bona fragmentació. A més, programari que s'ha desenvolupat recentment com pot ser el cas del SIEVE, permet de manera força senzilla la

detecció dels TPs generats mitjançant l'alineació i comparació cromatogràfica de les mostres tractades i les mostres control. Això també ens facilita poder treballar en concentracions on manualment ens resultaria molt complicat identificar TPs que no mostren un pic a l'escompratge total d'ions.

En el cas de l'estudi de biodegradació de les sulfonamides, previ als anàlisis quantitatius reportats en la publicació 4, es va realitzar un mètode d'escombratge de sospitosos mitjançant UPLC-HRMS. Per aquest treball es va realitzar una llista de masses dels TPs del SMX i de la SMZ identificats a la literatura (llistat de sospitosos). Les mostres es van injectar en mode d'escombratge complet amb obtenció dependent de fragments. Aquest mode realitza la fragmentació d'un nombre determinat de compostos detectats en cada escombratge, donant prioritat als ions de m/z inclosos a la llista.

Aquest escombratge es va realitzar per a veure quins TPs eren presents a les mostres i poder obtenir patrons de referència comercials per a la seva posterior quantificació. Així doncs, es va realitzar una base de dades amb els TPs de les sulfonamides identificats a la literatura i d'altres que es podien esperar per analogia amb reaccions de transformació conegudes. La base de dades contenia simplement el nom del compost, la seva composició elemental i la massa exacte del ió generat en mode positiu i en mode negatiu. Les mostres es van injectar mitjançant escombratge complet d'ions amb adquisició dependent d'espectres MS^2, donant prioritat als compostos inclosos en aquesta llista. Posteriorment les masses es van extreure a l'escombratge total d'ions de les mostres amb activitat microbiana i es van comparar amb les mostres control, per tal de veure la formació de nous pics corresponents als TPs generats. La taula 3 mostra els compostos sospitosos detectats a les mostres irradiades. Finalment es va tractar de confirmar la identitat d'aquests sospitosos (veure apartat 3.3.2) i comprar els patrons de referència per a realitzar l'esmentat estudi quantitatiu. Mitjançant aquesta quantificació es va constatar que a altes concentracions el paper de la degradació de les sulfonamides és més important, mentre que a baixes concentracions la adaptació dels bacteris mitjançant la propagació de gens resistents als antibiòtics cobra protagonisme.

TAULA 3. Compostos sospitosos detectats als estudis de biodegradació de les sulfamides.

		POSSIBLES TPs										
		(M+H) +	DESAMINO	HIDROXILACIÓ	CARBOXILACIÓ	ACETIL	HIDROXILACIÓ + ACETIL	SULFAT	GLUCURÒNIC	HIDROXILACIÓ + GLUCURÒNIC	HIDROXILACIÓ + SULFAT	DIHIDROXILACIÓ + GLUCURÒNIC
SULFAMETOXAZOL	Massa exacte (m/z)	254.0594	239.0485	270.0544	284.0336	296.0700	312.0649	N.D.	430.0915	N.D.	350.0111	N.D.
	TR (min)	3.69	4.48	3.43	4.84	3.73	1.88/3.62	N.D.	3.42	N.D.	4.27	N.D.
SULFAMETAZINA	Massa exacte (m/z)	279.0910	N.D.	295.0860	309.0652	321.1016	337.0965	359.0478	455.1231	471.1180	N.D.	487.1129
	TR (min)	2.9	N.D.	2.34	2.71	2.85	3.03	1.36	2.89	2.52	N.D.	8.3

3.3.2 Identificació de TPs

En l'elucidació estructural mitjançant els espectres obtinguts amb LC-HRMS, conèixer la fragmentació dels compostos inicials és clau per poder proposar una estructura plausible pels diferents TPs generats. Per aquest motiu, en tots els experiments s'ha elucidat el patró de fragmentació dels compostos pare.

En les publicacions centrades en la identificació de TPs dels inhibidors de la fosfodiesterasa V, el patró de fragmentació està clarament detallat. El fet de treballar amb compostos relacionats, va permetre observar fragments comuns de la part aromàtica de l'estructura del SDF (ions m/z 377, 311, 299 i 283) i les diferències en els ions de baix m/z rati degudes a les diferències en l'anell de piperazina. Les similituds i diferencies entre espectres facilita la identificació dels TPs per analogia.

De fet, estudiar compostos relacionats aporta informació útil pel coneixement del seu procés de degradació, ja que les seves diferències estructurals ens permeten veure el comportament d'aquella par de l'estructura. És el cas del NR-SDF, que no tenia l'anell de piperazina, ja que presenta un carboni en el lloc del nitrogen de l'amina terciària, i això va ser utilitzat per veure els efectes en la fototransformació que suposa no tenir aquest anell heterociclic. Per altre banda, l'estudi del TS-SDF, va permetre veure com es comporten els anàlegs obtinguts mitjançant la substitució de l'oxigen pel sofre, una altre estratègia, cada cop més comú, per a l'obtenció d'anàlegs.

Malgrat la informació que ens aporten els espectres de masses obtinguts pels diferents TPs, la seva comparació amb els patrons de fragmentació dels compostos pare i la informació de compostos relacionats, en alguns casos és necessari l'ús d'estratègies complementaries. En aquests estudis, la degradació de compostos deuterats ha aportat una informació addicional de gran valor per tal de postular la identitat d'alguns TPs.

Finalment, tota aquesta informació ens ha permès elucidar els diferents TPs però sobretot ens han permès veure un patró de fragmentació comú per a tots els compostos relacionats amb el SDF. Aquest es basa en transformacions

centrades en l'esmentada anella de piperazina. Els TPs generats poden ser comuns entre els diferents compostos, si es perd el diferent substituent de l'anell, o diferents, quan la transformació es produeix mantenint aquesta part

En quant al NR-SDF, el qual no té aquest anell, només s'observa la formació del TP de m/z 393, precisament el TP que ja no conte l'anell a l'estructura. Pel que fa al TS-SDF, s'observa que en els primers minuts d'irradiar la mostra es forma ràpidament un TP de m/z 475. L'estructura d'aquest TP es va comprovar amb un patró comercial que es tracta de SDF, és a dir, el TS-SDF en ser irradiat s'oxida invertint la substitució del sofre de l'anàleg per l'oxigen del compost original. Ja que aquesta conversió es produeix gairebé de forma immediata, la resta de TPs observats coincideixen amb els del SDF.

En l'estudi de biodegradació de SMX i SMZ en un mesocosm també es va començar per identificar la fragmentació dels compostos pare Figura 7.

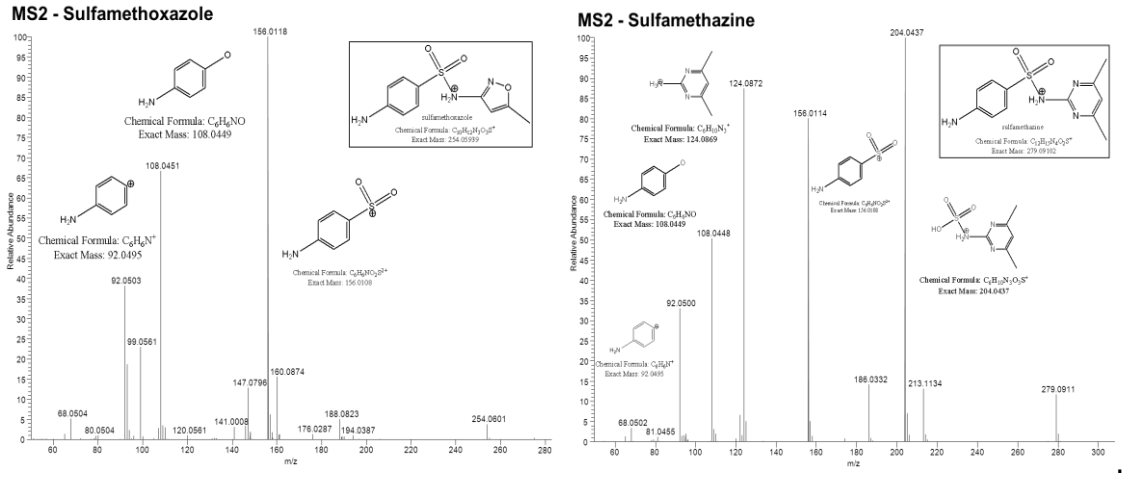

Figura 7. *Espectres MS/MS amb els fragments proposats pels compostos pares*

Aquests espectres s'utilitzaven per tal de confirmar la identitat dels compostos sospitosos mitjançant la comparativa amb els espectres dels TPs. El temps de retenció relatiu al compost pare, així com el perfil isotòpic, també ens dóna informació sobre els grups funcionals que s'han pogut transformar. Però l'avantatge d'aquest cas és que coneixíem la identitat del compost proposat i alguns han estat estudiats en altres processos. Així doncs, es va poder utilitzar

una llibreria d'espectres (massbank.eu) per tal de confirmar l'estructura dels TPs. Aquesta llibreria conté espectres en alta i baixa resolució introduïts per usuaris d'arreu del món i obtinguts mitjançant diferents instruments. Malgrat ser compostos força estudiats, tan sols es van poder trobar els espectres del Acetyl-sulfametoxazol i l' Acetyl-sulfametazina. Aquests espectres es van comparar amb els obtinguts i es va poder confirmar la seva identitat en un nivell 2 segons l'escala proposada per Schymanski [127]. La resta de TPs van ser confirmats mitjançant espectres o fragments publicats en altres estudis o proposats via elucidació estructural pròpia.

Aquests resultats, identificant principalment les mateixes reaccions en ambdós casos, ens mostren també una via de degradació comú per les sulfonamides estudiades. Finalment, es van escollir els TPs a quantificar basant-nos en un dels principals obstacles per a la quantificació dels mateixos, la viabilitat d'obtenir patrons comercials de referència.

3.3.3 Detecció de TPs en mostres ambientals

El darrer pas en els estudis basats en simulacions de degradació de fàrmacs a escala laboratori sòl ser freqüentment la constatació de la presencia d'aquests compostos al medi ambient. En l'article 3, després de la identificació dels diferents fotoTPs, s'han analitzat diferents mostres ambientals per tal de determinar-ne la seva presència. Per això es va realitzar un mètode quantitatiu amb un instrument de LC-QqQ-MS per analitzar diferents mostres i poder detectar-lo a baixes concentracions. Aquest fet, va comportar la primera detecció de dos TPs de SDF o d'un dels seus anàlegs en mostres reals. En aquestes mostres no es va detectar SDF ni cap dels compostos anàlegs estudiats, ressaltant la importància d'incloure els TPs en els estudis ambientals. A més, el TP488 detectat podria provenir del SDF, però també del H-SDF, del HH-SDF o del T-SDF. I per altre banda, el TP448 també podria provenir del SFD o del T-SDF. Això ens ha servit per corroborar que l'avaluació del destí ambiental del SDF és força complexa degut a que els anàlegs presenten rutes de degradació convergents. Malgrat tot, ser compostos tant semblants també pot resultar una avantatge i ser utilitzat com una estratègia per avaluar la

presència global d'aquests compostos. En aquest sentit, els patrons de fragmentació de compostos i TPs ens mostren fragments comuns, fet que es pot utilitzar per a realitzar un anàlisi de sospitosos a través de la cerca d'aquests fragments en mostres ambientals. És a dir, buscar aquests fragments mitjançant l'adquisició de dades independent i després tractar d'identificar el compost pare. Aquesta estratègia ja s'està utilitzant en la detecció d'anàlegs en mostres adulterades [146], ja que és més senzill degut a l'elevada concentració que presenta a la mostra. En mostres ambientals requereix d'estratègies per a l'assignació de l'ió parental amb l'ió producte.

CAPÍTOL 4.

ACUMULACIÓ I METABOLISME DE FÀRMACS A LA BIOTA

CAPITOL 4. ACUMULACIÓ I METABOLISME DE FÀRMACS A LA BIOTA

Al capítol 3 s'ha demostrat que els residus farmacèutics presents als ecosistemes aquàtics es degraden per fotòlisis i biodegradació. No obstant això degut a l'elevat consum i la seva pertinent entrada continua al medi, la fauna i la flora d'aquests ecosistemes hi estan constantment exposats. A la literatura hi ha diversos estudis que han reportat la seva presència en diferents organismes, principalment en peixos, i els possibles efectes adversos sobre la seva salut, creixement i reproducció. A més, a la literatura també s'han analitzat els diferents teixits i s'ha comprovat que els fàrmacs més liposolubles poden acumular-se al teixit adipós, amb el risc de passar a la cadena alimentaria.

Els productes farmacèutics s'han desenvolupat per produir un efecte biològic, i per tant diversos estudis s'han centrat en estudiar la seva toxicitat aguda sobre la biota. Weeb i col. [149] va estudiar-la per les diferents classes de fàrmacs i va reportar que els antidepressius, antibacterians i antipsicòtics van resultar ser els més tòxics. Cleuvers i col. [150, 151] també van avaluar la toxicitat aguda a curt termini de fàrmacs antiinflamatoris no esteroides (AINE), utilitzant algues i invertebrats. En general, aquests estudis conclouen que a concentracions ambientals no es preveuen efectes aguts sobre els organismes, ja que haurien de ser d'unes com 100 a 1000 vegades més altes. No obstant això, aquests estudis es realitzen de forma individual i aquests compostos es troben en mescles complexes que poden provocar efectes diferents, ja que es poden produir efectes sinèrgics o antagònics. A més a més, s'han de tenir en compte els efectes crònics ja que moltes espècies aquàtiques estan exposades de manera contínua a residus farmacèutics durant llargs períodes, fins i tot tot el seu cicle de vida.

En l'actualitat encara se sap molt poc sobre els processos d'absorció, metabolisme, acumulació o eliminació dels residus farmacèutics a peixos i plantes. El metabolisme dels fàrmacs consisteix en la modificació bioquímica del compost farmacèutic generalment a través d'enzims especialitzats. És sabut, que els fàrmacs com a tals estan dissenyats per ser ingerits per humans o animals, actuar segons el seu propòsit i ser excretats (Figura 8).

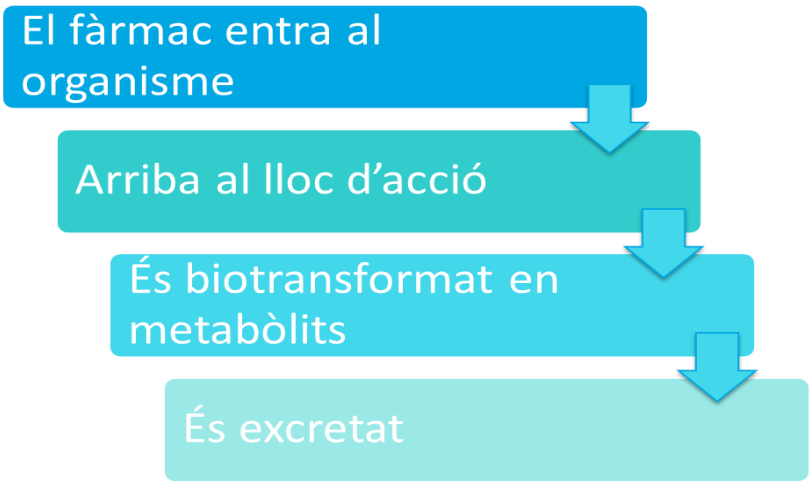

Figura 8. *Etapes del metabolisme dels fàrmacs*

Malgrat això, el seu disseny està dirigit i estudiat per a un tipus d'organisme concret i per tant la exposició d'altres éssers vius pot tenir diferent resultat. Se sap que els vegetals i els animals poden detoxificar i eliminar els contaminants després de l'absorció, però l'acumulació en el seu teixit adipós o l'absència dels sistemes d'enzims apropiats per al seu metabolisme poden dificultar-ne la seva excreció.

És per aquest motiu que en aquest capítol s'ha pretès estudiar el metabolisme de fàrmacs en diferents tipus d'organismes aquàtics, concretament en peixos i plantes, començant per entendre les seves reaccions principals mitjançant experiments dissenyats al laboratori i finalment acabant per avaluar la exposició i el metabolisme en la biota salvatge.

4.1 Estudi del metabolisme de fàrmacs en biota a escala laboratori

Degut a les baixes concentracions de fàrmacs ambientals, per tal d'estudiar en profunditat les rutes metabòliques de diferents organismes aquàtics, s'ha optat per realitzar experiments a escala laboratori en condicions controlades i amb l'exposició a un fàrmac determinat. En aquests estudis, són encara més necessàries les mostres control, que pels experiments de fotodegradació i biodegradació, ja que la detecció de metabòlits en matrius biològiques és encara mes complexa.

En aquest apartat també s'ha volgut estudiar les diferencies metabòliques entre els diferents organismes aquàtics. Per aquest motiu s'ha realitzat l'estudi d'un mateix fàrmac en plantes, utilitzant llenties d'aigua, i en peixos, concretament en llenguados. El fàrmac escollit a estat un dels AINE més coneguts; l'ibuprofè (IBU).

Per tal de realitzar els experiments a escala laboratori, es va realitzar una col·laboració amb l'Institut de Ciències del Mar de Barcelona, el qual disposava d'aquests peixos marins per a realitzar l'experiment. Els llenguados varen ser injectats amb IBU i CBZ i es van estudiar els metabòlits a la bilis. Per tal de identificar els metabòlits de l'IBU en plantes es va realitzar una col·laboració amb el consell d'investigacions d'Italia, concretament amb el Institut agro-ambiental i de biologia forestal de Roma, el qual realitza diferents estudis en Lemna Gibba. Les plantes van ser exposades a l'IBU a través de l'aigua on vivien. L'anàlisi es va realitzar mitjançant un sistema LC-HRMS, concretament utilitzant un Orbitrap Q-Exactive.

L'IBU es detecta freqüentment al medi ambient ja que, segons l'informe anual del sistema nacional de salut espanyol de l'any 2015, és el setè principi actiu més venut a l'estat en nombre d'envasos, amb 17.3 milions d'envasos que corresponen a uns 43.3 milions d'euros. Alguns estudis d'altres AINEs com l'àcid acetilsalicílic van demostrar que tenen efectes sobre la reproducció de la daphnia magna a concentracions al voltant de 1,8 mg/L. També estudis de toxicitat crònica del diclofenac van mostrar efectes histopatològics en la truita arc de Sant Martí després de 28 dies d'exposició, produint lesions renals a concentracions de 5 mg/L i efectes sub-cel·lulars a 1 mg/L [35].

Finalment, en l'estudi del metabolisme dels llenguados també es va optar per estudiar la carbamazepina (CBZ), un antiepilèptic bastant persistent a les EDARs, ja que com s'ha documentat a la literatura, els fàrmacs d'ús psiquiàtric són freqüentment detectats en peixos degut a la seva relativa lipo-solubilitat (pKa: 13.94 / log P:2.77). La CBZ presenta generalment un rati baix de degradació a les EDARs i el seu lleuger caràcter bàsic ens ajudarà al estudi de les vies metabòliques en contraposició al IBU, lleugerament àcid.

El resultat d'aquests estudis amb la detecció i identificació dels diferents metabòlits es troba a les dues publicacions següents.

Article nº 5: Metabolic profiling of ibuprofen and carbamazepine in juvenile Senegal soles (Solea senegalensis) using high-resolution mass spectrometry.

J. Aceña , S. Pérez, P. Eichhorn, M. Solé and D. Barceló.

Analytical and Bioanalytical Chemistry - 2017

Analytical & Bioanalytical Chemistry

METABOLITE PROFILING OF CARBAMAZEPINE AND IBUPROFEN IN SOLEA SENEGALENSIS BILE USING HIGH RESOLUTION MASS SPECTROMETRY

Journal:	*Analytical and Bioanalytical Chemistry*
Manuscript ID	ABC-00552-2017.R1
Type of Paper:	Research Paper
Date Submitted by the Author:	23-May-2017
Complete List of Authors:	Aceña, Jaume; IDAEA-CSIC, environmental chemistry department Perez, Sandra; IDAEA-CSIC, Environmental Chemistry Eichhorn, Peter; IDAEA-CSIC Sole, Montserrat; CSIC, ; PML-NERC, Barceló Culleres, Damià; IDAEA-CSIC, Department of Environmental Chemistry; Catalan Institute for Water Research (ICRA),
Keywords:	Ibuprofen, carbamazepine, Fish metabolites, Carboxylesterases, bile, High resolution Mass spectrometry

METABOLITE PROFILING OF CARBAMAZEPINE AND IBUPROFEN IN *SOLEA SENEGALENSIS* BILE USING HIGH RESOLUTION MASS SPECTROMETRY

Jaume Aceña[1], Sandra Pérez[1*], Peter Eichhorn[1], Montserrat Solé[2] and Damià Barceló[1]

[1] Water and Soil Quality Research Group, IDAEA-CSIC, c/Jordi Girona 18-26, 08034 Barcelona (Spain).
[2] Institute of Marine Sciences ICM-CSIC, Pg Marítim Barceloneta,37-49, Barcelona (Spain).

Corresponding author:

Sandra Pérez

IDAEA-CSIC

Water and Soil Quality Research Group

Jordi Girona 18-26

Barcelona 08034, Spain

E-mail: spsqam@idaea.csic.es

Phone: ++34-93 400 6100

Fax: ++34-93 204 5904

ABSTRACT

The widespread occurrence of pharmaceuticals in the aquatic environment has raised concerns about potential adverse effects on exposed wildlife. Very little is currently known on exposure levels and clearance mechanisms of drugs in marine fish. Within this context, our research was focused on the identification of main metabolic reactions, generated metabolites and caused effects after exposure of fish to carbamazepine (CBZ) and ibuprofen (IBU). To this end, juveniles of *Solea senegalensis* acclimated to two temperature regimes of 15ºC and 20ºC for 60 days received a single intraperitoneal dose of these drugs. A control group was administered the vehicle (sunflower oil). Bile samples were analyzed by ultra-high performance liquid chromatography - high-resolution mass spectrometry. on a Q Exactive (Orbitrap) system allowing to propose plausible identities for eleven metabolites of CBZ and thirteen metabolites of IBU in fish bile. In case of CBZ metabolites originated from aromatic and benzylic hydroxylation, epoxidation and ensuing O-gucuronidation; O-methylation of a catechol-like metabolite was also postulated. Ibuprofen in turn formed multiple hydroxyl metabolites, O-glucuronides and (hydroxyl) acyl glucuronides, in addition to several taurine conjugates. Enzymatic responses after drug exposures revealed a water temperature-dependent induction of microsomal carboxylesterases. The metabolite profiling in fish bile provides an important tool for pharmaceutical exposure assessment.

Keywords*:* Ibuprofen, Carbamazepine, Fish metabolites, Carboxylesterases, Bile, High resolution mass spectrometry

1. INTRODUCTION

During the last few years the presence of pharmaceuticals in riverine fish has been reported demonstrating that long-term exposure of aquatic organisms to pharmaceutical residues emitted from wastewater treatment plants may result in bioaccumulation [152-154]. Besides, marine species in coastal areas may also be exposed to pharmaceuticals through effluent discharges, waste disposal, and the use of drugs in aquaculture. The impact of this exposure, however, has received very little attention and studies reporting the detection of human drug residues in wild marine fish species is very scarce [63, 155, 156]. This is surprising because the occurrence of pharmaceuticals in estuaries and potential contaminated areas has raised concerns about potential adverse effects on the species living on them. The first report on the detection of pharmaceuticals in wild marine species dates back to 2009 [157]. In this study, diazepam was measured in marine flatfish collected near ocean discharges of municipal wastewater effluent. More recently, Alvarez-Muñoz reported the presence of several pharmaceuticals, including metoprolol, azithromycin and venlafaxine, in the different trophic levels of the food chain from coastal areas [63]. Other authors reported the presence of carbamazepine (CBZ) [158, 159] in different marine species being this compound one of the pharmaceutical compounds more frequently reported in marine species.

Through the gills, as one of the major ports of entry, drugs are taken up from the water reaching the blood stream. Upon passage through the liver hepatic detoxification systems recognize these xenobiotics and may bring about their transformation by phase I and II metabolizing steps into more readily excretable metabolites [160]. In fact, over 60% of clinically used drugs are metabolised by CYP-mediated (mostly CYP3A4) phase I metabolism [161]. Another phase I enzymes carboxylesterases (CbEs) are involved in the hydrolysis of many administered drugs and pro-drugs as well as endogenous compounds [162]. As yet only the metabolism in rainbow trout, representing a model freshwater species frequently used in environmental studies, has been investigated using the three non-steroidal anti-inflammatory drugs naproxen [48], diclofenac [51], ibuprofen (IBU) [49] as substrates. In all instances the metabolic pathways were studied under controlled laboratory conditions with exposure through either spiked tank water or intraperitoneal administration of the test compounds. In case of naproxen the analysis of the bile proved the acylglucuronides of the parent compound and its demethylated metabolite to be the major biotransformation products [48]. Detailed profiling of bile samples from the diclofenac experiments revealed a substantial overlap with the metabolic reactions observed in humans, including 4´- and 5-hydroxylations, acyl glucuronidation, sulfation and glucuronidation of hydroxyl metabolites, and hydroxyl-acylglucuronidation [51]. Rainbow trout dosed with ibuprofen in turn yielded apart from the hydroxylated metabolites, (hydroxylated) acylglucuronides, and ether glucuronides of hydroxyl-IBU also a number of taurine conjugates [49] although these were deemed of minor relevance.

In contrast to metabolism studies carried out with juvenile or adult fish, alternative test systems have been described exploring the use of zebra fish at larval or embryonic stage for elucidating the biotransformation of human drugs. Following exposure of larvae to ^{14}C-radiolabeled IBU, HRMS allowed to identify hydroxyl-IBU as a major metabolite while additional drug-related material accounting for a relatively low fraction of radioactivity could not be identified [54]. In contrast, a comprehensive characterization of the metabolites of clofibric acid was accomplished in extracts of zebrafish embryos [163]. Besides common reactions including oxygenation, glucuronidation, sulfation and combinations thereof, a series of less frequently observed conjugative reactions was reported involving the enzymes acyl-CoA synthetase, N-acetyl transferase, carnitine acyl transferase, and catechol O-methyltransferase (COMT) [15].

Taken together, the findings from laboratory exposure studies provide strong evidence for fish having an inherent capability for metabolizing pharmaceuticals using enzymatic pathways very similar to those involved in the hepatic clearance of drugs in the human body. Nonetheless, the rate of metabolic conversion in fish may vary largely between substrates as suggested by the quantitative results from in vitro studies obtained with trout liver S9 fractions [164] and trout liver spheroids [165]. Comparison of intrinsic clearance values and depletion rate constants, respectively, for sets of environmentally relevant drugs demonstrated extensive biotransformation in some cases while under the assay conditions other drugs were resistant to metabolic conversion. In both these model systems the anticonvulsant carbamazepine, representing one of the most frequently monitored drugs in the aquatic environment, proved to be metabolically stable. Conversely, recent data published on the occurrence of CBZ and two of its human oxidative metabolites, 2-hydroxy-CBZ and CBZ-epoxide, in *Gambusia affinis* and *Jenynsia multidentata*, having been captured in a wastewater-impacted Argentinian river, suggested biotransformation in these species [166]. Subsequent exposure experiments with *J. multidentata* at laboratory scale provided further support for this hypothesis by identifying both metabolites in various organs.

Given the still fragmentary information on the metabolic pathways of CBZ in fish, we set out to conduct a comprehensive characterization of its biotransformation by analyzing bile from the flatfish Senegalese sole (*Solea senegalensis*) as a species of great economic importance in fisheries and aquaculture. In addition to the dosing experiments of this marine species with CBZ, bile was harvested and profiled for drug metabolites after administration of IBU. The findings obtained for the marine fish were contrasted with those reported for rainbow trout inhabiting freshwater environments [49, 167]. The work presented here was carried out as part of a broader study on the biological interactions of human drugs with hepatic enzymes in fish [168].

2. EXPERIMENTAL

2.1 Chemical Reagents

IBU (≥98 %), 2-hydroxy-IBU (99.2%), IBU acyl glucuronide (98%), CBZ (≥99 %), , IBU-d_3 (99.4%), and CBZ-d_{10} (99.2%) were purchased from Sigma-Aldrich (Madrid, Spain) and 2-hydroxy-CBZ (99.3 %), 3-hydroxy-CBZ (99.4 %) from Toronto Research Chemicals (Toronto, Canada). All organic solvents used in LC analysis were Chromasol LC grade or equivalent. Ultra-pure water and LC/MS grade formic acid were purchased from Sigma-Aldrich (Munich, Germany). LC-grade acetonitrile was purchased from Riedel de Häen (Steinheim, Germany). KCl (99%), dithiothreitol (99%), ethylenediaminetetraacetic acid (EDTA; 99.5%), 4-nitrophenyl acetate (99%), and phenatroline (Reagent grade) were purchased from Sigma-Aldrich (Madrid, Spain).

2.2 Lab scale experiments

Solea senegalesis were obtained and maintained as in Solé et al. 2015 [169]. Juveniles were acclimated in tanks for a period of two months at water temperatures of 15 ºC and 20ºC in order to assess the influence of temperature on the formation of the metabolites. After the adaption phase the fish received a single intraperitoneal injection of IBU at a dose of 10 mg/kg (n=12) or CBZ at 1 mg/kg (n=12). Control animals (n=12) were administered the carrier (sunflower oil at 1 µl/g b.w.). After injection the fish were fasted and sacrificed 48 hours later. Their organs dissected and liver and bile immediately frozen in liquid nitrogen and stored at -80ºC until analysis. Livers were also weighed to calculate gross morphometric indexes (Table S-

3). Handling and sacrifice of the fish was done according to national and institutional regulations of the Spanish Council for Scientific Research (CSIC) and Directive 2010/63/EU.

2.3 Bile sample analysis

Ten microliter aliquots of the bile samples were diluted with 150 µl of acetonitrile/0.1 N HCl (1:3) to ensure the solubility of the metabolites and to inhibit their pH-dependent degradation. The latter was important as at elevated pH acylglucuronides (expected for IBU) are susceptible to chemical hydrolysis and to acyl migration. The diluted samples were centrifuged and the supernatants analyzed by ultra-high performance liquid chromatography–high resolution mass spectrometry (UPLC-HRMS) for comprehensive drug metabolite profiling.

2.4 UPLC/ESI-MS/MS analysis

Chromatographic separation was performed on a Waters ACQUITY BEH C18 column (50 × 2.1 mm, 1.7 µm particle size) equipped with a guard column (5 × 2.1 mm) of the same packing material and connected to a Waters Acquity liquid chromatograph. The mobile phases for IBU in negative mode were (A) 20 mM of ammonium acetate and (B) acetonitrile. The chromatographic run in these neutral conditions (pH 6.8) was started at 95% A. After 0.5 min isocratic elution at 95 % A, the proportion of A was linearly decreased to 5 % within 15 min. The percentage of A was then maintained at 5 % for 2 min and the initial mobile phase composition was reestablished within 1.0 min followed by a 2.0 min equilibration step at 95 % A.

For acid conditions the mobile phase A was 0.1 % formic acid and the chromatographic run for CBZ in the positive ion mode started at 90%A. After 0.5 min isocratic elution at 90 % A, the proportion of A was linearly decreased to 10 % within 6.5 min. The percentage of A was then maintained at 10 % for 1.0 min and the initial mobile phase composition was reestablished within 1.0 min followed by a 2.0 min equilibration step at 90 % A. The flow rate was 300 µL/min and the injection volume was 10 µL. Exact mass measurements of IBU, CBZ and their metabolites were carried out in full-scan and product ion scan mode on a Q Exactive mass spectrometer (Thermo Fisher Scientific, San Jose, CA) equipped with a heated electrospray ion source (HESI). Negative and positive ion modes were used for the analysis of the IBU and CBZ samples, respectively. The source parameters were as follows: spray voltage: +/-3000 V; sheath gas flow: 40 L/h; auxiliary gas flow: 10 L/h; capillary temperature: 350 °C; heater temperature: 300 °C. The Orbitrap mass analyzer was operated at a resolving power of 70,000 (FWHM) in full-scan mode and of 17,500 (FWHM) in the MS^2 mode. External mass calibration for positive and negative ESI mode was conducted weekly for the mass range of m/z 50-2000 by infusing a Pierce LTQ Velos ESI Positive and Negative Ion calibration solution from Thermo Fisher Scientific. MS data acquisition and processing was done using the software package XCalibur 2.2. The differential analysis software Sieve 2.1 was used to aid in the detection of metabolites. The chromatographic alignment allows the determination of relatively intensive peaks formed through higher injections of drugs. Detected peaks were elucidated through MS/MS accurate measurements obtained in data dependent mode. This approach is helpful to overcome the lack of authentic standards to propose metabolite identities.

2.5 Hepatic biochemical determinations

Liver samples (≈1g) were homogenized in ice-cold buffer phosphate (100 mM, pH 7.4), containing 150 mM KCl, 1 mM dithiothreitol (DTT), 0.1 mM phenatroline, 0.1mg/mL trypsin inhibitor and 1 mM EDTA in a 1:4 (w/v) ratio ratio between sample weight/volume using a Polytron blender. The obtained homogenate was centrifuged at consecutive steps of 10,000 g x 30 min and 100,000 g x 60 min at 4ºC to obtain the microsomal pellet which was resuspended in the homogenization buffer containing 20% glycerol in a 2:1

(w/v) ratio. Microsomal protein content was determined by the Bradford's method [170] adapted to microplate format and using the Bradford Bio-Rad Protein Assay reagent and bovine serum albumin as the standard (0.05–0.5 mg/ml). The absorbance was read at 595 nm. All protein determinations were performed in triplicate.

Carboxylesterase activity was measured in microsomes using a kinetic mode in 96-well microplates [171]. Twenty-five microliters of appropriately diluted microsomes were incubated with 200 µl 4-nitrophenyl acetate as substrate (1 mM of 4-NPA final concentration) in phosphate buffer (50 mM, pH 7.4) for 5 min at 25ºC. Formation of 4-nitrophenol was read at 405 nm in a TECAN Infinite 200 microplate reader. Carboxylesterase activity was measured in triplicate and results were expressed as nmol/min/mg protein.

2.6 Statistics

Student's t-test was applied to detect differences between metabolites formed at the two temperatures and between enzyme activities at a given temperature with respect to the carrier control.

3. RESULTS AND DISCUSSION

3.1. Detection and identification of drug metabolites

In order to facilitate a thorough and automated search for drug-related metabolites in a complex matrix such as the bile samples, differential analysis Sieve 2.1 software was used. By comparing the aligned total ion chromatograms of the samples from vehicle-treated animals with those collected from fish treated with CBZ or IBU (Figures 1 and 2), the presence of compounds unique to the drug-exposed group was indicated. After the chromatographic alignment, the software provided a list of candidates with accurate mass, retention time and several ratios of differences between treated and control samples. Finally, the most intensive and relevant peaks were checked manually to obtain all the available information, including their MS/MS spectra. This comparative approach allowed us to filter the most relevant metabolites in this complex biological matrix. In the resulting list of potential drug metabolites each hit was characterized by exact mass, chromatographic retention time and peak intensity. Based on the knowledge about common phase I and phase II metabolic reactions and combinations thereof, appropriate filters for the minimum and maximum number of the atoms (H, C, N, O, and S) were defined and applied to the aforementioned drug metabolite list. This produced elemental formulae alongside the relative mass errors between the experimentally measured values and the ones calculated for the respective elemental composition. This procedure allowed to propose the type of enzymatic reactions involved in the biotransformation of CBZ and IBU. The subsequent examination of the product ion spectra of the metabolites provided further support for the proposed metabolites. The identification of characteristic fragment ions helped determine the site of metabolism in the case of positional isomers originating from regioselective conversions.

Figure 1: Extracted ion chromatograms (XIC) of CBZ metabolites detected by HR-MS analysis of diluted bile of *Solea senegalensis*.

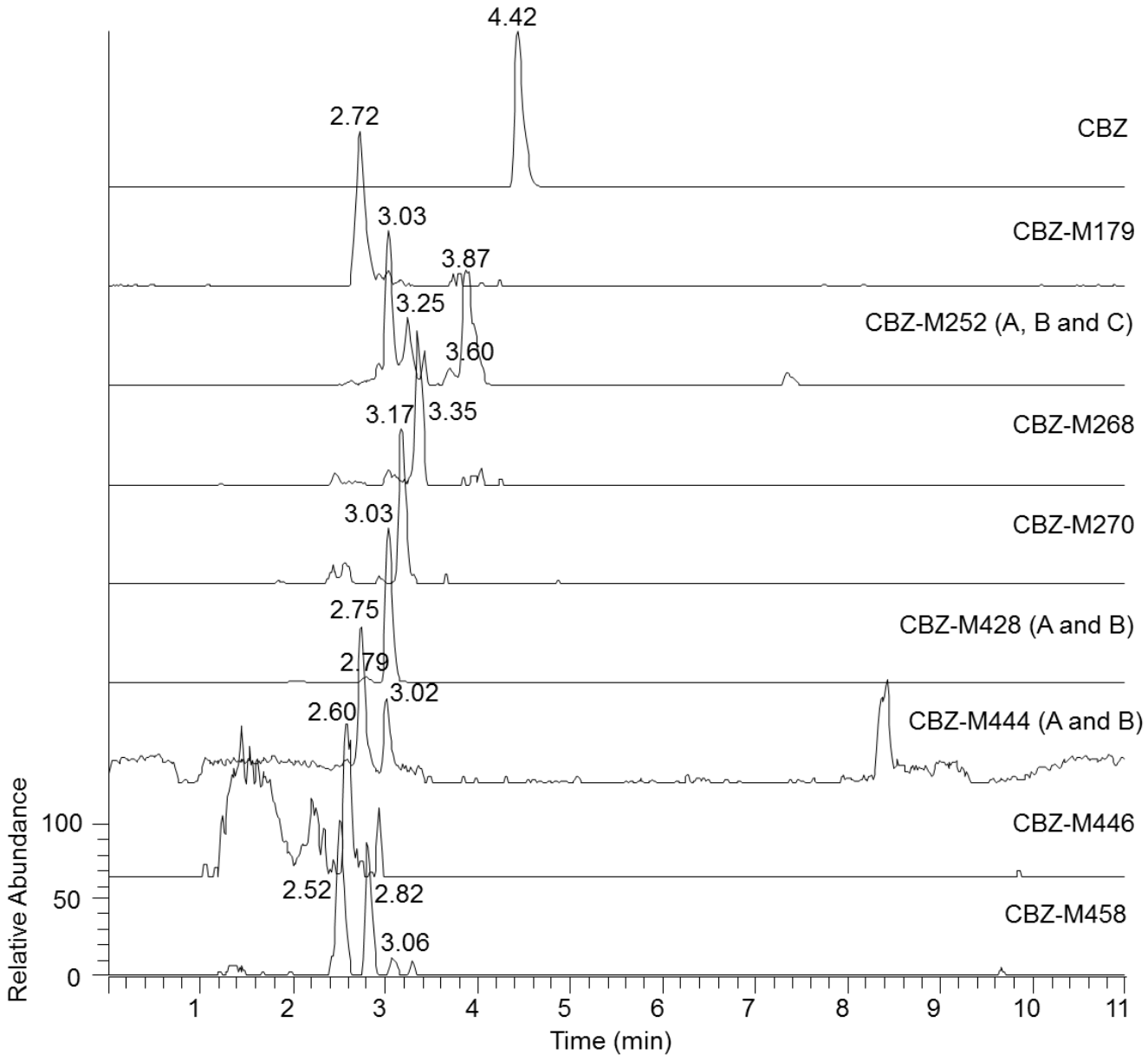

Figure 2. Extracted ion chromatograms (XIC) of detected IBU metabolites by direct analysis of treated bile sample.

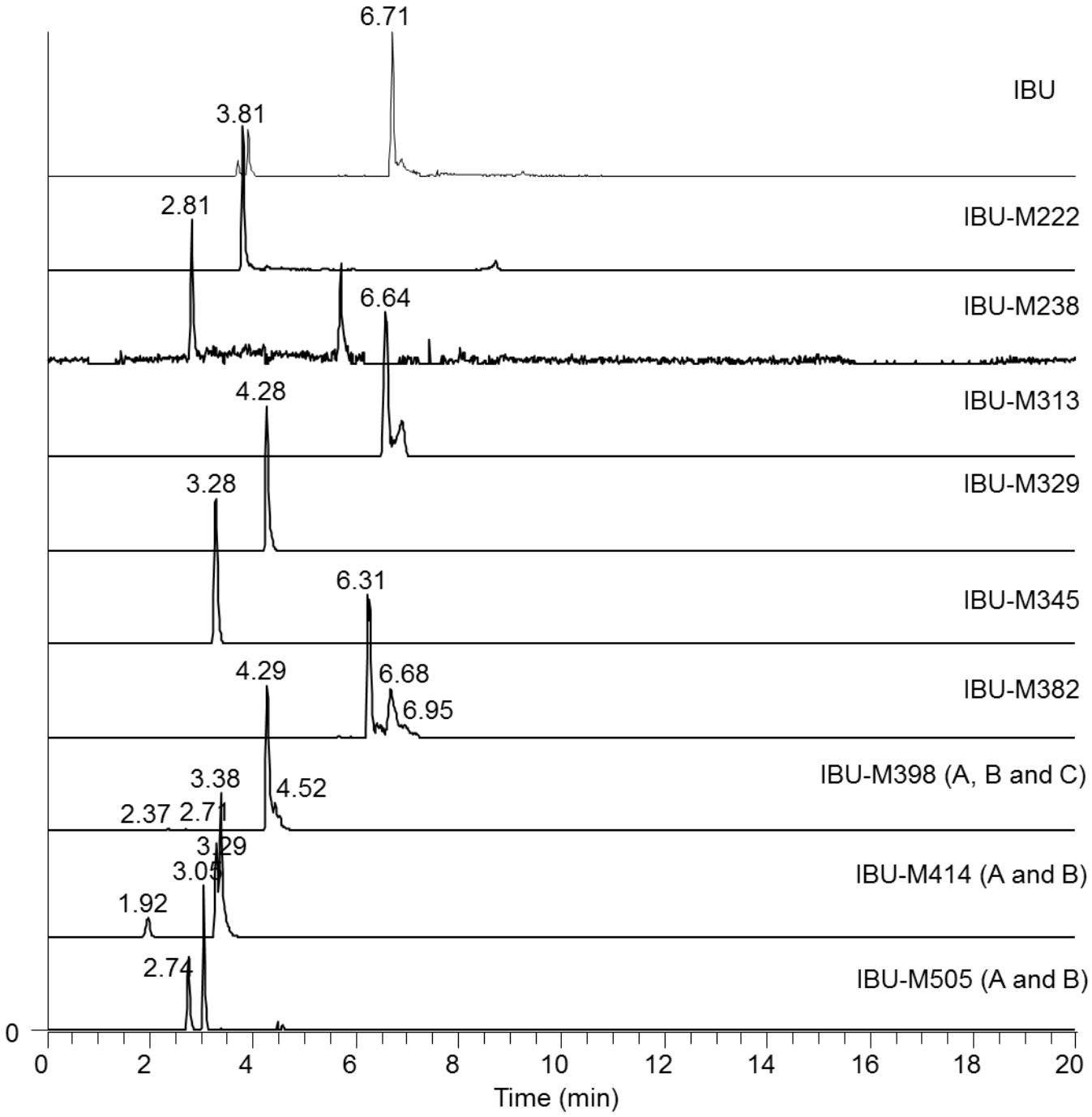

The proposed metabolites of CBZ and IBU are listed in Tables S-1 and S-2, respectively, in the order of increasing mass, and the postulated pathways leading to their formation are depicted in Figure 3 and 4. Since in this work only a few metabolites were available as authentic standards for ultimate confirmation of the metabolite identities, in most instances the exact positions of the hydroxyl groups – and any subsequent phase II reaction at those sites - could not be pinpointed. While this is a well-known limitation in the interpretation of ESI-MS/MS data in drug metabolism studies, it does not constitute an obstacle for elucidating the metabolic pathways and their respective enzymes. For the identification of the metabolites, the product ion spectra of the parent compounds CBZ and IBU, as well as those of their metabolites were recorded to determine plausible elemental compositions and structures of the fragment ions (Figure 5).

In case of CBZ (see Table S-1) three monooxygenated metabolites were detected (M252-A, M252-B, and M252-C) of which the first one was assigned as corresponding to the epoxidation of the double bond in the seven-membered central ring. That the other two metabolites were the product of aromatic hydroxylations occurring at adjacent positions in one of the phenyl rings is discussed further on (Figure 3). The structures of the two hydroxy metabolites were confirmed with authentic standards (Table S-1). Two further phase I metabolites were the doubly hydroxylated CBZ-M268 and the metabolite CBZ-M270 (Figure 3). Once oxidative reactions introduced suitable handles for ensuing conjugative reactions, hydroxylated metabolites yielded the corresponding glucuronides. By this route, CBZ-M428-A and its isomer CBZ-M428-B were formed whereas the two metabolites CBZ-M444-A and B were the products of glucuronidations of dihydroxylated metabolites (Table S-1). The identification of M-444 based on its mass spectrum is depicted in Figure 5C. The two metabolites with ion mass 445.1245 break easily in the ESI source to yield their precursor drug (m/z 269.0923). This neutral loss of 176 Da is diagonistic of glucuronides. Upon collision-induced dissociation of the protonated dihydroxylated CBZ molecule, fragment ions were detected at m/z 226 corresponding to the neutral loss of NH_3 and HNCO (43 Da) (Figure 5C). A third hydroxy-glucuronide (CBZ-M446) was proposed to arise from UGT-mediated conjugation of CBZ-M270 (Figure 3) which was in line with the order of elution from the LC column: M446 displayed weaker retention than the two M444 isomers just as M268 eluted before M270.

Besides the hydroxylations and epoxidation, belonging to the category of phase I reaction, and the subsequent conjugations with glucuronic acid as a phase II-type reaction (Figure 3), the elemental formula of the heaviest detected metabolite, M458, clearly indicated a gain of CH_2 with respect to M444. This methylation, likewise falling into the class of conjugations, was most likely the product of catechol-O-methyltransferase (COMT)-mediated conversion, thus requiring a substrate with two hydroxyl groups on adjacent carbon atoms within an aromatic ring, namely M268 (Figure 3). Unlike the various hydroxylation and glucuronidation reactions with their inherent introduction of polar groups and thus an overall increase in hydrophilicity, the generation of an O-methyl metabolite from a phenol generally produces a more lipophilic entity. Taking into account that the secretion of hepatic metabolites into bile occurs against a concentration gradient, suitable transporter proteins at the membrane separating the hepatocyte from the bile canaliculus are required. With specific transporters in place to recognize glucuronized species and thus to promote their secretion, the methylation was likely to precede the conjugation with glucuronic acid in M458. Consequently. it was produced from M268 with subsequent glucuronidation. In fact the importance of glucuronides in the elimination of CBZ from fish was reflected in the relative abundances of the oxidative vs. conjugated metabolites (Table 1): the biotransformation product with the highest relative abundance by far was M428-B, likely corresponding to the 3-hydroxy-glucuronide (Figure 3).

Table 1. Biological, hepatosomatic index [(liver weight/total weight)x100)] and microsomal activities of juvenile *Solea senegalensis* injected with vehicle (sun flower oil) and the drugs ibuprofen and carbamazepine Data are expressed as mean ± SEM (n=6).

Group	**Vehicle control**		**Carbamazepine-treated**	
Temperature (ºC)	15	20	15	20
N (male:female)	6 (1:5)	6 (4:2)	6 (2:4)	6 (5:1)
Length (cm)	25.3 ± 1.21	24.9 ± 1.24	26.2 ± 1.47	27.2 ± 1.72
Weight (g)	252.7 ± 36.1	254.8 ± 34.5	286.3 ± 37.2	264.8 ± 36.9
HSI	0.97 ± 0.08	0.81 ± 0.07	0.90 ± 0.08	0.62 ± 0.11
CbE (pNPA)	39.1 ± 1.4	17.1 ± 2.2	68.6 ± 7.8**	17.7 ± 2.1

t-test Contrasts were made between each treatment and its temperature control * denotes $p<0.05$

HSI as (liver weight/total weight) x 100

Figure 3. Proposed metabolic pathway of carbamazepine in *Solea senegalensis* based on the HR-MS analysis of bile. Annotations on arrows indicate enzyme likely involved in metabolic reaction: catechol-O-methyltransferase (COMT), cytochrome P450 (CYP), epoxide hydrolase (EH) uridine-diphospho-glucuronosyltransferase (UGT). Positions of glucuronide in M444-A and M444-B are inferred from chromatographic retention times (see Table S-1).

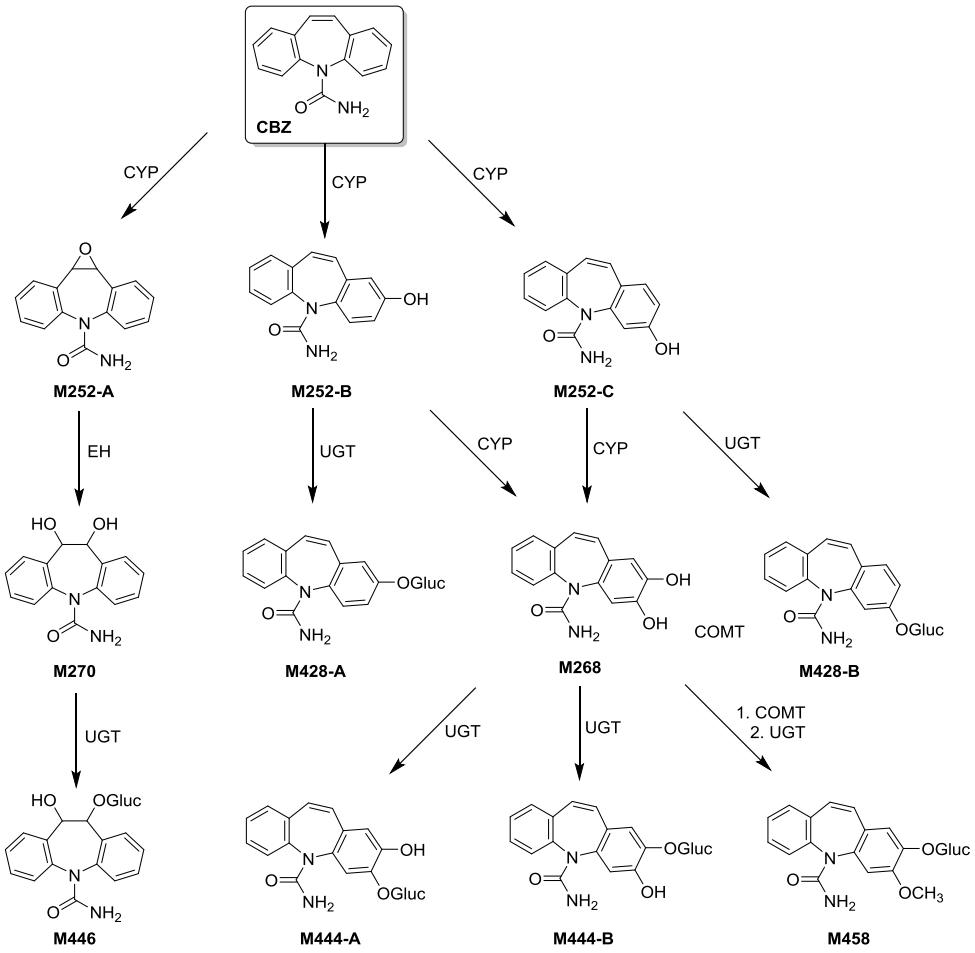

With respect of the functional groups in the chemical structure of IBU, the presence of a carboxyl group in this acidic compound made it directly amenable to phase II reactions, in particular to UGT-catalyzed glucuronidation (Figure 4). In addition, IBU features a series of chemically diverse C-H bonds (aromatic and benzylic; primary and secondary alkyl) rendering it attractive for CYP-mediated oxygenations. As compiled in Table S-2, one mono- and one dihydroxylated metabolite (M222 and M238) were detected. In contrast to CBZ where the glucuronidation of the (di)hydroxylated metabolites involved the formation of an ether bond, transfer of glucuronic acid to the carboxyl group IBU molecule produced the acylglucuronide (M382), i.e. an ester bond. The observation of a partially resolved peak cluster of M382 in the extracted ion chromatogram (m/z 381.1558) instead of a single peak with a defined retention time (see Table S-1) is typical of acylglucuronides because they are subject to acyl migration yielding positional isomers [172]. Taking advantage of this characteristic behaviour, the visual inspection of the peak profiles allowed to easily discriminate between the hydroxy-glucuronides bearing the glucuronic acid on the OH-group and the isobaric acylglucuronides. A second useful trait for telling apart O-glucuronides from acylglucuronides was the large difference in retention times: owing to the presence of two COOH groups the former were more polar, and thus exhibit faster elution as compared to the acylglucuronides in which the carboxy group is masked by the glucuronic acid (Figure 4). Applying these principles, two hydroxylated O-glucuronides (M398-A and M398-B) were proposed while M398-C corresponded to the hydroxyl acylglucuronides. Similarly, M414-A (1.92 min) is assigned to be the O-glucuronide of a dihydroxylated IBU whereas the isomeric acylglucuronides of dihydroxy IBU (M414-B) eluted at 3.29-3.38 min. Apart from substrate oxygenation and (subsequent) glucuronidation, a third category of metabolites could be unequivocally identified as originating from conjugation of the carboxyl group with taurine ($NH_2CH_2CH_2SO_3^-$). This comprised the series of M313 as the direct conjugate, its hydroxyl derivative M329, and its dihydroxylated form (M345) (Figure 4). Given the decrease in chromatographic retention times due to the presence of additional hydroxyl group in the metabolite structures, it appeared plausible to postulate that M329 (4.28 min) and M345 (3.28 min) were formed by taurine conjugation of M222 (3.81 min) and M238 (2.81 min), respectively. In the ESI-MS/MS spectrum of IBU-M345, the deprotonated taurine is detected at m/z 124.0062 (Figure 5D) Two further isomeric metabolites of minor intensity (M505-A and M505-B) were detected in the bile samples as a pair of unusual diconjugates bearing a taurine group at the carboxyl group as well as an O-glucuronide (Figure 4).

Figure 4. Proposed metabolic pathway of ibuprofen in *Solea senegalensis* based on the HR-MS analysis of bile. Annotations on arrows indicate enzyme likely involved in metabolic reaction: cytochrome P450 (CYP) and uridine-diphospho-glucuronosyltransferase (UGT).

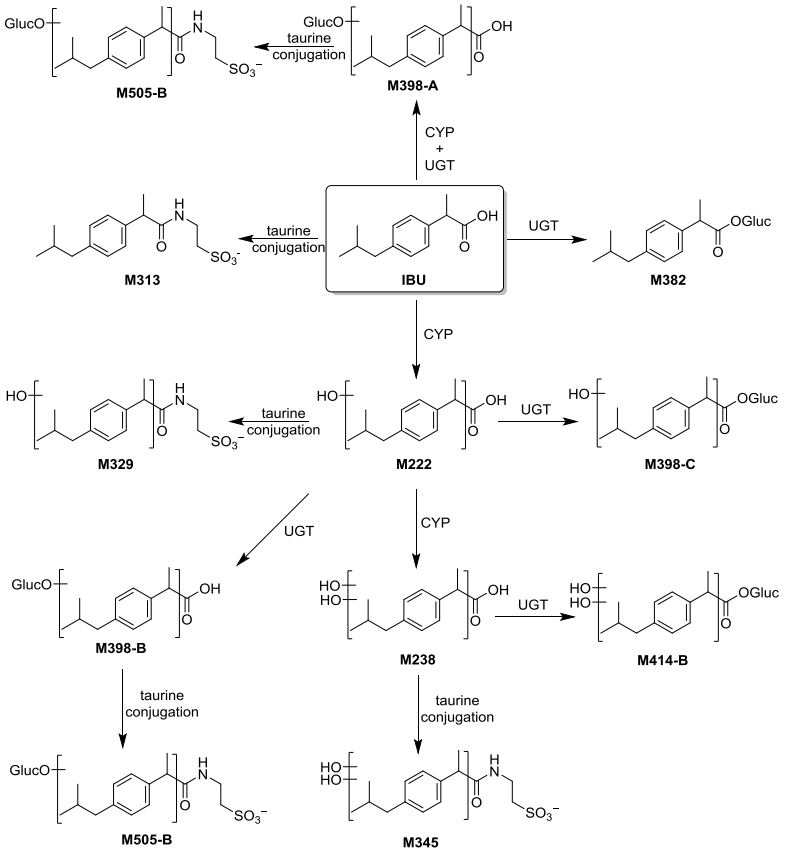

3.2. Qualitative analysis

Based on the qualitative analysis, eleven and 13 metabolites were detected for CBZ and IBU, respectively in bile samples from *Solea senegalensis*. The CBZ and IBU metabolites were identified as a combination of accurate mass measurements of the molecular ions and fragment ions detected in MS/MS experiments (Tables S-1 and S-2 as well as in Table S-4 and S5). Since authentic standards of most of the CBZ and IBU metabolites were not available, relative metabolite abundances were calculated as the ratio of the analyte MS peak area to the total peak areas of all metabolites and intact parent compound. Taking into account relative areas, the fraction of unmetabolized CBZ was much higher than that of IBU indicating limited capacity of hepatic enzymes in *S. senegalensis* to biotransform CBZ. This is in stark contrast to the hepatic disposition in humans where more than 95 % of the absorbed dose is transformed to a large number of metabolites [173]. Nonetheless, the overlap in metabolite identities of CBZ between human and the studied fish is surprisingly large. Although one of the principal metabolic reactions for CBZ and IBU was glucuronidation of the hydroxylated compound, IBU formed also taurine conjugates of hydroxylated IBU. In comparison to the findings in rainbow trout [49], previously not reported metabolites of IBU include an ether glucuronide and a taurine conjugate of the dihydroxylated substrate (M414-A and M345, respectively), as well as an acyl glucuronide of dihydroxy-IBU (M414-B).

The relative peak intensities of IBU, CBZ and their detected metabolites in fish bile were measured at two water temperatures. Although no pronounced differences were observed in the relative intensities of the metabolites (Tables S-1 and S-2), the effect of water temperature on hepatic enzyme activity is discussed in the next section.

Figure 5. ESI-MS/MS spectra of CBZ (A) and IBU (B) and their metabolites CBZ-M444 (C) and IBU-M345 (D).

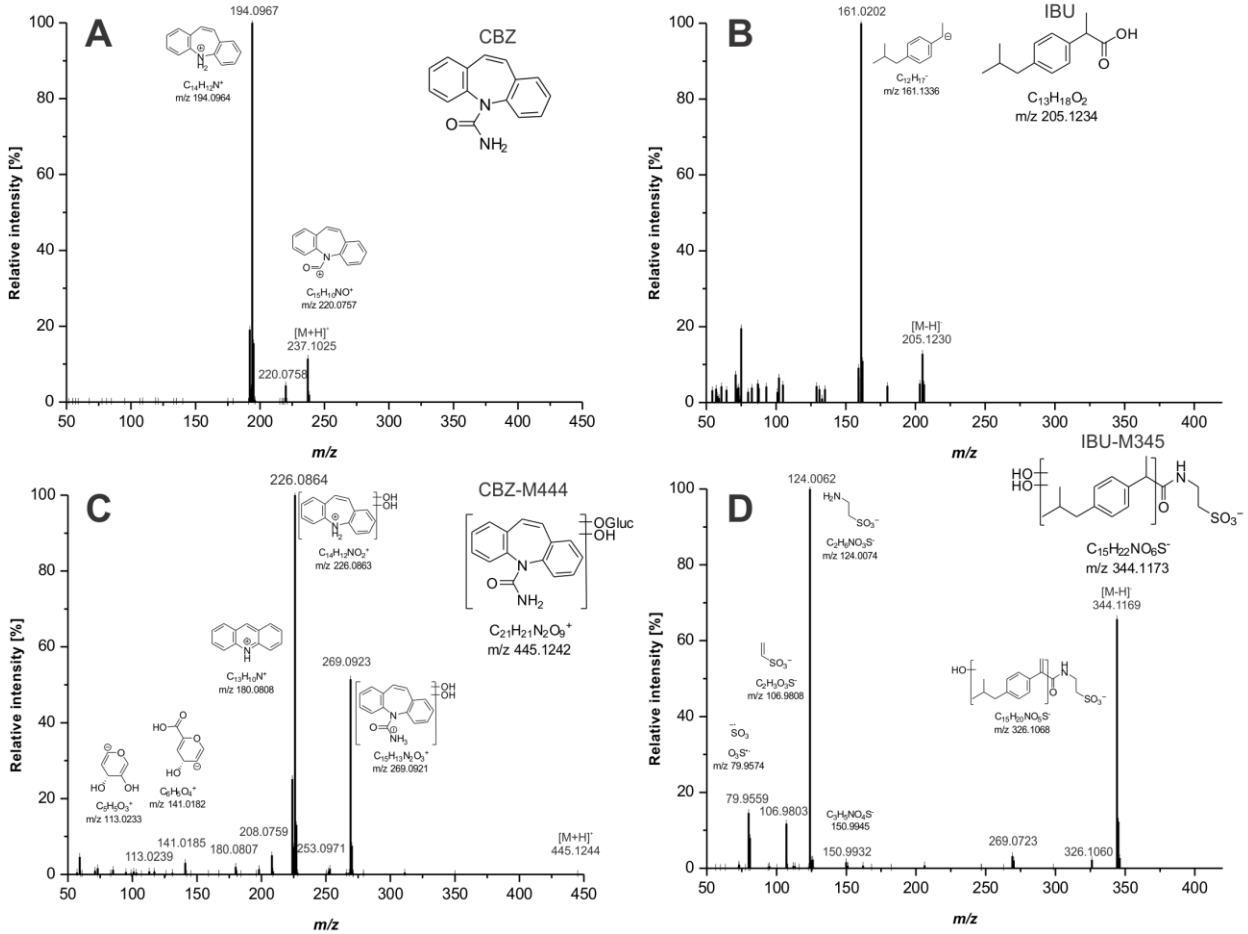

3.3. Biological effects on detoxification enzymes

There is proved evidence of metabolism of CBZ and IBU in fish at both temperatures by the action of phase I CYP and phase II UDPGT enzymes as revealed by the identity of the metabolites formed. The total amount of metabolites detected in bile after 48 h injection was not clearly seen as temperature dependent as only one metabolite of IBU and 3 of CBZ were significantly higher at 15ºC (Tables S-1 and S-2). By contrast, the enzymatic responses on CYP-dependent activities and CbEs were only traceable at 15ºC but not 20ºC (Table 1) [168]. An effect of rising temperature alone over these and other hepatic enzymes has been recently published for these same fish species with higher activities displayed at lower temperatures as a result of acclimation [174]. More recently, the combined effect of temperature and these same drug exposures on some of these enzymes and other metabolic and oxidative stress parameters has also been published [168]. In addition to former observations, both injections IBU ($p<0.05$) and CBZ ($p<0.01$) increased microsomal CbE activity. As an elevation of CYP3A4-mediated BFCOD activity also occurred with IBU ($p<0.05$) and CBZ (albeit not significant), while CYP1A-mediated EROD activity was not affected [168] it is plausible that induction of CYP3A4 and CbE may occur by the same mechanism such as via the nuclear receptor PXR as revealed in fish as well as in mammals [161] [175]. It could also be hypothesized that the lower response after IBU injection, despite the dose assayed was higher, could be due to the inhibition of CbEs by NSAID glucuronides formed as revealed in humans [176]. To the best of our knowledge this is the first report on CbE induction by these two pharmaceutical drugs in fish although an induction by other drugs such as gemfibrozil, nonylphenol and ethinylestradiol was formerly reported *in vivo* in the same fish species [177]. IBU and CBZ have also revealed to inhibit *in vitro* microsomal CbE activity in several marine species [174] and the lipid regulators simvastatin and fenofibrate interfere *in vitro* with microsomal CbE of either adults or juveniles of a related species *Solea solea* [174] [178]. Due to the importance of this enzyme family in drug and prodrug metabolism as well as its endogenous role in lipid homeostasis, we recommended its potential use as marker of drug exposures.

4. CONCLUSION

In the present study, we have identified thirteen metabolites of IBU and eleven metabolites of CBZ in fish bile. The structures of metabolites have been proposed using HRMS and HRMS/MS data. In particular, the combination of mass accuracy and the fragmentation patterns of metabolites and parent compounds allowed proposing plausible structures for each metabolite. The set of generated IBU metabolites was similar to those reported in a previous work on the metabolism of IBU in rainbow trout under similar experimental conditions [49].Three new IBU metabolites were identified formed as ether glucuronide and a taurine conjugate of the dihydroxylated substrate (M414-A and M345, respectively), as well as an acyl glucuronide of dihydroxy-IBU (M414-B). Regarding CBZ, the current work constitutes the first study on the identification of fish metabolites of CBZ (thirteen metabolites). We evaluated also the relative peak areas of CBZ, IBU and their metabolites in the fish exposed to two water temperatures. No quantitative/qualitative differences in metabolism of CBZ and IBU were observed at the two temperature regimes in terms of metabolite formation, however enzyme activities differed significantly at the two acclimation temperatures. This reveals that after 48 h drug injections, the hepatic response to the drugs was only traceable at the lowest temperature despite similar metabolism was achieved under both rearing conditions as revealed by biliary the metabolites formed. In sum, the findings of the present study enabled us to gain further insight into the metabolism of two pharmaceuticals (CBZ and IBU) in the marine fish and by extension to other pharmaceuticals detected in the aquatic environment.

ACKNOWLEDGEMENTS

This study has been financially supported by the EU through the FP7 project GLOBAQUA (Grant agreement No 603629), partly supported by the MEC [NET-SCARCE (CTM2015-69780-REDC) and by the Generalitat de Catalunya (Consolidated Research Group “2014 SGR 418—Water and Soil Quality Unit). This work is also integrated in the MINECO project CTM 2010-16611, DEPURAMAR.

REFERENCES

1. Zenker, A., et al., *Bioaccumulation and biomagnification potential of pharmaceuticals with a focus to the aquatic environment.* Journal of Environmental Management, 2014. **133**: p. 378-387.
2. Liu, J., et al., *Occurrence, bioaccumulation and risk assessment of lipophilic pharmaceutically active compounds in the downstream rivers of sewage treatment plants.* Science of The Total Environment, 2015. **511**: p. 54-62.
3. Tanoue, R., et al., *Uptake and Tissue Distribution of Pharmaceuticals and Personal Care Products in Wild Fish from Treated-Wastewater-Impacted Streams.* Environmental Science and Technology, 2015. **49**(19): p. 11649-11658.
4. Álvarez-Muñoz, D., et al., *Occurrence of pharmaceuticals and endocrine disrupting compounds in macroalgaes, bivalves, and fish from coastal areas in Europe.* Environmental Research, 2015. **143**: p. 56-64.
5. Wille, K., et al., *Development of analytical strategies using U-HPLC-MS/MS and LC-ToF-MS for the quantification of micropollutants in marine organisms.* Analytical and bioanalytical chemistry, 2011. **400**(5): p. 1459-1472.
6. Moreno-González, R., et al., *Do pharmaceuticals bioaccumulate in marine molluscs and fish from a coastal lagoon?* Environmental Research, 2016. **146**: p. 282-298.
7. Jeong-Wook Kwon, K.L.A., Doris E., Vidal-Dorsch, Steven M. Bay and Kang Xia1, , *Determination of 17α-ethynylestradiol, carbamazepine, diazepam, simvastatin, and oxybenzone in fish livers.* J AOAC Int. , 2009. **Jan-Feb;92**(1): p. 359-369.
8. McEneff, G., et al., *A year-long study of the spatial occurrence and relative distribution of pharmaceutical residues in sewage effluent, receiving marine waters and marine bivalves.* Science of the Total Environment, 2014. **476-477**: p. 317-326.
9. Martínez Bueno, M.J., et al., *Fast and easy extraction combined with high resolution-mass spectrometry for residue analysis of two anticonvulsants and their transformation products in marine mussels.* Journal of Chromatography A, 2013. **1305**: p. 27-34.
10. Pritchard, J.B. and J.R. Bend, *Relative roles of metabolism and renal excretory mechanisms in xenobiotic elimination by fish.* Environmental Health Perspectives, 1991. **90**: p. 85-92.
11. Corcoran, J., et al., *Effects of pharmaceuticals on the expression of genes involved in detoxification in a carp primary hepatocyte model.* Environmental Science and Technology, 2012. **46**(11): p. 6306-6314.
12. Fukami, T. and T. Yokoi, *The emerging role of human esterases.* Drug Metabolism and Pharmacokinetics, 2012. **27**(5): p. 466-477.
13. Brozinski, J.-M., et al., *Detection of naproxen and its metabolites in fish bile following intraperitoneal and aqueous exposure.* Environmental Science and Pollution Research, 2011. **18**(5): p. 811-818.
14. Kallio, J.-M., et al., *Metabolites of the Aquatic Pollutant Diclofenac in Fish Bile.* Environmental Science & Technology, 2010. **44**(19): p. 7213-7219.

15. Brozinski, J.-M., et al., *Identification and dose dependency of ibuprofen biliary metabolites in rainbow trout.* Chemosphere, 2013. **93**(9): p. 1789-1795.
16. Jones, H.S., et al., *Metabolism of ibuprofen in zebrafish larvae.* Xenobiotica, 2012. **42**(11): p. 1069-1075.
17. Brox, S., et al., *Metabolism of clofibric acid in zebrafish embryos (Danio rerio) as determined by liquid chromatography-high resolution-mass spectrometry.* Comparative Biochemistry and Physiology Part - C: Toxicology and Pharmacology, 2016. **185-186**: p. 20-28.
18. Connors, K.A., et al., *Comparative pharmaceutical metabolism by rainbow trout (Oncorhynchus mykiss) liver S9 fractions.* Environmental Toxicology and Chemistry, 2013. **32**(8): p. 1810-1818.
19. Baron, M.G., et al., *Pharmaceutical metabolism in fish: Using a 3-D Hepatic in Vitro model to assess clearance.* PLoS ONE, 2017. **12**(1).
20. Valdés, M.E., et al., *Bioaccumulation and bioconcentration of carbamazepine and other pharmaceuticals in fish under field and controlled laboratory experiments. Evidences of carbamazepine metabolization by fish.* Science of The Total Environment, 2016. **557-558**: p. 58-67.
21. Lahti, M., et al., *Uptake from water, biotransformation, and biliary excretion of pharmaceuticals by rainbow trout.* Environmental Toxicology and Chemistry, 2011. **30**(6): p. 1403-1411.
22. González-Mira, A., et al., *Drugs of environmental concern modify Solea senegalensis physiology and biochemistry in a temperature-dependent manner.* Environmental Science and Pollution Research, 2016. **23**(20): p. 20937-20951.
23. Solé, M., et al., *Xenobiotic metabolism modulation after long-term temperature acclimation in juveniles of Solea senegalensis.* Marine Biology, 2015. **162**(2): p. 401-412.
24. Bradford, M.M., *A rapid and sensitive method for the quantitation of microgram quantities of protein utilizing the principle of protein-dye binding.* Analytical Biochemistry, 1976. **72**(1-2): p. 248-254.
25. Hosokawa, M., Satoh, T., , *Measurement of carboxylesterase (CES) activities.* Curr Protoc Toxicol . 2002. **Chapter 4, Unit 47**.
26. Lassila, T., et al., *Toxicity of Carboxylic Acid-Containing Drugs: The Role of Acyl Migration and CoA Conjugation Investigated.* Chemical Research in Toxicology, 2015. **28**(12): p. 2292-2303.
27. Kim, K.A., et al., *Effect of probenecid on the pharmacokinetics of carbamazepine in healthy subjects.* European Journal of Clinical Pharmacology, 2005. **61**(4): p. 275-280.
28. Solé, M. and J.C. Sanchez-Hernandez, *An in vitro screening with emerging contaminants reveals inhibition of carboxylesterase activity in aquatic organisms.* Aquatic Toxicology, 2015. **169**: p. 215-222.
29. Xu, C., X. Wang, and J.L. Staudinger, *Regulation of tissue-specific carboxylesterase expression by pregnane X receptor and constitutive androstane receptor.* Drug Metabolism and Disposition, 2009. **37**(7): p. 1539-1547.
30. Inoue, N.R., et al., *Reversible inhibition of human carboxylesterases by acyl glucuronides.* Drug Metabolism and Disposition, 2013. **41**(4): p. 698-703.

31. Solé, M., A. Fortuny, and E. Mañanós, *Effects of selected xenobiotics on hepatic and plasmatic biomarkers in juveniles of Solea senegalensis.* Environmental Research, 2014. **135**: p. 227-235.
32. Crespo, M. and M. SolÃ©, *The use of juvenile Solea solea as sentinel in the marine platform of the Ebre Delta: in vitro interaction of emerging contaminants with the liver detoxification system.* Environmental Science and Pollution Research, 2016. **23**(19): p. 19229-19236.

Article nº 6: Ibuprofen exposure in Lemna gibba L.: evaluation of growth and phytotoxic indicators, detection of ibuprofen and identification of its metabolites in plant and in the medium

F. Pietrini, D. Di Baccio, **J. Aceña**, S. Perez, D. Barceló and M. Zacchini

Journal of Hazardous Materials - 2015

Journal of Hazardous Materials 300 (2015) 189–193

Contents lists available at ScienceDirect

Journal of Hazardous Materials

journal homepage: www.elsevier.com/locate/jhazmat

Ibuprofen exposure in *Lemna gibba* L.: Evaluation of growth and phytotoxic indicators, detection of ibuprofen and identification of its metabolites in plant and in the medium

F. Pietrini [a], D. Di Baccio [a], J. Aceña [b], S. Pérez [b], D. Barceló [b], M. Zacchini [a,*]

[a] Institute of Agro-environmental and Forest Biology, National Research Council of Italy, Via Salaria Km 29,300, 00015 Monterotondo Scalo, Roma, Italy
[b] Water and Soil Research Group, Department of Environmental Chemistry, IDAEA-CSIC, c/ Jordi Girona, 18-26, 08034 Barcelona, Spain

HIGHLIGHTS

- Assessment of high ibuprofen level on *Lemna gibba* L. growth and phytotoxic indicators.
- First detection of ibuprofen and its metabolites in plant was performed.
- Identification of ibuprofen metabolites suggested activation of detoxification pathways.
- Several ibuprofen metabolites in the plant growth medium were also detected.

ARTICLE INFO

Article history:
Received 11 May 2015
Received in revised form 25 June 2015
Accepted 30 June 2015
Available online 2 July 2015

Keywords:
Aquatic plants
Duckweed
Pharmaceuticals
Micro-contaminants
Water quality
Wastewater

ABSTRACT

Ibuprofen (IBU) is detected worldwide in water bodies due to the incomplete removal by wastewater treatments. Contrasting results have been reported on the toxicity of IBU on aquatic biomonitor plants such as duckweed, and no data about IBU detection and metabolism in plants has been reported. In this work, the effects of 1 mg L^{-1} IBU on *Lemna gibba* L. were monitored in an 8-day laboratory test. In particular, an increase in frond number (+12%) and multiplication rate (+10%) while no variations in photosynthetic pigment content were observed. Moreover, UPLC-HRMS analysis of the presence of IBU and its metabolites in plants and in the growth medium was performed. The results showed that, besides IBU, 11 IBU metabolites were detected in plants. Among the IBU metabolites, hydroxyl- and dihydroxyl-IBU were found, whereas carboxyl-IBU was undetectable. Interestingly, some IBU metabolites were detected in the plant growth solution at the end of the IBU treatment, while no IBU products were found in the IBU solution without plants, suggesting a role for *L. gibba* in IBU metabolism. The findings of this work represent an important step for a better evaluation of the effects of IBU and its metabolites in duckweed, with notable implications for the eco-toxicological assessment of IBU in the aquatic ecosystem.

1. Introduction

Pharmaceuticals and personal care products (PPCPs) are becoming an emerging problem because of their widespread occurrence in both fresh and reclaimed waters [1,2]. These organic pollutants are present at trace concentrations in surface waters, gaining the classification of micro-contaminants [3]. Nevertheless, little information is available in the literature about the toxicological effects of these compounds, the effective concentrations and persistence in the environment, and the toxicity of their possible metabolites [1,4].

Among these micro-contaminants, ibuprofen (IBU) is a non-steroidal anti-inflammatory drug (NSAID) of great concern for aquatic environments because of its high consumption worldwide and potential ecological impact [1,5]. It is one of the most frequently detected pharmaceuticals in freshwater, and as such it has been proposed as a marker of wastewater contamination [6]. Despite the high removal capability by wastewater treatment technologies [7], IBU and its major human metabolites (carboxyl-IBU and both hydroxyl-IBU isomers) are commonly detected in water bodies [1], representing a potential environmental hazard. In fact, it has been pointed out that chronic exposure to IBU may represent a non-negligible risk for aquatic organisms [8,9]. In this regard,

* Corresponding author. Fax: +39 069 067 2990.
E-mail address: massimo.zacchini@ibaf.cnr.it (M. Zacchini).

http://dx.doi.org/10.1016/j.jhazmat.2015.06.068
0304-3894/

very little is known about the effects of IBU, and other pharmaceuticals, on photosynthetic aquatic organisms such as duckweed (*Lemna* spp.). *Lemnaceae* are free-floating tiny macrophytes, whose species commonly grow naturally in wetlands, including some highly contaminated water bodies [10]. For this reason, *Lemna* spp. are commonly utilised in water quality biomonitoring studies [11,12], and are also used in standardised tests for environmental risk assessment [13], and have been proposed as a biological tool for wastewater reclamation [14,15]. Pomati et al. [16] showed that duckweed is more sensitive to IBU than other organisms, including bacteria and vertebrates. On the other hand, Brain et al. [17] did not observe phytotoxic effects in *Lemna gibba* plants exposed to similar concentrations to those used by Pomati et al. [16]. Moreover, in some cases, depending on the IBU concentration and the duration of exposure, a growth stimulation of *Lemna* was observed [16], and has also been reported for non-aquatic plant species [18]. In this regard, the enhancement of antioxidant enzyme activities [18–20] was reported in riparian plant species (*i.e. Typha*, *Populus*, and *Salix* spp.) exposed to IBU. Nevertheless, to date, no information has been reported in the literature about the fate of IBU within plant tissues, and the toxicity potential of its transformation products on plant metabolism.

This work was aimed at evaluating the effects of IBU on the growth and phytotoxic indicators in *Lemna gibba* L., which is a model plant species of the aquatic environment, and at studying the fate of IBU both in the plant tissues and in the growth medium. The IBU concentration (1 mg L^{-1}) was chosen as it is currently reported as a threshold dose to evaluate tolerance/sensitive responses in duckweed [16,17].

2. Experimental

2.1. Plant material, pre-culture conditions and experimental design

Duckweed (*Lemna gibba* L.) fronds were collected from a company producing aquatic cultivation systems (Anubias, Villanova (BO), Italy) and cultivated for one month in a growth chamber under the following controlled conditions: temperature 25 ± 3 °C, photosynthetic photon flux density (PPFD) 60–80 μmol m^{-2} s^{-1}, and a photoperiod of 14-h light/10-h dark. Prior to culture, *L. gibba* fronds were gently rinsed with a 0.25% bleach solution for five minutes and thoroughly washed with distilled and sterilized water and massed. The plants were grown and maintained in plastic vessels in sterilized half-strength Murashige and Skoog (MS) medium without vitamins (Duchefa, Burgh-Haamstede, The Netherlands) at pH 6.0 ± 0.3 until the beginning of the experiment. Sub-samples of *L. gibba* fronds were periodically transferred to fresh-sterilized medium to keep contamination by other organisms to a minimum, as indicated in the OECD 221 guideline [21]; at each transfer only uncontaminated fronds were used for further cultivation.

The experiment was run in transparent covered six-well plates (well volume of 15.53 mL, well surface area of 8.96 cm^2; TPP, Switzerland) in a growth chamber (PPFD 120–140 μmol m^{-2} s^{-1}, photoperiod 14-h light/10-h dark at 25/20 ± 3 °C day/night) for 8 days. For each plate, 4–5 colonies consisting of 2 to 4 visible fronds of *L. gibba* per well were placed (*i.e.* 79.4 ± 6 fronds per plate) and cultivated in half-strength MS (MS/2, 7.5 mL per well) without (control treatment) or with the addition of 1 mg L^{-1} IBU (IBU treatment). The experimental set-up consisted of 26 six-well plates. Each treatment was represented by 10 plates, and two additional plates with plants in half-strength MS were used to determine the initial *L. gibba* biomass immediately before the beginning of the IBU treatment (day 0). Moreover, two plates without plants for each treatment were used as negative and positive IBU blanks. The assay (8 days) was conducted by testing without renewal (static) of the test solutions [21], and the plates remained covered to minimise evaporation and accidental contamination. After 2, 6, and 8 days of treatment the number and area of the fronds were assessed. All chemicals were purchased from Sigma-Aldrich (Milan, Italy) unless otherwise stated.

2.2. Growth analysis and photosynthetic pigment contents

The number of duckweed plants (fronds) and area was determined for each single well for all of the treatments and replicates using imaging analysis software (ImageJ, IJ 1.46r, http://imagej.nih.gov/ij/). At the beginning (day 0, t_0), after 3 days of IBU treatment and at the end of the experiment (day 8, t_8) the plants were surface-dried between layers of paper towels and the fresh weight (FW) was immediately determined. Then, this plant material was oven dried at 60 °C to a constant weight for dry weight (DW) determination. For each well the frond area was correlated to the corresponding fresh and dry weights using linear regressions (r^2 values >0.96). These correlations were used to estimate the fresh and dry weight of plants without destructive sampling during all the experiment. The relative growth rate (RGR) of biomass production was calculated from the following equation with the measured parameter DW (x) at the start (t_0) and at the end (t_8) of the test: $RGR = (\ln xt_8 - \ln xt_0)/t_8 - t_0$.

The frond number (FN), the doubling time (T_d) of the frond number, and the average specific growth rate for the 8 days of the testing period (μ_{t0-8}) were determined according to the ISO 20,079 test protocol [22]. The multiplication rate (MR) was expressed as follows: $MR = 1000\ (\ln FNt_n - \ln FNt_m)/t_n - t_m$, where FNt_n is the number of fronds at day n (8) and FNt_m the number of fronds at day m (0) [23].

The chlorophyll and carotenoid contents were measured according to the method described by Wellburn [24]. Briefly, 50 mg of the fresh samples were homogenized with 80% (w/v) cold acetone, centrifuged at 5000 × g for 10 min at 4 °C, and the absorbance of the supernatant was read at 663, 646, and 470 nm.

2.3. Ibuprofen analysis and identification of its plant metabolites

Control and IBU-treated plants were extracted following the methodology of Wu et al. [25]. Briefly, the control and IBU-treated plants were freeze-dried and extracted three times by sonication with 8 mL of MeOH, and then the samples were centrifuged for 20 min at 4500 rpm. The supernatants were collected and concentrated to a volume of 1 mL by evaporation. A volume of 200 mL of water was added to each sample and then they were extracted by SPE using HLB cartridges. The extracts were evaporated and reconstituted prior to UPLC-HRMS analysis. The extracts and the nutrient solutions were injected directly onto a Waters ACQUITY BEH C18 column (100 × 2.1 mm, 1.7 μm particle size) equipped with a guard column (5 × 2.1 mm) of the same packing material. The mobile phases were (A) water and (B) acetonitrile, both with 20 mM NH_4OAc. After 0.5 min isocratic elution at 90% A, the proportion of A was linearly decreased to 10% within 6.5 min. The percentage of A was then maintained at 10% and held for 1.0 min. The initial mobile phase composition was re-established within 1.0 min followed by a 2.0 min equilibration step at 90% A. The flow rate was 300 μL/min and the injection volume was 10 μL. The exact mass measurements of IBU and its metabolites formed were carried out in full-scan and product ion scan modes on a Q Exactive mass spectrometer (Thermo Fisher Scientific, San Jose, CA, USA). All MS experiments were performed in the negative ion mode using heated electrospray ionization (HESI). All MS data acquisition and processing was done using the software package Xcalibur 2.2.

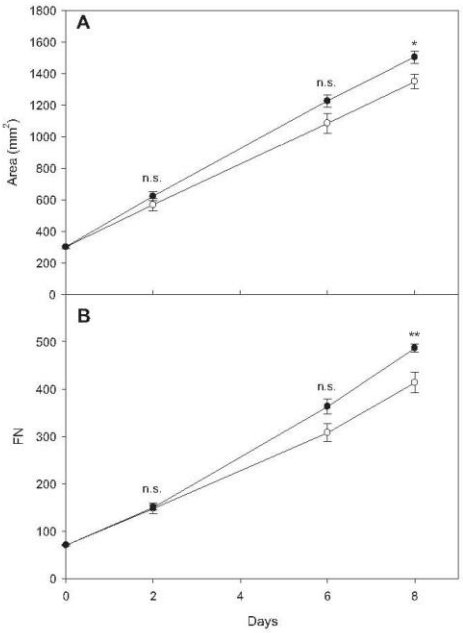

Fig. 1. Total frond area (A) and number (B) of *Lemna gibba* L. treated for 2, 6 and 8 days at 0 (Control, open circles) and 1 mg L^{-1} IBU (closed circles) solution. Data are the mean values of ten ($n = 10$) replicates ± SE. For each time point, asterisks represent significantly different data (*t*-test, $P \leq 0.05$); n.s. = not significant, *≤0.05, **≤0.01.

2.4. Statistical analysis

The data reported in the tables and figures refer to 10 replicates (six-well plates) for each treatment ($n = 10$). Normally distributed data were processed by one-way ANOVA in order to evaluate the effects of the control and IBU treatments using the SPSS (Chicago, IL, USA) software tool. The statistical significance of the mean data was assessed by *t*-test ($P \leq 0.05$).

3. Results and discussion

The total frond area and number were monitored after 2, 6, and 8 days of *L. gibba* exposure to IBU (Fig. 1). In comparison with the control samples, a significant increase of these two parameters was observed in IBU-treated plants only after 8 days of treatment. Growth and phytotoxic indicators (T_d, μ_{t0-8}, chlorophyll, and carotenoid content) were assessed after 8 days of IBU exposure (Table 1).

Except for the RGR, the T_d, and the pigment contents, all of the measured parameters exhibited significantly higher values in IBU-treated plants compared to the control plants. Particularly, the enhancement of frond number and area, in addition to biomass production, highlighted a growth stimulation effect exerted by 1 mg L^{-1} IBU. In the literature, contrasting results are reported on the plant response to IBU exposure. Pomati et al. [16] found a 25% inhibition of growth in *Lemna minor* L. cultures exposed to 1 mg L^{-1} IBU, even if in different experimental conditions, while Brain et al. [17] showed no decrease in the wet mass of *L. gibba* treated with

Table 1
Growth parameters and pigment contents of *Lemna gibba* L. treated with 0 (Control) and 1 mg L^{-1} IBU solution for 8 days. Data are the mean values of ten ($n = 10$) replicates ± SE. A *t*-test ($P \leq 0.05$) between control and IBU treatment was applied. Data followed by different letters in the same row are significantly different with the *P*-value indicated.

Parameter	Control	IBU	*P*
FW (mg)	301.0 ± 10.2b	335.7 ± 8.4a	0.016
DW (mg)	192.2 ± 6.6b	217.5 ± 5.4a	0.017
RGR (d^{-1})	0.68 ± 0.01	0.71 ± 0.003	0.071
MR	204.6 ± 6.8b	225.5 ± 2.2a	0.009
T_d	3.20 ± 0.10a	2.89 ± 0.03b	0.011
μ_{t0-8}	0.21 ± 0.007b	0.24 ± 0.002a	0.009
Chl *a* (μg g DW^{-1})	745.6 ± 54.1	808.9 ± 73.9	0.515
Chl *b* (μg g DW^{-1})	230.1 ± 22.7	254.2 ± 21.9	0.473
Chl *a*/Chl *b*	3.27 ± 0.12	3.18 ± 0.09	0.560
Carotenoids (μg g DW^{-1})	203.3 ± 11.1	221.6 ± 15.9	0.382

MR – Multiplication rate
Td – Doubling time of frond number
μ_{t0-8} – Average specific growth rate

the same IBU concentration for 7 days. In our experiment, 1 mg L^{-1} IBU stimulated the general multiplication capacity of *L. gibba* (MR: +10%), resulting in the increase of FN (+12%) and the average specific growth rate (μ_{t0-8}, +14%) after 8 days of IBU exposure. At the same time, the RGR remained unaltered and the doubling time of the frond number (T_d) decreased. These results indicate that IBU does not affect the rate at which the plants grow. Although the pharmaceutical reduced the time that it took for one plant multiplication to occur, the number of plants which multiply in the same time is higher, resulting in a general enhancement of the total fronds. According to Brain et al. [17], the unaltered chlorophyll and carotenoid contents (Table 1), as a consequence of IBU treatment, were consistent with the lack of inhibition effect caused by IBU to *L. gibba* in our bioassay conditions. Then, it can be stated that different growth and testing conditions, together with the use of *L. minor* or *L. gibba* (although both of these are indifferently recognised as test organisms [21]), are responsible for the observed variability in the plant response to IBU.

Few studies have been reported in the literature about the effects of IBU on non aquatic plants. In accordance with the results of Table 1, Kotyza et al. [26] and Iori et al. [18] found a growth stimulation in plant cell cultures (*Armoracia rusticana* L. and *Populus nigra* L., respectively), even when treated with a far higher IBU concentration than that used in the present experiment. On the contrary, a sensitive response to a high IBU concentration was reported in *Linus usitatissimum* L. cell culture by Kotyza et al. [26]. Different effects of IBU on the growth of *Salix alba* L. hydroponic cultures were shown by Iori et al. [20], depending on the IBU concentration, plant organ, and clone. A reduction of the RGR in *Typha* spp. exposed for 1 week at 1 mg L^{-1} IBU under hydroponics was also observed by Dordio et al. [19].

The qualitative assessment of the presence of IBU and its transformation products in *L. gibba* plants (Table 2) showed that, at the end of the experiment, IBU and 11 metabolic products were detected in *Lemna* plant extracts. Among these metabolic products, the presence of hydroxyl-IBU is consistent with results previously reported for the biological degradation of IBU in sludge [27]. Interestingly, carboxyl-IBU was not detected in *Lemna* plants, suggesting a different metabolic pathway with respect to humans and microbia, where this degradation product was found [28,29]. On the other hand, the lack of carboxyl-IBU and the presence of dihydroxyl-IBU allows for the hypothesis that, in these experimental conditions, the IBU metabolic pathway in *L. gibba* plants is more similar to that of fungi [30] than to the metabolism of other living organisms [29]. With regard to the other metabolic compounds, the detection of hydroxyl-IBU glucuronide suggests a possible activation

Table 2
Qualitative pattern of UPLC-HRMS identified metabolites in control and ibuprofen (IBU) treated *Lemna gibba* L. plants and relative growth solutions at the end of the experiment (8 days). D, detected; ND, not detected.

IBU metabolites' characterization					Bioassay			
Name	Formula (M-H)⁻	RT (min)	Accurate mass (M-H)⁻	Mass fragmentation	IBU treated plants	Control plants	IBU treated plant solution	Control plant solution
IBU	$C_{13}H_{17}O_2^-$	4.23	205.1234	*m/z* 159.1179	D	ND	D	ND
Hydroxyl-IBU	$C_{13}H_{17}O_3^-$	2.57	221.1183	*m/z* 73.0295, 177.1285	D	ND	D	ND
Dihydroxyl-IBU	$C_{13}H_{17}O_4^-$	2.65	237.1132	*m/z* 135.0815, 193.1234	D	ND	D	ND
Acetyl IBU	$C_{15}H_{19}O_3^-$	4.23	247.1340	*m/z* 59.0139, 201.1285, 219.139	D	ND	ND	ND
IBU hexoside	$C_{19}H_{27}O_7^-$	4.84	367.1762	*m/z* 101.0244, 113.0244, 159.1179, 219.139	D	ND	D	ND
Hydroxyl-IBU glucuronide	$C_{19}H_{25}O_8^-$	2.37	397.1504	*m/z* 73.0295, 191.1078, 233.1183, 249.1132	D	ND	ND	ND
IBU acetyl hexoside	$C_{21}H_{29}O_8^-$	4.23	409.1868	*m/z* 101.0244, 159.1179, 219.139, 247.1340	D	ND	D	ND
Hydroxyl-IBU acetyl hexoside	$C_{21}H_{29}O_9^-$	3.00	425.1817	*m/z* 101.0244, 113.0244, 133.0659, 177.1285, 235.1340	D	ND	D	ND
IBU malonyl hexoside	$C_{22}H_{29}O_{10}^-$	4.22	453.1766	*m/z* 101.0244, 219.1390, 247.1340	D	ND	D	ND
IBU deoxyhexosyl hexoside	$C_{25}H_{37}O_{11}^-$	4.51	513.2341	*m/z* 103.0401, 115.0401, 131.035, 159.1179, 219.1390	D	ND	ND	ND
IBU hexosyl hexoside	$C_{25}H_{37}O_{12}^-$	4.18	529.2291	*m/z* 101.0244, 113.0244, 159.1179, 205.1234	D	ND	D	ND
IBU acetyl desoxyhexosyl hexoside	$C_{27}H_{39}O_{12}^{2-}$	3.98	555.2452	*m/z* 103.0401, 115.0401, 131.035, 159.1179, 219.139	D	ND	ND	ND

The UPLC-HRMS analysis was also carried out on the initial 1 mg L^{-1} IBU stock solution and the positive IBU blank solution without plants, where only IBU was detected, and on the initial nutrient solution (MS/2 without vitamins) and the negative IBU blank solution without plants, where none of the identified compounds (included IBU) was detected.

of detoxification processes, as well as the presence of hexoside compounds which are commonly found in plants as a result of a conjugation step with xenobiotics [31]. It is worth underlining that, after 8 days of IBU treatment, some IBU metabolic products, namely hydroxyl-IBU, dihydroxyl-IBU, IBU hexoside, IBU acetyl hexoside, hydroxyl-IBU acetyl hexoside, IBU malonyl hexoside, and IBU hexosyl hexoside, were detected in the growth solution of treated plants (Table 2). As these compounds were not found in the positive IBU blank (growth solution supplied with IBU but without plants), it can be excluded that these metabolites were produced by physico-chemical degradation processes. Therefore, it can be hypothesised that *L. gibba* plants growing in these experimental conditions have a fundamental role in IBU metabolisation, and in the possible release of IBU-derived compounds into the medium.

In conclusion, to the best of our knowledge, this paper reports the first evidence of IBU absorption and its possible metabolisation by duckweed, demonstrating that, in addition to IBU, IBU metabolites are also detectable in plants and in the growth medium. These findings could have a notable ecological interest, as the genus *Lemna* is an important biological component of natural and constructed wetlands, and opens up intriguing questions for further research.

Acknowledgements

S. Pérez acknowledges the contract from the Ramon y Cajal Program of the Spanish Ministry of Economy and Competitiveness. This work has been financially supported by the Generalitat de Catalunya (Consolidated Research Groups "2014 SGR 418—Water and Soil Quality Unit", 2014 SGR 291–ICRA and 2014-SGR109 - Research Unit on Bioactive Molecules).

References

[1] L. Ferrando-Climent, N. Collado, G. Buttiglieri, M. Gros, I. Rodriguez-Roda, S. Rodriguez-Mozaz, D. Barceló, Comprehensive study of ibuprofen and its metabolites in activated sludge batch experiments and aquatic environment, Sci. Total Environ. 438 (2012) 404–413.
[2] R. Moreno-Gonzales, S. Rodríguez-Mozaz, M. Gros, E. Pérez-Cánovas, D. Barceló, V.M. León, Input of pharmaceuticals through coastal surface watercourses into a Mediterranean lagoon (Mar Menor, SE Spain): Sources and seasonal variations, Sci. Total Environ. 490 (2014) 59–72.
[3] T.A. Ternes, A. Joss, H. Siegrist, Scrutinizing pharmaceuticals and personal care products in wastewater treatment, Sci. Total Environ. 38 (2004) 392–399.
[4] K.E. Murray, S.M. Thomas, A.A. Bodour, Prioritizing research for trace pollutants and emerging contaminants in the freshwater environment, Environ. Pollut. 158 (2010) 3462–3471.
[5] M.D. Hernando, M. Mezcua, A.R. Fernández-Alba, D. Barceló, Environmental risk assessment of pharmaceutical residues in wastewater effluents, surface waters and sediments, Talanta 69 (2006) 334–342.
[6] D.N. Ribeiro de Sousa, A.A. Mozeto, R.L. Carneiro, P.S. Fadini, Electrical conductivity and emerging contaminant as markers of surface freshwater contamination by wastewater, Sci. Total Environ. 484 (2014) 19–26.
[7] L.H.M.L.M. Santos, M. Gros, S. Rodriguez-Mozaz, C. Delerue-Matos, A. Pena, D. Barceló, M.C.B.S.M. Montenegro, Contribution of hospital effluents to the load of pharmaceuticals in urban wastewaters:identification of ecologically relevant pharmaceuticals, Sci. Total Environ. 461–462 (2013) 302–316.
[8] S. Han, K. Choi, J. Kim, K. Ji, S. Kim, B. Ahn, J. Yun, K. Choi, J.S. Khim, X. Zhang, J.P. Giesy, Endocrine disruption and consequences of chronic exposure to ibuprofen in Japanese medaka (*Oryzias latipes*) and freshwater cladocerans *Daphnia magna* and *Moina macrocopa*, Aquat. Toxicol. 98 (2010) 256–264.
[9] M. Parolini, A. Binelli, A. Provini, Chronic effects induced by ibuprofen on the fresh water bivalve *Dreissena polymorpha*, Ecotoxicol. Environ. Saf. 74 (2011) 1586–1594.
[10] L.M. Stout, E.N. Dodova, J.F. Tyson, K. Nüsslein, Phytoprotective influence of bacteria on growth and cadmium accumulation in the aquatic plant *Lemna minor*, Water Res. 44 (2010) 4970–4979.
[11] H. Böcük, A. Yakar, O.C. Türker, Assessment of *Lemna gibba* L. (duckweed) as a potential ecological indicator for contaminated aquatic ecosystem by boron mine effluent, Ecol. Indic. 29 (2013) 528–538.
[12] M. Mkandawire, J.A. Teixeira da Silva, E.G. Dudel, The *Lemna* bioassay: contemporary issues as the most standardized plant bioassay for aquatic ecotoxicology, Crit. Rev. Environ. Sci. Technol. 44 (2014) 154–197.

[13] N. Rentz, M. Hanson, Duckweed toxicity tests are appropriate for ERA, Integr. Environ. Assess. Manage. 5 (2009) 350–351.
[14] D. Reinhold, S. Vishwanathan, J.J. Park, D. Oh, F.M. Saunders, Assessment of plant-driven removal of emerging organic pollutants by duckweed, Chemosphere 80 (2010) 687–692.
[15] A. Garcia-Rodríguez, V. Matamoros, C. Fontàs, V. Salvadó, The influence of *Lemna* sp. and *Spirogyra* sp. on the removal of pharmaceutical and endocrine disruptors in treated wastewaters, Int. J. Environ. Sci. Technol. (2014), http://dx.doi.org/10.1007/s13762-014-0632-x
[16] F. Pomati, A.G. Netting, D. Calamari, B.A. Neilan, Effects of erythromycin, tetracicline and ibuprofen on the growth of *Synechocystis* sp. and *Lemna* minor, Aquat. Toxicol. 67 (2004) 387–396.
[17] R.A. Brain, D.J. Johnson, S.M. Richards, H. Sanderson, P.K. Sibley, K.R. Solomon, Effect of 25 pharmaceutical compounds to *Lemna gibba* using a seven-day static-renewal test, Environ. Toxicol. Chem. 23 (2004) 371–382.
[18] V. Iori, F. Pietrini, M. Zacchini, Assessment of ibuprofen tolerance and removal capability in *Populus nigra* L. by *in vitro* culture, J. Hazard. Mater. 229–230 (2012) 217–223.
[19] A. Dordio, R. Ferro, D. Teixera, A.J. Palace, A.P. Pinto, C.M.B. Dias, Study on the use of *Typha* spp. For the phytotreatment of water contaminated with ibuprofen, Int. J. Environ. Anal. Chem. 91 (2011) 654–667.
[20] V. Iori, M. Zacchini, F. Pietrini, Growth, physiological response and phytoremoval capability of two willow clones exposed to ibuprofen under hydroponic culture, J. Hazard. Mater. 262 (2013) 796–804.
[21] OECD, 2002. OECD guideline 221. OECD Guidelines for the Testing of Chemicals: Revised Proposal for a New Guideline 221, Lemna sp. Growth Inhibition Test. Organization of Economic Cooperation and Development Paris, France.
[22] ISO/DIS 20,079, 2004. Water quality –determination of the toxic effect of water constituents and waste water to duckweed (*Lemna minor*)–Duckweed growth inhibition test. ISO TC 147/SC 5/WG 5.
[23] A. Severi, Toxicity of selenium to Lemna minor in relation to sulfate concentration, Physiol. Plant 113 (2001) 523–532.
[24] A.R. Wellburn, The spectral determination of chlorophylls a and b, as well as total carotenoids, using various solvents with spectrophotometers of different resolution, J. Plant Physiol. 144 (1994) 307–313.
[25] X. Wu, J.L. Conkle, J. Gan, Multi-residue determination of pharmaceutical and personal care products in vegetables, J. Chromatogr. A 1254 (2012) 78–86.
[26] J. Kotyza, P. Soudek, Z. Kafka, T. Vaněk, Phytoremediation of pharmaceuticals–preliminary study, Int. J. Phytoremed. 12 (2011) 306–316.
[27] N. Collado, G. Buttiglieri, L. Ferrando-Climent, S. Rodriguez-Mozaz, D. Barceló, J. Comas, J. Rodriguez-Roda, Removal of ibuprofen and its transformation products: experimental and simulation studies, Sci. Total Environ. 433 (2012) 296–301.
[28] C. Zwiener, S. Seeger, T. Glauner, F.H. Frimmel, Metabolites from the biodegradation of pharmaceutical residues of ibuprofen in biofilm reactors and batch experiments, Anal. Bioanal. Chem. 372 (2002) 569–575.
[29] S. Pérez, D. Barceló, Application of advanced MS techniques to analysis and identification of human and microbial metabolites of pharmaceuticals in the aquatic environment, Trends Anal. Chem. 26 (2007) 494–514.
[30] E. Marco-Urrea, M. Pérez-Trujillo, T. Vicent, G. Caminal, Ability of white-rot fungi to remove selected pharmaceuticals and identification of degradation products of ibuprofen by *Trametes versicolor*, Chemosphere 74 (2009) 765–772.
[31] P. Schröder, C. Collins, Conjugating enzymes involved in xenobiotic metabolism of organic xenobiotics in plants, Int. J. Phytoremed. 4 (2002) 247–265.

4.2 Avaluació del metabolisme a peixos de riu

Per tal d'avaluar el metabolisme de fàrmacs en peixos salvatges, es va realitzar un mostreig mitjanant pesca elèctrica a cinc punts diferents al llarg del riu Llobregat. En total es van recol·lectar més de 80 individus de dues espècies diferents, la carpa comú (Cyprinus carpio) i el barb de l'Ebre (Barbus graellsi). Amb aquest mostreig es pretenia determinar els fàrmacs que es detectaven als peixos de riu per poder detectar i identificar els seus principals metabòlits.

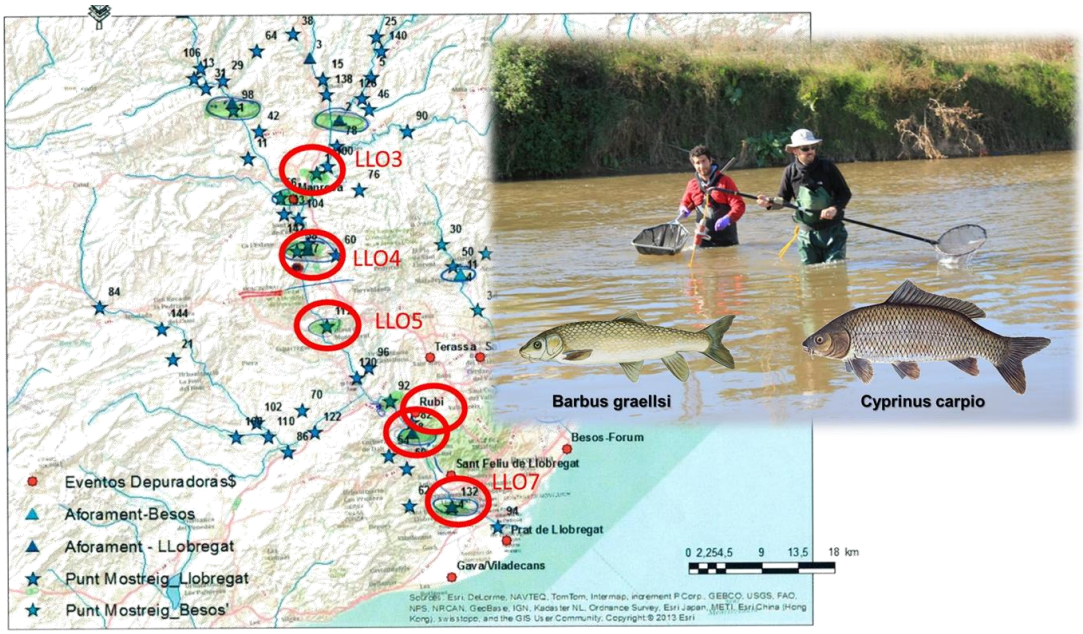

Figura 9. *Imatges dels punts de mostreig al riu Llobregat i les dues espècies seleccionades*

Amb aquest motiu, els peixos varen ser disseccionats per tal de poder analitzar els diferents teixits. En l'article 5 s'ha observat que la bilis pot ser analitzada de forma ràpida i senzilla però allà hi trobarem principalment els fàrmacs metabolitzats i per tant la seva detecció resulta més complexa. Així doncs, es va optar per analitzar primer el múscul amb un mètode d'anàlisi dirigit de més de 2000 contaminants orgànics polars. Per extreure el múscul es va utilitzar un mètode prèviament publicat a la literatura [40]. Aquest consistia amb una extracció amb 8 mL d'una solució de metanol i àcid acètic 0.1M (1:1) mitjançant ultrasons. Els extractes es van centrifugar a 2ºC per tal de fer precipitar els greixos I el sobrenedant es va evaporar i reconstituir per ser analitzat mitjançant un sistema LC-HRMS.

L'anàlisi de les mostres de múscul es va realitzar en col·laboració amb la universitat d'Atenes mitjançant LC-QTOF amb l'esmentat mètode d'escombratge, amb més de 2000 contaminant orgànics polars, entre ells més de 150 productes farmacèutics [179]. Aquest mètode l'havien desenvolupat prèviament, creant la base de dades a partir de la injecció dels compostos incloent el temps de retenció, la massa exacte, el perfil isotòpic i diversos fragments de confirmació. L'anàlisi es va realitzar mitjançant un sistema UHPLC (3000 DionexUltiMate RSLC, Thermo FisherScientific, Alemanya) acoblat a un espectròmetre de masses QTOF (MaxisImpact, Bruker Daltonics, Bremen, Alemanya) equipat amb una font d'ionització ESI. La columna cromatogràfica utilitzada va ser una AcclaimTM RSLC 120C18 (2,1 mm de diàmetre intern × 100 mm de longitud i 2,2 mμ de mida de partícula) de Thermo Fisher Scientific (Dreieich, Alemanya) amb una pre-columna del mateix material.

Les mostres es van analitzar a l'espectrometre de masses tant en mode d'ionització positiu com en negatiu. Les fases mòbils per la cromatografia en mode d'ionització positiu van ser (A) metanol amb 5 mM de formiat d'amoni i 0,01% (v/v) d'àcid fòrmic i (B) solució aquosa amb formiat d'amoni 5 mM, 10% de metanol i 0,01% d'àcid fòrmic. Pel mode d'ionització negativa, les fases mòbils van ser (A) MeOH amb acetat d'amoni 5 mM i (B) una solució aquosa amb acetat d'amoni 5 mM i 10% de metanol .

Mitjançant el software de Bruker "*TargetAnalysis*", es van rastrejar els compostos de la base de dades a les mostres de forma automatitzada. Per això es van fixar criteris d'error tolerable de ± 5 ppm per exactitud de massa, <200 mSigma pel perfil isotòpic i ± 0,2 minuts per al temps de retenció. Finalment per a determinar correctament la seva identitat es van comprovar de forma manual els fragments de confirmació.

Un cop es van determinar els fàrmacs acumulats al peixos de riu, es va optar per a desenvolupar un mètode per a la detecció del seus metabòlits. Per aquest motiu, es va utilitzat un mètode d'anàlisis de sospitosos. Per tal de generar la llista de compostos es van seleccionar cinc fàrmacs; l'IBU, la sertralina, la mepivacaina, la pregabalna i el gemfibrozil i es va utilitzar el software

Metabolite predict de Bruker. Per aquesta predicció es van incorporar també les reaccions observades en els peixos a escala laboratori.

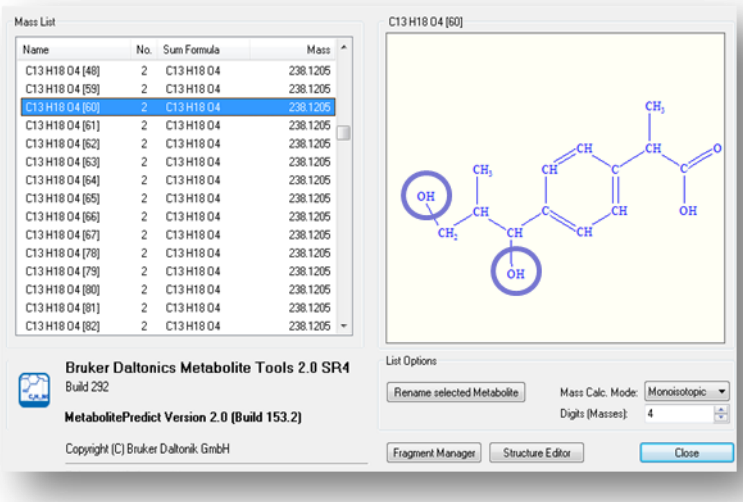

Figura 10. *Exemple de predicció de metabòlits de l'IBU a través dels software MetabolitePredict*

Aquesta aproximació, es va aplicar inicialment per a l'anàlisi de la bilis, mitjançant el mateix tractament que en l'article 5 però injectat mitjançant el mètode de la Universitat d'Atenes. Com hem vist l'anàlisi de la bilis evita els problemes d'extracció i recuperació que tenen els anàlisis d'altres teixits i a més, el metabòlits poden estar presents a altes concentracions. En segon lloc, per tal d'avaluar l'acumulació de metabòlits, l'escombratge de sospitosos també es va realitzar a les dades de les mostres de múscul. El següent esquema resumeix l'estratègia utilitzada al capítol 4.

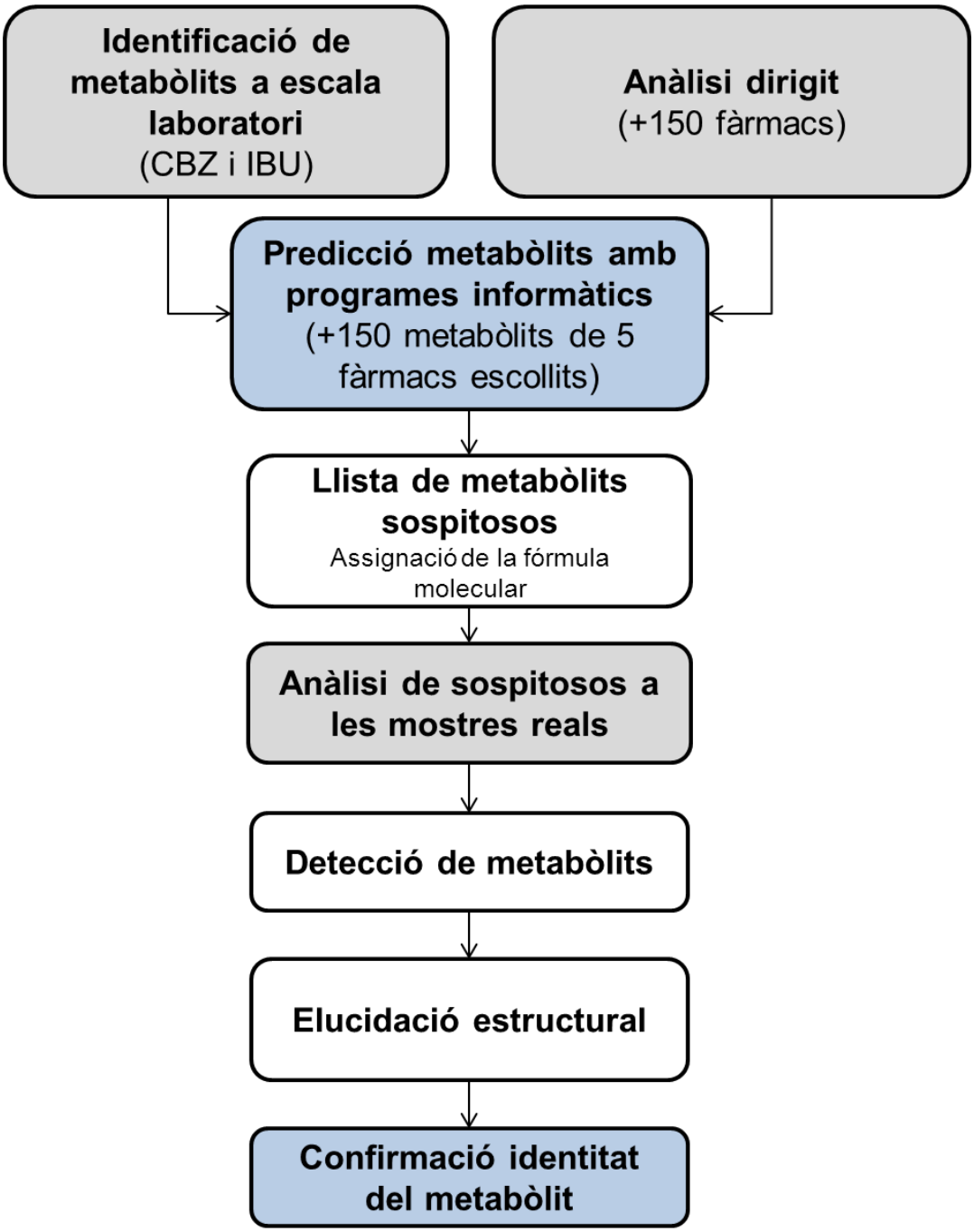

Figura 11. *Estratègia analítica utilitzada per a la detecció i identificació de metabòlits en peixos salvatges.*

4.3 Discussió de resultats

4.3.1 Identificació de les reaccions metabòliques a escala laboratori

Mitjançant la comparació de les mostres de bilis de llenguado tractades i les mostres control, s'han pogut determinar els pics corresponents als possibles metabòlits. Degut a la complexitat de les matrius aquesta s'ha realitzat de forma automatitzada mitjançant el software SIEVE. La figura 12 mostra un exemple de compost detectat a través de la comparació de les mostres control amb les mostres de bilis de peixos tractades amb carbamazepina i ibuprofè.

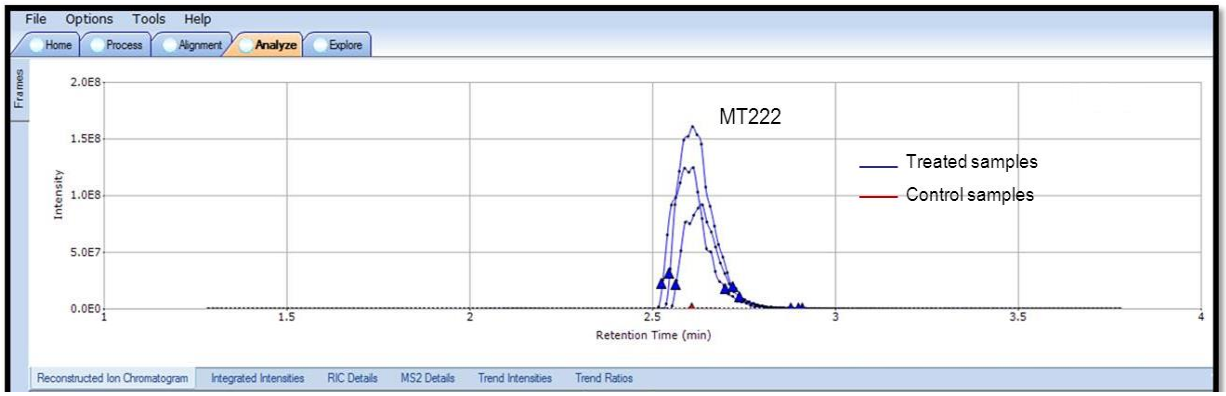

Figura 12. *Metabòlit de l'Ibuprofè (IBU-MET222) detectat a la bilis del peix mitjançant el software SIEVE*

Amb aquesta aproximació s'han pogut detectar els metabòlits més importants a la bilis, ja que el software proveeix un llistat amb un rati de diferència entre mostres control i mostres tractades. Aquest rati permet prioritzar en la identificació temptativa dels metabòlits, que continua sent la etapa més complexa de l'estudi. Per tal de identificar aquests metabòlits, s'ha tingut en compte la massa exacte, la possible composició elemental proposada per aquesta massa, el temps de retenció i el perfil isotòpic. Amb aquesta informació, s'ha procedit a l'estudi del patró de fragmentació de cada compost. Per a proposar la seva estructura s'ha comparat aquest amb el patró del principi actiu i s'han tingut en compte fragments específics de metabòlits reportats a la literatura. La figura 13 mostra un exemple de identificació mitjançant la observació de l'espectre. En ella hi podem veure fragments del IBU-MET398 determinants per a la seva temptativa identificació com a

l'hidròxid de l'acil glucurònic ibuprofè. Ràpidament podem observar que es tracta d'un glucurònic mitjançant els fragments de m/z 113 i 175, característics d'aquests compostos. A més, podem observar que el compost pateix inicialment la pèrdua de 176 unitats de massa, corresponents a la pèrdua de l'àcid glucurònic, fet que ens indica que es tracte de l'acil glucurònic ja que els èters glucurònics inicialment sofreixen la pèrdua del CO_2 de l'àcid carboxílic (figura 14).

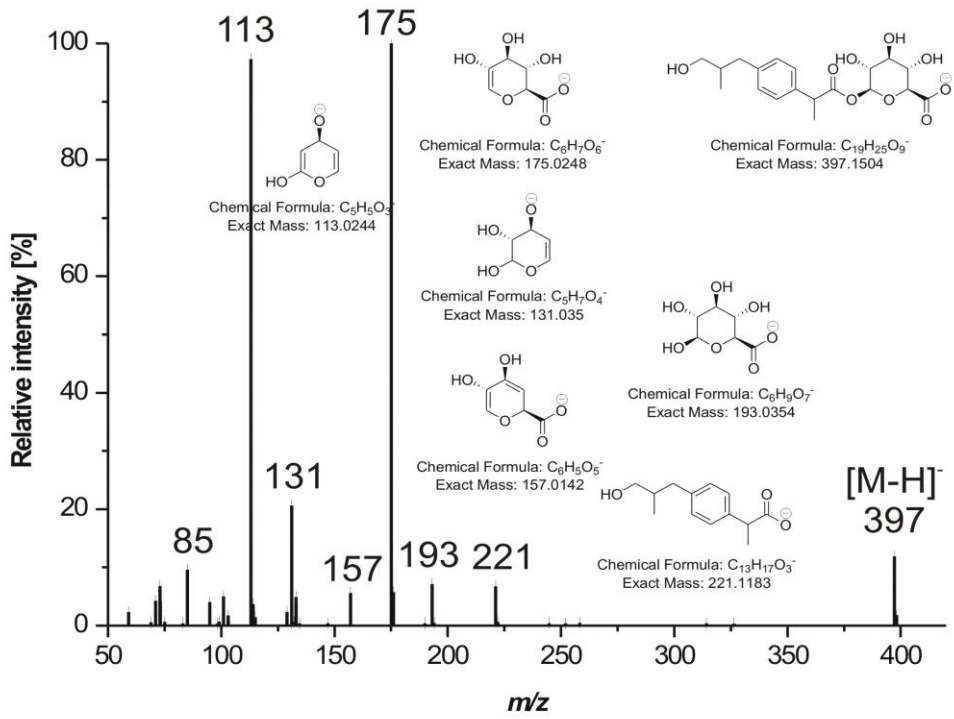

Figura 13. *Espectre de fragmentació proposat per l'hidròxid de l'acil glucurònic iburpofè (IBU-MET398- C).*

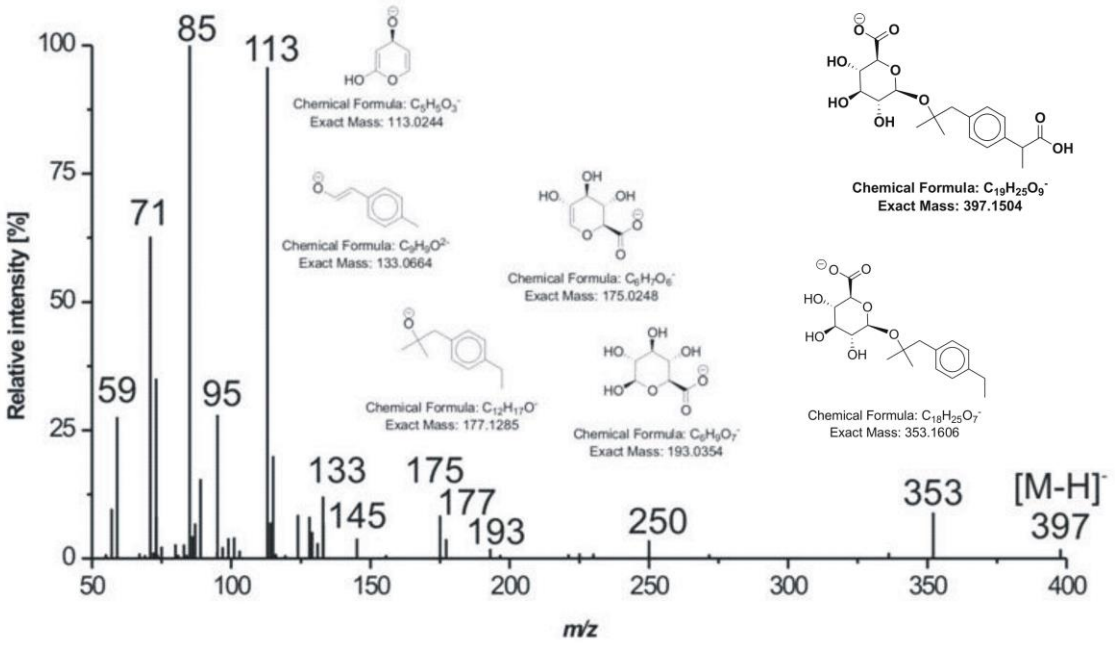

Figura 14. *Espectre de fragmentació proposat per l'èter glucurònic d'ibuprofè (IBU-MET398- A i B).*

De forma anàloga, s'han proposat estructures pels 13 metabòlits de la CBZ i els 11 metabòlits de l'IBU que es poden trobar a l'anterior publicació. En ella s'han reportat per primera vegada els metabòlits de la CBZ en peix i s'ha ampliat la llista de metabòlits de l'IBU. Concretament s'han identificat per primera vegada tres metabòlits provinents de la doble oxidació del IBU, el IBU-MET238, el IBU-MET345 i el IBU-MET414. Els seus espectres es troben a continuació (figura 15). Com es pot veure, pel metabòlit conjugat de taurina també es pot observar un fragment de m/z 124 molt característic d'aquesta classe de compostos.

.

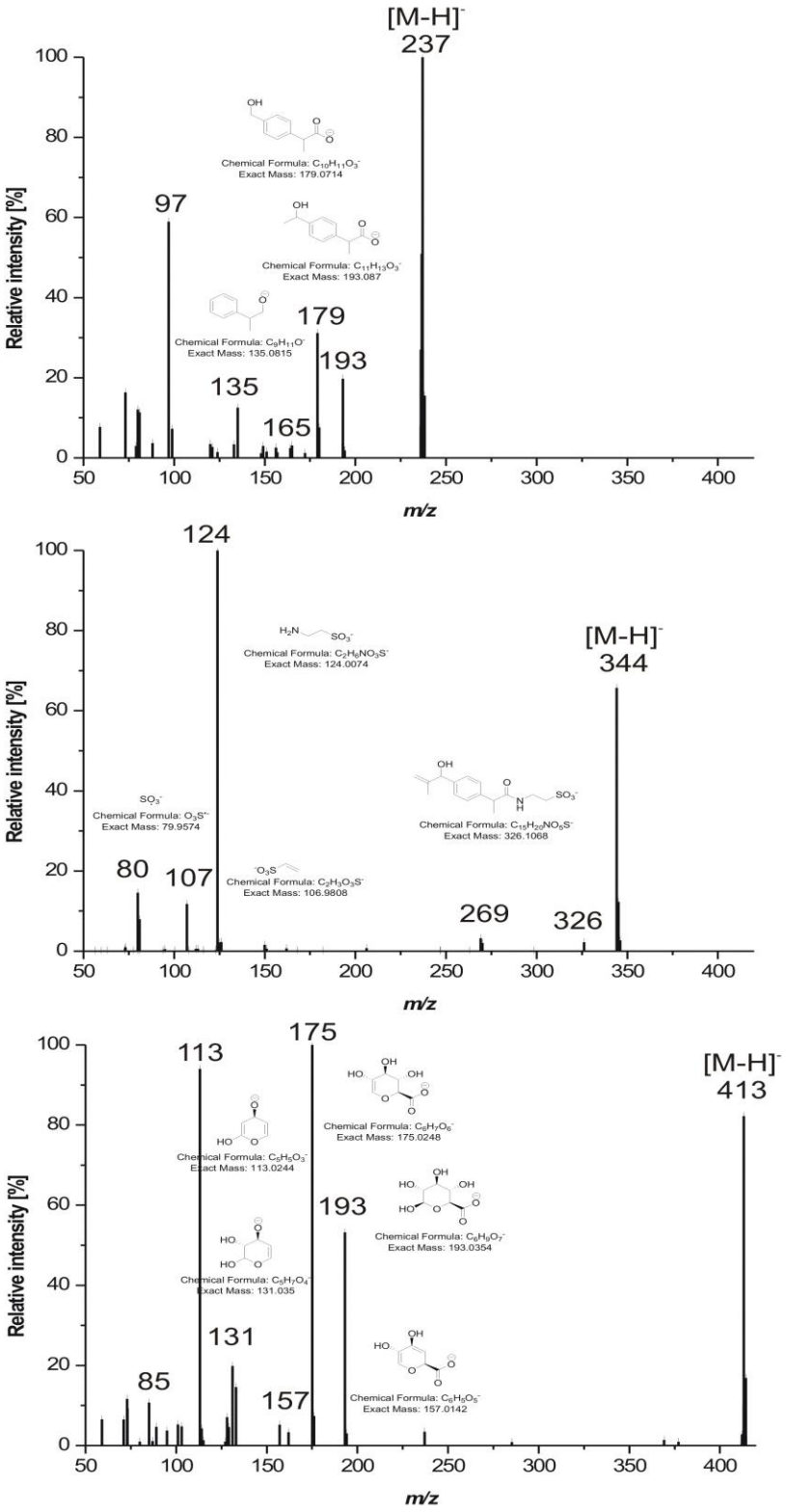

Figura 15. *Espectre de fragmentació dels metabòlits di-hidroxilats de l'IBU detectats per primera vegada a l'article 3.*

Precisament la conjugació amb taurina ha estat una de les principals diferències observades entre el metabolisme de CBZ i IBU. Aquesta es deu pròpiament a la naturalesa del compost amb la presència del grup carboxílic en la estructura del IBU. En l'estudi dels metabòlits de CBZ també s'han pogut observar algunes particularitats com és el cas de l'oxidació en forma d'epòxid. El que crida més l'atenció entre el comportament dels dos fàrmacs és el diferent grau de metabolització. Mentre que s'estima que l'IBU es metabolitza completament, més de dos terços de la CBZ roman inalterada.

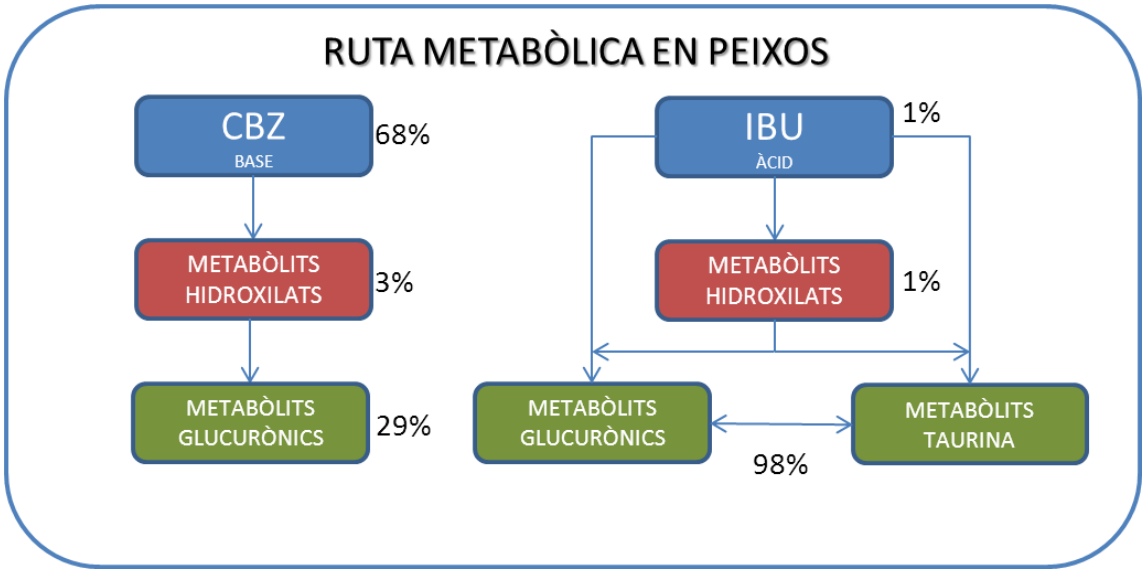

Figura 16. *Ruta metabòlica de la CBZ i l'IBU en SOLEA SENEGALENSIS.*

Finalment, l'estudi del metabolisme en les plantes aquàtiques, en ha permès veure com les capacitats i reaccions metabòliques són diferents en els diversos organismes aquàtics que poden ser exposats a residus farmacèutics. En els peixos, les reaccions principals es porten a terme al fetge i per tant l'anàlisi de la bilis ens ha permès estudiar-les. Les plantes no tenen un òrgan tant diferenciat on es porten a terme aquests processos i s'ha analitzat el conjunt de l'organisme. Malgrat això és sabut que les plantes tenen capacitat de detoxificar-se mitjançant la formació de metabòlits que els resultin més senzills d'excretar. Així s'ha pogut observar que els enzims de les reaccions en peixos són principalment el citocrom P450 (CYP), les uridinadifosfat glucuronosiltransferasa (UGTs) i les sulfotransferases (SULTs), amb reaccions similars a la majoria de vertebrats. A les plantes s'han observat metabòlits

comuns als peixos, com els hidroxilats i els glucurònics però també d'altres més característics de les plantes com la formació d'acetils, malonils i hexoses, alguns d'ells més similars als formats pels fongs. La següent taula resumeix les similituds i les diferències entre els dos organisme estudiats.

TAULA 4. Metabòlits del IBU identificats en peixos i en plantes.

Metabòlit	Fórmula (M-H)	Massa exacte (M-H)-	Detectat en:	
			Peixos	Plantes
Hidroxi-IBU	$C_{13}H_{17}O_3^-$	221.1183	x	x
Dihidroxi-IBU	$C_{13}H_{17}O_4^-$	237.1132	x	x
Acetil IBU	$C_{15}H_{19}O_3^-$	247.1340	n.d.	x
IBU taurina	$C_{15}H_{22}NO_4S^-$	312.1275	x	n.d.
Hidroxi-IBU taurina	$C_{15}H_{22}NO_5S^-$	328.1224	x	n.d.
Dihidroxi-IBU taurina	$C_{15}H_{22}NO_6S^-$	344.1173	x	n.d.
IBU hexosa	$C_{19}H_{27}O_7^-$	367.1762	n.d.	x
IBU acil glucurònic	$C_{19}H_{25}O_8^-$	381.1555	x	n.d.
Hidroxi-IBU glucurònic (acil)	$C_{19}H_{25}O_9^-$	397.1504	x	n.d.
Hidroxi-IBU glucurònic (éter)	$C_{19}H_{25}O_9^-$	397.1504	x	x
IBU acetil hexosa	$C_{21}H_{29}O_8^-$	409.1868	n.d.	x
Dihidroxi-IBU glucurònic (acil)	$C_{19}H_{25}O_{10}^-$	413.1453	x	n.d.
Dihidroxi-IBU glucurònic (éter)	$C_{19}H_{25}O_{10}^-$	413.1453	x	n.d.
Hidroxi-IBU acetil hexosa	$C_{21}H_{29}O_9^-$	425.1817	n.d.	x
IBU malonil hexosa	$C_{22}H_{29}O_{10}^-$	453.1766	n.d.	x
IBU desoxihexosa hexosa	$C_{25}H_{37}O_{11}^-$	513.2341	n.d.	x
IBU hexosil hexosa	$C_{25}H_{37}O_{12}^-$	529.2291	n.d.	x
IBU acetil desoxihexosil hexosa	$C_{27}H_{39}O_{12}^{2-}$	555.2452	n.d.	x
Hidroxi-IBU glucurònic taurina	$C_{21}H_{30}NO_{11}S^-$	504.1545	x	n.d.

4.3.2 Detecció de metabòlits de fàrmacs en peixos de riu

Amb el primer escombratge dirigit a les mostres de múscul, es van detectar més de 50 contaminants orgànics polars a cada punt de mostreig. Aquesta detecció automàtica proveïa d'indicadors de confidencialitat, tenint en compte el nombre de criteris d'error marcats anteriorment que satisfeia cada compost sospitós. A continuació es mostra una taula a mode d'exemple amb la detecció automatitzada de compostos sospitosos mitjançant el software *TargetAnalysis*.

Multi Target Screening with 'C:\Users\Jaume\Desktop\Athens\Negative_HPG.csv'

#	Id	Cmpd.Name	Formula	PMI	m/z calc.	m/z me...	Err...	E...	m...	RT ...	RT ...	del...	I	Area	Res.
58	+++	Carbetamide Fragm 116	C 5 H 10 N 1 O 2	[I]1-	116.0717	116.0720	-2.9	-0.3	1.4	6.54	6.49	0.05	9280	6937	17908
2	+++	ethyl sulfate	C 2 H 6 O 4 S 1	[M-H]-	124.9914	124.9912	-2.0	-0.2	18.6	1.44	1.41	0.03	256	1034	18251
61	+++	Carbetamide Fragm 116	C 5 H 10 N 1 O 2	[I]1-	116.0717	116.0719	-2.1	-0.2	3.8	6.54	6.56	-0.02	9348	12590	18274
63	+++	Pravastatin	C 23 H 36 O 7	[M-H]-	423.2388	423.2390	-0.5	-0.2	48.2	8.27	8.17	0.10	269	1490	31777
67	+++	Ibuprofen	C 13 H 18 O 2	[M-H]-	205.1234	205.1240	2.9	0.6	8.7	9.01	9.06	-0.05	430	3349	36295
76	+++	methenolone	C 20 H 30 O 2	[M-H]-	301.2173	301.2161	-3.9	-1.2	53.0	13.82	13.72	0.10	204	2106	37932
70	+++	19-norandrosterone	C 18 H 28 O 2	[M-H]-	275.2017	275.2026	3.4	0.9	14.2	12.51	12.47	0.04	421	4489	27360
72	+++	4-nonylphenol (4-NP)	C 15 H 24 O 1	[M-H]-	219.1754	219.1770	-7.0	-1.5	46.9	12.92	12.91	0.01	290	787	34148
17	+++	Imazapyr (Na)	C 13 H 13 N 3 Na 1 O 3	[I]1-	282.0860	282.0850	-3.4	-1.0	28.7	3.10	3.03	0.07	4455	41140	26490
71	+++	19-noretiocholanolone	C 18 H 28 O 2	[M-H]-	275.2017	275.2026	3.4	0.9	14.2	12.51	12.47	0.04	421	4489	27360
77	+++	methenolone met.1	C 20 H 30 O 2	[M-H]-	301.2173	301.2161	-3.9	-1.2	53.0	13.82	13.72	0.10	204	2106	37932
80	+++	Dodecyl-benzenesulfonate	C 18 H 29 O 3 S 1	[I]1-	325.1843	325.1850	2.2	0.7	40.7	14.15	14.12	0.03	2034	924	25742
73	+++	4-nonylphenol (4-NP)	C 15 H 24 O 1	[M-H]-	219.1754	219.1761	-3.0	-0.7	41.2	12.92	13.01	-0.09	480	3977	34348
27	+++	Butocarboxim-sulfoxid Fragm 84	C 4 H 6 N 1 O 1	[I]1-	84.0455	84.0461	-7.8	-0.7	4.7	3.36	3.34	0.02	215	1357	27655
79	+++	Dodecyl-benzenesulfonate	C 18 H 29 O 3 S 1	[I]1-	325.1843	325.1849	1.9	0.6	40.0	14.15	14.05	0.10	2281	2347	29279
31	+++	Butocarboxim-sulfoxid Fragm 74	C 2 H 4 N 1 O 2	[I]1-	74.0248	74.0251	4.5	0.3	38.3	3.36	3.44	-0.08	713	1289	20349
68	+++	Gemfibrozil (Fragm. 121)	C 8 H 9 O 1	[I]1-	121.0659	121.0664	-4.6	-0.6	37.8	10.89	10.96	-0.07	217	2271	30693
15	+++	benzoic acid	C 7 H 6 O 2	[M-H]-	121.0295	121.0290	4.0	0.5	49.4	2.88	2.94	-0.06	276	924	32567
47	+++	1.2.3.6-Tetrahydrophthalimide (cis-)	C 8 H 9 N 1 O 2	[M-H]-	150.0561	150.0565	-2.7	-0.4	7.3	4.36	4.31	0.05	773	1471	20645
37	+++	Butoxycarboxim Fragm 74	C 2 H 4 N 1 O 2	[I]1-	74.0248	74.0251	5.1	0.4	5.7	3.67	3.69	-0.02	661	1185	20668
60	++	probenecid	C 13 H 19 N 1 O 4 S 1	[M-H]-	284.0962	284.0992	-10.6	-3.0	n.a.	6.46	6.54	-0.08	216	758	53282
52	++	1-Naphthylaceticacid Fragm 141	C 11 H 9	[I]1-	141.0710	141.0740	-21.6	-3.0	57.6	5.70	5.53	0.17	161	1143	36323
69	++	4-tert-octylphenol (4-t-OP)	C 14 H 22 O 1	[M-H]-	205.1598	205.1607	-4.4	-0.9	8.4	12.30	12.41	-0.11	1581	14258	25028
36	++	Imazamox	C 15 H 19 N 3 O 4	[M-H]-	304.1303	304.1314	3.8	1.1	n.a.	3.74	3.64	0.10	335	1454	29094

Figura 17. *Exemple de taula de resultats per al escombratge dirigit de més de 2000 compostos en múscul de peix.*

D'entre els diferents contaminant orgànics detectats es va focalitzar en els productes farmacèutics presents al múscul dels peixos. Aquests resultats es resumeixen a la taula 5. La seva detecció al múscul demostra l'absorció dels residus farmacèutics per la biota salvatge que habita els rius, ja que la majoria d'aquests compostos ja havien estat detectats anteriorment a les aigües del riu Llobregat.

TAULA 5. Fàrmacs detectats en múscul de peixos del riu Llobregat

Fàrmac	Fórmula	Massa exacte (M±H)±
Amantadina	$C_{10}H_{17}N$	152.1434
Citalopram	$C_{20}H_{21}N_2OF$	325.1716
Carbamazepina	$C_{15}H_{12}N_2O$	237.1024
Gabapentina	$C_9H_{17}NO_2$	172.1332
Gemfibrozil	$C_{15}H_{22}O_3$	249.1489
Ibuprofè	$C_{13}H_{18}O_2$	205.1225
Lamotrigina	$C_9H_7Cl_2N_5$	256.0151
Mepivacaina	$C_{15}H_{22}N_2O$	247.1805
Pravastatina	$C_{23}H_{36}O_7$	423.2388
Pregabalina	$C_8H_{17}NO_2$	158.1187
Prolinamida	$C_5H_{10}N_2O$	115.0866
Sertralina	$C_{17}H_{17}NCl_2$	306.0811
Venlafaxina	$C_{17}H_{27}NO_2$	278.2117

D'aquests compostos es van escollir cinc fàrmacs per a l'estudi del metabolisme als peixos; l'Ibuprofè, el gemfibrozil, la pregabalina, la sertralina i la mepivacaina. Tots ells van ser freqüentment detectats en les mostres dels diferents punts excepte la sertralina i la mepivacaina. Aquestes només van ser detectades al darrer punt de mostreig però en un percentatge molt alt de les mostres (figura 18).

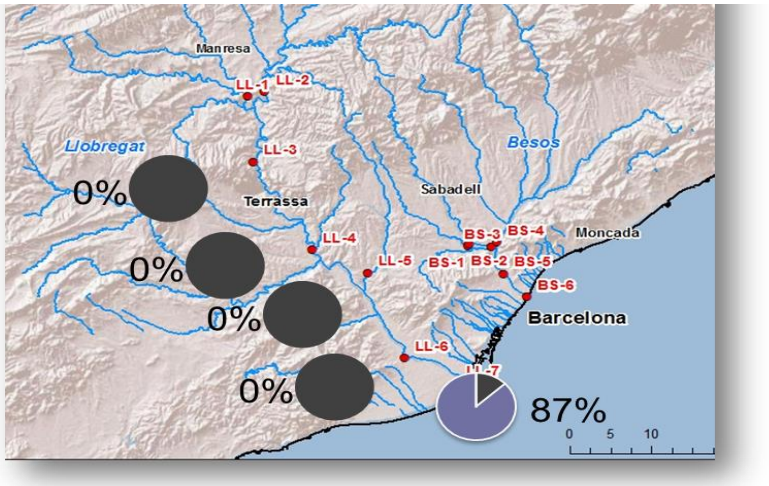

Figura 18. *Percentatge de detecció de la sertralina i mepivacaina als diferents punts de mostreig.*

Mitjançant el software de predicció es van preveure més de 150 metabòlits diferents. Després de l'escombratge d'aquesta llista de sospitosos es van detectar multitud de pics corresponents a possibles metabòlits, tant al múscul com a la bilis (Figura 19).

Multi Target Screening with 'C:\Users\Jaume\Desktop\Athens\SUSPECT METABOLITES\DATABASE SUSPECT METABOLITES.csv'

#	Id	Cmpd.Name	Formula	PMI	m/z calc.	m/z me...	Err [ppm]	Err [mDa]	mSigma	RT e...	RT me...	delt...	I	Area	Res.
45	+	Galaxolide MET	C 18 H 28 O 3	[M+H]-	291.1966	291.1980	-5.0	-1.4	14.6	0.00	9.59	-9.59	1077	5059	29888
42	+	Galaxolide MET	C 18 H 26 O 3	[M+H]-	289.1809	289.1814	1.6	0.5	24.6	0.00	6.82	-6.82	738	9822	21972
47	+	Galaxolide MET	C 18 H 28 O 3	[M+H]-	291.1966	291.1972	-2.2	-0.6	32.2	0.00	10.24	-10.24	882	3067	36301
51	+	Galaxolide MET	C 18 H 28 O 3	[M+H]-	291.1966	291.1978	4.2	1.2	20.1	0.00	12.46	-12.46	869	6825	26363
50	+	Galaxolide MET	C 18 H 28 O 3	[M+H]-	291.1966	291.1974	2.7	0.8	48.6	0.00	10.59	-10.59	709	5840	27978
46	+	Galaxolide MET	C 18 H 28 O 3	[M+H]-	291.1966	291.1978	-4.2	-1.2	n.a.	0.00	9.66	-9.66	670	4255	24376
41	+	Gemfibrozil MET	C 15 H 24 O 5	[M+H]-	283.1551	283.1557	2.0	0.6	56.7	0.00	6.66	-6.66	824	6667	24707
43	+	Gemfibrozil MET	C 15 H 24 O 5	[M+H]-	283.1551	283.1553	0.9	0.2	14.8	0.00	6.89	-6.89	775	6217	28428
35	+	Ibuprofen MET	C 13 H 18 O 4	[M+H]-	237.1132	237.1139	2.6	0.6	21.3	0.00	5.08	-5.08	1658	24149	22322
30	+	Ibuprofen MET	C 18 H 25 N 1 O 6	[M+H]-	350.1609	350.1622	3.6	1.3	40.6	0.00	4.19	-4.19	1725	11090	26886
38	+	Ibuprofen MET	C 13 H 20 O 4	[M+H]-	239.1289	239.1294	-2.2	-0.5	69.1	0.00	5.24	-5.24	974	17192	22997
40	+	Mepivacaine MET	C 15 H 22 N 2 O 3	[M+H]-	277.1558	277.1564	-2.5	-0.7	31.4	0.00	5.59	-5.59	24807	228897	26772
24	+	Mepivacaine MET	C 14 H 19 N 1 O 6	[M+H]-	296.1140	296.1145	1.7	0.5	n.a.	0.00	3.66	-3.66	603	2864	17934
37	+	Mepivacaine MET	C 15 H 22 N 2 O 3	[M+H]-	277.1558	277.1564	-2.4	-0.7	34.2	0.00	5.23	-5.23	5558	68969	22490
22	+	Mepivacaine MET	C 14 H 19 N 1 O 6	[M+H]-	296.1140	296.1147	2.6	0.8	58.3	0.00	3.59	-3.59	923	8192	21466
29	+	Pregabalin	C 8 H 17 N 1 O 2	[M+H]-	158.1187	158.1191	-2.6	-0.4	2.9	0.00	4.14	-4.14	3618	37861	18151
12	+	Pregabalin MET	C 10 H 20 N 2 O 3	[M+H]-	215.1401	215.1404	1.3	0.3	5.5	0.00	2.46	-2.46	2230	29015	25123
25	+	Pregabalin MET	C 15 H 27 N 3 O 6	[M+H]-	344.1827	344.1831	-1.0	-0.4	32.8	0.00	3.81	-3.81	1980	15025	27413
20	+	Pregabalin MET	C 10 H 18 N 2 O 3	[M+H]-	213.1245	213.1249	-1.9	-0.4	29.1	0.00	3.19	-3.19	1952	26826	20276
32	+	Pregabalin MET	C 8 H 14 O 3	[M+H]-	157.0870	157.0873	-1.7	-0.3	18.9	0.00	4.33	-4.33	1867	2787	18852
18	+	Pregabalin MET	C 10 H 18 N 2 O 3	[M+H]-	213.1245	213.1250	-2.5	-0.5	17.9	0.00	3.09	-3.09	1712	6033	23263
6	+	Pregabalin MET	C 10 H 20 N 2 O 3	[M+H]-	215.1401	215.1411	-4.6	-1.0	17.7	0.00	1.78	-1.78	1600	6677	22247
5	+	Pregabalin MET	C 6 H 10 O 7	[M+H]-	193.0354	193.0361	-3.6	-0.7	9.6	0.00	1.48	-1.48	10168	81908	19904
11	+	Pregabalin MET	C 10 H 20 N 2 O 4	[M+H]-	231.1350	231.1355	2.0	0.5	17.5	0.00	2.33	-2.33	1536	21167	22377

Figura 19. *Exemple de taula de resultats per al escombratge de metabòlits sospitosos en bilis de peix.*

Com es pot veure, el fet de no disposar de patrons de referència i per tant no disposar dels seus temps de retenció comporta disposar de menys criteris de confirmació i per tant va comportar l'obtenció de més falsos positius. A més, la manca d'espectres MS/MS de metabòlits en les poques biblioteques disponibles també en va dificultar la identificació dels mateixos.

Malgrat la complexitat s'han proposat identitats en grau de nivell 2 per a metabòlits de la majoria dels fàrmacs estudiats. Amb el mètode d'escombratge utilitzat en moltes ocasions no s'havia adquirit la informació MS/MS i per tant les mostres van ser reinjectades a Barcelona mitjançant un sistema Orbitrap Q-Exactive. Aquest fet també va facilitar la detecció dels metabòlits del IBU prèviament estudiats a escala laboratori i analitzats amb aquests mateix instrument (figura 20).

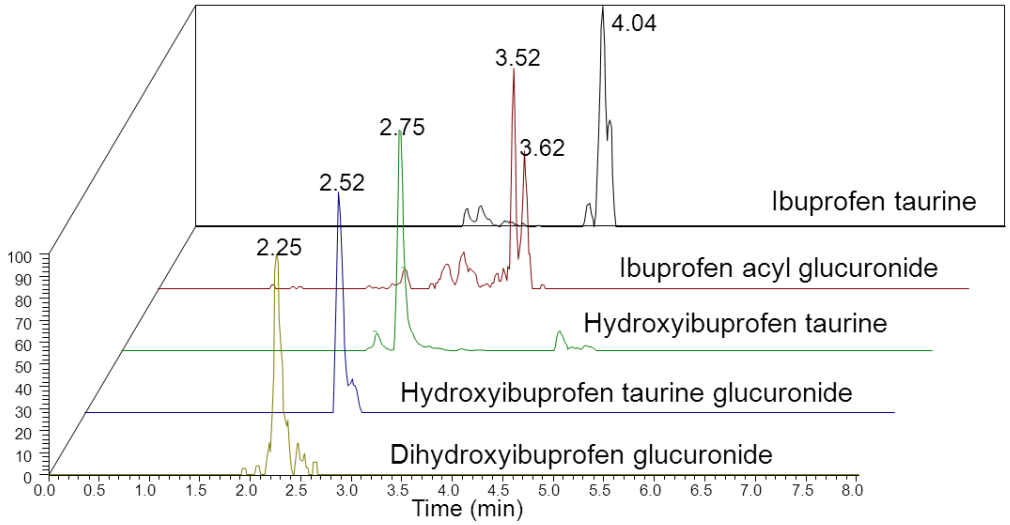

Figura 20. *Metabòlits del IBU detectats a les mostres de peixos del Llobregat*

En altres ocasions no es disposava ni tant sols del patró de fragmentació del compost pare ja que no disposàvem de patró. Per això s'han comparat els espectres obtinguts amb els disponibles a la biblioteca d'espectres NORMAN.

Per exemple, d'aquesta manera es va constatar que el patró de fragmentació de la sertralina era el mateix que el de la biblioteca. A més es va detectar un metabòlit corresponent a una possible desmetilació. L'espectre d'aquest, amb informació complementaria en va permetre una identificació temptativa. A la figura 21 es pot observar com el temps de retenció del possible metabòlit és lleugerament inferior al del compost pare, fet que correspondria a la identitat proposada.

Les reaccions identificades als experiments a escala laboratori, introduïdes al software de predicció ens han permès detectar possibles metabòlits per reaccions anàlogues. Aquest és el cas del gemfibrozil, que presenta una estructura amb un àcid carboxílic similar al IBU i que podria metabolitzar-se de manera similar. A la figura 22 es mostra la identificació temptativa del conjugat de taurina corresponent.

.

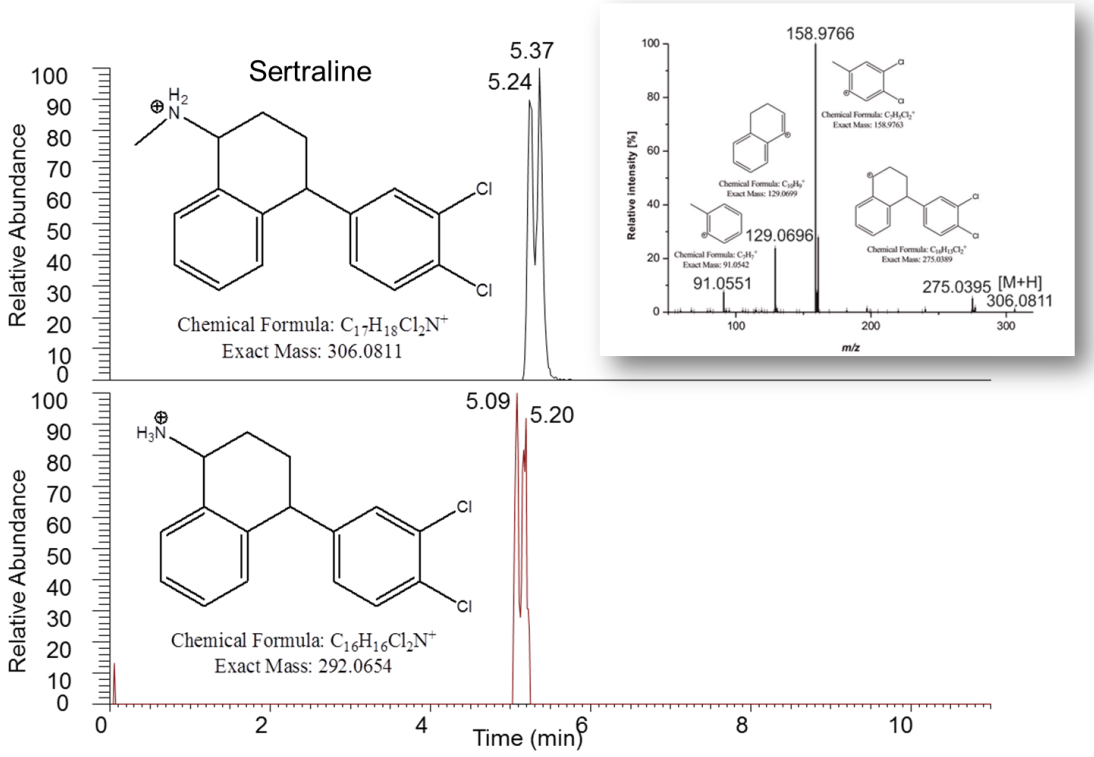

Figura 21. *Detecció de sertralina i metabòlit proposat com a desmetilsertralina*

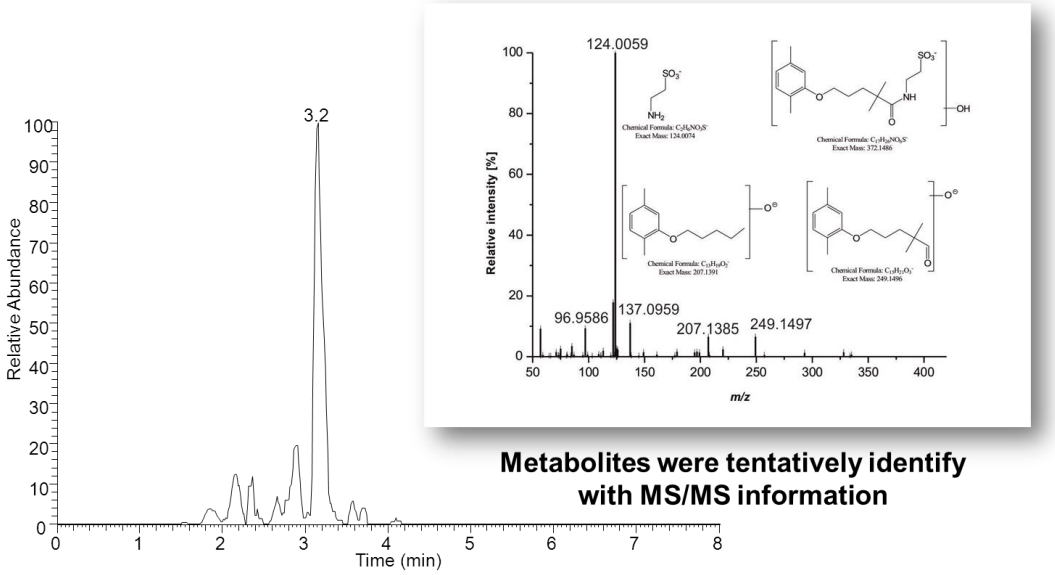

Figura 22. *Metabòlit proposat com a hidroxi-taurina de gemfibrozil*

Malgrat els esforços per a identificar els diferents metabòlits, molts d'ells encara no han pogut ser identificats. Tot i que cada dia els diferents softwares que subministren les diferents plataformes faciliten la seva identificació, aquesta encara requereix molt de temps i molts coneixements. La manca de bases de dades d'espectres en alta resolució per a metabòlits i la dificultat per obtenir patrons comercials d'aquests compostos fan que totes aquestes identitats no puguin ser confirmades amb un grau de confidència més elevat.

CAPÍTOL 5.

CONCLUSIONS

CAPITOL 5. CONCLUSIONS

Mitjançant aquesta tesis s'han pogut estudiar les **diferents transformacions que pateixen els fàrmacs al medi aquàtic**, incloent els processos biòtics més rellevant, la biodegradació per microorganismes i la detoxificació de la biota, i el principal procés abiòtic, la fotòlisi.

En el primer capítol s'han pogut revisar a fons els estudis més recents del destí ambiental dels **fàrmacs** i s'han pogut revisar les capacitats i limitacions més actuals que ens ofereix la **LC-HRMS**. A més, s'ha pogut constatar que els instruments de nova generació han superat certes limitacions en alguns factors, com la sensibilitat i la linealitat, que els converteixen en instruments realment poderosos tant per l'anàlisi qualitatiu com quantitatiu.

Mitjançant els estudis a escala laboratori s'han identificat les principals transformacions i finalment al medi natural s'han pogut constatar, **assolint els objectius marcats** al capítol 2.

En el capítol 3 s'ha estudiat el procés principal de transformació abiòtica, la **fotodegradació** de sildenafil i els seus anàlegs corresponents, i el procés principal de transformació biòtica en rius, la **biodegradació** bacteriana d'antibiòtics, concretament de dos sulfonamides (**sulfametazina i sulfametoxazol**) a **l'aigua superficial**. Aquests estudis s'han realitzat mitjançant incubacions a **escala laboratori** amb un simulador de llum solar pel **sildenafil** i els seus compostos estructuralment relacionats i un mesocosoms que contenia aigua superficial i pedres perquè es formés biofilm per degradar les sulfonamides. En el cas del sildenafil i els seus compostos estructuralment relacionats els fotoproductes es van formar de l'atac de l'anell de la piperazina arribant a deixar el àcid sulfònic lliure i els que tenien modificacions o no tenien aquest anell van formar primer el sildenafil (p.e. tiosildenafil que en comptes d'un oxigen presenta un sofre a l'anell de piperazina o directament el producte de transformació que contenia el àcid sulfònic lliure (p.e Norsildenafil). En canvi, els productes de biotransformació de les sulfonamides ja havien estat identificats abans com a metabòlits humans o productes de biotransformació en mostres ambientals (hidroxisulfametoxazol, desaminosulfametoxazol, acetil-

sulfametoxazol, nitro-sulfametoxazol i l'acetilsulfametazina). La novetat d'aquest treball és la manera de detectar aquests composostos, ja que es va fer una llista de sospitosos i es va crear un mètode al HRMS per detectar-los només amb la seva massa exacta.

Amb la identificació de TPs formats a incubacions amb aigua superficial a escala laboratori i la seva posterior detecció a mostres reals s'ha comprovat doncs que al medi ambient, els residus farmacèutics són susceptibles de patir transformacions abiòtiques i/o biòtiques.

Al capítol 4, mitjançant l'estudi a **escala laboratori** s'han pogut constatar els metabòlits formats per dos fàrmacs la **carbamazepina** i el **ibuprofè**, establint les reaccions principals produïdes pels sistemes enzimàtics dels **organismes aquàtics** estudiats. La capacitat de les **plantes aquàtiques (*Lemma gibba*)** per absorbir compostos de l'aigua en aquest cas **ibuprofè** i transformar-lo es va avaluar a l'article 6 i pels **peixos (*Solea senegalensis*)** a l'article 7. Els enzims característics de cada espècie han comportat la detecció de diferents conjugats. En el cas dels ***Solea senegalensis*** els 12 metabòlits conjugats de fase II que han estat temptativament identificats del **ibuprofè** són els glucurònics i taurines, mentre que per les ***Lemma gibba*** s'han proposat glucurònics, hexoses i malonils i també set metabòlits hidroxilats i glucurònics, demostrant que les plantes i els peixos presenten mecanismes de detoxificació pels compostos farmacèutics. En el cas dels peixos injectats amb **carbamazepina**, es van detectar 11 metabòlits nous de la hidroxilació tant aromàtica com benzílica, epoxidació, glucuronització, o-metilació i un metabòlit que es forma com un catecol.

Finalment, s'han aprofitar les capacitats de la **LC-HRMS** i els coneixements obtinguts mitjançant els experiments a escala laboratori per a estudiar el destí dels **fàrmacs en peixos salvatges del riu Llobregat**. Actualment, com s'ha demostrat en capítols anteriors, els espectròmetres de masses d'alta resolució, com l'Orbitrap i el TOF, són molt útils per a la identificació i elucidació de TP i/o metabòlits, gràcies a les mesures de massa exacta que ens proporcionem aquests analitzadors, però, mitjançant **combinacions híbrides** com l'Orbitrap,

el **Q Exactive**, el LTQ Orbitrap o el **QTOF MS**, ens han proporcionat una adquisició de dades MS/MS en diferents modes i en una única injecció. Això, com també s'ha vist, pot resultar de gran utilitat per a realitzar escombratge dirigit, de sospitosos i fins i tot de compostos desconeguts.

L'anàlisi dirigit ha permès la **detecció de** més de **12** fàrmacs amb l'escombratge de més de 2000 compostos que comprenia més **de 150 fàrmacs**. Pel nostre coneixement, és la **primera detecció d'amantadina, gabapentina, lamotrigina, mepivacaina, pravastatina, pregabalina i prolinamida en peixos salvatges**.

D'entre els fàrmacs detectats l'estudi s'ha centrat en **l'Ibuprofè, el gemfibrozil, la pregabalina, la sertralina i la mepivacaina**. La gran informació enregistrada també ha permès un **anàlisi de sospitosos** de forma retrospectiva en les mostres on s'havia realitzat l'anàlisi dirigit. Mitjançant **software de predicció** s'ha creat una base de dades de possibles metabòlits dels fàrmacs escollits. Mitjançant l'anàlisi de sospitosos s'han detectat multitud de pics que podrien correspondre als metabòlits predits. Mitjançant la massa exacta, el temps de retenció, perfil isotòpic i l'espectre de fragmentació, s'ha tractat **d'identificar els diferents metabòlits**. S'han identificat metabòlits de l'Ibuprofè identificats prèviament al laboratori. S'han proposat **metabòlits del gemfibrozil, detectats per primera vegada** en peixos salvatges, i de la sertralina. Molts metabòlits encara estan sent identificats. L'absència de patrons de referència impedeix la confirmació final de les identitats proposades.

Aquest darrer estudi demostra que si es disposes de l'espectre MS/MS dels metabòlits i dels seus temps de retenció, **l'anàlisi** directe de la **bilis** podria resultar un mètode ràpid i de grans prestacions per **avaluar l'exposició** dels peixos a fàrmacs. Els mètodes que no requereixen una extracció de la mostra ens permeten avaluar la presència dels diferents compostos sense el risc de no ser extrets. En aquest sentit, **softwares de predicció** MS/MS o de temps de retenció poden ser de gran utilitat, però sobretot **biblioteques d'espectres** obertes on s'incorpori la informació de TPs i metabòlits identificats. Malauradament, mentre aquesta informació encara no estigui disponible, la

identificació dels metabòlits fa que aquesta aproximació resulti encara molt complexa.

El fet de treballar directament en **mostres ambientals**, concretament en peixos salvatges, també facilita la **priorització** en l'elucidació dels metabòlits o TPs que realment tenen rellevància ambiental. En moltes ocasions a les simulacions a escala laboratori s'obtenen multitud de compostos que elucidar i molts d'ells no són detectats en les mostres reals.

En les diverses publicacions, centrades en l'estudi de les transformacions en diferents fàrmacs de rellevància ambiental, s'ha pogut constatar que la reproducció de les condicions ambientals i la comparació amb mostres control són una estratègia exitosa per a l'elucidació dels possibles TPs al medi, ja que alguns d'aquests TPs han estat finalment detectats en mostres reals.

També degut a l'evolució dels espectròmetres disponibles al laboratori, s'ha pogut demostrar com el creixement de la **LC-HRMS**, amb instruments cada dia més sofisticats, ens ofereix cada cop més poder de resolució i exactitud de massa, permetent tenir **més informació** per proposar de forma més acurada l'estructura de compostos desconeguts.

Després del desenvolupament d'aquests tesis es conclou que la presència dels fàrmacs al medi aquàtic és atenuada mitjançant diferents processos naturals. El fet de **conèixer els possibles destins** ambientals, les seves transformacions, degradacions i/o entrada a la cadena tròfica, pot facilitar poder **predir els efectes ambientals** associats i estimar-ne el seu risc. Per tal de realitzar una avaluació toxicològica dels fàrmacs als ecosistemes, és imprescindible considerar l'aportació dels seus TPs i metabòlits.

BIBLIOGRAFIA

1. Jones, O., N. Voulvoulis, and J. Lester, *Human pharmaceuticals in the aquatic environment a review.* Environmental technology, 2001. **22**(12): p. 1383-1394.
2. Evgenidou, E.N., I.K. Konstantinou, and D.A. Lambropoulou, *Occurrence and removal of transformation products of PPCPs and illicit drugs in wastewaters: a review.* Science of the Total Environment, 2015. **505**: p. 905-926.
3. Behera, S.K., et al., *Occurrence and removal of antibiotics, hormones and several other pharmaceuticals in wastewater treatment plants of the largest industrial city of Korea.* Science of the Total Environment, 2011. **409**(20): p. 4351-4360.
4. Heberer, T., *Occurrence, fate, and removal of pharmaceutical residues in the aquatic environment: a review of recent research data.* Toxicology letters, 2002. **131**(1): p. 5-17.
5. Schwarzenbach, R.P., et al., *The challenge of micropollutants in aquatic systems.* Science, 2006. **313**(5790): p. 1072-1077.
6. Carballa, M., et al., *Behavior of pharmaceuticals, cosmetics and hormones in a sewage treatment plant.* Water Research, 2004. **38**(12): p. 2918-2926.
7. Jones, O., N. Voulvoulis, and J. Lester, *Aquatic environmental assessment of the top 25 English prescription pharmaceuticals.* Water Research, 2002. **36**(20): p. 5013-5022.
8. Lindqvist, N., T. Tuhkanen, and L. Kronberg, *Occurrence of acidic pharmaceuticals in raw and treated sewages and in receiving waters.* Water Research, 2005. **39**(11): p. 2219-2228.
9. Vidal-Dorsch, D.E., et al., *Contaminants of emerging concern in municipal wastewater effluents and marine receiving water.* Environmental Toxicology and Chemistry, 2012. **31**(12): p. 2674-2682.
10. Zuccato, E., S. Castiglioni, and R. Fanelli, *Identification of the pharmaceuticals for human use contaminating the Italian aquatic environment.* Journal of Hazardous Materials, 2005. **122**(3): p. 205-209.
11. Zuccato, E., et al., *Source, occurrence and fate of antibiotics in the Italian aquatic environment.* Journal of Hazardous Materials, 2010. **179**(1): p. 1042-1048.
12. Mendoza, A., et al., *Pharmaceuticals and iodinated contrast media in a hospital wastewater: A case study to analyse their presence and characterise their environmental risk and hazard.* Environmental Research, 2015. **140**: p. 225-241.
13. Bottoni, P., S. Caroli, and A.B. Caracciolo, *Pharmaceuticals as priority water contaminants.* Toxicological & Environmental Chemistry, 2010. **92**(3): p. 549-565.
14. Emke, E., et al., *Enantiomer profiling of high loads of amphetamine and MDMA in communal sewage: a Dutch perspective.* Science of the Total Environment, 2014. **487**: p. 666-672.
15. Lapworth, D., et al., *Emerging organic contaminants in groundwater: a review of sources, fate and occurrence.* Environmental Pollution, 2012. **163**: p. 287-303.
16. McEneff, G., et al., *A year-long study of the spatial occurrence and relative distribution of pharmaceutical residues in sewage effluent, receiving marine waters and marine bivalves.* Science of the Total Environment, 2014. **476**: p. 317-326.
17. Patrolecco, L., et al., *Simultaneous determination of human pharmaceuticals in water samples by solid phase extraction and HPLC with UV-fluorescence detection.* Microchemical Journal, 2013. **107**: p. 165-171.
18. Osorio, V., et al., *Concentration and risk of pharmaceuticals in freshwater systems are related to the population density and the livestock units in Iberian Rivers.* Science of the Total Environment, 2016. **540**: p. 267-277.

19. da Silva, B.F., et al., *Occurrence and distribution of pharmaceuticals in surface water, suspended solids and sediments of the Ebro river basin, Spain.* Chemosphere, 2011. **85**(8): p. 1331-1339.
20. Viana, M., et al., *Cocaine and other illicit drugs in airborne particulates in urban environments: a reflection of social conduct and population size.* Environmental Pollution, 2011. **159**(5): p. 1241-1247.
21. Goncalves, C., et al., *Photofate of oseltamivir (Tamiflu) and oseltamivir carboxylate under natural and simulated solar irradiation: kinetics, identification of the transformation products, and environmental occurrence.* Environmental Science & Technology, 2011. **45**(10): p. 4307-4314.
22. Fono, L.J., E.P. Kolodziej, and D.L. Sedlak, *Attenuation of wastewater-derived contaminants in an effluent-dominated river.* Environmental Science & Technology, 2006. **40**(23): p. 7257-7262.
23. Kormos, J.L., et al., *Multistep approach for the structural identification of biotransformation products of iodinated X-ray contrast media by liquid chromatography/hybrid triple quadrupole linear ion trap mass spectrometry and 1H and 13C nuclear magnetic resonance.* Analytical Chemistry, 2009. **81**(22): p. 9216-9224.
24. Kormos, J.L., et al., *Biotransformation of selected iodinated X-ray contrast media and characterization of microbial transformation pathways.* Environmental Science and Technology, 2010. **44**(13): p. 4998-5007.
25. Trautwein, C. and K. Kummerer, *Incomplete aerobic degradation of the antidiabetic drug Metformin and identification of the bacterial dead-end transformation product Guanylurea.* Chemosphere, 2011. **85**(5): p. 765-73.
26. Nödler, K., et al., *Evidence for the microbially mediated abiotic formation of reversible and non-reversible sulfamethoxazole transformation products during denitrification.* Water Research, 2012. **46**(7): p. 2131-2139.
27. Trautwein, C., K. Kummerer, and J.W. Metzger, *Aerobic biodegradability of the calcium channel antagonist verapamil and identification of a microbial dead-end transformation product studied by LC-MS/MS.* Chemosphere, 2008. **72**(3): p. 442-50.
28. Barceló, D., *Emerging organic contaminants and human health*. Vol. 20. 2012: Springer.
29. Ben-Jonathan, N. and R. Steinmetz, *Xenoestrogens: The Emerging Story of Bisphenol A.* Trends in Endocrinology & Metabolism, 1998. **9**(3): p. 124-128.
30. Kasprzyk-Hordern, B., R.M. Dinsdale, and A.J. Guwy, *The occurrence of pharmaceuticals, personal care products, endocrine disruptors and illicit drugs in surface water in South Wales, UK.* water research, 2008. **42**(13): p. 3498-3518.
31. Lacey, C., et al., *Occurrence of pharmaceutical compounds in wastewater process streams in Dublin, Ireland.* Environmental Monitoring and Assessment, 2012. **184**(2): p. 1049-1062.
32. Parolini, M. and A. Binelli, *Adverse effects induced by ecgonine methyl ester to the zebra mussel: A comparison with the benzoylecgonine.* Environmental Pollution, 2013. **182**: p. 371-378.
33. Rabiet, M., et al., *Consequences of Treated Water Recycling as Regards Pharmaceuticals and Drugs in Surface and Ground Waters of a Medium-sized Mediterranean Catchment.* Environmental science & technology, 2006. **40**(17): p. 5282-5288.
34. Oaks, J.L., et al., *Diclofenac residues as the cause of vulture population decline in Pakistan.* Nature, 2004. **427**(6975): p. 630-633.

35. Schwaiger, J., et al., *Toxic effects of the non-steroidal anti-inflammatory drug diclofenac: Part I: histopathological alterations and bioaccumulation in rainbow trout.* Aquatic Toxicology, 2004. **68**(2): p. 141-150.
36. Corcoran, J., M.J. Winter, and C.R. Tyler, *Pharmaceuticals in the aquatic environment: a critical review of the evidence for health effects in fish.* Critical reviews in toxicology, 2010. **40**(4): p. 287-304.
37. Nagtegaal, M., et al., *UV-filtersubstanzen in wasser und fischen.* Umweltwissenschaften und Schadstoff-Forschung, 1997. **9**(2): p. 79-86.
38. Gago-Ferrero, P., M.S. Díaz-Cruz, and D. Barceló, *An overview of UV-absorbing compounds (organic UV filters) in aquatic biota.* Analytical and bioanalytical chemistry, 2012. **404**(9): p. 2597-2610.
39. Brooks, B.W., et al., *Determination of select antidepressants in fish from an effluent-dominated stream.* Environmental Toxicology and Chemistry, 2005. **24**(2): p. 464-469.
40. Ramirez, A.J., et al., *Analysis of Pharmaceuticals in Fish Using Liquid Chromatography-Tandem Mass Spectrometry.* Analytical Chemistry, 2007. **79**(8): p. 3155-3163.
41. Ramirez, A.J., et al., *Occurrence of pharmaceuticals and personal care products in fish: results of a national pilot study in the United States.* Environmental Toxicology and Chemistry, 2009. **28**(12): p. 2587-2597.
42. Subedi, B., et al., *Occurrence of Pharmaceuticals and Personal Care Products in German Fish Tissue: A National Study.* Environmental Science & Technology, 2012. **46**(16): p. 9047-9054.
43. Huerta, B., S. Rodríguez-Mozaz, and D. Barceló, *Pharmaceuticals in biota in the aquatic environment: analytical methods and environmental implications.* Analytical and bioanalytical chemistry, 2012. **404**(9): p. 2611-2624.
44. Tanoue, R., et al., *Uptake and Tissue Distribution of Pharmaceuticals and Personal Care Products in Wild Fish from Treated-Wastewater-Impacted Streams.* Environmental Science & Technology, 2015. **49**(19): p. 11649-11658.
45. Liu, J., et al., *Bioconcentration, metabolism, and biomarker responses in freshwater fish Carassius auratus exposed to roxithromycin.* Chemosphere, 2014. **99**: p. 102-108.
46. Mehinto, A.C., E.M. Hill, and C.R. Tyler, *Uptake and biological effects of environmentally relevant concentrations of the nonsteroidal anti-inflammatory pharmaceutical diclofenac in rainbow trout (Oncorhynchus mykiss).* Environmental Science & Technology, 2010. **44**(6): p. 2176-2182.
47. Brozinski, J.-M., et al., *The Anti-Inflammatory Drugs Diclofenac, Naproxen and Ibuprofen are found in the Bile of Wild Fish Caught Downstream of a Wastewater Treatment Plant.* Environmental Science & Technology, 2012. **47**(1): p. 342-348.
48. Brozinski, J.-M., et al., *Detection of naproxen and its metabolites in fish bile following intraperitoneal and aqueous exposure.* Environmental Science and Pollution Research, 2011. **18**(5): p. 811-818.
49. Brozinski, J.-M., et al., *Identification and dose dependency of ibuprofen biliary metabolites in rainbow trout.* Chemosphere, 2013. **93**(9): p. 1789-1795.
50. Alderton, W., et al., *Accumulation and metabolism of drugs and CYP probe substrates in zebrafish larvae.* Xenobiotica, 2010. **40**(8): p. 547-557.
51. Kallio, J.-M., et al., *Metabolites of the Aquatic Pollutant Diclofenac in Fish Bile.* Environmental Science & Technology, 2010. **44**(19): p. 7213-7219.
52. Lahti, M., et al., *Uptake from water, biotransformation, and biliary excretion of pharmaceuticals by rainbow trout.* Environmental Toxicology and Chemistry, 2011. **30**(6): p. 1403-1411.

53. Nallani, G.C., et al., *Bioconcentration of ibuprofen in fathead minnow (Pimephales promelas) and channel catfish (Ictalurus punctatus).* Chemosphere, 2011. **84**(10): p. 1371-1377.
54. Jones, H.S., et al., *Metabolism of ibuprofen in zebrafish larvae.* Xenobiotica, 2012. **42**(11): p. 1069-1075.
55. Xie, Z., et al., *Bioconcentration, metabolism and effects of diphenhydramine on behavioral and biochemical markers in crucian carp (Carassius auratus).* Science of the Total Environment, 2016. **544**: p. 400-409.
56. Valdés, M., et al., *Bioaccumulation and bioconcentration of carbamazepine and other pharmaceuticals in fish under field and controlled laboratory experiments. Evidences of carbamazepine metabolization by fish.* Science of the Total Environment, 2016. **557**: p. 58-67.
57. Brox, S., et al., *Metabolism of clofibric acid in zebrafish embryos (Danio rerio) as determined by liquid chromatography–high resolution–mass spectrometry.* Comparative Biochemistry and Physiology Part C: Toxicology & Pharmacology, 2016. **185**: p. 20-28.
58. Gaw, S., K.V. Thomas, and T.H. Hutchinson, *Sources, impacts and trends of pharmaceuticals in the marine and coastal environment.* Philosophical Transactions of the Royal Society of London B: Biological Sciences, 2014. **369**(1656).
59. Yan, C., et al., *Antibiotics in the surface water of the Yangtze Estuary: Occurrence, distribution and risk assessment.* Environmental Pollution, 2013. **175**: p. 22-29.
60. Thomas, K.V. and M.J. Hilton, *The occurrence of selected human pharmaceutical compounds in UK estuaries.* Marine Pollution Bulletin, 2004. **49**(5–6): p. 436-444.
61. Yang, Y., et al., *Occurrence and phase distribution of selected pharmaceuticals in the Yangtze Estuary and its coastal zone.* Journal of Hazardous Materials, 2011. **190**(1–3): p. 588-596.
62. Kwon, J.-W., et al., *Determination of 17-Ethynylestradiol, Carbamazepine, Diazepam, Simvastatin, and Oxybenzone in Fish Livers.* Journal of AOAC International, 2008. **92**(1): p. 359-370.
63. Álvarez-Muñoz, D., et al., *Occurrence of pharmaceuticals and endocrine disrupting compounds in macroalgaes, bivalves, and fish from coastal areas in Europe.* Environmental Research, 2015. **143**: p. 56-64.
64. Regulation, O., *No 1831/2003 of the European Parliament and the Council of 22 September 2003 on additives for use in animal nutrition.* Official J Eur Union, 2003.
65. Directive, C., *Council Directive 96/23/EC of 29 April 1996 on measures to monitor certain substances and residues thereof in live animals and animal products and repealing Directives 85/358/EEC and 86/469/EEC and Decisions 89/187/EEC and 91/664/EEC.* OJ EC L, 1996. **125**: p. 10-31.
66. Cháfer-Pericás, C., Á. Maquieira, and R. Puchades, *Fast screening methods to detect antibiotic residues in food samples.* TrAC Trends in Analytical Chemistry, 2010. **29**(9): p. 1038-1049.
67. Schröder, U. and A. Machetzki, *Determination of flumequine, nalidixic acid and oxolinic acid in shrimps by high-performance liquid chromatography with fluorescence detection.* European Food Research and Technology, 2007. **225**(5-6): p. 627-635.
68. Bringolf, R.B., et al., *Environmental occurrence and reproductive effects of the pharmaceutical fluoxetine in native freshwater mussels.* Environmental Toxicology and Chemistry, 2010. **29**(6): p. 1311-1318.
69. Li, W., et al., *Investigation of antibiotics in mollusks from coastal waters in the Bohai Sea of China.* Environmental Pollution, 2012. **162**: p. 56-62.

70. Vernouillet, G., et al., *Toxic effects and bioaccumulation of carbamazepine evaluated by biomarkers measured in organisms of different trophic levels.* Chemosphere, 2010. **80**(9): p. 1062-1068.
71. Marshall, A.G. and C.L. Hendrickson, *High-Resolution Mass Spectrometers.* Annual Review of Analytical Chemistry, 2008. **1**(1): p. 579-599.
72. Hopfgartner, G., et al., *Triple quadrupole linear ion trap mass spectrometer for the analysis of small molecules and macromolecules.* Journal of Mass Spectrometry, 2004. **39**(8): p. 845-855.
73. Yang, C. and J. Henion, *Atmospheric pressure photoionization liquid chromatographic–mass spectrometric determination of idoxifene and its metabolites in human plasma.* Journal of Chromatography A, 2002. **970**(1–2): p. 155-165.
74. Yost, R. and C. Enke, *Selected ion fragmentation with a tandem quadrupole mass spectrometer.* Journal of the American Chemical Society, 1978. **100**(7): p. 2274-2275.
75. Picó, Y., C. Blasco, and G. Font, *Environmental and food applications of LC–tandem mass spectrometry in pesticide-residue analysis: An overview.* Mass Spectrometry Reviews, 2004. **23**(1): p. 45-85.
76. Petrović, M., et al., *Liquid chromatography–tandem mass spectrometry for the analysis of pharmaceutical residues in environmental samples: a review.* Journal of Chromatography A, 2005. **1067**(1–2): p. 1-14.
77. Gago-Ferrero, P., M.S. Diaz-Cruz, and D. Barcelo, *Liquid chromatography-tandem mass spectrometry for the multi-residue analysis of organic UV filters and their transformation products in the aquatic environment.* Analytical Methods, 2013. **5**(2): p. 355-366.
78. Ortelli, D., P. Edder, and C. Corvi, *Multiresidue analysis of 74 pesticides in fruits and vegetables by liquid chromatography–electrospray–tandem mass spectrometry.* Analytica Chimica Acta, 2004. **520**(1–2): p. 33-45.
79. Gros, M., M. Petrović, and D. Barceló, *Development of a multi-residue analytical methodology based on liquid chromatography–tandem mass spectrometry (LC–MS/MS) for screening and trace level determination of pharmaceuticals in surface and wastewaters.* Talanta, 2006. **70**(4): p. 678-690.
80. Krauss, M., H. Singer, and J. Hollender, *LC–high resolution MS in environmental analysis: from target screening to the identification of unknowns.* Analytical and bioanalytical chemistry, 2010. **397**(3): p. 943-951.
81. Makarov, A.A., *Mass spectrometer*. 1999, Google Patents.
82. Benassi, M., et al., *Petroleum crude oil analysis using low-temperature plasma mass spectrometry.* Rapid Communications in Mass Spectrometry, 2013. **27**(7): p. 825-834.
83. Gonsior, M., et al., *Characterization of dissolved organic matter across the Subtropical Convergence off the South Island, New Zealand.* Marine Chemistry, 2011. **123**(1): p. 99-110.
84. Mesfioui, R., et al., *Reactivity and chemical characterization of effluent organic nitrogen from wastewater treatment plants determined by Fourier transform ion cyclotron resonance mass spectrometry.* water research, 2012. **46**(3): p. 622-634.
85. Shakeri Yekta, S., et al., *Characterization of dissolved organic matter in full scale continuous stirred tank biogas reactors using ultrahigh resolution mass spectrometry: a qualitative overview.* Environmental science & technology, 2012. **46**(22): p. 12711-12719.
86. Lehner, S.M., et al., *Evaluation of LC-high-resolution FT-Orbitrap MS for the quantification of selected mycotoxins and the simultaneous screening of fungal metabolites in food.* Food Additives & Contaminants: Part A, 2011. **28**(10): p. 1457-1468.

87. Bijlsma, L., et al., *Investigation of drugs of abuse and relevant metabolites in Dutch sewage water by liquid chromatography coupled to high resolution mass spectrometry.* Chemosphere, 2012. **89**(11): p. 1399-1406.
88. Calza, P., et al., *Identification of the unknown transformation products derived from lincomycin using LC-HRMS technique.* Journal of Mass Spectrometry, 2012. **47**(6): p. 751-759.
89. Hogenboom, A., J. Van Leerdam, and P. de Voogt, *Accurate mass screening and identification of emerging contaminants in environmental samples by liquid chromatography–hybrid linear ion trap Orbitrap mass spectrometry.* Journal of Chromatography A, 2009. **1216**(3): p. 510-519.
90. Krauss, M. and J. Hollender, *Analysis of nitrosamines in wastewater: exploring the trace level quantification capabilities of a hybrid linear ion trap/orbitrap mass spectrometer.* Analytical chemistry, 2008. **80**(3): p. 834-842.
91. Kumar, P., et al., *Targeted analysis with benchtop quadrupole–orbitrap hybrid mass spectrometer: Application to determination of synthetic hormones in animal urine.* Analytica chimica acta, 2013. **780**: p. 65-73.
92. Li, X., et al., *Rapid screening of drugs of abuse in human urine by high-performance liquid chromatography coupled with high resolution and high mass accuracy hybrid linear ion trap-Orbitrap mass spectrometry.* Journal of Chromatography A, 2013. **1302**: p. 95-104.
93. Michalski, A., et al., *Mass Spectrometry-based Proteomics Using Q Exactive, a High-performance Benchtop Quadrupole Orbitrap Mass Spectrometer.* Molecular & Cellular Proteomics, 2011. **10**(9).
94. Mol, H.J., P. Zomer, and M. de Koning, *Qualitative aspects and validation of a screening method for pesticides in vegetables and fruits based on liquid chromatography coupled to full scan high resolution (Orbitrap) mass spectrometry.* Analytical and bioanalytical chemistry, 2012. **403**(10): p. 2891-2908.
95. Scientific, T., *Thermo Scientific Orbitrap Fusion Tribrid Mass Spectrometer.* WWW Document, 2014.
96. Bijlsma, L., et al., *Performance of the linear ion trap Orbitrap mass analyzer for qualitative and quantitative analysis of drugs of abuse and relevant metabolites in sewage water.* Analytica chimica acta, 2013. **768**: p. 102-110.
97. Hopfgartner, G., D. Tonoli, and E. Varesio, *High-resolution mass spectrometry for integrated qualitative and quantitative analysis of pharmaceuticals in biological matrices.* Analytical and bioanalytical chemistry, 2012. **402**(8): p. 2587-2596.
98. Xian, F., C.L. Hendrickson, and A.G. Marshall, *High resolution mass spectrometry.* Analytical chemistry, 2012. **84**(2): p. 708-719.
99. Diaz, R., et al., *Target and non-target screening strategies for organic contaminants, residues and illicit substances in food, environmental and human biological samples by UHPLC-QTOF-MS.* Analytical Methods, 2012. **4**(1): p. 196-209.
100. Ojanperä, I., M. Kolmonen, and A. Pelander, *Current use of high-resolution mass spectrometry in drug screening relevant to clinical and forensic toxicology and doping control.* Analytical and bioanalytical chemistry, 2012. **403**(5): p. 1203-1220.
101. Hernández, F., et al., *Current use of high-resolution mass spectrometry in the environmental sciences.* Analytical and bioanalytical chemistry, 2012. **403**(5): p. 1251-1264.
102. Bijlsma, L., et al., *Fragmentation pathways of drugs of abuse and their metabolites based on QTOF MS/MS and MSE accurate-mass spectra.* Journal of Mass Spectrometry, 2011. **46**(9): p. 865-875.

103. Chiaia-Hernandez, A., et al., *Suspect and nontarget screening approaches to identify organic contaminant records in lake sediments.* Analytical and bioanalytical chemistry, 2014. **406**(28): p. 7323-7335.
104. Moschet, C., et al., *Alleviating the reference standard dilemma using a systematic exact mass suspect screening approach with liquid chromatography-high resolution mass spectrometry.* Analytical chemistry, 2013. **85**(21): p. 10312-10320.
105. Hug, C., et al., *Identification of novel micropollutants in wastewater by a combination of suspect and nontarget screening.* Environmental Pollution, 2014. **184**: p. 25-32.
106. Gallart-Ayala, H., E. Moyano, and M.T. Galceran, *Liquid chromatography/tandem mass spectrometry (highly selective selected reaction monitoring) for the analysis of isopropylthioxanthone in packaged food.* Journal of Chromatography A, 2008. **1208**(1–2): p. 182-188.
107. Martínez-Villalba, A., et al., *Fast liquid chromatography/tandem mass spectrometry (highly selective selected reaction monitoring) for the determination of toltrazuril and its metabolites in food.* Analytical and Bioanalytical Chemistry, 2010. **397**(7): p. 2893-2901.
108. Henry, H., et al., *Comparison between a high-resolution single-stage Orbitrap and a triple quadrupole mass spectrometer for quantitative analyses of drugs.* Rapid Communications in Mass Spectrometry, 2012. **26**(5): p. 499-509.
109. Zhang, H., et al., *Mass defect filter technique and its applications to drug metabolite identification by high-resolution mass spectrometry.* Journal of Mass Spectrometry, 2009. **44**(7): p. 999-1016.
110. Kaufmann, A., et al., *Comprehensive comparison of liquid chromatography selectivity as provided by two types of liquid chromatography detectors (high resolution mass spectrometry and tandem mass spectrometry): "Where is the crossover point?".* Analytica Chimica Acta, 2010. **673**(1): p. 60-72.
111. Kaufmann, A., et al., *Quantitative and confirmative performance of liquid chromatography coupled to high-resolution mass spectrometry compared to tandem mass spectrometry.* Rapid Communications in Mass Spectrometry, 2011. **25**(7): p. 979-992.
112. Ibáñez, M., et al., *Screening of antibiotics in surface and wastewater samples by ultra-high-pressure liquid chromatography coupled to hybrid quadrupole time-of-flight mass spectrometry.* Journal of Chromatography A, 2009. **1216**(12): p. 2529-2539.
113. Hermo, M.P., D. Barrón, and J. Barbosa, *Determination of multiresidue quinolones regulated by the European Union in pig liver samples: High-resolution time-of-flight mass spectrometry versus tandem mass spectrometry detection.* Journal of Chromatography A, 2008. **1201**(1): p. 1-14.
114. Ramanathan, R., et al., *It is time for a paradigm shift in drug discovery bioanalysis: from SRM to HRMS.* Journal of Mass Spectrometry, 2011. **46**(6): p. 595-601.
115. Grimalt, S., et al., *Quantification, confirmation and screening capability of UHPLC coupled to triple quadrupole and hybrid quadrupole time-of-flight mass spectrometry in pesticide residue analysis.* Journal of Mass Spectrometry, 2010. **45**(4): p. 421-436.
116. Wang, J., D. Leung, and W. Chow, *Applications of LC/ESI-MS/MS and UHPLC QqTOF MS for the Determination of 148 Pesticides in Berries†.* Journal of Agricultural and Food Chemistry, 2009. **58**(10): p. 5904-5925.
117. Gallart-Ayala, H., et al., *Preventing false negatives with high-resolution mass spectrometry: the benzophenone case.* Rapid Communications in Mass Spectrometry, 2011. **25**(20): p. 3161-3166.
118. Ferrer, I. and E.M. Thurman, *Analysis of 100 pharmaceuticals and their degradates in water samples by liquid chromatography/quadrupole time-of-flight mass spectrometry.* Journal of Chromatography A, 2012. **1259**(0): p. 148-157.

119. Chiaia-Hernandez, A.C., M. Krauss, and J. Hollender, *Screening of Lake Sediments for Emerging Contaminants by Liquid Chromatography Atmospheric Pressure Photoionization and Electrospray Ionization Coupled to High Resolution Mass Spectrometry.* Environmental Science & Technology, 2012. **47**(2): p. 976-986.
120. Shi, F., et al., *Application of a high resolution benchtop quadrupole-Orbitrap mass spectrometry for the rapid screening, confirmation and quantification of illegal adulterated phosphodiesterase-5 inhibitors in herbal medicines and dietary supplements.* Journal of Chromatography A, (0).
121. Tseng, L.Y., et al., *Comparison of effluent organic matter from parallel activated sludge and integrated fixed-film activated sludge (IFAS) processes.* Proceedings of the Water Environment Federation, 2013. **2013**(7): p. 6553-6562.
122. Schymanski, E.L., et al., *Strategies to Characterize Polar Organic Contamination in Wastewater: Exploring the Capability of High Resolution Mass Spectrometry.* Environmental science & technology, 2014. **48**(3): p. 1811-1818.
123. Jelic, A., et al., *Degradation of carbamazepine by Trametes versicolor in an air pulsed fluidized bed bioreactor and identification of intermediates.* Water Research, 2012. **46**(4): p. 955-964.
124. González-Mariño, I., et al., *Screening and Selective Quantification of Illicit Drugs in Wastewater by Mixed-Mode Solid-Phase Extraction and Quadrupole-Time-of-Flight Liquid Chromatography–Mass Spectrometry.* Analytical chemistry, 2012. **84**(3): p. 1708-1717.
125. Bletsou, A.A., et al., *Targeted and non-targeted liquid chromatography-mass spectrometric workflows for identification of transformation products of emerging pollutants in the aquatic environment.* TrAC Trends in Analytical Chemistry, 2015. **66**: p. 32-44.
126. Heuett, N.V., S.R. Batchu, and P.R. Gardinali, *Understanding the magnitude of emergent contaminant releases through target screening and metabolite identification using high resolution mass spectrometry: Illicit drugs in raw sewage influents.* Journal of Hazardous Materials, 2015. **282**: p. 41-50.
127. Schymanski, E.L., et al., *Identifying Small Molecules via High Resolution Mass Spectrometry: Communicating Confidence.* Environmental science & technology, 2014. **48**(4): p. 2097-2098.
128. Zonja, B., et al., *LC-HRMS Suspect Screening for Detection-Based Prioritization of Iodinated Contrast Media Photodegradates in Surface Waters.* Environmental science & technology, 2015. **49**(6): p. 3464-3472.
129. Jeon, J., D. Kurth, and J. Hollender, *Biotransformation Pathways of Biocides and Pharmaceuticals in Freshwater Crustaceans Based on Structure Elucidation of Metabolites Using High Resolution Mass Spectrometry.* Chemical Research in Toxicology, 2013. **26**(3): p. 313-324.
130. Kern, S., et al., *Identification of Transformation Products of Organic Contaminants in Natural Waters by Computer-Aided Prediction and High-Resolution Mass Spectrometry.* Environmental science & technology, 2009. **43**(18): p. 7039-7046.
131. Postigo, C. and S.D. Richardson, *Transformation of pharmaceuticals during oxidation/disinfection processes in drinking water treatment.* Journal of Hazardous Materials, 2014. **279**: p. 461-475.
132. Segura, P.A., et al., *Quantification of carbamazepine and atrazine and screening of suspect organic contaminants in surface and drinking waters.* Chemosphere, 2011. **84**(8): p. 1085-1094.
133. Batchu, S.R., et al., *RESEARCH ARTICLE Open Access.* 2013.

134. Nácher-Mestre, J., et al., *Qualitative Screening of Undesirable Compounds from Feeds to Fish by Liquid Chromatography Coupled to Mass Spectrometry.* Journal of Agricultural and Food Chemistry, 2013. **61**(9): p. 2077-2087.
135. Plassmann, M.M., W. Brack, and M. Krauss, *Extending analysis of environmental pollutants in human urine towards screening for suspected compounds.* Journal of Chromatography A, 2015. **1394**: p. 18-25.
136. Solliec, M., A. Roy-Lachapelle, and S. Sauvé, *Development of a suspect and non-target screening approach to detect veterinary antibiotic residues in a complex biological matrix using liquid chromatography/high-resolution mass spectrometry.* Rapid Communications in Mass Spectrometry, 2015. **29**(24): p. 2361-2373.
137. Kinyua, J., et al., *A data-independent acquisition workflow for qualitative screening of new psychoactive substances in biological samples.* Analytical and bioanalytical chemistry, 2015. **407**(29): p. 8773-8785.
138. Halling-Sørensen, B., G. Sengeløv, and J. Tjørnelund, *Toxicity of tetracyclines and tetracycline degradation products to environmentally relevant bacteria, including selected tetracycline-resistant bacteria.* Archives of Environmental Contamination and Toxicology, 2002. **42**(3): p. 263-271.
139. Sunderland, J., et al., *Ofloxacin photodegradation products possess antimicrobial activity.* Drugs, 1999. **58**: p. 171-172.
140. Howard, P.H. and D.C.G. Muir, *Identifying New Persistent and Bioaccumulative Organics Among Chemicals in Commerce II: Pharmaceuticals.* Environmental Science & Technology, 2011. **45**(16): p. 6938-6946.
141. Amr Abdel Raheem and P. Kell, *Patient preference and satisfaction in erectile dysfunction therapy: a comparison of the three phosphodiesterase-5 inhibitors sildenafil, vardenafil and tadalafil.* Patient Prefer Adherence, 2009. **3**: p. 99–104.
142. RM, C. and C. CC, *Tadalafil in the treatment of erectile dysfunction.* Ther Clin Risk Manag, 2008.
143. Gregory A Broderick, *Oral Pharmacotherapy and the Contemporary Evaluation and Management of Erectile Dysfunction.* Rev Urol, 2003. **5**.
144. Aytaç, McKinlay, and Krane, *The likely worldwide increase in erectile dysfunction between 1995 and 2025 and some possible policy consequences.* BJU International, 1999. **84**(1): p. 50-56.
145. Cooper, J.D.H., et al., *Development of an assay for the simultaneous determination of sildenfail (viagra) and its metabolite (UK-103,320) using automated sequential trace enrichment of dialysates and high-performance liquid chromatography.* Journal of Chromatography B: Biomedical Sciences and Applications, 1997. **701**(1): p. 87-95.
146. Singh, S., et al., *Strategies for characterizing sildenafil, vardenafil, tadalafil and their analogues in herbal dietary supplements, and detecting counterfeit products containing these drugs.* TrAC Trends in Analytical Chemistry, 2009. **28**(1): p. 13-28.
147. Caracciolo, A.B., E. Topp, and P. Grenni, *Pharmaceuticals in the environment: biodegradation and effects on natural microbial communities. A review.* Journal of Pharmaceutical and Biomedical Analysis, 2015. **106**: p. 25-36.
148. Gutiérrez, I.R., et al., *Effect of sulfonamide antibiotics on microbial diversity and activity in a Californian Mollic Haploxeralf.* Journal of Soils and Sediments, 2010. **10**(3): p. 537-544.
149. Webb, S., *A data based perspective on the environmental risk assessment of human pharmaceuticals II—Aquatic risk characterisation*, in *Pharmaceuticals in the Environment*. 2001, Springer. p. 203-219.
150. Cleuvers, M., *Aquatic ecotoxicity of pharmaceuticals including the assessment of combination effects.* Toxicology letters, 2003. **142**(3): p. 185-194.

151. Cleuvers, M., *Mixture toxicity of the anti-inflammatory drugs diclofenac, ibuprofen, naproxen, and acetylsalicylic acid.* Ecotoxicology and Environmental Safety, 2004. **59**(3): p. 309-315.
152. Zenker, A., et al., *Bioaccumulation and biomagnification potential of pharmaceuticals with a focus to the aquatic environment.* Journal of Environmental Management, 2014. **133**: p. 378-387.
153. Liu, J., et al., *Occurrence, bioaccumulation and risk assessment of lipophilic pharmaceutically active compounds in the downstream rivers of sewage treatment plants.* Science of The Total Environment, 2015. **511**: p. 54-62.
154. Tanoue, R., et al., *Uptake and Tissue Distribution of Pharmaceuticals and Personal Care Products in Wild Fish from Treated-Wastewater-Impacted Streams.* Environmental Science and Technology, 2015. **49**(19): p. 11649-11658.
155. Wille, K., et al., *Development of analytical strategies using U-HPLC-MS/MS and LC-ToF-MS for the quantification of micropollutants in marine organisms.* Analytical and bioanalytical chemistry, 2011. **400**(5): p. 1459-1472.
156. Moreno-González, R., et al., *Do pharmaceuticals bioaccumulate in marine molluscs and fish from a coastal lagoon?* Environmental Research, 2016. **146**: p. 282-298.
157. Jeong-Wook Kwon, K.L.A., Doris E., Vidal-Dorsch, Steven M. Bay and Kang Xia1, , *Determination of 17α-ethynylestradiol, carbamazepine, diazepam, simvastatin, and oxybenzone in fish livers.* J AOAC Int. , 2009. **Jan-Feb;92**(1): p. 359-369.
158. McEneff, G., et al., *A year-long study of the spatial occurrence and relative distribution of pharmaceutical residues in sewage effluent, receiving marine waters and marine bivalves.* Science of the Total Environment, 2014. **476-477**: p. 317-326.
159. Martínez Bueno, M.J., et al., *Fast and easy extraction combined with high resolution-mass spectrometry for residue analysis of two anticonvulsants and their transformation products in marine mussels.* Journal of Chromatography A, 2013. **1305**: p. 27-34.
160. Pritchard, J.B. and J.R. Bend, *Relative roles of metabolism and renal excretory mechanisms in xenobiotic elimination by fish.* Environmental Health Perspectives, 1991. **90**: p. 85-92.
161. Corcoran, J., et al., *Effects of pharmaceuticals on the expression of genes involved in detoxification in a carp primary hepatocyte model.* Environmental Science and Technology, 2012. **46**(11): p. 6306-6314.
162. Fukami, T. and T. Yokoi, *The emerging role of human esterases.* Drug Metabolism and Pharmacokinetics, 2012. **27**(5): p. 466-477.
163. Brox, S., et al., *Metabolism of clofibric acid in zebrafish embryos (Danio rerio) as determined by liquid chromatography-high resolution-mass spectrometry.* Comparative Biochemistry and Physiology Part - C: Toxicology and Pharmacology, 2016. **185-186**: p. 20-28.
164. Connors, K.A., et al., *Comparative pharmaceutical metabolism by rainbow trout (Oncorhynchus mykiss) liver S9 fractions.* Environmental Toxicology and Chemistry, 2013. **32**(8): p. 1810-1818.
165. Baron, M.G., et al., *Pharmaceutical metabolism in fish: Using a 3-D Hepatic in Vitro model to assess clearance.* PLoS ONE, 2017. **12**(1).
166. Valdés, M.E., et al., *Bioaccumulation and bioconcentration of carbamazepine and other pharmaceuticals in fish under field and controlled laboratory experiments. Evidences of carbamazepine metabolization by fish.* Science of The Total Environment, 2016. **557-558**: p. 58-67.
167. Lahti, M., et al., *Uptake from water, biotransformation, and biliary excretion of pharmaceuticals by rainbow trout.* Environmental Toxicology and Chemistry, 2011. **30**(6): p. 1403-1411.

168. González-Mira, A., et al., *Drugs of environmental concern modify Solea senegalensis physiology and biochemistry in a temperature-dependent manner.* Environmental Science and Pollution Research, 2016. **23**(20): p. 20937-20951.
169. Solé, M., et al., *Xenobiotic metabolism modulation after long-term temperature acclimation in juveniles of Solea senegalensis.* Marine Biology, 2015. **162**(2): p. 401-412.
170. Bradford, M.M., *A rapid and sensitive method for the quantitation of microgram quantities of protein utilizing the principle of protein-dye binding.* Analytical Biochemistry, 1976. **72**(1-2): p. 248-254.
171. Hosokawa, M., Satoh, T., , *Measurement of carboxylesterase (CES) activities.* Curr Protoc Toxicol . 2002. **Chapter 4, Unit 47**.
172. Lassila, T., et al., *Toxicity of Carboxylic Acid-Containing Drugs: The Role of Acyl Migration and CoA Conjugation Investigated.* Chemical Research in Toxicology, 2015. **28**(12): p. 2292-2303.
173. Kim, K.A., et al., *Effect of probenecid on the pharmacokinetics of carbamazepine in healthy subjects.* European Journal of Clinical Pharmacology, 2005. **61**(4): p. 275-280.
174. Solé, M. and J.C. Sanchez-Hernandez, *An in vitro screening with emerging contaminants reveals inhibition of carboxylesterase activity in aquatic organisms.* Aquatic Toxicology, 2015. **169**: p. 215-222.
175. Xu, C., X. Wang, and J.L. Staudinger, *Regulation of tissue-specific carboxylesterase expression by pregnane X receptor and constitutive androstane receptor.* Drug Metabolism and Disposition, 2009. **37**(7): p. 1539-1547.
176. Inoue, N.R., et al., *Reversible inhibition of human carboxylesterases by acyl glucuronides.* Drug Metabolism and Disposition, 2013. **41**(4): p. 698-703.
177. Solé, M., A. Fortuny, and E. Mañanós, *Effects of selected xenobiotics on hepatic and plasmatic biomarkers in juveniles of Solea senegalensis.* Environmental Research, 2014. **135**: p. 227-235.
178. Crespo, M. and M. SolÃ©, *The use of juvenile Solea solea as sentinel in the marine platform of the Ebre Delta: in vitro interaction of emerging contaminants with the liver detoxification system.* Environmental Science and Pollution Research, 2016. **23**(19): p. 19229-19236.
179. Bletsou, A.A., et al., *Targeted determination of more than 1500 micropollutants & transformation products in wastewater samples by liquid chromatography quadrupole-time-of-flight mass spectrometry with an accurate-mass database.* 2016.

ANNEX

INDEX DE TAULES

TAULA 1. Resum dels principals estudis de biodegradació ambiental, TPs identificats i principals reaccions de transformació. 27

TAULA 2. Metabòlits dels fàrmacs identificats als peixos..... 34

TAULA 3. Compostos sospitosos detectats als estudis de biodegradació de les sulfamides. 162

TAULA 4. Metabòlits del IBU identificats en peixos i en plantes. 215

TAULA 5. Fàrmacs detectats en múscul de peixos del riu Llobregat 217

INDEX DE FIGURES

Figura 1. Concentracions de fàrmacs al riu Llobregat l'any 2011 [18]. 24

Figura 2. Història de la espectrometria de masses 39

Figura 3. Esquema de la generació e identificació dels TPs a mostres ambientals 47

Figura 4. Detecció de TPs a mostres reals aplicant anàlisi de sospitosos 50

Figura 5. Esquema del estudi ambiental dels fàrmacs..... 75

Figura 6. Estructures del SDF i els seus anàlegs 80

Figura 7. Espectres MS/MS amb els fragments proposats pels compostos pares 164

Figura 8. Etapes del metabolisme dels fàrmacs..... 171

Figura 9. Imatges dels punts de mostreig al riu Llobregat i les dues espècies seleccionades 206

Figura 10. Exemple de predicció de metabòlits de l'IBU a través dels software MetabolitePredict 208

Figura 11. Estratègia analítica utilitzada per a la detecció i identificació de metabòlits en peixos salvatges..... 209

Figura 12. Metabòlit de l'Ibuprofè (IBU-MET222) detectat a la bilis del peix mitjançant el software SIEVE 210

Figura 13. Espectre de fragmentació proposat per l'hidròxid de l'acil glucurònic iburpofè (IBU-MET398- C). 211

Figura 14. Espectre de fragmentació proposat per l'èter glucurònic d'ibuprofè (IBU-MET398- A i B). 212

Figura 15. Espectre de fragmentació dels metabòlits di-hidroxilats de l'IBU detectats per primera vegada a l'article 3. 213

Figura 16. Ruta metabòlica de la CBZ i l'IBU en SOLEA SENEGALENSIS. 214

Figura 17. Exemple de taula de resultats per al escombratge dirigit de més de 2000 compostos en múscul de peix. 216

Figura 18. Percentatge de detecció de la sertralina i mepivacaina als diferents punts de mostreig. 217

Figura 19. Exemple de taula de resultats per al escombratge de metabòlits sospitosos en bilis de peix. 218

Figura 20. Metabòlits del IBU detectats a les mostres de peixos del Llobregat 219

Figura 21. Detecció de sertralina i metabòlit proposat com a desmetilsertralina 220

Figura 22. Metabòlit proposat com a hidroxi-taurina de gemfibrozil..... 220

LLISTAT D'ACRÒNIMS

- **ADC:** Detector d'analògic a digital.
- **AINE:** Antiinflamatoris No Esteroides.
- **APCI:** Ionització Química a Pressió Atmosfèrica, del anglès "Atmospheric Pressure Chemical Ionization".
- **API:** Ionització a Pressió Atmosfèrica, del anglès "Atmospheric Pressure Chemical Ionization".
- **APPI:** FotoIonització a Pressió Atmosfèrica, del anglès "Atmospheric Pressure PhotoIonization".
- **BCF:** Factors de Bioconcentració, del anglès "Bioconcentration Factors".
- **CBZ:** Carbamazepina.
- **CYP:** Citocrom P450.
- **DBPs:** Subproductes de Desinfecció, de l'anglès "Desinfection ByProducts".
- **DM-SDF:** Desmetilsildenafil.
- **EDAR:** Estació Depuradora d'Aigües Residuals.
- **ESI:** Ionització per Electrospray, de l'anglès "Electrospray Ionization".
- **FWHM:** Amplada total a mitja alçada, de l'anglès "Full Width at Half Maximum".
- **FT-ICR:** Ressonància ciclotrònica d'ions per transformada de Fourier, de l'anglès "Fourier Transform Ion Cyclotron Resonance".
- **GC:** Cromatografia de gasos, de l'anglès "Gas Chromatography".
- **HR:** Alta Resolució, de l'anglès "High resolution".
- **HH-SDF:** Hidroxihomosildenafil.
- **H-SDF:** Homosildenafil.
- **IBU:** Ibuprofè.
- **ICM:** Mitjans de Contrast Iodats de l'anglès "Iodinated Contrast Media".
- **LC:** Cromatografia de Líquids, de l'anglès "Liquid Chromatography".
- **LR:** Baixa resolució, de l'anglès "Low resolution".
- **MDF:** Filtrat per Defecte de Massa, de l'anglès "Mass Defect Filtering".
- **MS:** Espectrometria de Masses, de l'anglès "Mass Spectrometry".

- **MS/MS:** Espectrometria de Masses en tandem.
- **NR-SDF:** Norneosildenafil.
- **QqLIT:** Quadrupol - Trampa lineal d'Ions, de l'anglès "Quadrupole-Linear Ion Trap".
- **QqQ**: Analitzador d'espectrometria de masses en tàndem de triple quadrupol, de l'anglès " Triple Quadrupole".
- **QqTOF:** Quadrupol-Temps de Vol, de l'anglès "Quadrupole-Time-of-flight".
- **RMN:** Ressonància Magnètica Nuclear.
- **SDF:** Sildenafil.
- **SULTs:** sulfotransferases
- **SMX:** Sulfametoxazol.
- **SMZ:** Sulfametazina.
- **SRM:** "Selected Reaction Monitoring".
- **TDC:** Detector de temps a digital.
- **TIC:** Total Ion Chromatogram.
- **TP:** Producte de transformació, del anglès "Transformation product".
- **TS-SDF:** Tiosildenafil.
- **UGTs:** uridinadifosfat glucuronosiltransferasa
- **UM-PPS:** Sistema de Predicció de la Universitat de Minnesota, de l'anglès "University of Minesota - Pathway Prediction System".
- **UPLC:** Cromatografia de Líquids d'Ultra-Eficiència de l'anglès, "Ultraperformance Liquid Chromatography".
- **XIC:** Cromatograma d'ions extrets.